Optimisation Approaches for Energy Supply Chains

Andrés Joaquín Calderón Vergara

Department of Chemical Engineering

University College London

A Thesis Submitted to University College London for the Degree of Doctor of Philosophy

April 2017

Declaration

I, Andrés J. Calderón, confirm that the work presented in this thesis is my own. Where information has been derived from other sources, I confirm that this has been indicated in the thesis.

Signature: _____

Date: _____

Acknowledgements

Without the support of the people who helped throughout my Doctorate studies, this thesis would not have been possible and my experience would not have been as enjoyable. Therefore, I would like to acknowledge them here.

First, my deepest gratitude goes to my supervisor, Prof. Lazaros Papageorgiou, for the time he spared to discuss our work, to provide me with his guidance and feedback, and to support my ideas for this research.

Then, I would like to thank my secondary supervisor, Dr. Paolo Agnolucci, for giving me useful comments on our common publications. During the months I spent at Purdue University as a visiting scholar, I learnt new optimisation techniques and was immersed in an inspiring environment, for which I would like to express my appreciation towards Prof. Gintaras Reklaitis.

Next, I would like to acknowledge the collaboration and productive conversations regarding the mathematical framework we developed together with my colleague and a true friend, Dr. Omar Guerra.

My baby steps in optimisation of unconventional fossil fuels and GAMS language programming I owe to the group from the Colombian Petroleum Institute. Further, I would like to express my gratitude to Dr. Astley Hastings for his generosity in sharing important data for the BioSNG project with me. Also, I would like to acknowledge Dr. Sergei Kucherenko and Yemi Zaccheus for the invaluable inputs in the implementation of the global sensitivity analysis in this thesis.

I would like to thank Masha for her unconditional support and infinite supplies of cupcakes and cheesecakes.

The people from room 203 in Roberts Building, where the Process Systems Engineering group is located, made this PhD ride an amazing journey so, thanks to Cristian, Carlos, Adrian, Javier, Charry, Matt, Di, Marta, Will, Billy, Mayo, Shade and the rest of the gang.

I would like to pay my sincere admiration and gratitude to my mum, dad and sister in Colombia, for their continuing love and patience during those four years.

Last but not least, I would like to acknowledge the financial support of COLCIENCIAS and the Administration of the Chemical Engineering Department at UCL.

Abstract

This research presents decision-support tools for the assessment of energy systems development at national and regional scales. For this purpose, mathematical frameworks for the design and optimisation of energy systems are developed.

A methodology is proposed as a preliminary assessment of shale gas development. For this purpose, economic and environmental metrics are proposed to address different aspects of well-pad designs such as productivity and water intensity. The outcome of this methodology is included in a comprehensive optimisation-based decision-support tool developed to address the design of shale gas supply chains along with water management strategies. In this framework, the optimisation of well-pad designs is regarded as a critical decision variable. Next, implications of water scarcity, the role of economy of scales, and the impact of wastewater quality are addressed through a case study focusing on the development of shale gas supply chains in Colombia.

The production of synthetic natural gas is studied as a possible substitute of natural gas. In this case, an optimisation approach is proposed to address decisions such as feedstock procurement, transportation and optimal production schemes of BioSNG and power. The mathematical framework can be implemented to investigate policies that encourage the development of renewable energy sources. The impact of uncertainty in input data is addressed through a global sensitivity analysis (GSA). The implementation of GSA assists not only in the identification of key parameters in the design of BioSNG supply chains, but also in revealing recurring trends in light of uncertainty. Finally, the development of BioSNG supply chains in the UK is investigated through the implementation of the proposed mathematical framework.

Table of Contents

List of Figures

List of Tables

Chapter 1. Introduction

The world's primary energy supply mix has faced recurring changes over the last century (1900 - 2000), period in which the primary energy consumption exhibited an almost 14-fold growth [1]. In earlier times, and until the end of 19th century, the world was fuelled mainly by traditional biomass-based fuels including wood, charcoal and crop residues [2]. Subsequently, driven by the development of the steam engine and the need of a higher energy density fuel [3], coal became the overriding primary energy source through the first two-thirds of the 20th century. This changed since the 1960s, when crude oil became the main source of primary energy.

The BP Statistical Review of World Energy estimated that 86.7% of the total primary energy consumption was supplied by fossil fuels in 2013 [4], in which oil and coal is the world's leading fuel followed closely by coal with 32.9% and 30.1% of total global consumption, respectively. Natural gas accounted for 23.7%. A growth in energy consumption is expected for the years to come in which fossil fuels will continue to be the major source of energy. According to the BP Energy Outlook 2035 [5], the world's primary energy consumption will increase 41% in 2035 compared to 2012, which means an average annual growth rate of 1.5%. The world's primary energy mix is moving to its third transition; from crude oil to natural gas, which is a cleaner and more efficient fuel for power generation when compared with coal or oil. Indeed currently natural gas is the fastest growing fossil fuel, with an estimated average growth rate of 1.9% per year between 2013 and 2035 [5]. Roughly, 50% of this growth in gas supply will be led by shale gas, which is classified as unconventional gas.

The growing demand for primary energy have spurred the development of new energy sources, with shale gas and shale oil among the unconventional fuels receiving most attention. Even though the development of these unconventional

fossil fuels has brought new business opportunities to the energy sector [6], their exploitation relies on the implementation of more sophisticated and costly production techniques, specifically, horizontal drilling and hydraulic fracturing, which make their economics especially susceptible to volatile prices in the spot market. Additionally, the implementation of artificial stimulation techniques, used in hydraulic fracturing operations, has raised concerns regarding potential negative environmental impacts, especially the depletion and possible degradation of fresh water resources [7–10]. Thus, a rigorous quantification of the trade-offs associated with the development of shale gas plays is essential for evaluating the economics of these unconventional fossil fuel projects as well as for formulating policies and regulations for their adequate exploitation and development [11].

The exploitation of fossil fuels is facing important challenges as the effects of climate change become more evident. The energy sector has become the major source of anthropogenic greenhouse gas (GHG) emissions, accounting for roughly two-thirds of global GHG emissions in recent years [12]. Furthermore, an energy supply chain based primarily on fossil fuels could raise concerns regarding energy supply security and energy sustainability. Consequently, the development of sustainable energy sources is gaining momentum mainly driven by a worldwide tendency of establishing policies that support the development of these technologies. For instance, the European Commission (EC) has devoted big efforts in designing and implementing policies that support the development of alternative energy sources, e.g. solar, windmill, advanced gasification, hydrogen production. Based on 1990's levels, the EC has set binding targets to reduce 20% of the greenhouse gas (GHG) emissions by 2020, increase the share of renewable energy up to 20% and increase the energy efficiency to 20% [13]. Additionally, new targets for 2030 are under consultation with the intention of giving continuity and driving progress towards a low-carbon economy [14].

The scientific community has also played an important role in the development of reliable, cost-efficient renewable technologies. For instance, Kim et al. [15] designed a superstructure for the assessment of optimal biomass-to-fuel production strategies. Swanson et al. [16] developed a process for the production of gasoline and

diesel from renewable resources via gasification and Fischer-Tropsch (FT). Moreover, the concept of hydrocarbon biorefineries has been subject of extensive research in which economic and environmental criteria are considered for the process synthesis [17–20]. Natural gas, being a cleaner substitute to coal in power generation applications, could play an important role in the transition from fossil to renewable fuels [21]. Accordingly, several processes have been developed for the production of synthetic natural gas from renewable resources (BioSNG) via gasification [22–25]. In order to improve the general efficiency of the process, energy integration for heat and power cogeneration [26–28] has been proposed. It has been reported that with the current state-of-the-art the production of BioSNG in the UK is technically feasible with the main risks being related to management and financing rather than technical aspects [29].

The main challenge lies on how to design energy systems while considering three crucial aspects: environmental sustainability, energy security and energy equity. Certainly, this could be achieved through coordinated actions between governments, markets, and industry. Mathematical modelling and optimisation techniques are powerful tools that provide a systematic methodology to tackle decision problems of these kinds [30–35]. A mathematical framework that incorporates important decision variables allows researchers, policy makers and shareholders to achieve a better understanding of the energy systems, identify key elements and trade-offs, and disclose synergies inherent to the nature of the problem. This work focuses on the development of optimisation approaches for the design of energy systems at regional and national scales. Specifically, two energy systems are investigated: shale gas supply chains and BioSNG supply chains. The novelty of this work stems from integration of shale gas supply chain with water management, and identification of critical components for the production of BioSNG at national scales.

The rest of the thesis is organised as follows:

The state of art of the three selected energy systems is discussed in Chapter 2. A thorough description of the challenges associated with their development is provided and opportunities for research are identified.

In Chapter 3, a methodology is presented as an alternative approach to integrate well-pad designs as decision variable in an optimisation framework. This methodology allows to investigate different design parameters along with characteristics of a shale reservoir in order to identify key well-pad designs to be included in a optimisation framework. Different performance metrics are proposed to evaluate the economics and the environmental impact of different well-pad designs.

In Chapter 4, a mathematical formulation and implementation of a comprehensive optimisation framework for the assessment of shale gas resources is presented. A set of case studies are discussed which provide insights on the water availability implications on the economic performance of shale gas supply chains. In addition, the role of economies of scale in scenarios under water scarcity, and the implications of wastewater quality on the economics of shale gas development are also investigated.

In Chapter 5, a general optimisation framework based on a spatially-explicit multiperiod mixed integer linear programming (MILP) model is proposed to address the strategic design of BioSNG supply chains. The capabilities of the proposed model are illustrated through the implementation of a set of case studies based on the UK. The results reveal the importance of power cogeneration and government subsidisation.

In Chapter 6, the optimisation framework introduced for the strategic design of BioSNG supply chains is extended to account for pretreatment technologies. Moreover, the role of the government in the economic performance of BioSNG production is further investigated via subsidisation schemes. Finally, a global sensitivity analysis approach is implemented in order to quantify the effect of uncertainties associated to input parameters and identify those that have the major impacts.

Finally, Chapter 7 provides the main conclusions and insights derived from the implementation of the optimisation frameworks. In addition, possible directions for future work are discussed.

Chapter 2. An overview of energy systems[1]

This chapter provides a broad discussion of different aspects related to shale gas development and production of synthetic natural gas from sustainable resources (BioSNG). The development of shale gas resources is highly complex since it poses several challenges regarding its economic benefits and potential associated environmental impacts. In this chapter, these challenges are classified and discussed in the context of global and local scales. Furthermore, the development of sustainable supply chains for production of BioSNG is examined. Current policies for promoting the development of renewable energy sources are presented and associated challenges for large-scale implementations are identified. Moreover, the relevance of BioSNG production in the UK is investigated. Finally, the review serves as a basis to identify opportunities for developing optimisation-based methodologies that contribute in elucidating some of the pinpointed challenges.

2.1 Shale gas development

Shale gas development has drawn the attention of countries around the world, stimulated by its observed impacts in the United States not only on the economy but also on the increasing burden on water resources required for fracking operations [6,36]. Accordingly, this increasing interest has resulted in numerous research studies addressing different aspects regarding the exploitation of shale gas resources. Some researchers have focused on the geologic characterisation, including prospect and play assessment [37,38] and productivity evaluation based on the identification of the naturally-fracture networks [39]. Reservoir modelling and simulation techniques have been implemented to investigate the productivity of shale gas plays by integrating petrophysical and geomechanical characterisation along with different

[1] This chapter is based on manuscripts IV and V of the list of publications presented at the end of this thesis

artificial stimulation strategies [40,41]. Moreover, the economic assessment of shale gas plays has also drawn the attention of the research community. Simulation-based and data driven tools have been reported for the preliminary evaluation of shale gas development [42,43]. Furthermore, given the complexity of the decision-making problem, optimisation models have been developed and implemented for the tactical and strategic planning of shale gas fields and supply chains [44,45]. In addition to modelling, simulation, and economic evaluation of shale gas resources, the assessment of environmental impacts, in terms of CO_2 emissions, associated with the development of shale gas resources, has also been subject of extensive research [46–48]. Wastewater management is another crucial aspect, which is being considered in the development of shale gas plays. However, despite the extensive studies reported to date on shale gas issues, the integration of water management within the design and planning of shale gas supply chains remains one of the key areas where additional research efforts are needed. In particular, the interaction between the well-pad configuration and water management strategies could reveal synergies that can be exploited in the planning of the shale gas supply chain. In the following sections the main challenges and implications of shale gas development are classified as global and local challenges and a broad analysis is provided.

2.1.1 Global challenges and implications

2.1.1.1 Shale gas resources, gas market, and water stress

Natural gas, including unconventional gas, is a key energy source, supplying about 21.4% (~ 3,507 billion cubic meters (bcm)) of world primary energy demand in 2013 [49]. The United States was the largest natural gas consumer accounting for roughly 27.1% of the global demand, followed by Russia, Europe, Middle East, and China with shares of 17.5%, 17.2%, 15.3%, and 6.3%, respectively (see Figure 2.1). Moreover, among fossil fuels, natural gas is the fastest growing fossil fuel whose consumption is expected to increase roughly 60% from 2013 to 2040 [49], giving natural gas an even more prominent role in the global energy mix. By way of comparison, oil and coal consumption will increase about 27% and 43% by 2040, respectively. Despite China's low gas consumption in 2013 by comparison to the global gas demand, China and the Middle East are expected to be the dominant areas

of gas demand growth, together accounting for ~44.6% of total gas demand increase by 2040. Specifically, by 2040 China's gas consumption will increase by more than three-fold with respect to the 2013 level, reaching 15.0% of the global gas demand. This increase, in combination with a reduction in gas demand in Russia and Europe, will position China as the third largest gas consumer, behind only the United States and the Middle East, which are expected to account for about 21.5% and 18.7% of the global gas demand by 2040 [49]. Consequently, the global gas market is expected to expand. This expansion will be mostly driven by LNG trade, which is increasing faster than delivery of gas via pipelines. The main reason is that LNG enables a worldwide distribution of natural gas, adding flexibility to the gas market by allowing trading of the commodity without requiring fixed distribution infrastructure with long-term agreements between supplier and consumer. However, shale gas could be produced at advantageous domestic prices in comparison to importing gas as LNG (between 2010 and 2014 the prices for shale gas varied from 2 $/MBtu to 6 $/MBtu, whereas for LNG prices ranged from 10 $/MBtu to 18 $/MBtu). Moreover, the efficiency for delivering natural gas via LNG is ~75% (energy penalty of about 25%), while for gas pipeline it ranges from 85% to 90% (energy penalty ranging from 10% to 15%) [50].

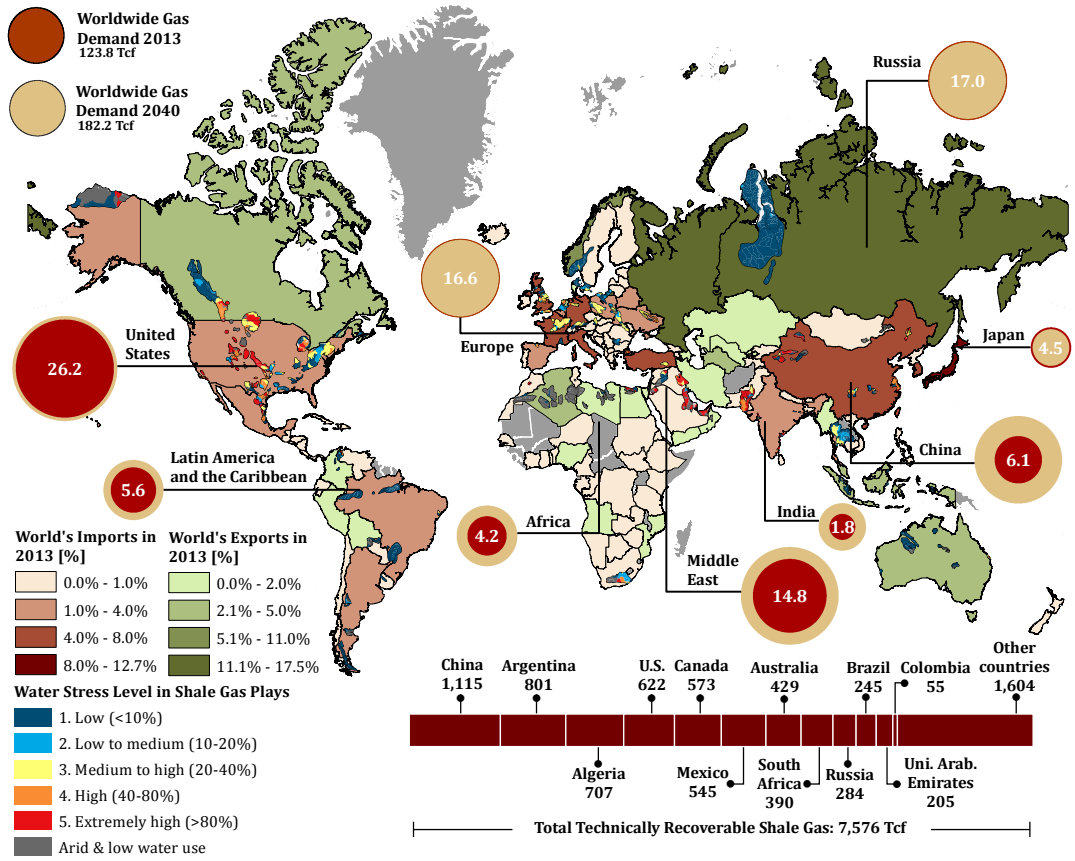

Figure 2.1 Global gas demand and supply [49,51], shale gas reserves [52], and water stress [53,54]. Numbers inside the bubbles indicate the natural gas demand in 2013.

The growing demand for natural gas together with the depletion of conventional gas reserves has spurred the development of unconventional gas, in particular, shale gas. Unconventional gas, mostly shale gas, is expected to represent ~60% of the total growth in gas supply from 2013 to 2040. The distribution of prospective and developed shale gas plays around the world is shown in Figure 2.1. In 2014, the IEA estimated the total technically recoverable shale gas to be 7,576 trillion cubic feet (Tcf) (227.3 tcm), which would be enough to supply the world's 2040 gas demand for ~40 years. China holds the largest shale gas reserves, comprising around 14.7% of the total availability, followed by Argentina, Algeria, and U.S. with 10.6%, 9.3%, and 8.2% of the world's shale gas reserves, respectively. Currently, the majority of plays in commercial shale gas operation are located in the United States, and only a minor fraction is located in Canada and China.

The development of shale gas has had remarkable repercussions on the US economy and this has caught the attention of governments around the world, who

now are seeking to replicate the precedent set by the United States in their economies. Nonetheless, the opportunities and urgency for developing shale gas resources are specific for every country.

It appears that shale gas holds the key for nations with shale resources to secure a short-term energy supply. However, the development of shale gas does come at potential cost in terms of its environmental impact. The exploitation of these resources could increase the stress on local fresh water sources; a crucial challenge that must be cautiously addressed [55]. It has been reported that 38% of the global shale gas resources are affected by limited fresh water access which can curb the successful development of these resources [53]. From the list of countries with the largest shale gas reserves shown in Figure 2.1, China, Mexico and South Africa, are, on average, under high water stress levels, and Algeria and Saudi Arabia are classified to be in the arid category. In China, 60% of the shale resources are located in areas with high or extremely high water stress. In the case of Mexico and South Africa these figures are 61% and 75%, respectively. In Algeria more than 90% of the prospective areas are located in the Sahara desert, whereas in Saudi Arabia 100% of the shale plays are placed in arid areas. Europe has a comparative advantage in this respect, since most of the prospective areas for shale gas production are classified in the first three categories of water stress: low, low to medium, and medium to high. This resource quandary presents significant challenges not only in terms of environmental aspects, but also in social and economic elements, which require that governments and decision makers join in efforts to establish regulatory frameworks that allow the sustainable development of shale gas while also securing the water supply necessary for agriculture, industry and domestic consumption.

2.1.1.2 Decoupling of fuel prices

Exploitation of shale gas resources dates back to 1800's when several wells were drilled in shallow shale formations in the Appalachian and Michigan basins in the United States [56]. However, their further development was overshadowed by the production of conventional fossil fuels. During the 1970's alternative hydraulic fracturing techniques were tested in the Barnett Shale Play, Texas and by 2000 about 726 vertical wells had been drilled. Horizontal drilling techniques, previously

developed for conventional reservoirs, were implemented along with multistage fracturing techniques. The first shale gas wells featuring this design appeared in 2003 in the Barnett Shale basin. The combination of these techniques has been an extraordinary innovation that allowed the development of new reserves thought previously to be either impossible or non-profitable for exploitation. The commercial success in the Barnett Shale Play together with high crude oil and natural gas prices, encouraged oil and gas companies to explore and develop other shale basins such as the Hayneville, Fayetteville, Woodford, Marcellus, among others. Drilling and fracturing techniques have been in continuing development with multilateral wells one of the latest advances. Certainly, during the last decade the production of shale gas has progressively altered the energy mix in the United States. In 2007, 7.67% of the total gross gas withdrawals occurred from shale gas wells. In the following three years, the share of shale gas increased substantially to 20.4% and by 2015 it reached 46.3%. This has influenced significantly the economy and energy security of the U.S [57,58]. For instance, gas imports have experienced a drop of 41.0% by 2015 after reaching a peak of 4.61 Tcf in 2007 [59]. Moreover, since 2000 natural gas exports have been steadily increasing registering an increase of almost 7-fold by 2015 [59].

The increase in supply has been reflected in lower prices, as can be seen when the price of shale gas in the U.S. is compared with the price of Henry Hub natural gas (see Figure 2.2a). The availability of cheaper natural gas is also transforming the U.S. power sector. For instance, the net electricity generation from natural gas plants have increased from 567.3 TWh in 2003 to 1,240.9 TWh in 2015 (an increase of more than two-fold or 673.6 TWh). By contrast, net electricity generation from coal power plants has decreased from 1,952.7 TWh to 1,343.9 TWh (a drop of about 31.2% or 608.8 TWh) in the same time period [60]. The U.S. shale gas revolution has also influenced the global chemical industry. For instance, in 2013 a total investment of $71.7 billion (bn) in 97 projects related to the petrochemical sector was announced spanning the period 2010-2020, with roughly half of the investments coming from foreign companies [61]. In 2015, the total number of projects increased to 226 with a corresponding investment of $138bn of which 61% is coming from companies based outside the U.S [62].

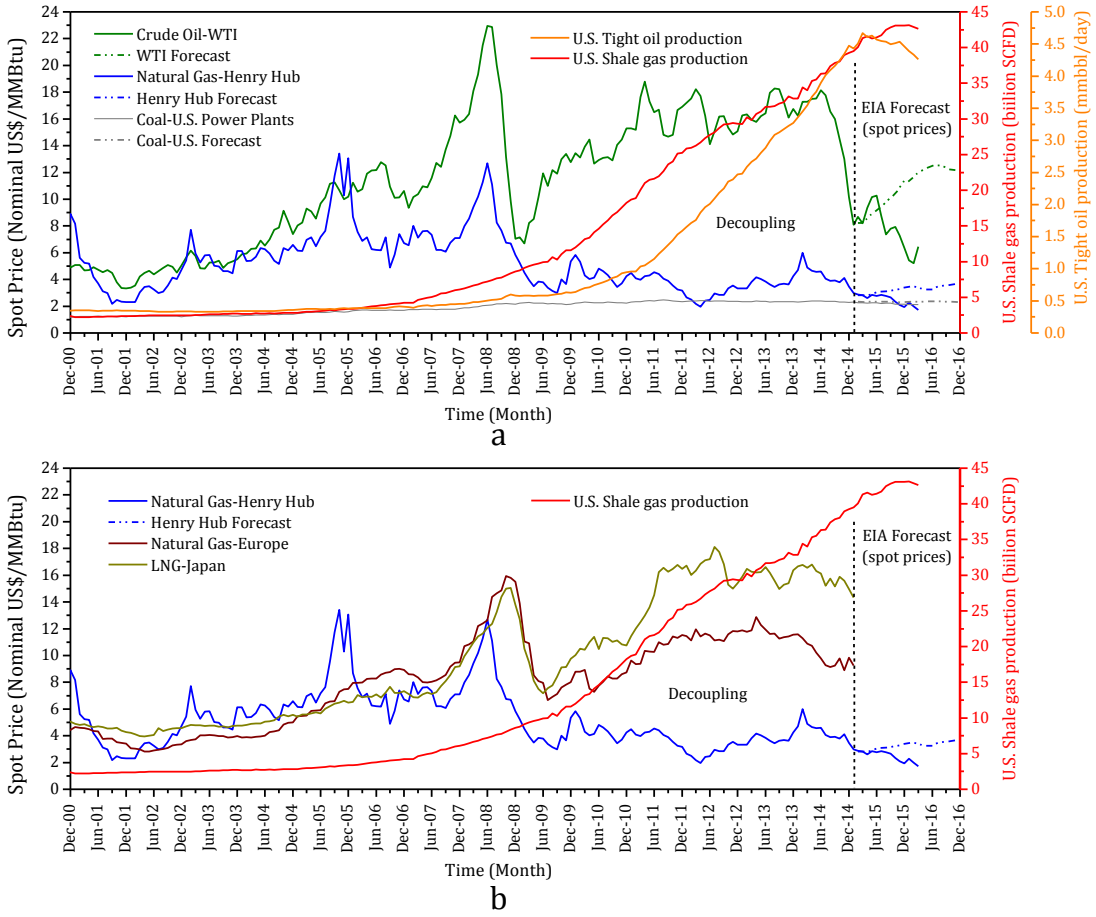

Figure 2.2. Effects of shale gas and oil production in global fossil fuel market: (a) U.S. unconventional fossil fuel production [63], prices forecast [64], and spot prices for coal [64], oil [65], and gas [66]. (b) U.S. shale gas production [63], prices forecast [64], and spot prices of natural gas in different markets [66,67].

Shale gas is not the only unconventional energy source that has caught the attention of oil and gas companies. Tight oil reserves are being developed in parallel with shale gas and these developments are displaying similar trends in the last decade. For example, in 2007, 8.4% of the total crude oil production in United States was associated with tight oil. Since then, the share of tight oil has increased reaching 48.2% in 2015.

The exploitation of unconventional resources (shale gas and tight oil) in the United States has brought about economic consequences not only at the national level but also at the global scale. For example, tight oil has played a major role in almost doubling the total crude oil production in the United States from 2007 to 2015 [68]. This scenario in combination with other factors such as aggressive policies of major oil producers for securing their global market share, resulted in a

surplus of oil production [64] that caused the abrupt reduction of 60.7% in the oil price over a time period of just two years (2014 and 2015). As a consequence, the production of tight oil, which in general entails higher production costs by comparison to conventional oil, was affected by the low prices causing a shift in the production rate since 2015 (see Figure 2.2a). Regarding the gas market, an interesting phenomenon has been occurring since 2008, in which the price of gas in the United States (tracked by the Henry Hub index), that historically has mirrored the behaviour of the oil price, has decoupled and it is no longer affected by the variability in the oil price. Moreover, the gas price variability is comparatively lower than in previous years. It is reasonable to point to the increasing production of shale gas during the last decade as the main cause of this situation. As a consequence, the production of shale gas has not been noticeably affected by low oil prices in the last years. Coal, an important traditional source of primary energy, has shown a stable behaviour along the last 15 years, and its price remains unaffected by the oil and gas market. In addition, a similar pattern can be noticed when the Henry Hub index is compared to the spot market price in Europe and the LNG price in Japan (see Figure 2.2b). These three markets have shown a strong historical correlation in terms of prices; nonetheless, since 2008 this correlation is no longer valid resulting in gas prices in the United States considerably lower than in Europe or Japan. Moreover, it is evident from Figure 2.2 that the oil and gas market is highly dynamic, which makes price forecasts highly uncertain. Certainly the United States provides an example of the potential of unconventional resources for impacting the energy mix of a country, especially for countries with abundant shale gas and shale oil reserves, such as China.

2.1.1.3 Greenhouse gas emissions: A shift from coal to gas

Besides the repercussions on commodity prices, energy security, and local and global economy, the development of shale gas resources entails potential environmental impacts that represent the major barrier for the global deployment of such energy source. The quantification of greenhouse gas emissions and carbon footprint of shale gas as a potential substitute of coal in electricity generation is subject of intense debate [46–48,69,70]. It is worthwhile to mention that there is not

a consensus in the research community regarding the life cycle greenhouse gas (GHG) emissions of shale gas. For instance, findings by Jiang et al. [69] suggest that shale gas use in electricity generation leads to higher GHG emissions than use of conventional gas, although by contrast, Burnham et al. [46] concluded the opposite. While these authors agreed on the potential emission reduction benefits of shale gas in the power sector by comparison to the use of coal, another study reports that the GHG emissions of shale gas surpasses the coal carbon footprint [47]. However, using a meta-analytical approach, a recent study suggested that emissions from electricity generation using shale gas are comparable to that from the use of natural gas, with both having considerably less emissions than those resulting from the use coal [71]. One of the major sources of uncertainty in the analysis of the life cycle greenhouse gas emissions of shale gas is the quantification of fugitive methane emissions. If they are proved to be an important fraction of the daily production of a gas field, they can severely affect the environmental benefits of shale gas over coal [72]. Accordingly, a number of methodologies have been proposed to shed light on this issue [73,74].

Despite the lack of consensus, and as explained previously in this work, the shift from coal to gas is materialising in the United States' power sector. Partially driven by this fuel switching, CO_2 emissions associated with electricity generation in the United States are decreasing in recent years. For example, CO_2 emissions faced a 16% drop from 2005 to 2012 in the United States' power sector [75]. However, abundant shale gas could decrease electricity generation from both coal and renewable energies in the power sector [76]. Therefore, the environmental benefits and impacts on climate change of abundant natural gas and the shift from coal to natural gas in the power sector are not clear yet [75–79]. It is noteworthy that even though energy transitions, e.g., from coal to gas, could occur fast (few years or decades) at a regional or national scale [80], global energy transitions take many decades to occur, i.e., from 50 to 60 years [2,81].

2.1.2 Local challenges

2.1.2.1 Regional water-energy nexus

The exploitation of shale gas imposes water resource risks, including the depletion, degradation, and contamination, of both underground and surface water sources (See Figure 2.3).

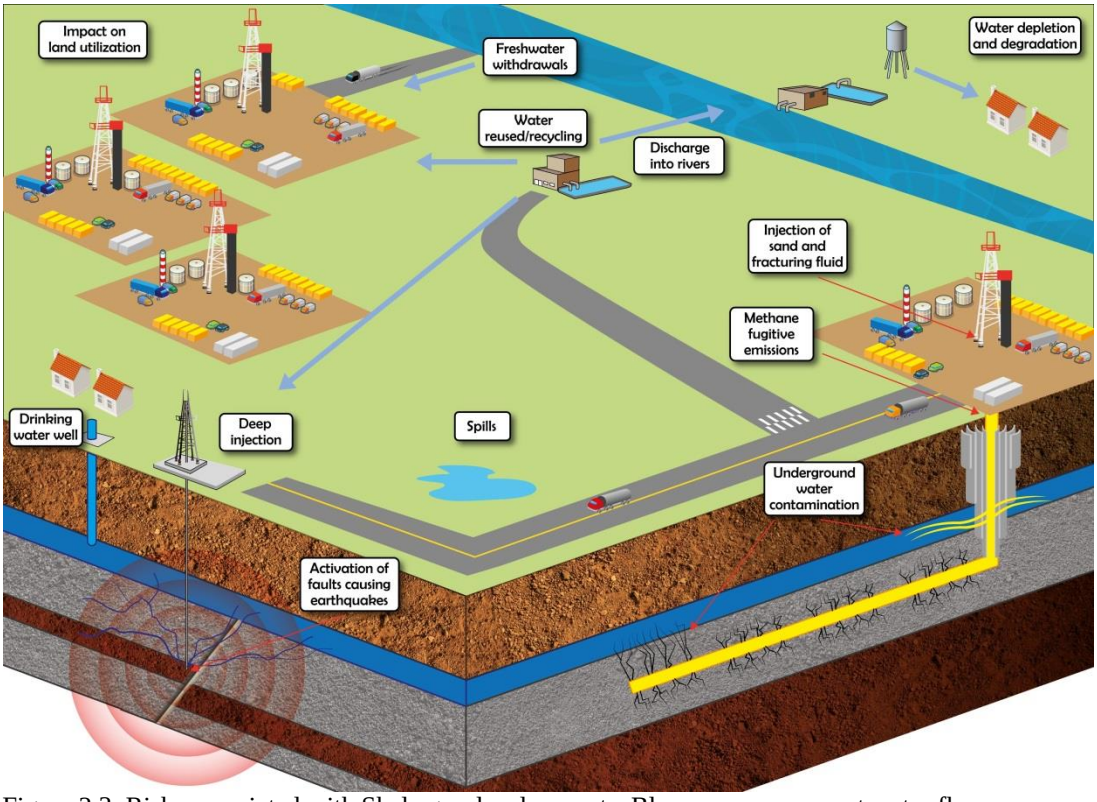

Figure 2.3. Risks associated with Shale gas developments. Blue arrows represent water flows.

First, fracking operations demand large amount of water and consequently water intensity for shale gas development is higher than that of conventional natural gas, e.g. water consumption for shale gas in U.S. plays ranges from 13-37 L/GJ (3.63-10.32 gallon/ million Btu) whereas for natural gas it varies from 9.3-9.6 L/GJ (2.59-2.68 gallon/ million Btu) [7]. However, the water intensity of shale gas is on the same order as other fossil energy sources, e.g. 8.3-27.0 L/GJ for coal [82,83]. Moreover, other issues have also been identified [9,84,85]. For instance, shallow aquifers and groundwater resources can be contaminated with fugitive hydrocarbons. Indeed, studies have associated high hydrocarbon concentrations in drinking water with shale gas production in U.S. plays [86,87]. Additionally, the inadequate management of wastewater can lead to the contamination of surface water as well as

shallow groundwater sources. Also, the accumulation of radioactive and toxic materials in hydraulic fracturing fluid spills or wastewater disposal sites could lead to the degradation of water sources. Furthermore, some studies have reported induced seismicity from hydraulic fracturing activities and injection of wastewater from shale gas operations into depleted formations. The latter represents a major risk since it could activate faults that can induce seismic events of considerable magnitude [88,89]. Consequently, water management has been recognised as one of the most important issues associated with the development of shale gas plays [90–92]. The water management encompasses fresh water procurement as well as flowback and produced water (wastewater) disposal or treatment for re-use, recycle, or discharge. Re-use generally involves treatment of the waste water to remove suspended solids (TSS) and occasionally reduce TDS concentration. The process is usually implemented on site and the treated water can be blended with freshwater for fracturing of new wells. Depending on the quality of water required for fracturing, the technologies for re-use include basic TSS removal, media filtration, membrane filtration, and ion exchange or nanofiltration to reduce TDS [93]. Recycle of water occurs when the TDS concentration of wastewater is high and therefore it is necessary the implementation of specialised technologies such as distillation and crystallisation in order to produce water within the technical specifications required for fracturing operations. Disposal of wastewater through injection in depleted wells is often preferred over recycle because of low associated costs. However, due to increasingly strict regulations, the injection into depleted wells is no always a feasible option and the aforementioned alternatives have to be implemented. The design and planning of an effective water management strategy is site dependent and is driven by, among other factors, availability of injection wells, disposal costs, treatment cost, local regulation, and blending compatibility in fracking operations.

2.1.2.2 Public perception

Shale gas development faces both positive and negative perceptions worldwide [94–97]. Job creation and growth of local economies are perceived as benefits associated with the deployment of shale gas, while impacts on water sources and increased traffic are perceived as risks [97]. In general, there are mixed levels of

awareness in United States and Canada [94,97], while greater awareness of potential environmental and social impacts than economic benefits is observed in UK [95]. Moreover, it was found that awareness varies spatially, i.e. national, regional, and local levels, and it tends to intensify in regions where shale gas has been developed [97]. Ethical issues and lack of transparency are issues that have been brought up. Moreover, it has been argued that the influence of communities on decisions related to shale gas development is minimal or non-existent, which derives in developments that lack social justice and procedural fairness [98]. Therefore, public perception represents a crucial aspect for the worldwide exploitation of shale gas resources, since social licenses to operate depend mostly on the community engagement.

2.1.2.3 Shale gas supply chains

The methods required for producing shale gas make the exploitation of these resources highly dependent, among other factors, on spot market prices and water resources. Therefore, flexibility, robustness, and efficiency are crucial elements that must be considered in the design, planning, and operation of the shale gas supply chain. This requires integration of the decisions regarding the exploration, production, transportation and processing of these unconventional resources with the corresponding water management decisions within a comprehensive decision-support framework. This section discusses the various elements that must be considered in the design and planning of shale gas supply chains which will be the basis of a series of case studies designed to investigate their interplay at local scales.

A thorough characterisation of the prospective shale basin is critical for a successful exploitation of these resources; this entails: (1) geochemical characterisation, which defines the potential of a formation to contain fossil fuels, (2) sedimentology characterisation, which describes the lithology of the different formations of the reservoir, (3) characterisation of the fracture network system in order to estimate the orientation of the natural fractures, and properties such as fracture aperture and fracture conductivity, (4) petrophysical characterisation, required to estimate properties of the formations such as absolute and relative permeability, porosity, net pay thickness and depth, pressure and temperature, (5) fluid characterisation in terms of the composition, viscosity, sweetness and

condensable hydrocarbons, and (6) geomechanical characterisation, necessary to study the state of stress of the reservoir, wellbore stability, and rock strength; crucial factors for successful drilling and fracturing operations [37,38]. The geological characterisation is the basis for assessing the productivity of a shale gas reservoir. This task could be carried out using specialised reservoir simulation tools [99] that allow the integration of geological information along with technical aspects regarding the design of horizontal wells to predict the impact on the production profile. In recent years, advances in horizontal drilling and fracturing techniques have made it possible to drill several horizontal wells in a well-pad configuration, reducing water trucking costs, drilling times and associated costs, and impacts on land utilisation. In a previous work [43], three key well-pad design parameters were identified to have the major impact on gas production: (1) number of wells, (2) horizontal length, and (3) spacing of fracture stages. These parameters, along with petrophysical properties of the reservoir, define not only the gas production profiles of a well-pad but also the water quantity necessary to drill and perform the hydraulic fracturing processes. In general, it can be said that under the same geological conditions, increasing the productivity of a well-pad requires higher water demand so that a wider area of the shale play can be stimulated.

The design of the gas supply chain involves the construction of the gas pipeline network, which involves selection of capacity of pipelines, and locations and capacities of compressor stations, for transporting raw gas from productive well-pads to processing facilities. Location and capacity of processing facilities must be also considered as important decision variables. The design of the water supply chain involves the procurement of fresh water sources, distribution of water for fracking operations, and the handling of flowback and produced water (wastewater). Water availability and water quality are two important aspects regarding the procurement of fresh water. Moreover, the distribution of water refers to selection and sizing of water transportation modes from water sources to well-pads and the allocation and capacity of water storage tanks. Wastewater, either the flowback water-fracturing fluid that returns to the surface during the first or second week after fracturing- or produced water -water from the formation that is produced at the surface, can be

treated for re-use (using primary treatment), recycling (using both primary and secondary treatment), or disposal (deep injection or environmental discharge). Important aspects in water management are the technical specifications regarding the composition of the fracturing fluids as well as quality regulations for environmental discharge, which are defined by the regional or national regulatory bodies.

The main economic aspects regarding the development of shale gas supply chains are capital expenditures, operational expenditures, royalties, and taxes. The development of shale gas resources is mostly dominated by capital expenditures, which at the early stages of a project, are mainly related to drilling and fracturing operations. This trend is shifted at later stages of a project in which investments related to infrastructure for treatment of gas and wastewater, and transportation of raw gas and final products are the main component [100]. Operational costs are a small fraction of the total costs, and can be surpassed by taxes and royalties which for some case studies have been reported to represent around 20% of the total costs [45]. Consequently, taxes and royalties are essential mechanisms for governments to implement policies that promote the development of shale gas resources, being Mexico, Canada, and China some of the many examples [101,102].

2.1.3 Challenges and opportunities

Despite the economic success of shale gas in the United States, the development of these resources is still facing important challenges that can potentially thwart their exploitation at a global scale. In light of the previous review, 6 main challenges can be identified that call for cooperation between governments, private sectors, and scientific community: (1) *Market conditions*: Since drilling campaigns are highly capital intensive and production lifespans are relatively short, shale gas development is critically dependent on favourable market conditions. The recently observed rapid response of developers to reduce exploration and drilling in the light of price drops illustrates this vividly. (2) *Water availability*: Access to fresh water sources is crucial for the exploitation of shale gas resources. However, many of the prospective areas are located in regions of high water scarcity. (3) *Contaminated water production*: A robust wastewater management strategy is essential to avoid contamination of surface or ground water sources and reduce freshwater withdrawals. (4)

Environmental impacts: The debate regarding shale gas as a "*greener*" replacement for coal is still unresolved. The scientific community is devoting great efforts in developing quantitative methodologies to shed light on this topic. (5) *Supply chain complexity*: Shale gas supply chains involve technical, operational, and strategic decisions that are highly interrelated which can make their design challenging. (6) *Poor public perception*: Concerns continue to be raised regarding the effects of fracking on environment and public health, largely independent of the specific context of the development in question. In some cases, strong public opposition has resulted in blanket moratoriums or bans of shale-related operations.

Some of these challenges can be tackled if a comprehensive approach is implemented in which the most critical decisions are addressed and evaluated in an integrated fashion. Accordingly, mathematical modelling and optimisation techniques have been implemented to develop a decision-support tool in order to simultaneously investigate aspects of challenges (1), (2), (3), and (5). In this study, challenges (2), (3), and (5) are systematically addressed through a novelty methodology for the analysis of the water-energy-economy of scales nexus in the development of shale gas resources. The methodology involves off-line integration of petrophysical properties of a reservoir and technical parameters of well-pad designs along with integrated optimisation of shale gas supply chain with water management.

2.2 Sustainable production of synthetic natural gas (BioSNG)

2.2.1 Government legislation

The UK has set targets regarding reduction of GHG emissions, which resulted in the Fourth Carbon Budget policy included in the Climate Change Act 2008. Targets for reducing 26% and 80% of GHG emissions (1990's baseline) are proposed for 2020 and 2050, respectively [103]. In terms of energy consumption, it is expected that 15% of the total demand in the UK will be supplied by renewable energy in 2020 [104]. Additionally, a target regarding energy savings was set to 17.9% for 2020 compared to the energy consumption in 2007, and projected to increase to 29.3% by 2030 [105]. As a result, the UK government has implemented mechanisms to promote the development of renewable energy projects.

- The Feed-in Tariff (FIT) scheme is a government funding program designed to support the development of a range of small-scale renewable and low-carbon electricity generation technologies. To be eligible for the FIT scheme, the total installed capacity of an installation must not exceed 5 MW. This limit is 2kW in the case of micro Combined Heat and Power (CHP). Eligible renewable and low carbon technologies are:•Solar Photovoltaic (PV), wind, hydro, anaerobic digestion and micro CHP [106].
- The Renewable Obligation Certificates (ROCs) have been designed to support the deployment of large-scale renewable electricity generating stations in the UK. Each supplier in the UK interconnected system must comply with a number of ROCs based on their annual energy generation. The ROCs are allocated to accredited operators for the electricity they generate from renewable sources. The ROCs can be traded among operators in spot markets. The scheme aims to increase the levels of supplied electricity coming from renewable resources. The obligation level is set annually by the UK and devolved governments [107].
- The Renewable Heat Incentive (RHI) is a government financial incentive designed to subsidy technologies for generation of renewable heat in order to reduce GHG emissions. The RHI is fundamental for the UK to meet its renewable energy target of 15% by 2020, as required by the European Union. Among the eligible technologies are: Solid biomass, heat pumps, geothermal, solar, biogas combustion (the biogas must come from anaerobic digestion, gasification or pyrolysis), CHP, and biomethane injection [108].

These initiatives are focused on increasing the contribution of alternative energies in the UK energy mix by encouraging private sectors to invest in low-carbon generation technologies.

2.2.2 Renewable energy challenges

Despite the increasing support from different sectors, penetration of renewable technologies in a market mostly dominated by fossil fuels can be highly expensive, considering that the current infrastructure is adequate mainly for conventional energy sources. While extensive research has been devoted to developing efficient and

scalable low-carbon technologies, their application is rarely regarded as profitable and their use is still limited. Some of the challenges include:

- The implementation of low-carbon conversion technologies requires high capital investments in comparison to conventional technologies, for example, the investment for power generation based on a gas open cycle was reported to be 650 €/kw in 2011, whereas for power from biomass the investment was 2500 €/kw [109].
- The production of first-generation biofuels can have negative impacts on agricultural markets given the competition for land and water resources, which can lead to increments in food and biofuels prices [110].
- Second-generation biofuels are an alternative to overcome the competition for land and food [111]. Nonetheless, most of the technologies for second-generation biofuels are still in developing stage. Commercial applications are scarce and their associated costs are estimated to be high in comparison to first-generation conversion technologies.
- Usually, the cultivation of conventional arable crops, such as wheat or corn, is a more profitable activity for farmers and landowners than growing energy crops such as SRC or miscanthus, which risks a continuous supply of feedstock to conversion facilities [112].
- Biomass resources are, in general, highly dispersed in a territory, which results in significant higher costs related to handling machinery, transportation capacity, and skilled labour. Additionally, the energy density of biomass resources is significantly low, e.g. 3.6 kWh/kg for miscanthus bales compared to 12.9 kWh/kg for liquefied petroleum gas (LPG). This is reflected in higher transportation and storage costs due to poor utilisation of the infrastructure capacity [112]. The implementation of pretreatment technologies is regarded as one way of decreasing transportation costs by preprocessing raw materials and producing higher energy density intermediate products that require of smaller infrastructure for their transportation [113–115] and further processing.

2.2.3 The role of BioSNG in the UK energy mix

During the last decade, the interest from the scientific community and private sectors in developing low-carbon technologies for sustainable energy generation has been steadily increasing, notably stimulated by the growing support from governments through funding research programmes and subsidisation policies. This has created a dynamic and collaborative environment for the different sectors to contribute in addressing challenges associated with sustainable energy development (Figure 2.4).

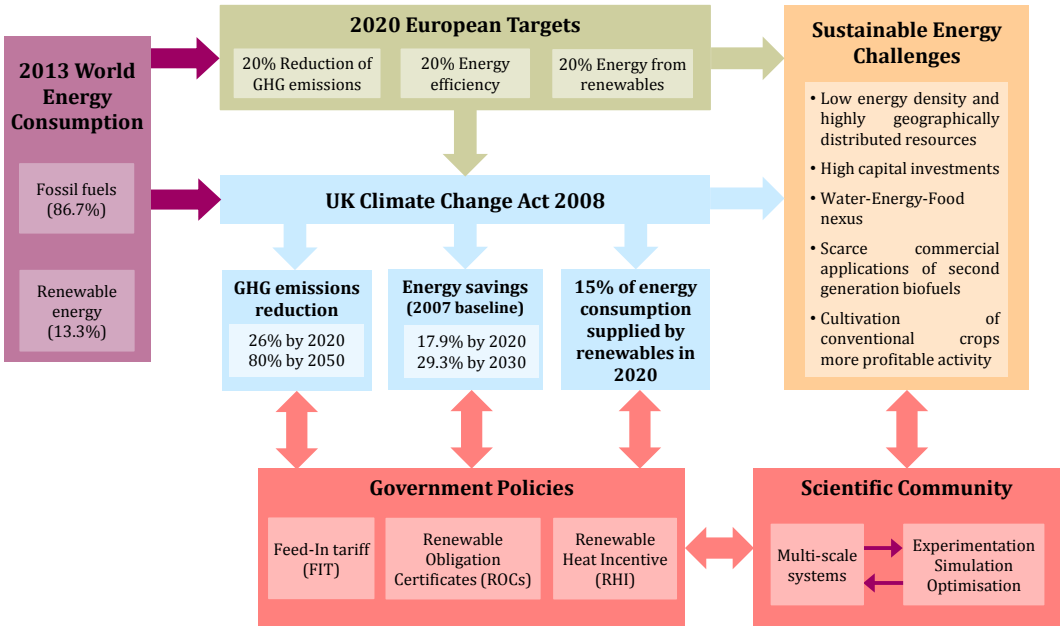

Figure 2.4. Global context

Renewable energy sources and biofuels are expected to become the dominant energy source for power generation and transportation sectors. These sectors have been traditionally driven by fossil fuels, which are regarded as the major contributors of GHG emissions. Nonetheless, the transition from a predominantly fossil-fuel based economy to a more diverse energy mix is challenging. Natural gas, being a cleaner substitute to coal in power generation applications, could play an important role in the transition from fossil to renewable fuels [21]. In the UK, natural gas is a key energy source with a reported share of 33.9% (77.9 bcm) of the total primary energy consumption in 2012 [116]. The UK gas infrastructure is well developed with a marked coverage across the country and capacity for gas imports by pipeline of

99.6 bcm/y and 51.4 bcm/y of LNG in 2010 [117]. Since 2004, when the UK became a net gas importer, the net gas imports by pipeline from Norway and Europe have steadily increased reaching a supply of 45% of the total gas consumption in 2014, putting at risk the energy security of England, Scotland, Wales, and Northern Ireland [118]. This scenario offers an excellent opportunity to investigate alternative processes for the production of natural gas from renewable resources in the UK. Among these, gasification of biomass or waste streams (e.g. wood waste, forestry residues, and residual waste) for the production of synthetic natural gas (BioSNG), which can be delivered using the current gas pipeline network [119], is an important alternative to be considered in order to reach the objectives set by the UK government and contribute to the national energy security. Accordingly, the installation of a 50-MWth demonstration facility has been proposed in Teesside in order to investigate technical uncertainties associated with BioSNG production such as injection of BioSNG into the national grid and feedstock procurement schemes, and to encourage investment from private sectors [29].

2.2.4 Technical aspects of BioSNG production

BioSNG is typically produced via an initial gasification step followed by gas conditioning (tar removals), BioSNG synthesis (methanation) and gas upgrading [120]. Gasification was initially developed for production of gas from coal in 1800's and its applications have been extended to production of methane and liquid fuels from coal [121,122]. Coal gasification has been successfully implemented at commercial scales in South Africa, China and United States [123]. However, the application of gasification as a renewable technology is a recent concept still in development stage. Currently, the Energy Research Centre of Netherlands (ECN), the Centre for Solar Energy and Hydrogen Research (ZSW) in Germany, and the Paul-Scherrer Institut (PSI) in Switzerland are leading the investigation of gasification for woody biomass [120]. van der Meijden et al. [25] and van der Drift et al. [124] identified the concept developed by ECN, based on allothermal gasification, as the preferred technology for the production of BioSNG with efficiencies ranging from 67 to 70%. The production cost for a 100 MWth input capacity plant in Netherlands was estimated between 7.8 €/GJ and 8.5 €/GJ in 2004

[22]. The authors also determined that pressurization of the indirect gasifier will further improve the efficiency of the process.

A gasification-based plant requires high initial investments which can affect negatively its economics. As the gasification step has been identified to have the highest exergy losses in the production of BioSNG [125], energy integration has been suggested in order to improve not only the economic performance but also the process sustainability [126]. Heyne et al. [23] reported global efficiencies between 90% and 96% for a BioSNG production process integrated with an existing biomass CHP steam power cycle. The authors concluded that the production of BioSNG is not affected by the different methods of integration. Likewise, Tremel et al. [24] reported global efficiencies of up to 90% when a fully integrated process is considered. Moreover, optimisation techniques have been implemented in single-site applications to address diverse energy integration strategies for the polygeneration of BioSNG, heat, and power from biomass [26–28]. The authors concluded that process integration and energy recovery enables an energetically and economically viable process.

The production of BioSNG can substantially benefit from a well-developed national gas pipeline network, traditionally used for transportation of conventional gas. However, the injection of BioSNG into a conventional gas pipeline network represents a major concern within the research and engineering community. Nonetheless, some authors have reported to be technically feasible to transport BioSNG through the conventional gas pipeline networks [127,128]. This has important repercussions on the development of BioSNG in a regional or national context as it facilitates the transportation of BioSNG from processing facilities to final customers and reduces considerably investments in transportation infrastructure. Regarding the development of BioSNG in a regional and/or national context, it has been suggested the installation of 12 BioSNG plants each with input capacity of 1000 MWth to supply 9% of the total primary energy consumption in Netherlands [129]. Furthermore, feedstocks such as stemwood, forestry residues, arboricultural arisings, sawmill coproducts, and clean wood waste were identified as suitable raw materials for BioSNG production in the short-term (before 2020)

whereas BioSNG production from straw, miscanthus, and municipal solid waste is considered to be attainable in the long-term (after 2020) [130].

2.2.5 Challenges and opportunities

The effects of global warming call for urgent actions for the decarbonisation of our energy systems. Renewable technologies can play a great part in this, although the transition is a challenging task. Based on the previous review, it is possible to identify 4 challenges and opportunities that are critical for a large-scale development not only of BioSNG supply chains but also analogous sustainable supply chains. (1) *Engagement of different sectors:* The efforts must aim to the generation of adequate scenarios where the development and implementation of renewable supply chains are economically attractive. This will only happen if governments create robust policy frameworks that stimulate the participation of private sectors and scientific community. (2) *Technologies still under development:* biomass gasification, which is the basis for BioSNG production, is still in development stage. Although significant advances have been achieved, this technology is yet to prove economic feasibility at commercial scales. Therefore, high initial capital investments are expected. (3) *Feedstocks supply:* A critical aspect in sustainable supply chains is to secure a stable source of raw materials for production of renewable fuels. The location of feedstocks, however, tends to be dispersed across a region or country which increments logistics complexity for their transportation and associated costs. Dependence on feedstocks such as waste streams and residues (forestry and agricultural) is risky since their availability can be high on a daily basis. This can affect the operation of the processing facilities. Cultivation of energy crops is an option to secure constant supply, however, this raises concerns regarding land competition and negative impacts on the food supply chain. Moreover, cultivation of crops for energy-related applications is a risky business for farmers. (4) *Supply chain complexity:* Numerous variables should be considered such as study of different schemes for reducing transportation costs, selection and location of technologies and capacities for new facilities, and evaluation of the most convenient strategy for production and supply, i.e., centralised vs distributed.

Accordingly, a mathematical framework for the strategic optimisation of BioSNG supply chains is presented. The proposed framework allows to address aspects of challenge (3), specifically waste streams and residues usage, transportation logistics, and energy crops cultivation, and challenge (4).

Chapter 3. Simulation of shale gas reservoirs[2]

One of the key elements in the design of shale gas supply chains has been identified to be the design of the well-pads (see section 2.1.2.3). However, the simultaneous optimisation of a shale gas supply chain and well-pad designs entails the implementation of highly non-linear models that depend not only on the design parameters of a well-pad but also on the characteristics of the shale reservoir. This would result in complex optimisation frameworks whose capabilities would be considerably limited to small-scale case studies. Accordingly, this chapter presents a methodology for the preliminary assessment of well-pad designs as an alternative to integrate this feature in an optimisation framework without increasing considerably the complexity of the optimisation model. The assessment is carried out by implementing reservoir simulations tools so as to address the productivity of a well-pad by considering the intrinsic properties of a reservoir along with the design parameters of the well-pad. Moreover, different performance metrics are proposed to evaluate not only the economics of developing a well-pad but also the environmental impact of its operation, including total gas production, and water consumption. In this chapter, 18 well-pad designs were initially proposed exploring 3 design parameters: number of wells per well-pad, horizontal length of each well, and spacing of fracture stages. The performance metrics were implemented in order to classify the 18 well-pad designs according to their economic and environmental benefits. From the results, two well-pad designs were selected such that one of the designs presents high economic benefits, labelled as "MaxNPV", and a second design presents high environmental benefits in terms of water consumption, labelled as "MinWI". Both well-pad designs are then utilised as input parameters in an

[2] This chapter is based on manuscript I of the list of publications presented at the end of this thesis

optimisation framework that addresses the optimisation of the entire supply chain which is outline in Chapter 4.

3.1 Literature review

The exploitation of shale gas resources has been possible due to advancements in horizontal drilling and the progress of hydraulic fracturing technology [9,44,78,84,131]. Despite the advances in drilling and stimulation techniques, the production of shale gas resources still is heavily constrained by production costs and productivity. Minor changes in these factors can make the difference between a resource that is economically and environmentally viable and one that is unattractive at current market conditions and regulations. For instance, the extraction of shale gas is more aggressive in terms of environmental impacts when compared to conventional gas. In particular, high water consumption and the potential for underground water contamination represent major concerns, which can and do hinder the development of shale gas plays [7,8,10,77,132]. A comprehensive summary of the different risk factors associated with shale gas development is presented by Logan et al. (2012) [133]. Four potential risk categories are identified, namely those associated with air, community, land, and water. It is worth mentioning that the majority of the risk factors are linked either to water management or to the design of the well-pad. Therefore, those two aspects must be taken into account when evaluating projects seeking to develop this unconventional energy source.

To reveal the possible trade-offs between the economics and environmental impacts of the development of shale gas resources, a methodology for the preliminary assessment of shale gas resources is introduced. The proposed methodology includes the ranking of different well-pad designs using various types of indices as metrics for the quantification of well-pad performance.

3.1.1 Shale Gas Reservoirs

3.1.1.1 Reservoir Characterisation

Shale gas reservoirs possess unique properties that set them apart from conventional reservoirs. As a consequence, efforts are needed to reflect the complex interactions between the fluids and the geological formation in which they are

contained. Although world reserves seem to be promising, in most cases the production from shale formations is particularly challenging since artificial stimulation processes are required to make these reservoirs economically attractive. The main characteristics of shale reservoirs are described in detail in the following sections.

3.1.1.2 Fluid Classification

The organic matter (kerogen) contained in shale formations is responsible for the generation of oil and gas. The formation of hydrocarbons is controlled by temperature and pressure which are determined by the burial conditions of the reservoir. These conditions define the thermal maturity of the rock. The vitrinite reflectance (%Ro) is a frequently used indicator of the thermal maturity and allows one to infer qualitatively the type of hydrocarbons trapped in the formation. The generation stages in shale deposits are shown in Table 3.1.

Table 3.1. Generation window in shale gas[a]

Ro%	Generation stage
< 0.6	Immature
0.6 – 1.0	Oil
1.0 – 1.3	Condensates
1.3 – 2.0	Wet gas
2.0 – 3.0	Dry gas
> 3.0	Over mature

[a] Data based on a report from the ANH-Colombia [134]

3.1.1.3 Storage Mechanisms

Shale gas is stored in the formation mainly as free gas, adsorbed gas and, in smaller proportion, as absorbed gas; which is often neglected. The free gas resides in the matrix porosity as well as in the natural fracture system[135]. The free gas content is almost linearly dependent to the pressure and can be modelled by an equation of state. In the present work, the Peng-Robinson (1976) equation will be used for this purpose[136].

The adsorbed gas is found mainly on the surface of the organic matter in the rock. The adsorption capacity of shale formations depends on properties such as surface area, temperature, reservoir pressure, shale composition, and sorption

affinity[137]. Many studies have demonstrated that the capacity of adsorption with pressure variation can be described with adequate precision by the Langmuir equation [138–140]. The general form of the Langmuir isotherm is presented in Equation (3.1).

$$V_E = \frac{V_L * b * P}{1 + b * P} \tag{3.1}$$

where V_L denotes the maximum storage capacity at infinite pressure, P refers to the reservoir pressure and b is the inverse of the pressure at which the stored volume, V_E, equals half of the maximum capacity. Nonetheless, in order to use the Langmuir equation as a measure of the actual adsorbed gas content, the reservoir must be assumed to be initially in equilibrium conditions. The extended version of the Langmuir equation can be used to model the desorption in multicomponent systems as shown in Equation (3.2) [141].

$$V_{E_i} = \frac{V_{L_i} * b_i * P * y_i}{1 + \sum_j b_j * P * y_i} \tag{3.2}$$

where the index i (and j) denotes the components in the mixture and y_i is the corresponding molar composition. Currently, the published data regarding the adsorption of mixtures or individual components on shale rocks is scarce.

3.1.1.4 Matrix Porosity and Permeability

Studies involving many different shale gas formations around the world have shown that the matrix porosity is associated with characteristics such as the organic content [142] the lithology as well as the level of diagenesis, which denotes chemical and mechanical processes that transform sediments into rock [143]. A higher porosity is desirable which results in better capacity for free gas storage. Some typical values for shale formations in United States indicate certain variability in this property. For example, the Lewis formation has an average porosity between 2% and 5%; the Barnett formation porosity ranges between 4% and 5%; Fayetteville can have values from 2% up to 8%; Marcellus has 10% of matrix porosity and New Albany has the highest porosity ranging from 10% to 14% [144].

Furthermore, the permeability of a formation is also an important parameter since it measures the capacity of the rock to transmit fluids. However, the extremely low permeability of shale rocks (on the order of 10^{-3} and 1000 nd [145]) makes it difficult to measure this characteristic parameter using conventional techniques. Digital Rock Physics (DRP) is a new approach that allows evaluation of the matrix permeability of tight formations, their pore sizes and connectivity [146]. Using this technique, samples from the Eagle Ford formation have been found to have a permeability ranging between 1 nd and 1000 nd while permeability values of up to 10000 nd have been measured for some shale formations in Colombia [147]. In addition, the existence of anisotropy has been demonstrated, as shown by measurements of different horizontal and vertical permeability.

3.1.1.5 Relative Permeability

Relative permeability is of great importance in describing adequately the multiphase fluid transport in a reservoir [148]. Usually, relative permeability curves are obtained by setting up an experiment that recreates the flow of a component (i.e. gas) through a porous medium (i.e. shale sample) in the presence of other fluids (i.e. water and/or oil). DRP also has application in estimating these properties, which otherwise, are challenging to measure with conventional techniques [147].

For the current study, only gas and water are considered to be in the reservoir. The corresponding relative permeability curves correspond to a sample from La Luna formation in Colombia whose values were determined by DRP [147]. For this sample, relative permeability of the gas, K_{rg}, ranges from 0.745 at the critical water saturation of 0.2, down to 0 when the water saturation is 0.636, which is equivalent to a gas critical saturation of 0.364. Similarly, the relative permeability of water, K_{rw}, ranges from 0 to 0.47 in the same range of water saturation. The corresponding relative permeability curves are shown in Figure 3.1.

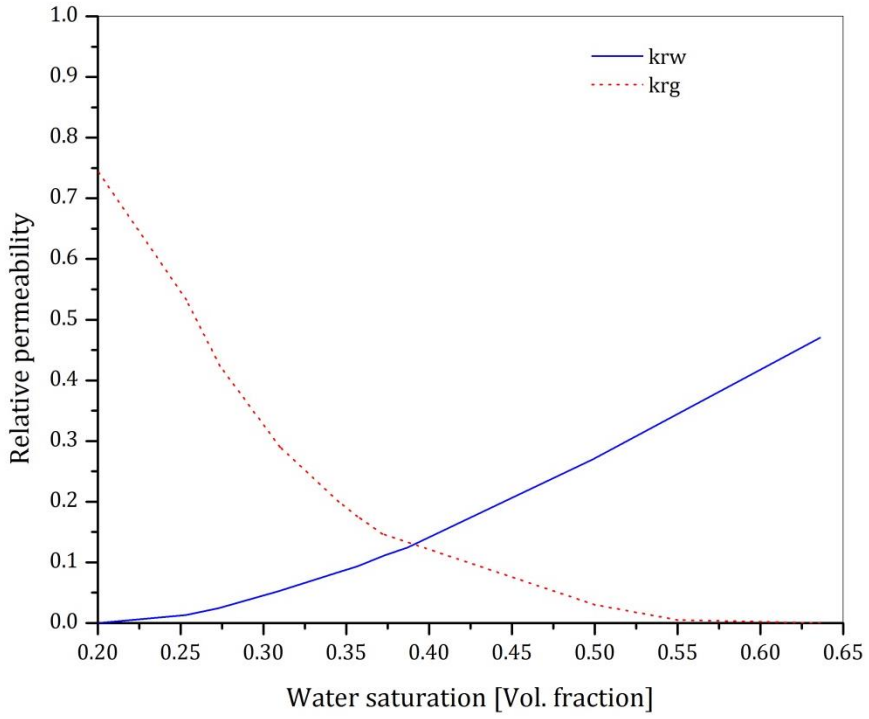

Figure 3.1. Relative permeability for the water-gas system.

3.1.1.6 Natural Fractures

The presence of natural fractures (joints) allows better connectivity between the matrix and the induced fractures (hydraulic fractures) which results in higher production. Natural fractures play an important role on fluid flow. For instance, open fractures can enhance fluid flow. Conversely, filled fractures can inhibit the fluid flow within the shale formation. The hydraulic fracturing process stimulates closed, or partially sealed natural fractures within the Stimulated Reservoir Volume (SRV) [41,149,150] which could facilitate the flow of gas from the porous media into the fracture network and then to the wellbore. A second important aspect to consider is the fracture spacing. This parameter measures the "density" of the natural fractures in the producing formation. Due to the heterogeneity of shale formations, it is difficult to arrive at an average value that represents the whole system properly, especially when there is a phenomenon called "fracture clustering" in which open fractures exist in clusters that are separated by hundreds of feet; this is a common occurrence in formations such as Barnett [151]. Consequently, different studies have focused on the measurement, modelling and characterisation of natural fractures in shale [152–155]. Statistical methods have been developed to describe the distribution

frequency of fracture properties in a layer by correlating experimental data to distributions such as power, lognormal, gamma, and exponential laws [156]. Optional methods to represent the geometry of the fracture network are based on fractal theory [157,158]. Although these methods could provide a better representation of the fractured system; in general, a simplified version of the fractured media must be assumed for simulation purposes in order to avoid highly computational demands. The critical parameter in these simplifications is the fracture spacing and the possible discrepancies due to simplification are assessed by carrying out sensitivity analysis. Some numerical studies measure the impact of this parameter by varying its magnitude with values between 40 ft and up to 300 ft [149,159].

3.1.1.7 Reservoir Pressure and Bottom Hole Pressure (BHP)

A reservoir can be classified into one of three types based on the pressure gradient. Normally pressured reservoirs correspond to a formation where the pressure is caused by a column of water; therefore the pore pressure is proportional to the hydrostatic gradient of 0.433 psi/ft. An underpressured reservoir occurs when the gradient pressure is less than the hydrostatic gradient. Finally, an overpressured reservoir presents moderately higher gradients, between 0.5 psi/ft and 0.75 psi/ft, or significant overpressured gradients, between 0.75 psi/ft and an upper limit determined by the fracture gradient or the overburden pressure, which is caused by the lithostatic column of the reservoir [160].

The Bottom Hole Pressure (BHP) defines the differential pressure between the reservoir and the wellhead. The BHP has an important impact on the production of the well, however its value depends largely on the reservoir characteristics (tendency to produce sand) and on safety conditions.

3.1.2 Production

3.1.2.1 Drilling

The production of shale gas requires both vertical and horizontal drilling. Vertical drilling, a commonly used technology in the conventional oil and gas industry, is used to reach the deep shale formation. Nonetheless, vertical wells can

intersect a limited amount of the shale reservoir, since shale formations are usually thin layers, less than 90 m (295.3 ft), extending over areas of thousands of acres [161]. Horizontal drilling is then needed in order to extend the vertical well horizontally to access a wider area of the formation, reducing the need for surface disturbance. Metal casing and cement are used to secure each section of the well. Although, drilling a horizontal well could cost between three or four times more than a vertical well, total drilling costs for intersecting the same area is much lower when horizontal wells are used. Drilling costs depend on a number of variables, including depth, well configuration and design, location, and formation type.

3.1.2.2 Stimulation

Due to the low permeability of shale formations, successful production is only achievable by means of stimulation techniques such as hydraulic fracturing. Therefore, after drilling the well, the cemented casing across the formation is perforated in order to stimulate the reservoir and start the production of shale gas. The design of the hydraulic fracture is a crucial step in achieving good performance of a well in terms of productivity. A proper design seeks to maximise the SRV by contacting as much as possible of the natural fractures with the wellbore. Local geological stresses are essential parameters to predict the hydraulic fracture growth in the formation. Commonly, the fracture stages are located perpendicular to the natural fracture network to intersect as many fractures as possible [162].

In reservoir simulation, a hydraulic fracture can be modelled as a complex geometry, commonly driven by microseismic data [149], or as a simple planar structure [159]. Usually, due to limitations in the information about the formation, preliminary assessments of the performance of a fracture are based on the planar structure approach. Five parameters are necessary to define the properties of a hydraulic fracture: width, permeability, half-length, height and fracture spacing. Figure 3.2 illustrates some of these parameters.

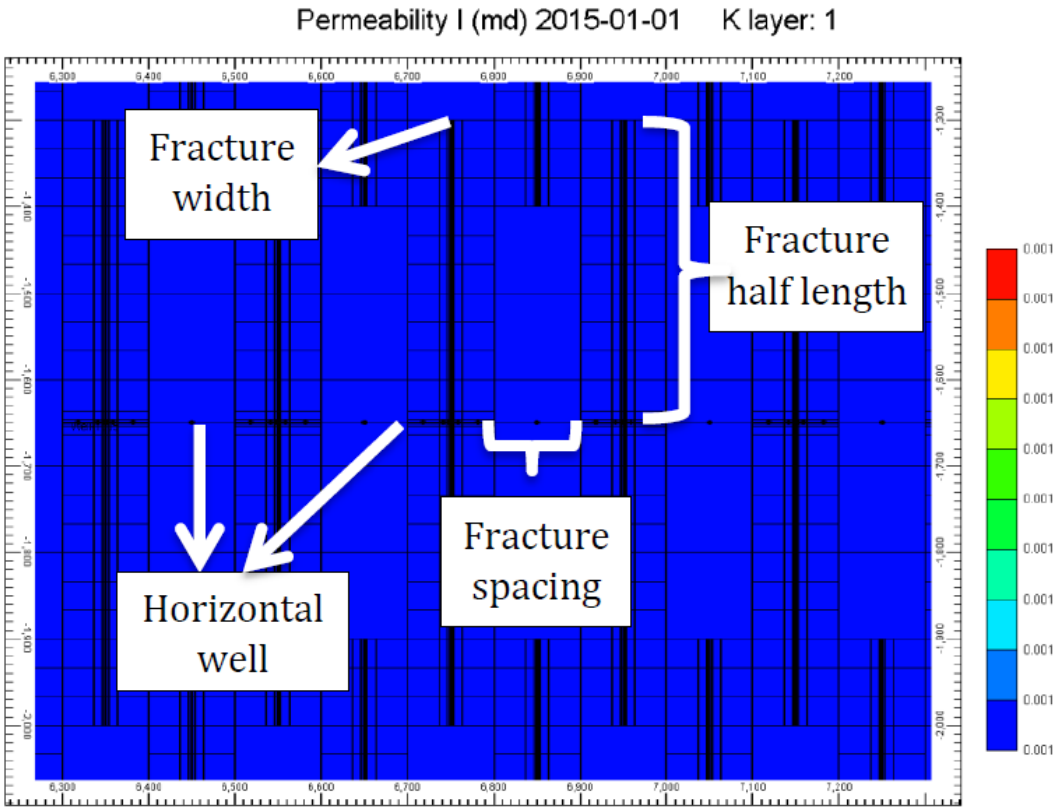

Figure 3.2. Hydraulic fracture components (x-axis ranges from 6,300 ft to 7,300 ft, and y-axis ranges from -2,000 ft to -1,300 ft).

3.2 Performance Metrics

In order to quantify the performance of a well-pad design from economic and environmental perspectives, different performance metrics are relevant and are presented next. The first metric is related to the efficiency of the investment, denoted as the Profitability Index $PI(d)$, where index d is used to denotes the design of a specific well-pad. Another valuable metric, particularly from an environmental point of view, is the Water Intensity $WI(d)$. The calculation of the above mentioned metrics are summarised in the following sections.

3.2.1 Economic model

3.2.1.1 Net Present Value

The Net Present Value (NPV), associated with the implementation of a specific well-pad design, is defined as the difference between the present value of the cash inflows $CashFlow(d,t)$ and the initial capital investment, $Capex(d)$, as stated

in Equation (3.3). The capital investment depends on the fracture dimensions and the total number of fractures completed at each well, as well as on the total number of wells drilled on the single well-pad. Scalar r represents the discount rate. Additionally, index t is used to denote number of time periods in years within the time horizon of interest.

$$NPV(d) = \sum_{t} \frac{CashFlow(d,t)}{(1+r)^{t-1}} - Capex(d) \quad \forall d \tag{3.3}$$

3.2.1.2 Cash Flow

The cash flow, for a specific design and during a given time period, is calculated from the cash balance expressed in Equation (3.4)

$$CashFlow(d,t) = Profit(d,t) + Dep * Capex(d) - Taxes(d,t) \quad \forall d,t \tag{3.4}$$

where $Profit(d,t)$ and $Taxes(d,t)$ denote the profit, and taxes fees respectively. Additionally, scalar Dep represents the depreciation rate.

3.2.1.3 Profit and Taxes

The profit refers to the surplus remaining once total cash outflows are deducted from the revenue. The profit is estimated as stated in Equation (3.5). Here, $Revenue(d,t)$, $Royalty(d,t)$, and $Opex(d,t)$ represent the revenue, the royalties, and the total operating expenditures, respectively.

$$\begin{aligned} Profit(d,t) = Revenue(d,t) - Royalty(d,t) - Opex(d,t) \\ -Dep * Capex(d) \quad \forall d,t \end{aligned} \tag{3.5}$$

Taxes are fees levied by governments on profit that is generated from business activities. Taxes paid are defined in Equation (3.6), the scalar tr represents the tax rate.

$$Taxes(d,t) = tr * Profit(d,t) \quad \forall d,t \tag{3.6}$$

3.2.1.4 Revenue

The amount of money received by the company from selling the shale gas to the market is defined as revenue, which is expressed as the product of product prices and total amount sold to the market. The revenue can be estimated from Equation (3.7); where $Price(k,t)$, $Com(k)$, and $Prod(d,t)$ are the unit price of gas products, the shale gas composition, and the total shale gas production during each period of time, respectively.

$$Revenue(d,t) = \sum_{k} Price(k,t) * Com(k) * Prod(d,t) \quad \forall d,t \tag{3.7}$$

3.2.1.5 Royalties

When a company wants to develop a natural resource, shale gas in this case, it has to pay compensation to the owner of the mineral rights, for instance, a person or government. This compensation is known as royalty, and is usually defined as a percentage of total production or an amount of money agreed in the contract between the company and the mineral rights owner. In this work, the royalties are defined as a percentage of the revenue, as expressed in Equation (3.8). The scalar *roy* represents the royalty rate.

$$Royalty(d,t) = roy * Revenue(d,t) \quad \forall d,t \tag{3.8}$$

3.2.1.6 Operating Expenditures

Wellhead shale gas is usually a mixture of different hydrocarbons, gases such as carbon dioxide and nitrogen, as well as flowback or produced water. In order to meet gas quality requirements, shale gas should be transported and processed. In addition, flowback and produced water may require physical and chemical treatment to meet regulations for discharge or water quality specifications for re-use and recycling. The total cost associated with these activities is defined as the operating expenditures, and is given by Equation (3.9). The scalar *WellOpex* represents the unit operating cost for gas, while scalar *TreatCost* denotes the unit cost for the

treatment of the flowback and produced water. Total water production (flowback and/or produced water) is denoted by parameter $Water(d,t)$.

$$Opex(d,t) = WellOpex * Prod(d,t) + TreatCost * Water(d,t) \quad \forall d,t \tag{3.9}$$

3.2.2 Profitability Index

The profitability index, which is a cost benefit relationship for a given well-pad, is defined as the ratio of the NPV to the capital investment, as expressed by Equation (3.10). The higher the profitability index is, the more economically attractive the proposed investment is. The variables $NPV(d)$ and $Capex(d)$ are estimated as described previously in Section 3.2.1.

$$PI(d) = \frac{NPV(d)}{Capex(d)} \quad \forall d \tag{3.10}$$

3.2.3 Water Intensity

Water intensity, defined as the ratio of water consumption $WatDem(d)$ to Estimated Ultimate Energy Recovery $EUER(d)$, is a measurement of water use efficiency. A lower value of water intensity means a higher efficiency in the use of water resources and consequently less environmental impact associated with water supply and management. Regarding water use, different studies have been reported on the life cycle of water consumption associated with the development of shale gas resources [7,163,164]. The life cycle includes not only water consumption for drilling and hydraulic fracturing operations but also flowback, produced, and disposed water. This study focuses principally on water consumption during the drilling and hydraulic fracturing operation. That is, given that the wastewater management is not addressed in this work, flowback and produced water, as well as water disposed are not included in the water balance. In addition, the $EUER(d)$ is estimated as the product of the energy density of the shale gas (MM Btu/MMSCF) and the estimated ultimate recovery $EUR(d)$. The water intensity associated with a specific well-pad design is determined as shown in Equation (3.11).

$$WI(d) = \frac{WatDem(d)}{EUER(d)} \quad \forall d \tag{3.11}$$

3.3 Reservoir Simulation

Reservoir simulation is a robust tool that allows to study the influence of formation properties along with well-pad designs on production profiles. In this section, a discussion regarding the state of art of available tools for reservoir simulation is presented. In particular, it is highlighted the extension of well-established methods developed primarily for conventional reservoirs and their application in more complex systems such as unconventional reservoirs.

3.3.1 Background

Reservoir simulation (RS) has long been used in the oil and gas industry to carry out preliminary studies supporting the development of a new oil and/or gas field. It holds the key to evaluation and understanding of shale plays by bringing laboratory and petrophysical measurements together, which can likely lead to improved evaluations and predictions [165]. In addition, RS is especially effective when historical production data is available and a better estimation of reserves and future production of an active field are required.

The first model for simulation applied in the Oil and Gas industry was based on the dual porosity method that featured single – phase flow in naturally fractured reservoirs [166]. In this modelling approach, the reservoir was assumed to consist of matrix and fracture networks which are connected by isotropic and homogeneous gridblocks [167]. In the following years, this model was improved significantly and acquired additional and advanced elements. Some of the models involved 2D radial systems [168] with transient fluid transfer between domains [169], multi-phase flow [170,171], and multiple interacting continua (MINC) model, which assumed that surfaces at equal distance from the fracture exhibit the same flow potential and 3D - three-phase flow [172,173]. The uniformity assumption in continuum models resulted in substantial divergence from reality due to the inadequate representation of fractures' physical properties [174,175]. This led to the introduction of Discrete Fracture Models (DFM) which used unstructured grids for describing the fracture

geometry and connections. The finite element method was then applied incorporating gravity and capillary phenomena [176–178].

With the recent focus on unconventional gas and, in particular, shale gas production, shale gas reservoir simulation has advanced considerably. Concepts, methods and models have been borrowed from conventional gas formation simulations to assist the characterisation of unconventional reservoirs and support their further development. Continuum approaches have now been extended to triple and quadruple porosity methods [159,179]. Additionally, since shale gas reservoirs require stimulation via hydraulic fracturing to create fracture networks for practical exploitation [180], methodologies and approaches have been reported for representing heterogeneous fracture networks and multi-scaled fractures [181,182]. The extensive developments in shale gas models and solution methods are classified and summarised in Table 3.2.

Table 3.2. Summary of Existing Shale Gas Reservoir Modelling and Simulation Methods shale

Shale gas reservoir simulation models	**Key authors**
Model types	
Continuum models	
Single porosity models	Blasingame, 2008 [183]; Li et al., 2011 [184]; Ding et al., 2014 [185]
Dual porosity models	Warren and Root, 1963 [166]; Kazemi, 1969 [168]; Du et al., 2010 [186]; Rubin, 2010 [187]; Li et al., 2011[184]; Ding et al., 2014 [185]; Sun et al., 2015 [188]
Triple porosity models	Huang et al., 2015 [179];
Quad porosity models	Patwardhan et al., 2014 [159]
Multiple interacting continua	Rubin, 2010 [187]; Wu et al., 2014 [182]; Farah et al., 2014 [180]; Ding et al., 2014 [185]
Discrete fracture models	Karimi-Fard et al. 2004 [178]; Noorishad and Mehran, 1982 [189]; Baca et al., 1984 [165]; Gong et al. 2011 [190]; Darishchev et al., 2013 [181]; Moinfar et al., 2013 [167]
Model features	
Flow phase	
Single – phase flow	Kazemi, 1969 [168]; Baca et al., 1984 [165]; Cipolla et al., 2010 [40]; Wu et al., 2014 [182]; Moridis and Freeman, 2014 [191]
Multi-phase flow	Kazemi et al., 1976 [170]; Rossen 1977 [171]; Thomas et al., 1983 [173]; Wu et al., 2014 [182]; Kam et al., 2014[167]; Sun et al., 2015 [188]
Number of wells	
Single - well model simulations	Bazan et al., 2010[192]; Rubin, 2010[187]; Chaudhri, 2012[193]; Cipolla et al., 2010[40]; Meyer et al., 2010[194]; Samandarli et al., 2011[195]
Full-field model simulations	Diaz de Souza et al., 2012 [196]; Altman et al., 2012 [197]; Kam et al., 2014 [198]; Esmaili and Mohaghegh, 2015 [199]
Model dimension	

2 – D models	Kazemi, 1969 [168]; Noorishad and Mehran, 1982 [189]; Baca et al., 1984 [165]; Rubin, 2010 [187];
3 – D models	Thomas et al., 1983 [173]; Mayerhofer et al., 2013 [41]; Gong et al., 2011 [190];
Well completion type	
Horizontally drilled	Sadrpanah et al., 2006 [200]; Zhang et al., 2009 [201]; Cipolla et al., 2010 [40]; Olorode, 2011 [202]; Guo et al., 2014 [203]; Esmaili and Mohaghegh, 2015 [199]
Vertically drilled	Rubin, 2010 [187]; Huang et al., 2015 [179]
Grid type	
Unstructured grids	Olorode, 2011 [202]; Gong et al., 2011 [190]; Wu et al., 2014 [182]; Moridis and Freeman, 2014 [191]
Structured grids	Moridis and Freeman, 2014 [191]
Fine grids	Balogun et al., 2007 [204]; Ramirez et al., 2009 [205]; Al-Kobaisi et al., 2009 [206]; Freeman et al., 2011 [207]
Decline Curve Analysis (DCA)	Boulis, 2009 [208]; Cheng et al., 2010 [209]; Mattar, 2008 [210]; Johnson et al., 2009 [211]
Rate Transient Analysis (RTA)	Bello 2010 [212]; Al-Ahmadi 2010 [213]; Anderson 2010 [214]; Nobakht and Clarkson, 2012 [215]; Ilk 2011 [216]; Anderson et al. 2013 [217]
Explicit Hydraulic Fracture (EHF)	Sadrpanah et al., 2006[200]; Moinfar et al., 2013[167]; Wu et al. 2014 [182]
Stimulated Reservoir Volume (SRV)	Mayerhofer et al., 2013 [41]; Cipolla et al., 2010 [40]; Guo et al., 2014 [203]; Yin et al, 2015 [218]; Lian et al., 2015 [219]
Model solution methods	
Analytical methods	Ikewun and Ahmadi, 2012 [220]; Can and Kabir, 2012 [221]; Can and Kabir, 2014 [222];
Numerical methods	Freeman et al., 2011 [207]; Darishchev et al., 2013 [181]; Wu et al., 2014 [182]; Ning et al. 2014 [223]; Sun et al. 2015 [188];
Data – driven	
Top-down Modelling	Mohaghegh et al., 2011 [224]; Mohaghegh, 2013 [225]; Esmaili and Mohaghegh, 2015 [199]

Despite the progress in reservoir simulation, there are numerous issues yet to be addressed to fully capture important aspects of shale gas systems. Some of these arise due to the multi-stage and multi-fracture nature of the reservoir, their low matrix permeability and small pore size. Currently, there are four methods that are used to model reservoirs displaying the aforementioned features. These methods are: Decline Curve Analysis (DCA), Rate Transient Analysis (RTA), Explicit Hydraulic Fracture (EHF), and (SRV). The DCA and RTA methods allow the user to easily set up case studies since they require relatively limited amounts of input data. Nevertheless, on the downside, the former method lacks sensitivity to physical phenomena and does not approach optimality, whereas the latter fails to generate adequate production forecasts [225].

The Explicit Hydraulic Fracture (EHF) model, which can be analytical, numerical or data-driven, is the most robust method but it comes at the expense of complexities which translate into higher computational times. Alternatively, the SRV model is a much simpler and computationally less demanding way of handling multi-cluster, multi-stage hydraulic fractures. Within a SRV, gas flows from the matrix to the complex fracture network and then to the well for production. Low permeabilities lead to highly complex interactions among the fluids present in the formation [182]. As a result, processes that can usually be ignored in high-permeability reservoirs (i.e. conventional reservoirs), such as non-Darcy flow and Klinkenberg effect, become important in low permeability systems. In shale gas reservoirs, the deviations from Darcy's law could be manifested not only at high velocities but also at low velocities. Forchheimer extended Darcy's Law by adding a quadratic velocity term, to account for some of the observed discrepancies [226]. When a formation exhibits values of permeability lower than $1x10^{-4}$ md [159], the gas permeability deviates significantly from the initial value as the conditions in the reservoir vary. Wang et al. [227] showed that the permeability of a sample from Marcellus shale changes from $1.96x10^{-2}$ md at 1000 psi to $54x10^{-2}$ md at 80 psi. This phenomenon is known as gas slippage flow and it is believed that it affects the gas production by giving misleading lower gas rates at low-pressure zones. This was described by Klinkenberg [228] who proposed an equation to correct the deviations

of the gas permeability as a function of the current pressure as shown in Equation (3.12).

$$K_g = K_\infty \left(1 + \frac{\beta}{P}\right) \tag{3.12}$$

where K_g is the apparent gas permeability, K_∞ is the intrinsic permeability, β is the slippage factor and P is the pressure. The modelling of stimulated shale gas formations by the SRV approach is based on a 3D volume around a wellbore with enhanced permeability. The SRV representation has the ability to match real production behaviour with time. As long as rigorous data is used, SRV is the preferred approach to providing a general understanding of a shale gas reservoir. Consequently, it was the selected method in the current work [225].

The major application of reservoir simulation is to generate different scenarios of shale gas and water production based on the petrophysical (e.g. porosity, permeability, water saturation) and geomechanical (e.g. total minimum horizontal stress, Young's modulus, shear ratio) properties of the fossil-fuel-bearing formation. The geomechanical properties, however, are beyond the scope of this work. With some simplifications, described by Wu et al. 2014 [182], the isothermal shale gas-water system subject to multiphase flow and adsorption can be adequately described by the mass balance expressed by Equation (3.13), for $f = \{g \ \textit{for gas}, w \ \textit{for water}\}$.

$$\frac{\partial}{\partial t}\left(\emptyset * S_f * \rho_f + m_f\right) = -\nabla.\left(\rho_f * v_f\right) + q_f \quad \forall f \tag{3.13}$$

where ϕ denotes the effective porosity of the shale formation and terms S_f and ρ_f represent the saturation and the density of fluid f, respectively. Similarly, m_f and ν_f denote the adsorption or desorption mass term and the volumetric velocity vector of fluid f, respectively. Additionally, q_f represents the sink/source term of phase f per unit volume of shale formation. The adsorption or desorption mass term m_f can be expressed as function of the gas content V_E given by the Langmuir adsorption isotherm, as stated in Equation (3.14).

$$m_f = \rho_R * \rho_f * V_E \quad \forall f \tag{3.14}$$

where ρ_R denotes the rock bulk density. The mass balances expressed in Equation (3.13), coupled with Darcy's law or any of its respective variants for non-Darcy flow, can be solved numerically via discretisation in space with a control volume or using finite-differences. In the following sections, the key petrophysical properties are described. The specific parameter values which will be used in the simulation case studies are summarised in Table 3.3. These values correspond to averages of the properties of a reservoir located in the Middle Magdalena Valley Basin in Colombia.

Table 3.3. Key parameters or variables for the assessment of shale gas reservoir.

Parameter	Value	Unit
Formation depth, D	9000	ft
Net pay, h	150	ft
Rock density, ρ_r	156	lb/ft^3
Rock compressibility, C_r	1x10^{-5}	psi^{-1}
Pore pressure gradient, ΔP	0.72	psi/ft
Initial pressure, P	6480	psi
Bottom Hole Pressure (BHP), P_w	3240	psi
Reservoir temperature, T	200	°F
Water saturation, S_w	30	%
Gas saturation, S_g	70	%
Matrix Porosity, ϕ_m	8	%
Matrix Permeability, $K_{m,i}$, $K_{m,\mathrm{j}}$, $K_{m,\mathrm{k}}$	(5x10^{-4}, 5x10^{-4}, 5x10^{-5})	md
Fracture Porosity, ϕ_f	4.10x10^{-3}	%
Fracture Permeability, $K_{\mathrm{f},i}$, $K_{\mathrm{f,j}}$, $K_{\mathrm{f,k}}$	6x10^{-5}	md
SRV fracture permeability, $K_{f,i}^{SRV}$, $K_{f,\mathrm{j}}^{SRV}$	2 x10^{-3}	md
Hydraulic fracture width, W_f	8 x10^{-3}	ft
Hydraulic fracture permeability, K_f^{hy}	6000	md
Fracture conductivity, F_c	48	md-ft
Hydraulic fracture half length, X_f	350	ft
Fracture spacing, F_s	100, 200	ft
Hydraulic radius, r_w	0.25	ft

3.3.2 Case Study: Input Data

In order to model the reservoir, a SRV-based strategy has been implemented. The simulation strategy includes a dual-porosity model that takes into account the

following interactions: matrix-natural fracture, natural fracture-hydraulic fracture, hydraulic fracture-well and matrix-well. In addition, a local refined and logarithmically spaced grid was implemented to be able to track the pressure changes between the matrix and the fractures, and allow better modelling of the stimulated zone. This approach is denoted as the "DP-LS-LGR method" (i.e. dual-porosity, logarithmically spaced, local grid refinements).

The reservoir is modelled as a rectangular block whose dimensions, length and width, are variables and depend on the number of wells considered for the production scheme. Only one uniform layer is used to represent the geological formation with a net pay of 150 ft and a top depth of 9000 ft. The reservoir is discretised with blocks of 100 ft x 100 ft x 150 ft for length, width and thickness, respectively. The density of the formation is set at 156 lb/ft^3 and the rock compressibility is $1x10^{-5}$ psi^{-1}.

For the numerical simulations, it is assumed that the reservoir is in the wet gas generation window (1.3 <Ro%<2). In total, 9 components were included to make up the "raw gas" in- situ. The Langmuir parameters are taken from Freeman [141]. The corresponding data is presented in Table 3.4.

Table 3.4. Gas concentration and Langmuir parameters [141]

Component	Molar fraction
Methane	0.75
Ethane	0.08
Propane	0.05
Isobutane	0.03
n-Butane	0.02
Isopentane	0.02
n-Pentane	0.02
Carbon Dioxide	0.02
Nitrogen	0.01

Component	bi [1/psi]	VL [scf/Ton]
Methane	$1.37x10^{-2}$	69
Ethane	$1.51x10^{-4}$	7612
Propane	$4.26x10^{-5}$	1614
Butane	$2.57x10^{-5}$	2875
Pentane	$1.05x10^{-5}$	1506
Carbon Dioxide	$1.55x10^{-3}$	80

As stated by the author, these data do not correspond to actual tests and the parameters were proposed merely to represent the correct functional behaviour. As there is not enough information available, adsorption for Nitrogen was not considered and the Langmuir parameters for butane and pentane were also used for

isopentane and isobutene, respectively. The effect of including the adsorption mechanism in numerical simulations is reflected during the later stages of gas production and contributes to increasing the EUR. Some authors have reported increments of the EUR ranging from 5% to 17% after 30 years of production [229]. The fact that desorption for nitrogen is not considered might lead to underestimation of the EUR; however, based on the low composition of the nitrogen, usually less than 1%, and when used in investigating shorter production periods (10 years), it seems reasonable to assume that the EUR will not be significantly affected. Additionally, the nitrogen is not considered a valuable component in the evaluation of the economics of a well-pad. The corresponding adsorption curves are shown in Figure 3.3.

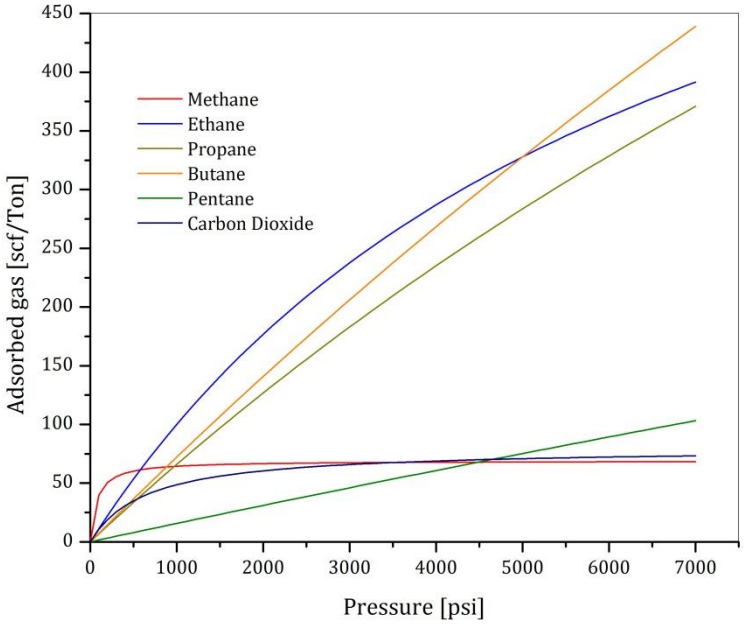

Figure 3.3. Langmuir isotherms.

Based on the values previously discussed, the matrix porosity for the simulated reservoir was set at 8% and the horizontal matrix permeability was set to $5x10^{-4}$ md; additionally, the effect of anisotropy was taken into account by setting the vertical permeability to be 10% of the horizontal permeability [159,188]. The water saturation, S_w, in the matrix and natural fracture system was assumed to be 30% [159,230]. Since the critical water saturation is 20%, associated water will be produced along with the shale gas. The corresponding costs of the water treatment are included in the economic model.

The fracture stages were simulated using a planar structure approach. The width of the fracture is $8x10^{-3}$ ft, and the permeability was assumed to be 6000 md. The resulting fracture conductivity; which is defined as the product of the fracture width and the fracture permeability, is 48 md-ft, which falls in the range of a fracture developed using a multi-layer propping technique. The half-length, which is the lateral distance between the tip of the fracture and the well, was fixed at 350 ft. Some authors assumed that the fracture height would cover the net pay of the studied formation. Works by Mayerhofer et al., 2013 [41] and Cipolla et al., 2013 [40] made this assumption for a net pay of 300 ft. Consequently, it is reasonable to assume the fracture height to be 150 ft. Two values for fracture spacing, 100 ft and 200 ft, were selected to study their impact on well performance. Finally, it was assumed that these properties hold for every fracture along the horizontal well. In order to reduce computational time, the fracture was discretised in 7x7x1 cells for the i, j, and k directions, respectively as shown in Figure 3.4.

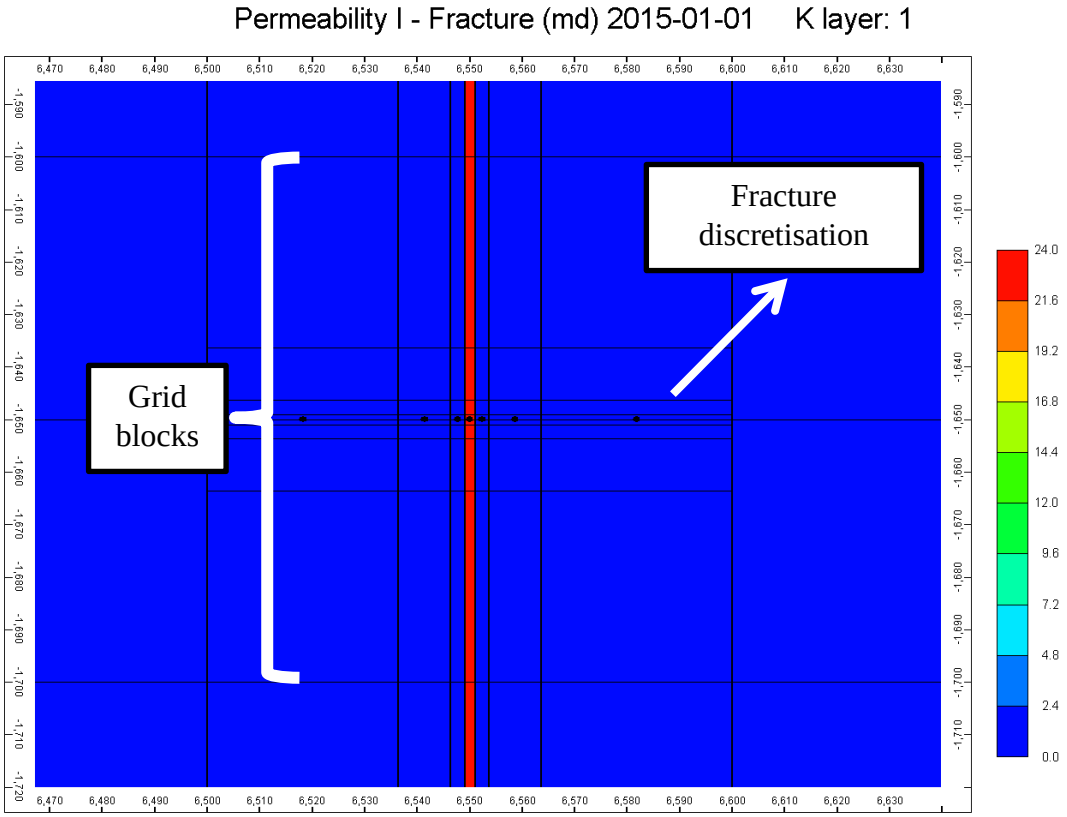

Figure 3.4. Hydraulic fracture discretisation (x-axis ranges from 6,470 ft to 6,630 ft, and y-axis ranges from -1,710 ft to -1,590 ft).

The effect of an enhanced natural fracture network, induced by fracturing the rock, is taken into account by modifying the permeability for natural fractures located in the stimulated region delimited by the hydraulic fractures. Additionally, the natural fractures are assumed to be unpropped. Consequently, the permeability and the porosity fraction are set at $6x10^{-5}$ md and $4.1x10^{-5}$ md respectively, for the entire reservoir, which would correspond to a very low connectivity with the hydraulic fractures. However, this value is updated in the fracture zone to take into account the induced connectivity of the natural fractures within the SRV by increasing the fracture permeability to $2x10^{-3}$ md. Furthermore, the natural fractures are considered to be located parallel and perpendicular to the hydraulic fractures and spaced 100 ft from each other, a value which is an acceptable average based on the literature presented previously. Finally, a moderate overpressured gradient of 0.72 psi/ft was chosen for the reservoir, corresponding to a reservoir pressure of 6480 psi. The pressure was assumed to be constant across the reservoir. For this study, the pressure drawdown was assumed to be 50% of the initial pressure of the reservoir. Therefore, the BHP was fixed a constant value of 3240 psi.

3.3.3 Case Study: Well-pad Designs

The development of shale gas plays started with the drilling of vertical wells with only one fracture stage. Due to advances in horizontal drilling and multi-fracture techniques, the trend of drilling several wells in a small area (well-pad) is becoming prevalent. A well-pad presents many advantages with respect to single wells, e.g. lower water trucking for fracturing, lower unitary drilling costs, less impact on the surface, etc. Consequently, our study is focused on the performance of several wells operating in a well-pad configuration. For this purpose, three main design parameters were identified and are the basis for the well-pad configurations [231]. These parameters are the number of wells per well-pad, the lateral length of a well and the fracture spacing. Three levels were chosen for the number of wells (6, 10 and 14), similarly three levels for the lateral length (5000 ft, 7000 ft and 9000 ft), finally two levels for the fracture spacing were included (100 ft and 200 ft). The combination of these three variables results in 18 different well-pad designs, listed in Table 3.5.

Table 3.5. Well-pad design candidates

Number of wells	Lateral length [ft]	Fracture spacing [ft]	Nomenclature	Running time [min]
6	5000	100	6w_5000L_100s	83.0
6	5000	200	6w_5000L_200s	49.5
10	5000	100	10w_5000L_100s	138.7
10	5000	200	10w_5000L_200s	74.0
14	5000	100	14w_5000L_100s	191.0
14	5000	200	14w_5000L_200s	107.7
6	7000	100	6w_7000L_100s	120.1
6	7000	200	6w_7000L_200s	63.3
10	7000	100	10w_7000L_100s	205.6
10	7000	200	10w_7000L_200s	105.6
14	7000	100	14w_7000L_100s	274.1
14	7000	200	14w_7000L_200s	154.6
6	9000	100	6w_9000L_100s	143.8
6	9000	200	6w_9000L_200s	76.7
10	9000	100	10w_9000L_100s	240.1
10	9000	200	10w_9000L_200s	131.6
14	9000	100	14w_9000L_100s	336.7
14	9000	200	14w_9000L_200s	189.0

Every design was set up in CMG Builder and solved with GEM Suite, a commercial simulator for shale gas reservoirs [99]. The CPU time for numerical simulations was between 0.8 and 5.6 hours per simulation, as shown in Table 3.5. All runs were performed using an Intel i-7 @ 2.40 GHz processor with 8 GB RAM, running 64-bit Windows 8.1. Figure 3.5 corresponds to the configuration for a well-pad composed of 6 horizontal wells, with a lateral length of 5000 ft and fractures every 200 ft. The upper graph shows the entire shale gas reservoir. The dense grid on the surface represents the fractures stages completed in every well. The lower graph shows the fracture stages in more detail.

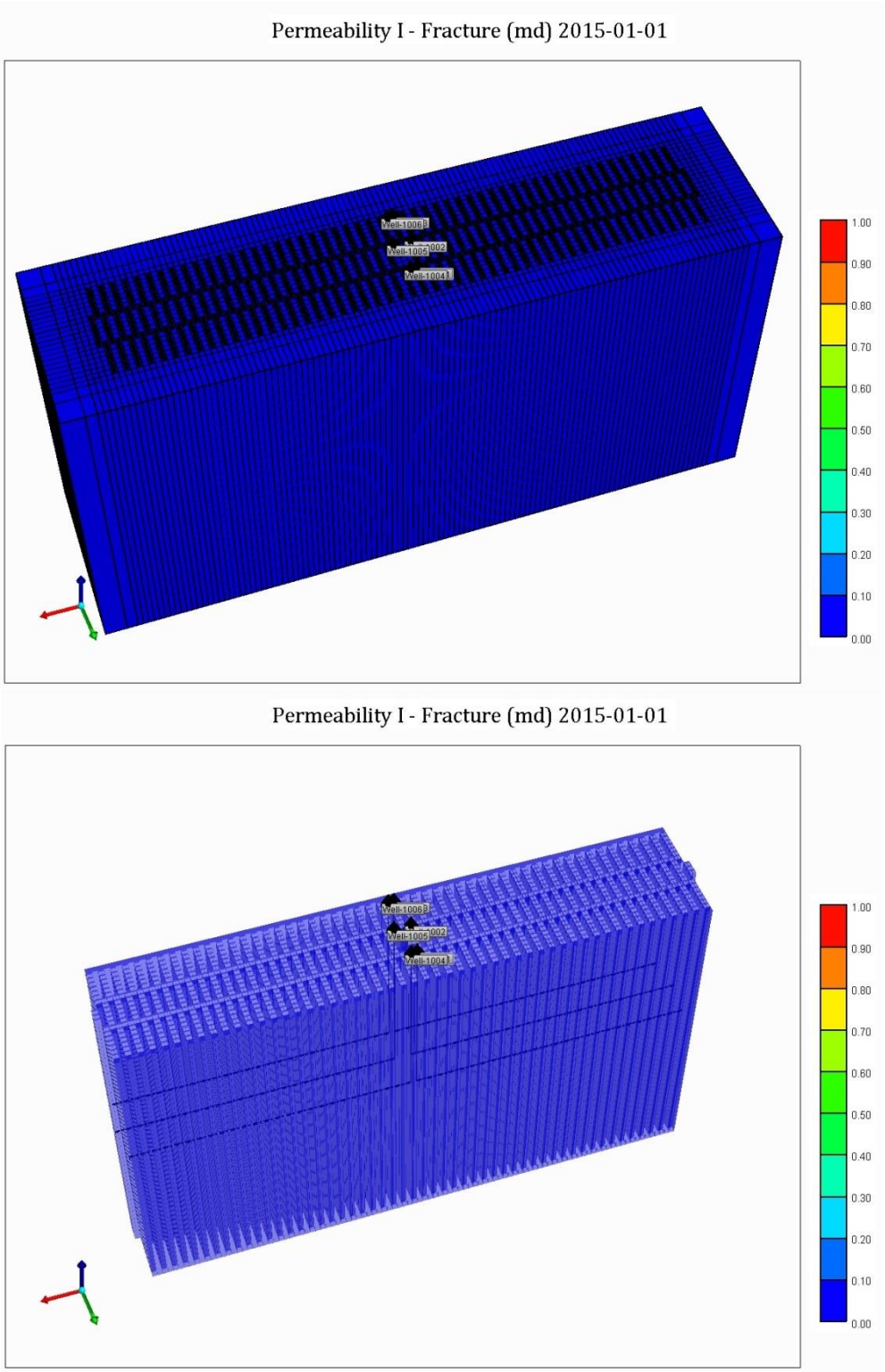

Figure 3.5. Design setup in CMG for 6w_5000L_100s (upper figure showcases the fracturing stages along 6 horizontal wells. Lower figure shows the horizontal wells across the reservoir).

3.4 Results and Discussion

Reservoir simulation was used to study the performance of a well-pad by considering typical petrophysical properties of a shale formation subject to different designs. This approach allows us to quantify the gas and water production rate, the estimated ultimate recovery (EUR) and the recovery factor. An example of some of the results that can be obtained is shown in Figure 3.6, where the evolution of the pressure profiles for the design composed by 6 wells with 5000 ft of lateral length and a total of 25 fractures is presented.

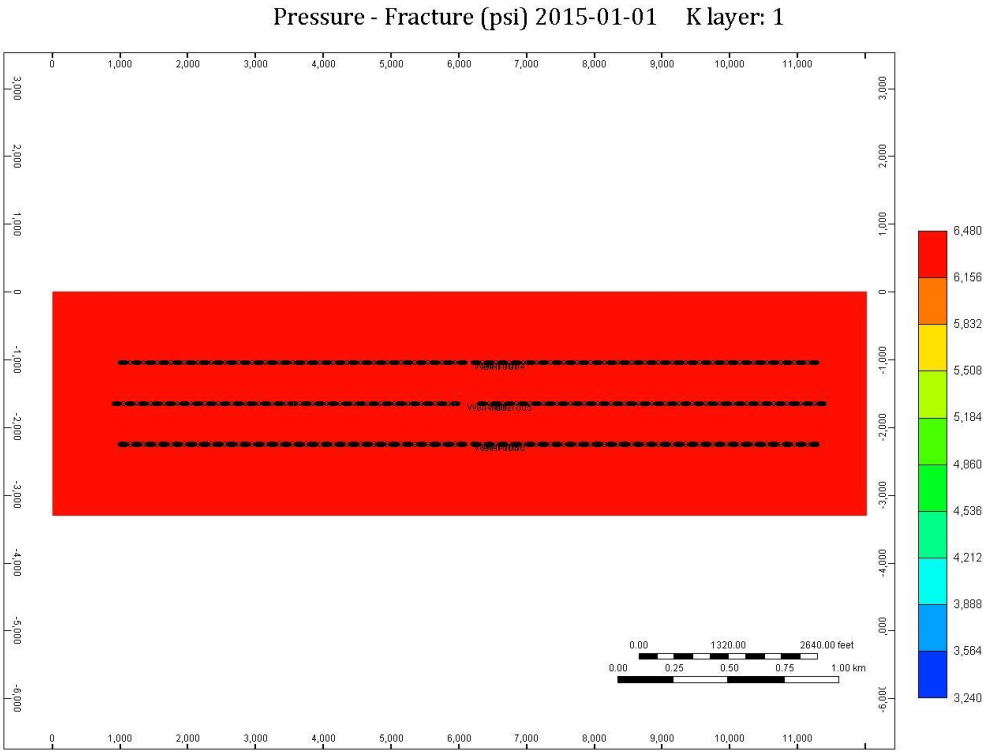

Pressure - Fracture (psi) 2017-12-01 K layer: 1

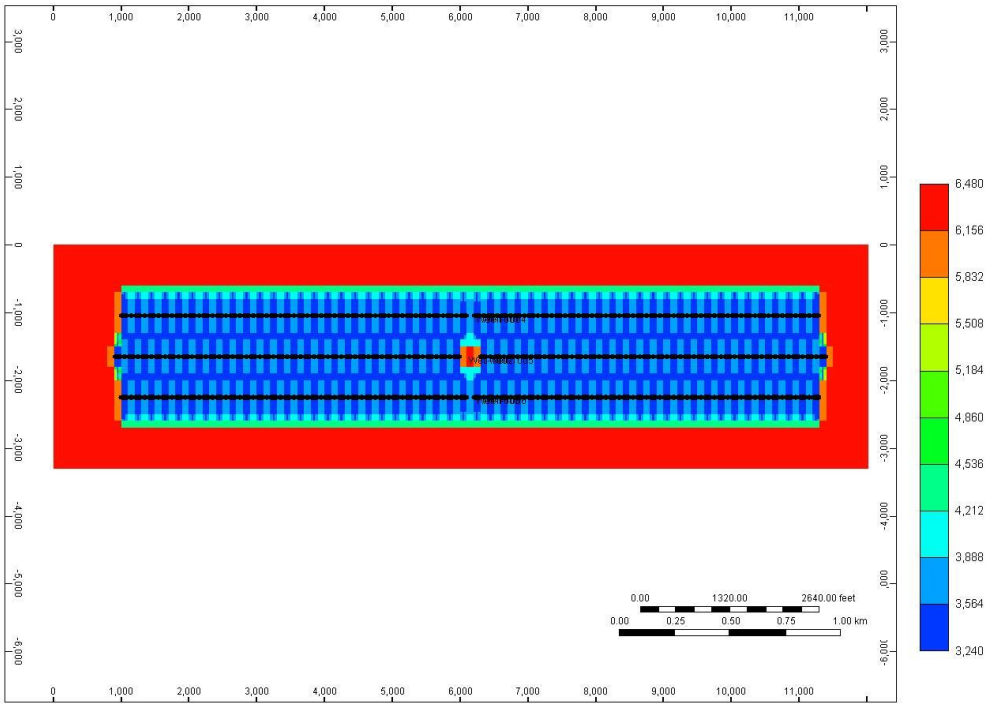

Pressure - Fracture (psi) 2015-12-01 K layer: 1

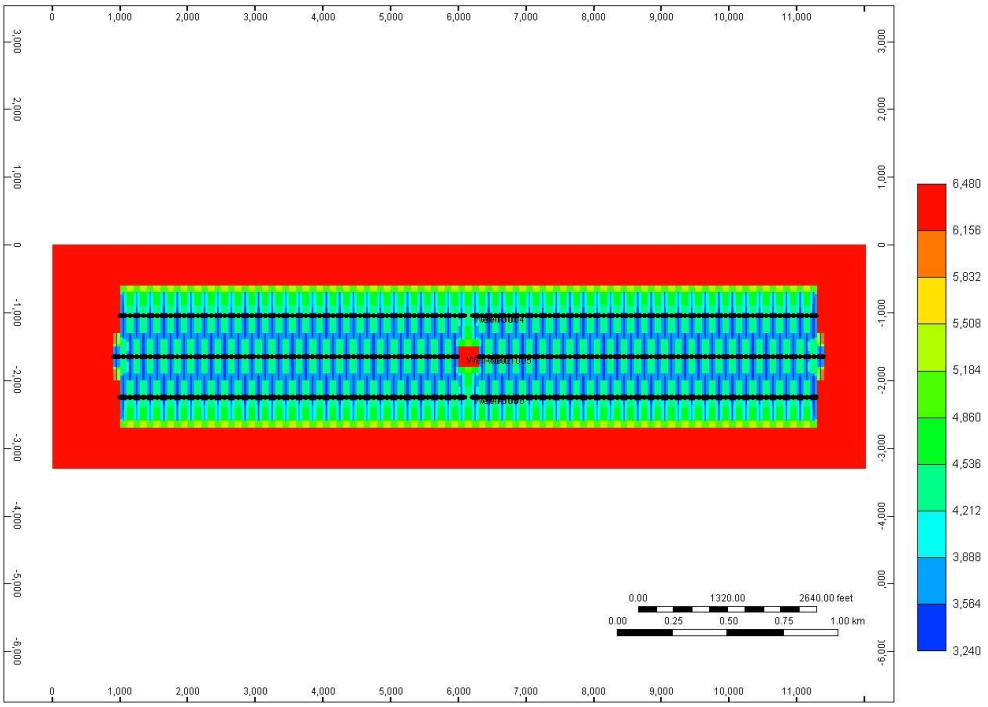

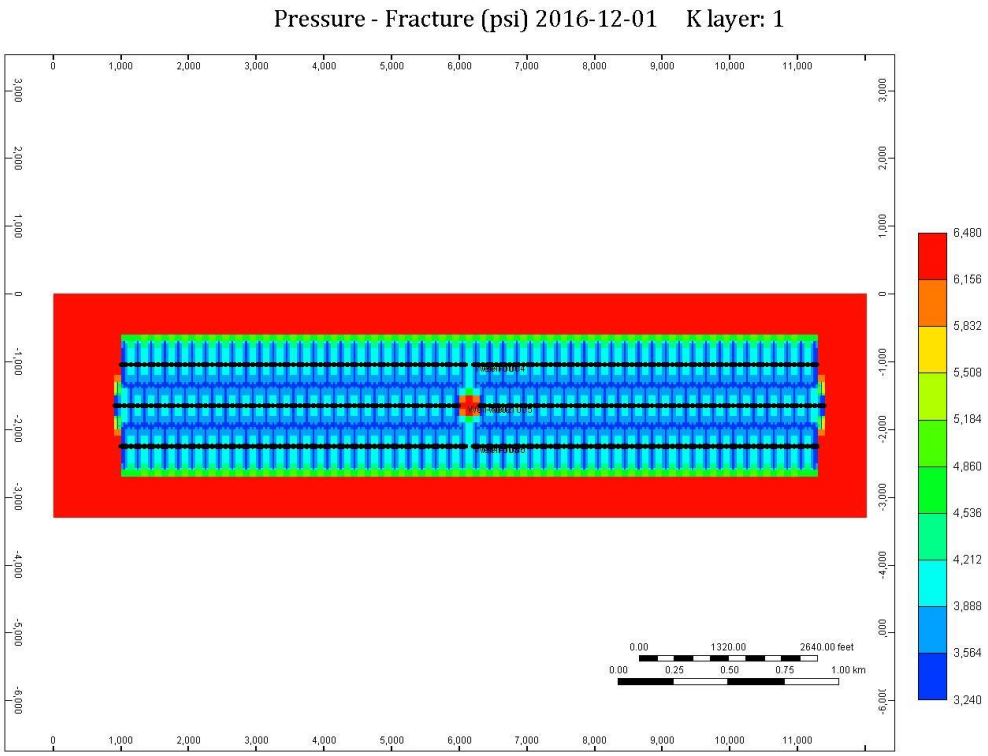

Figure 3.6. Changes of pressure profile in time for the design 6w_5000L_200s (x-axis ranges from 0 ft to 12,000 ft, and y-axis ranges from -6,000 ft to 3,000 ft).

Initially, the reservoir pressure is constant with a value of 6480 psi (first graph). After one year of production (second graph), the reservoir pressure has decreased only in the area affected by the hydraulic fracturing, which is expected since the permeability in this zone is higher in comparison with the rest of the reservoir. Furthermore, the blue areas that correspond to the fracture stages have a lower pressure, between 3564 psi and 3888 psi, in comparison to the surroundings (green areas) whose pressure ranges between 4536 psi and 4860 psi. The pressure distribution after two years of production is shown in the third graph. A pattern is observed around the central wells where the pressure is especially lower closer to the BHP. This can be explained by the relative location of the wells in the well-pad. For wells with a fracture spacing of 200 ft, this has allowed a certain degree of overlapping in the drainage areas by intercalating the fracture stages. This procedure is not uncommon in field applications and is intended to improve the general performance of the well-pad. Finally, the fourth graph shows the pressure profile after 3 years of operation. In this case the pressure is more homogeneous across the SRV. A tendency of the system to even out the pressures can be noted.

3.4.1 Impact of Well-pad Design on Gas Production

It was mentioned previously that the design of a well-pad is an important decision that directly affects the economy of shale gas project. In this study, different production schemes are taken into account by considering the effect of the total number of wells per well-pad, the length and the total number of fractures on the final production of gas (EUR) and consumption of fresh water. The impact of the well-pad design parameters on the gas production profiles is summarised in Figure 3.7.

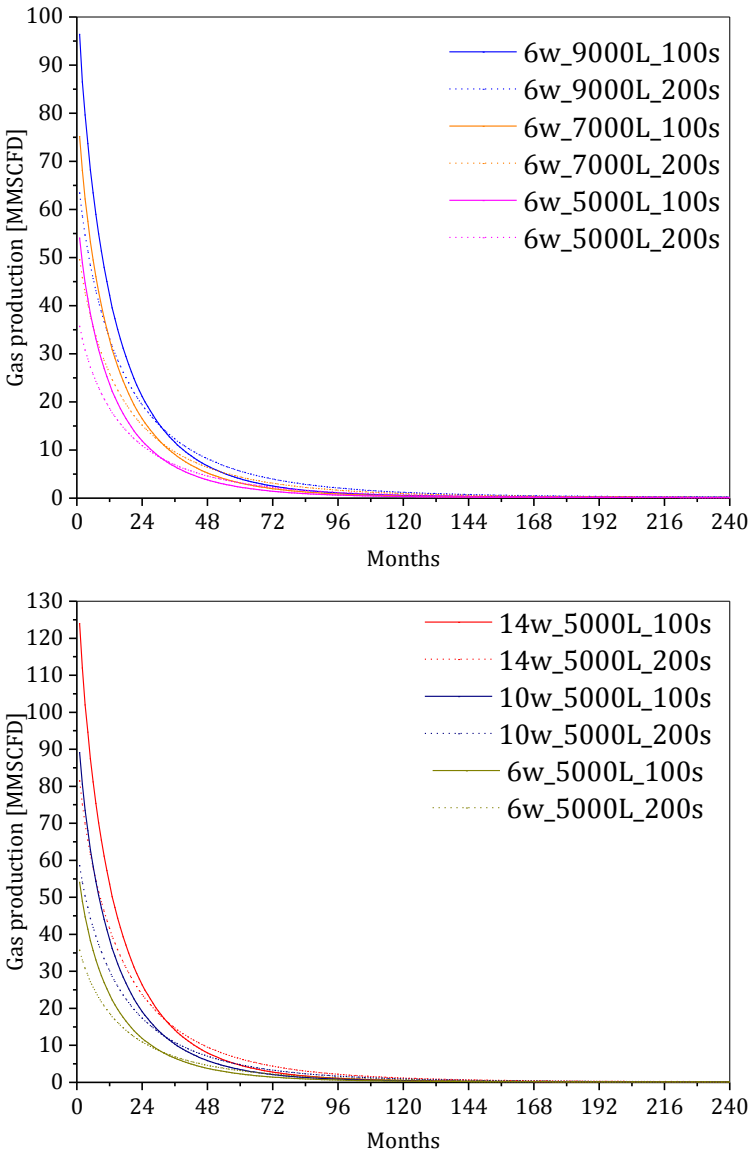

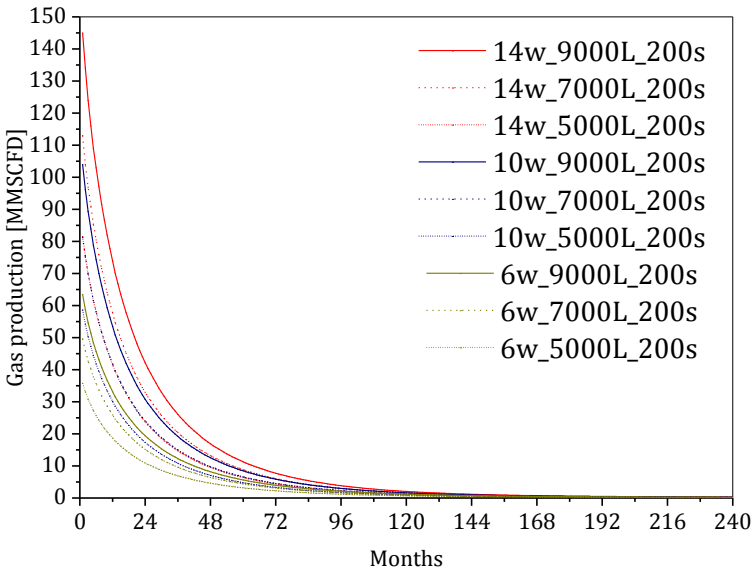

Figure 3.7. Well-pad gas production profiles: constant number of wells (upper left graph), constant horizontal length (upper right graph), and constant fractures spacing (bottom graph).

The initial gas production decreases as the length of the well decreases or as the primary fracture spacing increases (fewer fractures). However, for wells with the same length, the trend regarding the effect of the fracture spacing on gas production is reversed as time progresses and from between 912-1095 days (≈ 2.5-3 years), wells with a higher space between fractures (less number of fractures) produce more gas than wells with a lower fracture spacing. This could be due to the high initial production that causes faster pressure depletion of the SRV. By contrast, the wells with fracture spacing of 200 ft, have lesser connectivity to the SRV which results in lower initial production but also lower production drop. Additionally, it was found that, for constant fracture spacing, the gas production increases as the number of wells and the length of each well increase. This situation is expected given the fact that either higher number of wells per pad or higher horizontal length implies a higher stimulated volume, and thus that a higher gas production can be achieved. Figure 3.8 presents the effect of well-pad design parameters on the estimated ultimate recovery (EUR).

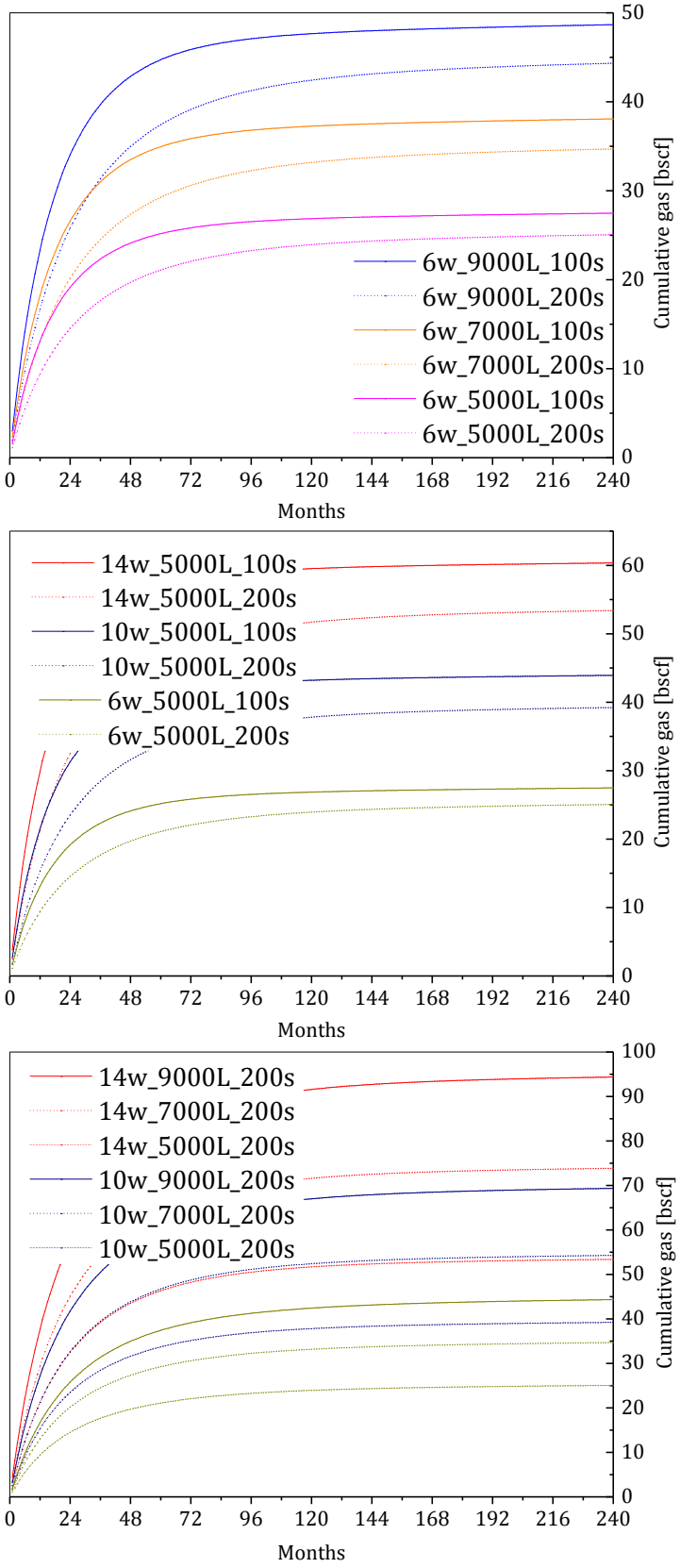

Figure 3.8. Well-pad cumulative gas production profiles: constant number of wells (upper graph), constant horizontal length (middle graph), and constant fractures spacing (bottom graph).

It was observed that for a constant number of wells, the EUR increases as the length of the well increases or as the fracture spacing decreases. Moreover, for a constant well length, the EUR increases as the number of wells increases or as the fracture spacing decreases. A similar situation is observed for constant fracture spacing, where the EUR increases as the number of wells or the length of each well increases. Again, this trend regarding the EUR is explained by the fact that a higher stimulated volume indicates a higher EUR.

3.4.2 Assessment of the Well-pad Designs

Once the technical performance of a well-pad is fully characterised (production and EUR), the results can serve as input to evaluate economic metrics such as net present value (NPV) and the profitability index (PI). The specific economic model parameters used in this evaluation are summarised in Table 3.6.

Table 3.6. Economic parameters.

Parameter	Value	Unit
Discount rate	8	%/year
Royalty rate	6	%
Taxes rate	33	%
Depreciation rate	1.67	%/month
Water treatment cost	0.048	$/gallon
Drilling cost (vertical plus horizontal length)	250	$/ft
Completion cost (fracture half-length = 350 ft)	210,000	$/fracture stage
Total Opex	1.91	$/Mscf

In addition, the use of fresh water per produced gas, defined as water intensity (WI) can also be calculated. With some exceptions in the case of NPV and WI, it was noted that for a constant fracture spacing, the EUR, the NPV, and the WI metric increase as the number of fractures increases (see Figure 3.9).

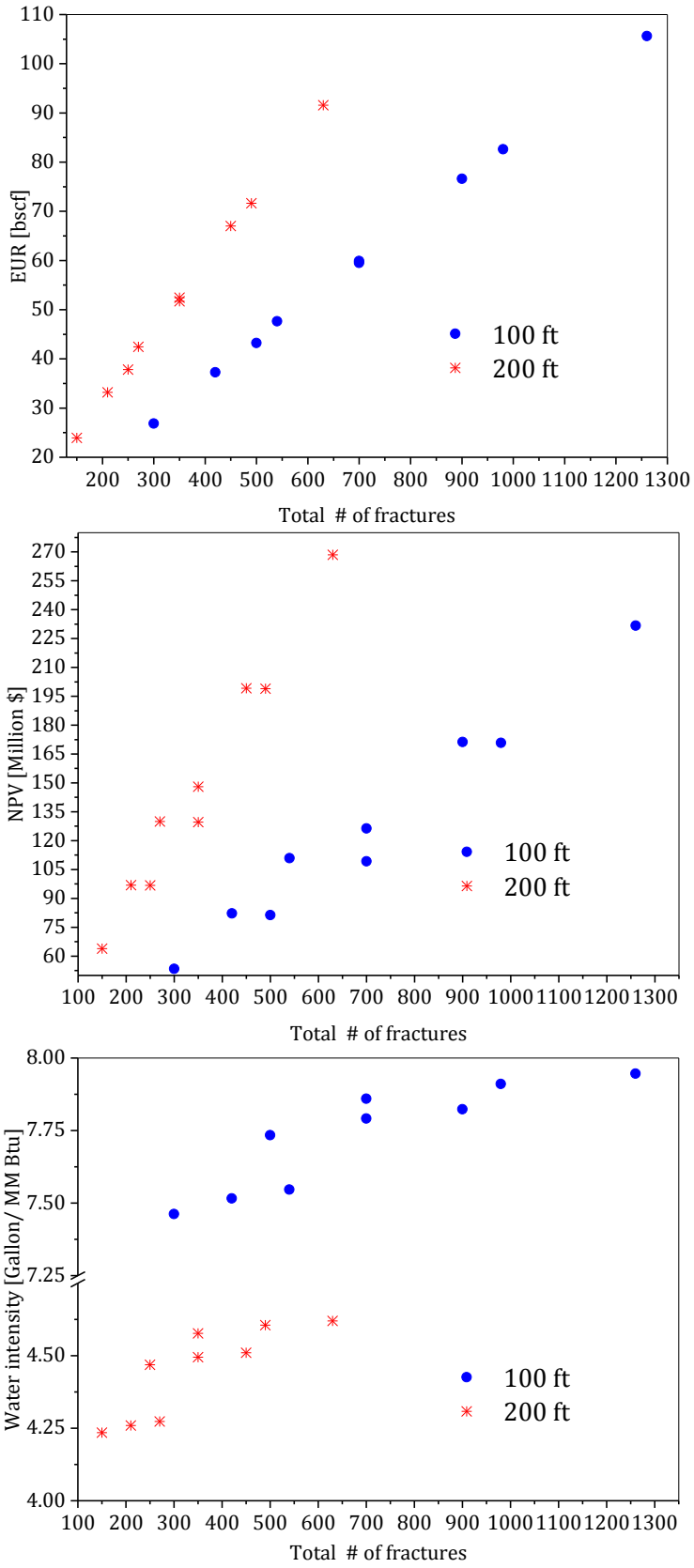

Figure 3.9. Well-pad EUR (upper graph), well-pad net present value (middle graph), and well-pad water intensity (bottom graph).

It is also important to note that the effect of increasing the number of fractures on the EUR and NPV is more significant on wells with 200 ft of fracture spacing than on wells with 100 ft of well fracture spacing. This is inferred from the higher slope of the path described by the points associated with wells with 200 ft separation. The well-pad designs with the highest EUR (105.6 bscf) and NPV (268.53 million $) were the "14w_9000L_100s" and the "14w_9000L_200s" cases, respectively. Regarding the performance metrics, it was observed that PI decreases as the length of the well decreases, but increases as the number of wells decrease, (see left graph in Figure 3.10).

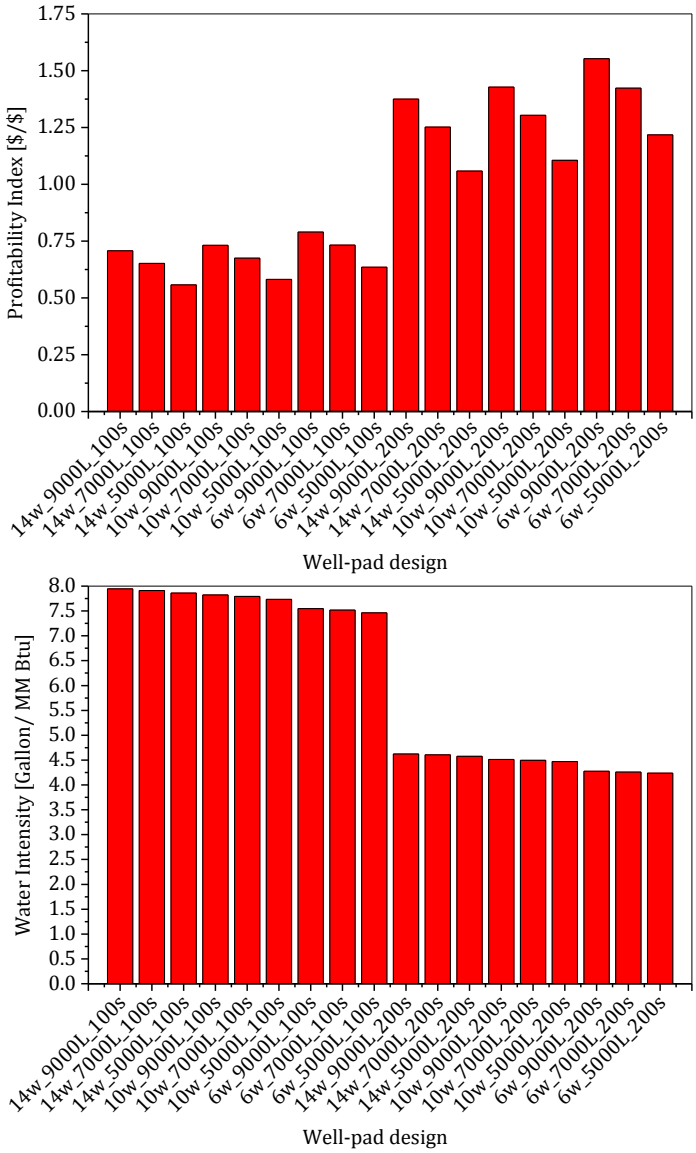

Figure 3.10. Summary of the probability index ranking (upper graph), and water intensity ranking (lower graph)

The well pad design with the highest PI (1.55 $/$) was “6w_9000L_200s”. From these cases, it can be concluded that in terms of gas production and economic performance, a length of 9000 ft is the best choice among the three potential well lengths evaluated in this study. Nevertheless, the lowest WI is achieved by the design “6w_5000L_200s” (see right graph in Figure 3.10). Despite this fact, it is important to clarify that the water intensity was more sensitive to the fracture spacing than to the length of the well and the number of wells per well-pad. Finally, the cumulative cash flow for the designs with maximum EUR, maximum NPV, maximum PI, and lower WI is presented in Figure 3.11.

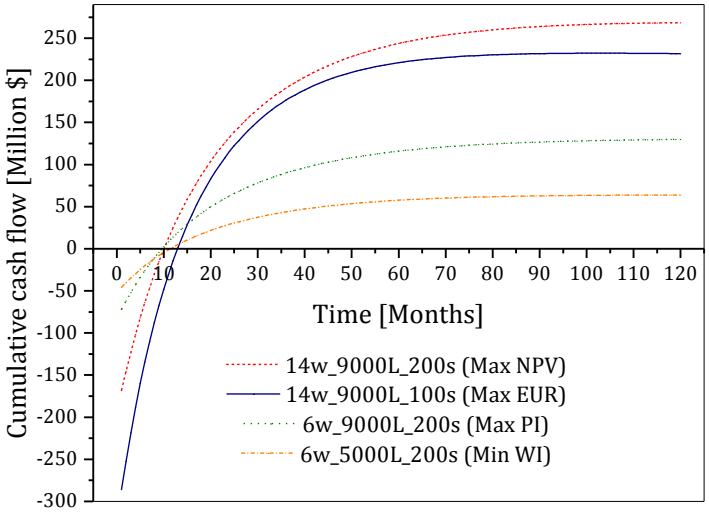

Figure 3.11. Well-pad cumulative cash flow

On average, the break-even point is achieved after 10 months of operation. By comparing the curves for the maximum EUR and NPV, it is interesting to note that a high EUR does not necessarily correspond to higher NPV. In this case, an extra cost in capital investments to increase the fracture stages is reflected on the EUR. However, the net increment in gas production does not compensate for the additional incurred costs. In case of water restrictions, one might want to consider well-pad designs that minimise the use of water per unit of produced gas. In this case, although the NPV is not as high as for the other cases, this design is still a feasible economic option in areas with water scarcity or strict environmental regulation. Lastly, a well-pad with a high profitability index (PI) is desirable if the position of a company is risk-adverse, since high PI seeks to minimise the risk of investment by

maximising the net profit per capital invested. Regarding the risk of the development of shale gas, it can be said that the well-pad design with the lowest water intensity is the one with the best performance. For instance, in terms of land disturbance and ecosystem degradation, the lowest water intensity achieved by design "6w_5000L_200s" implies less truck journeys per well to bring the fracking fluid to the well-pad location and less negative impacts associated with the management of flowback and produced water. Consequently, a decrease in drilling and fracturing operations would contribute to the abatement of noise pollution as well as reduce the possibilities of local seismic events, reducing the negative impacts to the community. Moreover, lower water intensity implies a better performance in terms of regional water depletion, surface water degradation, and Green House Gas (GHG) emissions. It is important to clarify that this analysis is qualitative and that the implementation of a detailed Life Cycle Analysis (LCA) is required in order to make a quantitative analysis and provide a more rigorous assessment of the risk associated with the implementation of those designs for the development of shale gas resources.

From the results, two well-pad designs, MaxNPV and MinWI, are selected to be included in the optimisation framework presented in Chapter 4. These designs present either economic or environmental benefits that can add flexibility in the optimal design of a shale gas supply chain.

3.5 Conclusions

This chapter introduces a methodology for the preliminary assessment of well-pad designs which are a crucial component in the shale gas supply chain. The proposed methodology allows to select key well-pads designs to be considered within an optimisation framework without impacting significantly the combinatorial complexity. The assessment is carried out through the implementation of different performance metrics. As a first step, reservoir simulations were developed to estimate gas and water production profiles from the shale formation for different well-pad configurations. An economic model was proposed and evaluated for each well-pad configuration to estimate the net present value, a commonly used criterion for the evaluation of oil and gas industry related projects. Furthermore, the

profitability index (PI) and water intensity (WI) were proposed as additional metrics to carry out a more complete assessment of a well-pad. 18 well-pad designs were initially set up to explore the impact of three key design parameters: number of wells per well-pad, horizontal length, and spacing of fracturing stages. It was observed that only when the economic aspects are considered for the assessment, well-pad configurations with higher length and lower density of hydraulic fractures are preferred. Furthermore, based on the results, it is possible to suggest that water intensity strongly depends on the density of hydraulic fractures; with a lower density of hydraulic fractures meaning lower water consumption per unit of energy recovery from the well. Regarding the effect of well-pad configuration on the break-even point, there was no significant (less than three months and a half) differences for the four well-pad designs identified using the metrics evaluated in this work.

Finally, based on environmental and economic criteria, 2 well-pad designs were selected from the initial 18 designs which will included as part of an optimisation framework that addresses the design of shale gas supply chains.

Chapter 4. Optimisation of shale gas development

This study presents the mathematical formulation and implementation of a comprehensive optimisation framework for the assessment of shale gas resources. The framework simultaneously integrates water management and the design and planning of the shale gas supply chain, from the shale formation to final product demand centres and from fresh water supply for hydraulic fracturing to water injection and/or disposal. The framework also addresses some issues regarding wastewater quality, i.e. total dissolved solids (TDS) concentration, as well as spatial and temporal variations in gas composition, features that typically arise in exploiting shale formations. In addition, the proposed framework also considers the integration of different modelling, simulation and optimisation tools that are commonly used in the energy sector to evaluate the technical and economic viability of new energy sources (see Chapter 3). First, the impact of water resources on the development of shale gas resources is investigated by means of a parametric analysis. Then, the water-energy-economy of scale nexus is addressed via different number of potential well-pads. The relevance of wastewater quality is also discussed.

4.1 Literature review

A potential shale gas field is represented as a superstructure composed by a number of interconnected echelons such as well-pads, compressors, processing facilities and demand centres [35]. The trade-offs between environmental and economic performance of the shale gas supply chain have been addressed by means of multi-objective optimisation techniques [232]. As water management is considered a key issue in shale gas projects, some works have addressed the minimisation of total water treatment related costs through MILP models with time-discrete representation [233]. A different approach has been investigated in which the objective is defined as the maximisation of profit per unit of fresh water

consumption, the model is formulated as a mixed-integer linear fractional programming (MILFP) problem [234]. In addition, an MILP model has been developed to address the optimal re-use of flowback water from hydraulic operations while considering fresh water seasonality, and economic and environmental aspects [235]. Finally, the effects of uncertainty has been studied through two-stage stochastic MILFP models for the optimal design of shale gas supply chains [236]. In addition, uncertainty has also been considered in the optimisation of water management strategies [237].

In this work, an optimisation–based decision-support tool is presented for the design of shale gas supply chains. The framework simultaneously addresses the strategic design and planning of drilling and fracturing operations as well as gas and water supply chains via maximising the corresponding net present value (NPV) using mathematical programming approaches.

The analysis makes use of a set of case studies carried out using a decision-supporting tool presented in [43,45]. The case studies consider different options regarding the configuration of the well pads, transportation and processing infrastructure from well-pad locations to deliver nodes and from well-pad locations to disposal sites for gas and water, respectively.

4.2 Problem statement[3]

This section presents an overview of the issues that must be considered in the development of shale gas reservoirs, the design of the gas supply chain, and its integration with water management strategies. A generic shale gas supply chain superstructure is presented in Figure 4.1.

[3] This section is based on manuscript III of the list of publications presented at the end of this thesis

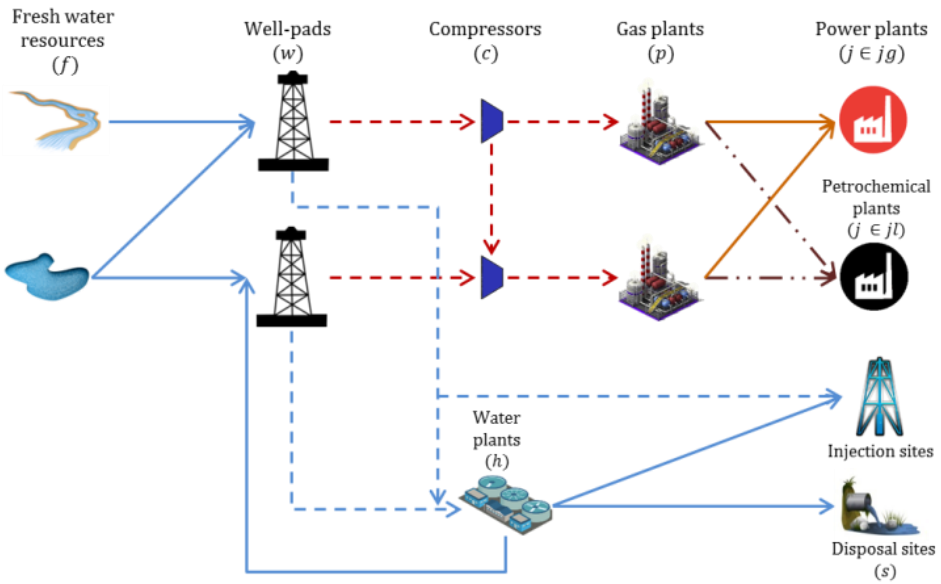

Figure 4.1. Generic superstructure for shale gas supply chain (Reproduced from Guerra et al., 2016 [45]).

Initially, fresh water is transported via trucks or pipelines from sources such as rivers and lakes to locations with high prospective production of shale gas. The transported water is mainly used to produce a fracturing fluid necessary for drilling and hydraulic fracturing operations, the latter activity being highly water-intensive as it accounts for about 86% of the total water consumption over the life-cycle of a well-pad [163]. The fracturing fluid is composed mainly of water (≈90-95 vol%), sand (≈ 4-9 vol%), which is used as a proppant to maintain high permeability of the artificial fractures, and chemical additives (≈ less than 1 vol%). A well-pad can be defined as a cluster of single wells connected at the wellhead to a common point. In its most general form, the design of a well-pad can be described in terms of the number of wells, the horizontal length of each well, and the number of hydraulic fractures per well. The design of a well-pad is a critical aspect in the shale gas supply chain design and planning, since it affects the productivity of the well-pad and also the water requirements. During the early stage of the production of a well-pad, from 1 to 2 weeks, a fraction of the fracturing fluid returns to the wellhead. This fractions is highly variable, ranging between 10%-40% and it depends on geomechanical properties of the formation as well as on the composition of the fracturing fluid. This stream is known as flowback water and presents an average flow rate of 1000 m^3/day. There can be additional production of water due to the presence of formation

water. This stream is known as produced water and its flow rate is significantly lower than the flowback water, around 2–8 m^3/day. Total suspended solids (TSS) and total dissolved solids (TDS) are two important parameters for the characterisation of the wastewater (flowback and produced water) associated with the production of shale gas [85]. For flowback water, the TSS concentration varies from 0.001-0.5 g/L and the concentration of TDS ranges between 5 to 250 m/L. The same ranges of TSS concentration apply to produced water, however, the TDS concentration varies between 10 and 336 g/L [238]. Concentration of TDS in flowback water increases with time, given that minerals and organic constituents present in the formation dissolve into the fracturing fluid [90,239]. Given these characteristics, water management strategies clearly play an important role in dealing with the wastewater associated with shale gas production. According to the wastewater characterisation and its final use, produced and flowback water can be sent either to water treatment plants, for primary and/or secondary treatment, or to deep-injection sites. Primary treatment processes only TSS and re-uses the treated water in new well-pad locations provided that the concentration of TDS is low. Secondary treatment is required if the TDS are higher than the specifications required for drilling and fracturing. In this case, the treated wastewater can be recycled to new well-pad locations or discharged into rivers. Finally, if the technology is available on-site, deep-injection is the most-preferred option as it avoids water treatment costs. However, if the injection point is located far from the reservoir, the trucking costs can be high enough to consider water treatment technologies instead. The concentration of TDS is one of the most important evaluation parameters for wastewater treatment economics and management strategy.

The composition of the produced shale gas depends on the geochemical characterisation of the shale formation. Shale gas can be classified as dry gas (methane > 90%, with the rest largely CO2 and N2) or wet gas (methane, ethane, condensable fractions of propane, butane, iso-butane, CO2, N2). Usually, the composition of shale gas varies not only with location but also as the production progresses. The produced shale gas is sent to gas treatment facilities via pipelines

either directly or through compressor stations. The gas is separated into different fractions and then the final products are sent to final customers, i.e. petrochemical plants, power stations, national gas pipeline network, etc. The novelties of the optimisation framework are summarised as follows:

- Off-line integration of reservoir simulation tools in shale gas supply chain design and planning: Implementation of reservoir simulation techniques that allow the assessment of optimisation of shale gas supply chains by taking into account geological properties of the shale reservoirs.
- Off-line integration of geographic information systems (GIS): ArcGIS® 10.2 [240] is implemented in order to design of potential infrastructure of shale gas and water supply chains. In addition, this tool is used to carry out a national hydrological balance to estimate water availability based on historical data on precipitation, evapotranspiration, infiltration, and downstream demand.
- Novel formulation of water management aspects: The explicit modelling of water blending for fracturing operations as well as in wastewater treatment plants considered. The formulation also takes into account constraints on spatial and temporal variations of Total Dissolved Solid (TDS) in fracturing operations and wastewater treatment plants.
- Integration of design and planning of the gas supply chain along with water management: The optimisation framework allows the simultaneous optimisation of the decisions involved in the design and planning of the gas supply chain and the water management.

The corresponding optimisation framework is presented in section 4.3

4.3 Shale gas mathematical formulation[4]

This section presents the deterministic optimisation model for the design and planning of shale gas supply chains, with water supply and wastewater management considerations. The mathematical model is as follows:

[4] This chapter is based on manuscript II of the list of publications presented at the end of this thesis

4.3.1 Nomenclature

Indices

c, c'	Compressor stations
d	Design of well-pads
f	Fresh water sources
g	Gas treatment plant sizes
h	Water plants
i	Products
j	Demand centres
k	Water treatment plant sizes
m	Compressor sizes
p	Gas plants
q	Set of pipeline sizes for gas and liquids products
s	Disposal sites
t, t'	Time periods
w	Well-pads

Sets

jg	Set of demand centres of gaseous products
jl	Set of demand centres of liquid products
lcc	Set of feasible connections between compressor stations c and c'
lcp	Set of feasible connections between compressor stations c and gas processing plants p
lfw	Set of feasible connections between fresh water sources f and well pads w
lhs	Set of feasible connections between water treatment plants h and disposal sites s
lhw	Set of feasible connections between water treatment plants h and well-pads w
lij	Set of feasible connections between products i and demand centres j
lwc	Set of feasible connections between well-pads w and compressor stations c
lwp	Set of feasible connections between well-pads w and gas processing plants p
lws	Set of feasible connections between well-pads w and disposal sites s
u	Set of pipeline sizes for liquid products
v	Set of pipeline sizes for gas products

Scalars

$MaxExp$	Maximum number of expansions for gas processing plants
$MaxInv$	Maximum budget available for investment
$MaxTDS$	Max TDS concentration on water blend for hydraulic fracturing
$MaxWell$	Maximum number of wells that can be drilled per period
roy	Royalty rate
tc	Lead time for installing a new compressor
td	Lead time for building a pipeline either for liquids or gas transportation
tg	Lead time for installing a new gas treatment plant
th	Lead time for installing a new water treatment plant
tx	Taxes rate
γ	Discount rate

Parameters

$CapDis(s,t)$	Maximum capacity for disposal sites s in time period t
$CapexCom(m,c)$	Capital investments for installing compressor c with capacity m
$CapexGas(g,p)$	Capital investments for installing Gas treatment plant p with capacity g
$CapexPcc(c,c',q)$	Capital investments for installing a pipeline to transport gas from compressor c to compressor c' with a diameter size q
$CapexPcp(c,p,q)$	Capital investments for installing a pipeline with size q to transport gas from compressor c to gas treatment plants p
$CapexPpj(p,j,q)$	Capital investments for installing a pipeline between gas treatment plants p and demand centres j to transport product type q
$CapexPwc(w,c,q)$	Capital investments for installing a pipeline to transport gas from well-pad w to compressor c with a diameter size q
$CapexPwp(w,p,q)$	Capital investments for installing a pipeline to transport gas from well-pad w to gas treatment plants p with a diameter size q
$CapexWate(k,h)$	Capital investments for installing a water treatment plant h with capacity k
$CapexWell(d,w)$	Capital investments for drilling a well-pad w with a design d
$Comp(i,d,w,t)$	Gas composition of product i for design d in well-pad w and time period t
$CostAcq(f)$	Fresh water cost acquisition for source f supplying well-pad w
$CostFres(f,w)$	Fresh water cost transportation for source f supplying well-pad w

$CostRech(h,w)$	Water transportation cost from water treatment plants h to well-pads w
$CostRecs(h,s)$	Water transportation cost from water treatment plants h to disposal sites s
$CostWateh(w,h)$	Water transportation costs from well-pads w to water treatment plants h
$CostWates(w,s)$	Water transportation costs from well-pads w to disposal sites s
$Dem(i,j,t)$	Demand of product i in demand centre j in time period t
$Dep(t,t')$	Depreciation rate for investments in time period t during periods t'
$MaxTDSt(h)$	Max TDS concentration in wastewater for treatment in water plant h
$NumWell(d)$	Number of wells per design d
$OpexWell(w)$	Operational costs for well-pad w
$OpexCom(c)$	Operational costs for compressor c
$OpexDis(s)$	Operational costs for water disposal in site s
$OpexGas(p)$	Operational costs for gas treatment plant p
$OpexWate(h)$	Operational costs for water treatment plant h
$Price(i,j,t)$	Price for products i paid in demand centres j during period t
$PriceC3(p,t)$	Price for C_{3+} at location of gas plant p during period t
$RawTankCap(k)$	Size discretisation for water tanks
$Sizec(m)$	Capacity for compressors of size m
$Sizeg(g)$	Capacity of water treatment plants of size g
$Sizeh(k)$	Capacity of water treatment plants of size k
$Sizep(q)$	Size discretisation for gas pipelines transportation of size q
$Sizepl(q)$	Size discretisation for liquids pipelines transportation of size $q \mid \in u$
$TankCap(k)$	Capacity of water tanks of size k
$TDSf(f)$	TDS concentration in fresh water sources f
$TDSh(h)$	TDS concentration in treated water from water plant h
$TDSw(w)$	TDS concentration in wastewater from well-pads w
$WatDem(d,w)$	Water demand for fracturing depending on design d and well-pad w
$WateAvai(f,t)$	Maximum fresh water availability at source f in time period t

$WellGas(d,w,t)$	Gas production profiles corresponding to design d at well-pad w in time period t
$WellWate(d,w,t)$	Water production profiles corresponding to design d in a well-pad w in time period t
$\psi(h)$	Water Recovery factor for water treatment plant h
$\phi(i,p)$	Separation efficiency for product i in gas treatment plant p

Positive continuous Variables

$Capex(t)$	Total capital investments in time period t
$CapexCO(t)$	Capital investments for in new compressors during time period t
$CapexGA(t)$	Capital investments for new gas treatment plants in time period t
$CapexPI(t)$	Capital investments for new pipelines in time period t
$CapexPJ(t)$	Capital investments for new pipelines transporting final products in time period t
$CapexWA(t)$	Capital investments for new water treatment plants in time period t
$CapexWE(t)$	Capital investments for new well-pads in time period t
$CompC(i,c,t)$	Compressor output composition for product i in compressor c in time period t
$CompW(i,w,t)$	Well-pad output composition for product i in well-pad w in time period t
$CostCC(t)$	Transportation costs between compressors in time period t
$CostFW(t)$	Total transportation costs for fresh water in time period t
$CostHS(t)$	Total transportation costs for treated water from water treatment plants to disposal sites in time period t
$CostHW(t)$	Transportation costs from water treatment plants to well-pads in time period t
$CostWH(t)$	Transportation costs from well-pads to water treatment plants in time period t
$CostWS(t)$	Transportation costs from well-pads to disposal sites in time period t
$Dep(t,t')$	Depreciation rate factor for investments in time t during periods t'
$FlowCC(c,c',t)$	Gas flow between compressor c and c' in time period t
$FlowCP(c,p,t)$	Gas flow from a compressor c to a gas treatment plant p in time period t
$FlowFW(f,w,t)$	Fresh water flow from source f to a well-pad w in time period t
$FlowHS(h,s,t)$	Treated water flow from water treatment plant h to disposal

	sites s in time period t
$FlowHW(h,w,t)$	Treated water flow from water treatment plant h to a well-pad w in time period t
$FlowPJ(p,i,j,t)$	Final products flow from gas treatment plant p sending products i to final demand centres j in time period t
$FlowWC(w,c,t)$	Gas flow from a well-pad w to a compressor c in time period t
$FlowWH(w,h,t)$	Wastewater flow from well-pad w to water treatment plant h in time period t
$FlowWP(w,p,t)$	Gas flow from a well-pad w to a gas treatment plant p in time period t
$FlowWS(w,s,t)$	Wastewater flow from well-pad w to disposal sites s in time period t
$Opex(t)$	Total operational costs in time period t
$OpexCO(t)$	Operational costs for new compressors in time period t
$OpexDI(t)$	Operational costs for disposal in time period t
$OpexGA(t)$	Operational costs for new gas treatment plants in time period t
$OpexWA(t)$	Operational costs for new water treatment plants in time period t
$OpexWC(t)$	Operational costs for transportation from well-pads to compressors in time period t
$OpexWE(t)$	Operational costs for new well-pads in time period t
$OpexWP(t)$	Operational costs for transportation from well-pads to gas treatment plants in time period t
$Pro(i,w,t)$	Individual component flow i from well-pad w in time period t
$RawTank(h,t)$	Raw water storage in water treatment plant h in time period t
$Revec3(t)$	Income from selling C_{3+} hydrocarbons at gas processing plant locations during period t
$Revenue(t)$	Revenue in time period t
$Royalty(t)$	Royalty in time period t
$ShalProd(w,t)$	Shale gas production profile in well-pad w in time period t
$Taxes(t)$	Taxes in time period t
$TransCost(t)$	Total water transportation costs in time period t
$WateProc(h,t)$	Raw water processed in water treatment plant h during time period t
$WateProd(w,t)$	Water production profile in well-pad w in time period t
$WateTank(h,t)$	Treated Water storage in water treatment plant h in time period t

Free continuous variables

$CashFlow(t)$	Cash flow after taxes in time period t
NPV	Net present value
$Profit(t)$	Profit after depreciation and operational costs in time period t

Binary variables

$InstC(m,c,t)$	Equal to 1 if a capacity expansion of size m is selected for a compressor c in time period t; 0 otherwise
$InstG(g,p,t)$	Equal to 1 if a capacity expansion of size g is selected for a gas treatment plant p in time period t; 0 otherwise
$InstH(k,h,t)$	Equal to 1 if a capacity expansion of size k is selected for a water treatment plant h in time period t; 0 otherwise
$InstPcc(q,c,c',t)$	Equal to 1 if a capacity expansion of size q is selected for a pipeline connecting a compressor c with a compressor c' in time period t; 0 otherwise
$InstPcp(q,c,p,t)$	Equal to 1 if a capacity expansion of size q is selected for a pipeline connecting a compressor c with a gas treatment plant p in time period t; 0 otherwise
$InstPpj(q,p,j,t)$	Equal to 1 if a capacity expansion of size q is selected for a pipeline connecting a gas treatment plant p with demand centres j in time period t; 0 otherwise
$InstPwc(q,w,c,t)$	Equal to 1 if a capacity expansion of size q is selected for a pipeline connecting a well-pad w with a compressor c in time period t; 0 otherwise
$InstPwp(q,w,p,t)$	Equal to 1 if a capacity expansion of size q is selected for a pipeline connecting a well-pad w with a gas treatment plant p in time period t; 0 otherwise
$PlanSite(p)$	Equal to 1 is a gas processing plant p is selected, 0 otherwise
$WellDes(d,w,t)$	Equal to 1 if the design d is selected for a well-pad w in time period t; 0 otherwise

4.3.2 Objective function

The objective function is to maximise the Net Present Value (NPV), defined as the cash flow $CashFlow(t)$ minus capital expenditures $Capex(t)$, associated with the design of the shale gas supply chain, as described in Equation (4.1). The scalar γ

represents the annual interest rate and t is the index for time periods, quarters in this case.

$$max \quad NPV = \sum_{t} \frac{CashFlow(t) - Capex(t)}{(1+\gamma)^{t-1}} \tag{4.1}$$

4.3.2.1 Cash flow

Cash flow is defined as the profit before taxes $Profit(t)$ plus depreciation minus tax amount $Taxes(t)$, as described in Equation (4.2). Here, depreciation is expressed as a linear function of the capital expenditures using a given depreciation rate $DepR(t', t)$.

$$CashFlow(t) = Profit(t) + \sum_{t'} DepR(t', t) * Capex(t') - Taxes(t) \quad \forall\, t \tag{4.2}$$

4.3.2.2 Capital expenditures

Capital expenditures consist of the sum of the investment in well-pads drilling and hydraulic fracturing, pipelines for transport raw gas, compressor stations, water treatment plants, gas processing plants, and pipeline for deliver final products, as shown in Equation (4.3)

.

$$\begin{aligned} Capex(t) = {} & CapexWE(t) + CapexPI(t) + CapexCO(t) + CapexWA(t) \\ & + CapexGA(t) + CapexPJ(t) \quad \forall\, t \end{aligned} \tag{4.3}$$

4.3.2.3 Profit and taxes

The profit associated with the shale gas supply chain operation is estimated as the revenue $Revenue(t)$ minus royalties $Royalty(t)$, water transportation cost $TransCost(t)$, operating expenditures $Opex(t)$, and depreciation, as defined in Equation (4.4). For periods in which the profit is positive, a taxation charge is typically imposed. The taxation charge is defined as the tax rate *tr* times profit. Equations (4.5) and (4.6) guarantee that taxes are applied only when profit is positive: taxes are set to zero otherwise. However, it is important to clarify that in

some situations; tax laws allow losses in one or more years to be carried over so as to reduce the tax burden in profitable years. In this case, Equations (4.5) and (4.6) should be modified accordingly to the tax system that is applicable for the study.

$$Profit(t) = Revenue(t) - Royalty(t) - TransCost(t) - Opex(t) - \sum_{t'} DepR(t', t) * Capex(t') \quad \forall\, t \tag{4.4}$$

$$Taxes(t) \geq tr * Profit(t) \quad \forall\, t \tag{4.5}$$

$$Taxes(t) \geq 0 \quad \forall\, t \tag{4.6}$$

4.3.2.4 Revenue

The revenue from selling final products to markets, is estimated as stated in Equation (4.7), where $Price(i, j, t)$ is the price for product i in market j during period t and $FlowPJ(p, i, j, t)$ is the flow rate of product i from gas plant p to demand centre j during period t. In addition, the variable $ReveC3(t)$ represents the income from selling C_{3+} hydrocarbons at gas processing plant locations.

$$Revenue(t) = \sum_{j} \sum_{i|(i,j)\in lij} Price(i, j, t) * \sum_{p} FlowPJ(p, i, j, t) + ReveC3(t) \quad \forall\, t \tag{4.7}$$

4.3.2.5 Royalties

Royalties are payment to resource owners for the permission to explore and exploit the resources found in their lands (shale gas in this case); this cost component is modelled through Equation (4.8), here scalar *roy* represents the royalty rate.

$$Royalty(t) = roy * Revenue(t) \quad \forall\, t \tag{4.8}$$

4.3.2.6 Water transportation cost

Total water transport cost $(TranCost(t))$ consist of the sum of the cost of transportation from freshwater suppliers to well-pads, from well-pads to water treatment plants, from well-pads to disposal sites, from water treatment plants to well-pads, and from water treatment plants to disposal sites, as shown in Equation (4.9).

$$TranCost(t) = CostFW(t) + CostWH(t) + CostWS(t) + CostHW(t) + CostHS(t) \quad \forall\, t \tag{4.9}$$

4.3.2.7 Operating expenditures

Operating expenditures include the annual cost of operating well-pads $OpexWE(t)$, gas pipelines for transporting raw gas from well-pads to either compressor stations $OpexWC(t)$ or gas plants $OpexWP(t)$, compressor stations $OpexCO(t)$, water treatment plants $OpexWA(t)$, gas processing plants $OpexGA(t)$, and pipelines for transporting final products to demand centres $OpexDI(t)$ are estimated from Equation (4.10).

$$Opex(t) = OpexWE(t) + OpexWC(t) + OpexWP(t) + OpexCO(t) + OpexWA(t) + OpexGA(t) + OpexDI(t) \quad \forall\, t \tag{4.10}$$

4.3.2.8 Investment budget

Since there is a significant risk associated with the shale gas businesses and at the same time oil and gas companies usually have limited budgets for investment on specific projects, Equation (4.11) ensures that capital expenditures do not exceed the maximum capital budget $MaxInv$ that is available for investment on shale gas projects.

$$\sum_{t} \frac{Capex(t)}{(1+\gamma)^{t-1}} \leq MaxInv \tag{4.11}$$

4.3.3 Freshwater supply

Freshwater sources are required to provide freshwater for hydraulic fracking at well-pads locations. These sources are constrained in water availability, since local water resources are not infinitely available. In addition, freshwater should be transported from freshwater sources to well-pad locations, which entails a transportation cost.

4.3.3.1 Availability

The availability of freshwater from a specific source may depend on the season, environmental flow, and downstream water demand. Equation (4.12) accounts for the freshwater availability restriction, where $FlowFW(f,w,t)$ is the

flow rate of freshwater transported from source f to well-pad location w during period t. The linkage between freshwater source and potential well-pad locations is defined by the set lfw.

$$\sum_{w|(f,w)\in lfw} FlowFW(f,w,t) \leq WateAvai(f,t) \ \forall f,t \tag{4.12}$$

4.3.3.2 Acquisition and Transportation costs

Acquisition and transportation costs related to the supply of freshwater for hydraulic fracking depend on both well-pad location and total freshwater withdrawal, as stated in Equation (4.13). The parameter $CostFres(f,w)$ refers to the unit transportation cost for freshwater from source f to well-pad location w. Similarly, parameter $CostAcq(f)$ denotes the unit water acquisition cost for source f.

$$CostFW(t) = \sum_{f} \left(CostAcq(f) * \sum_{w|(f,w)\in lfw} FlowFW(f,w,t) + \sum_{w|(f,w)\in lfw} CostFres(f,w) * FlowFW(f,w,t) \right) \ \forall t \tag{4.13}$$

4.3.4 Well-pads

In order to produce shale gas from potential well-pad locations, vertical and horizontal wells need to be drilled and hydraulically fractured. The water demand for fracking the shale formation as well as wastewater production profiles depends on both well-pad location and design. Well-pad design is expressed in terms of total number of wells, length of each well, and number of hydraulic fractures completed in each well. From the supply chain point of view, the design of well-pads is a key decision variable. In particular, the optimal design for a specific well-pad location can be a function of gas prices, water availability constraints, and petrophysical properties of the formation, such as porosity and permeability. For Instance, the U.S. Energy Information Administration, in 2012, reported that the total average cost, including drilling and completion expenses, per horizontal well in Bakken, Eagle Ford, and Marcellus formations varies between approximately $6.5 million and $9

million (http://www.eia.gov/todayinenergy/detail.cfm?id=7910&src=email). Therefore, well-pad design is an important variable to be considered when designing a shale gas supply chain.

4.3.4.1 Well-pad design

In this work, well-pad design, location, and timing are considered the most important decisions related to shale gas production. These decisions are captured in the binary variable $WellDes(d,w,t)$. This variable is equal to one if well-pad design d is selected for potential well-pad w during period t; the variable is equal to zero otherwise. The well-pad designs are decision variables in our model. They are implicitly represented by different potential gas and wastewater production profiles for each well-pad location based on shale gas reservoir simulations. Among these, the most appropriate well-pad design or configuration for each location is selected as well as the timing of drilling operations. Then, the binary variable $WellDes(d,w,t)$ is used to estimate gas and wastewater production profiles for each location, which change with time. Since only one well-pad design can be activated during the whole time horizon for a specific potential well-pad location, the constraint defined in Equation (4.14) needs to be imposed on the binary variable $WellDes(d,w,t)$. In addition, for each time period, the total number of wells drilled should not exceed the maximum number of wells $MaxWell$ that can be drilled, as expressed in Equation (4.15). The maximum number of wells $MaxWell$ is determined by the total number of rigs that are available times the number of wells that a single rig can drill during one period of time. Parameter $NumWell(d)$ is defined as the number of wells considered in design d.

$$\sum_{d}\sum_{t} WellDes(d,w,t) \leq 1 \quad \forall\, w \tag{4.14}$$

$$\sum_{d}\sum_{w} NumWell(d) * WellDes(d,w,t) \leq MaxWel \quad \forall\, t \tag{4.15}$$

4.3.4.2 Shale gas production

Shale gas production is expressed as a function of the well-pad design chosen for each potential well-pad location, as defined in Equation (4.16). Here, the parameter $WellGas(d,w,t')$ represents current gas production associated with design d for well-pad w of age t'. Shale gas production from well-pads can be either sent to compressor stations or directly to gas processing plants, as stated in Equation (4.17). The variable $FlowWC(w,c,t)$ represents the flow rate of shale gas transported from well-pad w to compressor station c during period t. Similarly, $FlowWP(w,p,t)$ represents the flow rate of shale gas transported from well-pad w to gas processing plant p during period t. The set lwc contains all of the possible connections between well-pads and compressor stations. Similarly, set lwp contains all of the possible connections between well-pads and gas plants.

$$ShalProd(w,t) = \sum_{d} \sum_{t' \le t-1} WellGas(d,w,t') * WellDes(d,w,t-t') \quad \forall\, w,t \tag{4.16}$$

$$ShalProd(w,t) = \sum_{c|(w,c)\in lwc} FlowWC(w,c,t) + \sum_{p|(w,p)\in lwp} FlowWP(w,p,t) \quad \forall\, w,t \tag{4.17}$$

4.3.4.3 Shale gas composition and component flows

With regard to the shale gas composition, three cases can be considered. First, in order to avoid bilinear terms in the problem formulation, shale gas composition can be set at constant values; however this assumption may not represent the real situation in shale gas formations. Secondly, shale gas composition can be considered as a function of well-pad location and design, due to the fact that shale gas formations are highly heterogeneous. Lastly, shale gas composition can be function of well-pad location and design as well as well-pad age, as shale gas is made up of different components whose desorption is selective, such that some components are produced first and others later. Here, shale gas composition is expressed as function of the binary variable $WellDes(d,w,t)$, as given in Equation (4.18). The parameter $Comp(i,d,w,t')$ represents the composition of component i

associated with design d for well-pad w of age t'. Equation (4.18) is general and can represent any of the cases mentioned above. However, if shale gas composition is assumed to be constant everywhere and over time, then Equation (4.18) is not needed due to the fact that shale gas composition becomes a known parameter.

Moreover, there is a particular case where even with variable gas composition the bilinear terms related to material balances in compressor stations can be avoided. That case happens when the supply chain model is forced to choose only one gas processing plant. In this case, estimation of component flows becomes more appropriate than the estimation of gas composition. Individual component flows from well-pads are estimated through Equation (4.19), where the variable $Prod(i,w,t)$ represents the production of shale gas component i from well-pad w during period t

$$CompW(i,w,t) = \sum_{t' \leq t-1} \sum_{d} Comp(i,d,w,t') * WellDes(d,w,t-t') \quad \forall\, i,w,t \tag{4.18}$$

$$Prod(i,w,t) = \sum_{t' \leq t-1} \sum_{d} Comp(i,d,w,t') * WellGas(d,w,t') * WellDes(d,w,t - t') \quad \forall\, i,w,t \tag{4.19}$$

4.3.4.4 Water demand and specifications for hydraulic fracturing

Water demand for hydraulic fracking $WatDem(d,w)$, which is a function of both design and well-pad location, can be supplied from freshwater resources and water treatment plants as expressed in Equation (4.20). Flow rates from freshwater sources and water treatment plants are represented by variables $FlowFW(f,w,t)$ and $FlowHW(h,w,t)$, respectively. The link between water treatment plants and potential well-pads is defined by the set lhw. In addition, in order to avoid scaling and other issues, treated water and fresh water blends for hydraulic fracturing have to meet the specification regarding TDS concentration, as expressed in Equation (4.21). Parameters $TDSf(f)$ and $TDSh(h)$ represent the TDS concentration in water stream from freshwater sources and water treatment plants, respectively. In addition, parameter $MaxTDS$ represents the maximum allowed TDS concentration in the

water blend. This specification could be a function of well-pad location, in which case the parameter $MaxTDS$ must be indexed by well-pad location w ($MaxTDS(w)$). It is important to note that there could be additional specifications imposed on the water blend, for instant maximum allowed concentration of hardness ions like Calcium, Chlorides, Barium and Strontium. In this case equations similar to Equation (4.21) should be included for those additional requirements on water blend quality.

$$\sum_{f|(f,w)\in lfw} FlowFW(f,w,t) + \sum_{h|(h,w)\in lhw} FlowHW(h,w,t) = \sum_{d} WatDem(d,w) * WellDes(d,w,t) \quad \forall\, w,t \tag{4.20}$$

$$\sum_{f|(f,w)\in lfw} TDSf(f) * FlowFW(f,w,t) + \sum_{h|(h,w)\in lhw} TDSh(h) * FlowHW(h,w,t) \leq MaxTDS * \sum_{d} \sum_{t'\leq t-1} WellWate(d,w,t') * WellDes(d,w,t-t') \quad \forall\, w,t \tag{4.21}$$

4.3.4.5 Water production

Water production profiles, flowback plus produced water, are calculated using Equation (4.22). The parameter $WellWate(d,w,t')$ represents the water production flow rate associated with design d for well-pad w of age t'. This parameter includes the flowback water after a fracturing process and the produced water inherent to the shale formation. The water production balance is described in Equation (4.23). The variable $FlowWH(w,h,t)$ represents the water flowrate from well-pad w to treatment plant h during period t. Likewise, variable $FlowWS(w,s,t)$ represents the water flowrate from well-pad w to disposal site s during period t. The linkage between well-pads and disposal sites is defined by the set lws.

$$WateProd(w,t) = \sum_{d} \sum_{t'\leq t-1} WellWate(d,w,t') * WellDes(d,w,t-t') \quad \forall\, w,t \tag{4.22}$$

$$WateProd(w,t) = \sum_{h|(h,w)\in lhw} FlowWH(w,h,t) + \sum_{s|(w,s)\in lws} FlowWS(w,s,t) \quad \forall\, w,t \tag{4.23}$$

4.3.4.6 Water transportation cost

The cost of transporting water from well-pads to water treatment plants and disposal sites is estimated through Equations (4.24) and (4.25), respectively. Unit transportation cost for water from well-pads to water treatment plants and disposal sites are defined in parameters $CostWateh(w,h)$ and $CostWates(w,s)$.

$$CostWH(t) = \sum_{w} \sum_{h|(h,w)\in lhw} CostWateh(w,h) * FlowWH(w,h,t) \quad \forall\, t \tag{4.24}$$

$$CostWS(t) = \sum_{w} \sum_{s|(w,s)\in lws} CostWates(w,s) * FlowWS(w,s,t) \quad \forall\, t \tag{4.25}$$

4.3.4.7 Capital and operating expenditures

Capital expenditures $CapexWE(t)$ associated with well-pads are estimated as stated in Equation (4.26), where parameter $CapexWell(d,w)$ represents the capital expenditures associated with the implementation of design d in well-pad w. In addition, operating expenditures $OpexWE(t)$ are calculated as defined in Equation (4.27). Here, the parameter $OpexWell(w)$ represents the operating expenditure for well-pad w.

$$CapexWE(t) = \sum_{w} \sum_{d} CapexWell(d,w) * WellDes(d,w,t) \quad \forall\, t \tag{4.26}$$

$$OpexWE(t) = \sum_{w} OpexWell(w) * ShalProd(w,t) \quad \forall\, t \tag{4.27}$$

4.3.5 Gas pipelines and compressor stations for raw gas transportation

Pipelines and compressor stations are required in order to allow the transportation of raw gas from well-pads to gas plants. Different capacities can be selected for both pipelines and compressor stations, depending on the amount of gas to be transported and the distances between well-pads and gas plants. In this work, the gas pipelines and compressor stations are not modelled using compressive flow equations. Instead, the potential pipeline network is designed based on fixed pressures at each node and using a process simulator to estimate capital and

operating cost for different pipeline or compressor capacities. It is important to note that, for pipes, each capacity corresponds to a specific commercial size depending on the length of the pipe as well as the pressure drop between the inlet and output nodes.

4.3.5.1 Gas pipeline capacity: Well-pad to compressor stations

The capacity of a gas pipeline, for a given time period, is equal to the cumulative capacity expansion from the first period until period $t^{'} - t_d$, as stated in Equation (4.28). Scalar t_d represents the lead time for gas pipeline construction. Capacity expansions can take discrete sizes only, which are defined by parameter $Sizep(q)$. The binary variable $InstPwc(q, w, c, t' - t_d)$ is equal to one if a capacity expansion of size q is assigned to gas pipeline from well-pad w to compressor station c during period t, the binary variable is equal to zero otherwise. Set v defines all of the possible sizes for gas pipelines. Equation (4.29) is used to guarantee that up to one size is selected for capacity expansions of a specific gas pipeline from well-pads to compressor stations during a given time period.

$$FlowWC(w,c,t) \leq \sum_{t' \leq t} \sum_{q \in v} Sizep(q) * InstPwc(q,w,c,t' - t_d) \quad \forall (w,c) | (w,c) \in lwc, t \tag{4.28}$$

$$\sum_{q \in v} InstPwc(q,w,c,t) \leq 1 \quad \forall (w,c) | (w,c) \in lwc, t \tag{4.29}$$

4.3.5.2 Material balance for compressor stations

The gas flow balances in compressor stations are expressed in Equation (4.30). The connections between compressor station and gas plants are defined by the set lcp. Additionally, set lcc contains the linkage between compression stations. The variables $FlowCC(c, c', t)$ and $FlowCP(c, p, t)$ represent the gas flow rate transported between compressor stations and from compressor stations to gas plants, respectively. Outlet stream compositions for compressor stations $CompC(i, c, t)$ are estimated from Equation (4.31), which is bilinear. It is important to note that if the composition of shale gas at well-pads is considered constant or if only one gas plant is allowed to be installed, the Equation (4.31) is not needed and can be removed

from the model formulation. In the first case of constant gas composition, the compressor outlet stream compositions become a known parameter equal to gas composition at well-pad locations. In the second case, where only one gas plant is allowed to be installed, individual component flows are used instead of gas composition.

$$\sum_{p|(c,p)\in lcp} FlowCP(c,p,t) + \sum_{c\prime|(c,c\prime)\in lcc} FlowCC(c,c',t) = \sum_{w|(w,c)\in lwc} FlowWC(w,c,t) + \sum_{c\prime|(c\prime,c)\in lcc} FlowCC(c',c,t) \quad \forall\, c,t \tag{4.30}$$

$$CompC(i,c,t) * \left(\sum_{p|(c,p)\in lcp} FlowCP(c,p,t) + \sum_{c\prime|(c,c\prime)\in lcc} FlowCC(c,c',t) \right) = \sum_{w|(w,c)\in lwc} CompW(i,w,t) * FlowWC(w,c,t) + \sum_{c\prime|(c\prime,c)\in lcc} CompC(i,c',t) * FlowCC(c',c,t) \quad \forall\, i,c,t \tag{4.31}$$

4.3.5.3 Capacity for compressor stations

Constraints on the maximum capacity for compressor stations are defined in Equation (4.32), using a similar approach to that in the gas pipeline case. The parameter $Sizec(m)$ defines the potential capacities for the expansion of compressor stations. Additionally, the binary variable $InstC(m,c,t)$ is equal to one if a capacity expansion of size m is assigned to compressor station c during period t, the binary variable is equal to zero otherwise. Equation (4.33) is used to guarantee that up to one size is selected for capacity expansions of compressor stations during a given time period.

$$\sum_{p|(c,p)\in lcp} FlowCP(c,p,t) + \sum_{c\prime|(c,c\prime)\in lcc} FlowCC(c,c',t) = \sum_{t\prime\le t} \sum_{m} Sizec(m) * InstC(m,c,t'-t_c) \quad \forall\, c,t \tag{4.32}$$

$$\sum_{m} InstC(m,c,t) \leq 1 \quad \forall\, c,t \tag{4.33}$$

4.3.5.4 Gas pipeline capacity: Between compressor stations

Analogous to capacity constraints for gas pipelines from well-pads to compressor station, capacity for gas pipelines between compressors is defined in Equation (4.34). Here, the binary variable $InstPcc(q,c,c',t)$ is equal to one if a capacity expansion of size q is assigned to gas pipeline from compressor station c to compressor station c' during period t, the binary variable is equal to zero otherwise. Equation (4.35) guarantees that up to one size is selected for capacity expansions of gas pipelines between compressor stations in a single period.

$$FlowCC(c,c',t) \leq \sum_{t' \leq t} \sum_{q \in v} Sizep(q) * InstPcc(q,c,c',t'-t_d) \quad \forall\, (c,c') | (c,c') \in lcc,t \tag{4.34}$$

$$\sum_{q \in v} InstPcc(q,c,c',t) \leq 1 \quad \forall\, (c,c') | (c,c') \in lcc,t \tag{4.35}$$

4.3.5.5 Gas pipeline capacity: Compressor stations to gas plants

The maximum capacity for gas pipelines between compressor stations and gas plants is defined in Equation (4.36). The binary variable $InstPcp(q,c,p,t)$ is equal to one if a capacity expansion of size q is assigned to gas pipeline from compressor station c to gas plant p during period t; the binary variable is equal to zero otherwise. Equation (4.37) guarantees that up to one size is selected for capacity expansions of gas pipelines from compressor stations to gas plants in a single period.

$$FlowCP(c,p,t) \leq \sum_{t' \leq t} \sum_{q \in v} Sizep(q) * InstPcp(q,c,p,t'-t_d) \quad \forall\, (c,p) | (c,p) \in lcp,t \tag{4.36}$$

$$\sum_{q \in v} InstPcp(q,c,p,t) \leq 1 \quad \forall\, (c,p) | (c,p) \in lcp,t \tag{4.37}$$

4.3.5.6 Gas pipeline capacities: Well-pads to gas plants

The capacity constraint for gas pipelines from well-pads to gas plants is expressed in Equation (4.38). The binary variable $InstPwp(q,w,p,t)$ is equal to one if a capacity expansion of size q is assigned to gas pipeline from well-pad w to gas plant p during period t; the binary variable is equal to zero otherwise. Equation (4.39) guarantees that up to one size is selected for capacity expansions of gas pipelines between well-pads and gas plants in a single period.

$$FlowWP(w,p,t) \leq \sum_{t' \leq t} \sum_{q \in v} Sizep(q) * InstPwp(q,w,p,t'-t_d) \quad \forall (w,p)|(w,p) \in lwp,t \tag{4.38}$$

$$\sum_{q \in v} InstPwp(q,w,p,t) \leq 1 \quad \forall (w,p)|(w,p) \in lwp,t \tag{4.39}$$

4.3.5.7 Capital and operating expenditures

Capital expenditures for new gas pipelines are calculated using Equation (4.40). Parameters $CapexPwc(w,c,q)$ and $CapexPwp(w,p,q)$ are related to capital expenditures for gas pipelines from well-pads to compressor stations and from well-pads to gas plants, respectively. Similarly, parameters $CapexPcc(c,c',q)$ and $CapexPcp(c,p,q)$ are related to capital expenditures for gas pipelines between compressor stations and from compressor stations to gas plants, respectively. Capital expenditures for compressor stations are estimated using Equation (4.41), where parameter $CapexCom(m,c)$ represents the Capex for compressor stations as function of their capacities. In addition, operating expenditures for compressor stations are estimated in terms of total output gas flow, as stated in Equation (4.42). The parameter $OpexCom(c)$ is defined as the unit operating expenditures for compressor stations.

$$\begin{aligned} CapexPI(t) = & \sum_{w} \sum_{c|(w,c)\in lwc} \sum_{q\in v} CapexPwc(w,c,q) * InstPwc(q,w,c,t) \\ & + \sum_{w} \sum_{p|(w,p)\in lwp} \sum_{q\in v} CapexPwp(w,p,q) * InstPwp(q,w,p,t) \\ & + \sum_{c} \sum_{c\prime|(c,c\prime)\in lcc} \sum_{q\in v} CapexPcc(c,c',q) * InstPcc(q,c,c',t) \\ & + \sum_{c} \sum_{p|(c,p)\in lcp} \sum_{q\in v} CapexPcp(c,p,q) * InstPcp(q,c,p,t) \quad \forall\, t \end{aligned} \tag{4.40}$$

$$CapexCO(t) = \sum_{c} \sum_{m} CapexCom(m,c) * InstC(m,c,t) \quad \forall\, t \tag{4.41}$$

$$\begin{aligned} OpexCO(t) = & \sum_{c} OpexCom(c) \\ & * \left(\sum_{c\prime|(c,c\prime)\in lcc} FlowCC(c,c',t) + \sum_{p|(c,p)\in lcp} FlowCP(c,p,t) \right) \quad \forall\, t \end{aligned} \tag{4.42}$$

4.3.6 Wastewater treatment plants

Wastewater recovered from well-pads can be treated in water plants to meet quality requirements either for re-use or recycling. Moreover, wastewater and treated water can be stored in tanks located in water plants in order to be treated or used when needed. The corresponding layout of the water treatment process is presented in Figure 4.2.

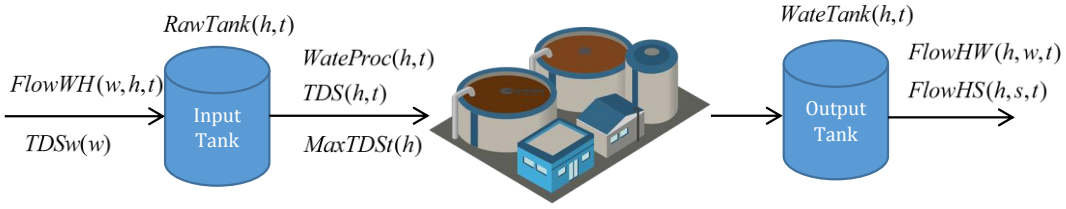

Figure 4.2. Water treatment plant schematics

4.3.6.1 Maximum treatment capacity and specifications for wastewater

The amount of wastewater that can be processed by a plant, $WateProc(h,t)$, is limited by the water plant capacity which is equal to the cumulative capacity expansion from the first period until period $t' - t_h$; this constraint is defined in Equation (4.43). The parameter $Sizeh(k)$ represents the potential sizes for capacity

expansions of water treatment plants. The scalar t_h represents the lead time for water treatment plant construction. The binary variable $InstH(k,h,t)$ is equal to one if a capacity expansion of size k is assigned to plant h during period t, the binary variable is equal to zero otherwise. Equation (4.44) ensures that no more than one size is assigned to capacity expansions of a specific plant in a given time period.

$$WateProc(h,t) \leq \sum_{t' \leq t} \sum_{k} Sizeh(k) * InstH(k,h,t'-t_h) \quad \forall\, h,t \tag{4.43}$$

$$\sum_{k} InstH(k,h,t) \leq 1 \quad \forall\, h,t \tag{4.44}$$

Likewise, wastewater has to meet some specifications (i.e maximum TDS concentration) in order to be treated by a specific treatment plant, depending on its technology (i.e. distillation, crystallisation, and reverse osmosis). In order to simplify the mathematical formulation to be linear, the restriction on the maximum TDS concentration treatable by a certain technology is imposed before the input tank shown in Figure 4.2. This is modelled by the Equation (4.45) that accounts for the specification on the maximum TDS concentration on wastewater. The parameters $TDSw(w)$ and $MaxTDSt(h)$ represent the TDS concentration in wastewater from each well-pad and the maximum TDS concentration that each treatment plant can handle, respectively. In this formulation only the specification for TDS concentration is considered. However, the formulation can be easily extended to account for the treatment of additional contaminants.

$$\begin{aligned} \sum_{w|(h,w)\in lhw} TDSw(w) * FlowWH(w,h,t) \\ \leq MaxTDSt(h) * \sum_{w|(h,w)\in lhw} FlowWH(w,h,t) \quad \forall\, h,t \end{aligned} \tag{4.45}$$

It is worth mentioning that although the linear version of the maximum TDS constraint is an approximation, it ensures that the technical limitations of a plant operating with a certain technology are still valid. If a more general formulation is required, then Equation (4.45) should be replaced by Equations (4.46) and (4.47). In this case, the variable $TDS(h,t)$ is introduced to account for the TDS concentration

in the input tank, which is equal to the TDS concentration in the stream $WateProc(h,t)$. The material balance for the input tank is presented in Equation (4.46). The right and left-hand side of this equation introduces a nonlinearity due to the product of the TDS concentration and the variables $RawTank(h,t)$ and $WateProc(h,t)$. The maximum TDS concentration that can be processed by a plant is expressed by the Equation (4.47). The variable $RawTank(h,t)$ refers to the quantity of water stored in inlet tank associated with water plant h in period t.

$$\sum_{w|(h,w)\in lhw} TDSw(w) * FlowWH(w,h,t) + TDS(h,t-1) * RawTank(h,t-1) \leq TDS(h,t) * \ (RawTank(h,t) + WateProc(h,t)) \ \forall\, h,t \tag{4.46}$$

$$TDS(h,t) \leq MaxTDS(h) \ \forall\, h,t \tag{4.47}$$

4.3.6.2 Material balance

Tanks for storage of wastewater are included in the formulation as an optional step before the water treatment process. The corresponding material balance is presented in Equation (4.48). The storage of wastewater is limited by the maximum capacity of a tank, $RawCap(k)$, and conditioned on the availability of a water plant represented by the binary variable $InstH(k,h,t'-t_h)$; this is modelled by means of equation (4.49). The material balance across water plants is described in Equation (4.50), where set lhs defines the linkage between water treatment plants and disposal sites. The variable $FlowHS(h,s,t)$ defines the flow rate of treated water from plant h to disposal site s during period t. The water recovery factor for each water treatment plant is defined by the parameter $\psi(h)$. In addition, variable $WateTank(h,t)$ is defined as the volume of treated water that remains in the storage tank associated with plant h at the end of period t. Since storage tanks have finite capacities, Equation (4.51) guarantees that water storage capacities are not exceeded. The parameter $TankCap(k)$ represents the potential capacities for expansions of storage tanks in water plants.

$$\sum_{w|(h,w)\in lhw} FlowWH(w,h,t) + RawTank(h,t-1) = WateProc(h,t) + RawTank(h,t) \;\; \forall\, h,t \tag{4.48}$$

$$RawTank(h,t) = \sum_{t\prime \le t} \sum_{k} RawCap(k) * InstH(k,h,t'-t_h) \;\; \forall\, h,t \tag{4.49}$$

$$\psi(h) * WateProc(h,t) + WateTank(h,t-1) = \sum_{w|(h,w)\in lhw} FlowWH(h,w,t) + \sum_{s|(h,s)\in lhs} FlowHS(h,s,t) + WateTank(h,t) \;\; \forall\, h,t \tag{4.50}$$

$$WateTank(h,t) \le \sum_{t\prime \le t} \sum_{k} TankCap(k) * InstH(k,h,t'-t_h) \;\; \forall\, h,t \tag{4.51}$$

4.3.6.3 Treated water transportation costs

The costs related to water transportation from water treatment plants to well-pads are estimated using Equation (4.52). The parameter $CostRech(h,w)$ represents the unit transportation cost for treated water from plant h to well-pad w. Moreover, the cost related to water transportation from water treatment plants to disposal sites is given by Equation (4.53), where the parameter $CostRecs(h,s)$ represents the unit transportation cost for treated water from treatment water plants to disposal sites.

$$CostHW(t) = \sum_{h} \sum_{w|(h,w)\in lhw} CostRech(h,w) * FlowHW(h,w,t) \quad \forall\, t \tag{4.52}$$

$$CostHS(t) = \sum_{h} \sum_{s|(h,s)\in lhs} CostRecs(h,s) * FlowHS(h,s,t) \quad \forall\, t \tag{4.53}$$

4.3.6.4 Capital and operating expenditures

Capital expenditures associated with the installation of new water treatment plants are estimated using Equation (4.54). The parameter $CapexWate(k,h)$ defines the capital cost for potential capacities of water treatment plants. Operating

expenditures are estimated as described in Equation (4.55), where the parameter $OpexWate(h)$ represents the operating cost associated to plant h.

$$CapexWA(t) = \sum_{h}\sum_{k} CapexWate(k,h) * InstH(h,t) \quad \forall t \tag{4.54}$$

$$OpexWA(t) = \sum_{h} OpexWate(h) * \sum_{w|(h,w)\in lhw} FlowWH(w,h,t) \quad \forall t \tag{4.55}$$

4.3.7 Gas treatment plants

In order to deliver gas and liquid products to final customers, the raw gas needs to be treated and separated in gas processing plants.

4.3.7.1 Processing capacity

The gas processing capacity is defined as the cumulative capacity expansion from the first period until period $t - t_g$, as expressed in capacity constraint defined in Equation (4.56). The parameter $Sizeg(g)$ defines the potential capacities for installation and expansion of gas plant. The scalar t_g accounts for the lead-time for construction of gas plants. The binary variable $InstG(g,p,t)$ is equal to one if a capacity expansion of size g is assigned to plant p during period t, the binary variable is equal to zero otherwise. Equation (4.57) ensures that capacity expansions take only one size at a time. If the supply chain model is forced to choose only one gas processing plant, Equations (4.58) and (4.59) should be added to the mathematical formulation. Binary variable $PlanSite(p)$ is equal to 1 is a gas processing plant p is selected: the binary variable is equal zero otherwise. Additionally, the scalar $MaxExp$ denotes the maximum number of expansions that is allowed for gas processing plants.

$$\sum_{w|(w,p)\in lwp} FlowWP(w,p,t) + \sum_{c|(c,p)\in lcp} FlowCP(c,p,t) \leq \sum_{t'\leq t}\sum_{g} Sizeg(g) * InstG(g,p,t'-t_g) \quad \forall p,t \tag{4.56}$$

$$\sum_{g} InstG(g,p,t) \leq 1 \quad \forall\, p,t \tag{4.57}$$

$$\sum_{p} PlanSite(p) \leq 1 \tag{4.58}$$

$$\sum_{t}\sum_{g} InstG(g,p,t) \leq MaxExp * PlanSite(p) \quad \forall\, p \tag{4.59}$$

4.3.7.2 Material balance

The material balance for gas plants is given by Equation (4.60). As defined in previous sections, terms $CompW(i,w,t)$ and $CompC(i,c,t)$ are related to the composition of shale gas streams from well-pads and compressor stations, respectively. These terms can be constants in the case that shale gas composition is considered to be constant everywhere and over the planning time. Nevertheless, in the general case these terms will be variable and thus Equation (4.60) becomes bilinear. The parameter $\phi(i,p)$ accounts for the separation efficiency in gas plants. The linkage between gas components and demand centres is defined by the set lij. The variable $FlowPJ(p,i,j,t)$ denotes the flow rate of component i from gas plant p to demand centre j during period t. If only one gas plant is allowed to be installed, then the material balance across the gas plants is reduced to Equation (4.61), which is linear.

$$\phi(i,p) * \left(\begin{array}{l} \sum_{c|(c,p)\in lcp} CompC(i,c,t) * FlowCP(c,p,t) + \\ \sum_{w|(w,p)\in lwp} CompW(i,w,t) * FlowWP(w,p,t) \end{array} \right) = \sum_{j|j\in lij} FlowPJ(p,i,j,t) \quad \forall\, i | i \neq C_{3+}, p, t \tag{4.60}$$

$$\phi(i,p) * \sum_{w} Prod(i,w,t) = \sum_{j|j\in lij} FlowPJ(p,i,j,t) \quad \forall\, i | i \neq C_{3+}, p, t \tag{4.61}$$

4.3.7.3 Income from selling C_{3+} at gas processing plant locations

As was mentioned before, C_{3+} hydrocarbons are assumed to be sold at gas processing plant locations. Equations (4.62) and (4.63) are used to calculate the

revenue from selling C_{3+} hydrocarbons for the general case (variable composition) and the case with only one gas processing plant , respectively. The parameter $PriceC3(p,t)$ represents the prices of C_{3+} hydrocarbons at gas processing plant p during period t.

$$ReveC3(t) = \sum_{p}\left(PriceC3(p,t) * \phi('C_{3+}', p) * \left(\sum_{c|(c,p)\in lcp} CompC('C_{3+}', w, t) * FlowCP(c, p, t) + \sum_{w|(w,p)\in lwp} CompW('C_{3+}', w, t) * FlowWP(w, p, t) \right) \right) \quad \forall t \tag{4.62}$$

$$ReveC3(t) = \sum_{p} Price(p,t) * \phi('C_{3+}', p) * \sum_{w} Prod('C_{3+}', w, t) \quad \forall t \tag{4.63}$$

4.3.7.4 Capital and operating expenditures

Capital and operating expenditures for gas processing plants are estimated using Equations (4.64) and (4.65), respectively. The parameter $CapexGas(g,p)$ represents capital investment for potential capacities of gas plants. Similarly, parameter $OpexGas(p)$ represents the unit operating expenditures for gas plants.

$$CapexGA(t) = \sum_{p}\sum_{g} CapexGas(g, p) * InstG(p,t) \quad \forall t \tag{4.64}$$

$$OpexGA(t) = \sum_{p} OpexGas(p) * \left(\sum_{w|(w,p)\in lwp} FlowWP(w, p, t) + \sum_{c|(c,p)\in lcp} FlowCP(c, p, t) \right) \quad \forall t \tag{4.65}$$

4.3.8 Product pipelines and Demand centres

Final products can be transported to demand centres through either gas or liquid pipelines, depending on the nature of the final product that is required.

4.3.8.1 Capacity for product pipelines between gas plants and demand centres

Capacity constraint for gas pipelines between gas plants and demand centres is defined in Equation (4.66). Similarly, Equation (4.67) defines the capacity constraint for liquid pipelines between gas plants and demand centres. Equation

(4.68) is used to guarantee that no more than one size is selected for capacity expansions of a specific pipeline from gas plants to demand centres during a given time period. The parameter $Sizepl(u)$ defines potential sizes for liquid pipelines, where set u defines the sizes available for liquid pipelines. The variable $InstPpj(q,p,j,t)$ is equal to one if a capacity expansion of size q is assigned to gas pipeline from gas plant p to demand centre j during period t, the binary variable is equal to zero otherwise. Demand centres associated to gas products are defined by set jg, while demand centres associated with liquid products are defined by set jl. It is assumed here that each demand centre is associated with only one product.

$$\sum_{i|(i,j)\in lij} FlowPJ(p,i,j,t) \le \sum_{t'\le t}\sum_{q\in v} Sizep(q) * InstPpj(q,p,j,t'-t_d) \quad \forall\, p,j \,|\, j \in jg, t \tag{4.66}$$

$$\sum_{i|(i,j)\in lij} FlowPJ(p,i,j,t) \le \sum_{t'\le t}\sum_{q\in u} Sizepl(q) * InstPpj(q,p,j,t'-t_d) \quad \forall\, p,j \,|\, j \in jl, t \tag{4.67}$$

$$\sum_{q} InstPpj(q,p,j,t) \le 1 \quad \forall\, p,j,t \tag{4.68}$$

4.3.8.2 Capital expenditures and final product demands

Capital expenditures for pipelines transporting final products are estimated from Equation (4.69). The parameter $CapexPpj(p,j,q)$ represents capital investment for product pipelines. Equation (4.70) ensures that final product flows do not exceed maximum demand for final products in any demand centre during each time period. Product demand is denoted by the parameter $Dem(j,t)$.

$$CapexPJ(t) = \sum_{p}\sum_{j}\sum_{q} CapexPpj(p,j,q) * InstPpj(q,p,j,t) \quad \forall\, t \tag{4.69}$$

$$\sum_{i|(i,j)\in lij}\sum_{p} FlowPJ(p,i,j,t) \le Dem(j,t) \quad \forall\, j,t \tag{4.70}$$

4.3.9 Disposal sites

There are different types of water disposal sites, for instance, rivers and injection sites. Each disposal site can have limitations in terms of capacity, as stated in Equation (4.71). The parameter $CapDis(s,t)$ represents the capacities for disposal sites. In addition, some of those disposal sites can entail operating expenditures, as is the case for underground injection sites. Operating expenditures for disposal sites are estimated by using Equation (4.72), where operating cost are represented by parameter $OpexDis(s)$. It is important to clarify that, only certain water treatment plants can discharge water into rivers, this depends on their technology and on the water quality constraints for disposal established by local regulations.

$$\sum_{w|w\in lws} FlowWS(w,s,t) + \sum_{h|h\in lhs} FlowHS(h,s,t) \le CapDis(s,t) \quad \forall\, s,t \tag{4.71}$$

$$OpexDI(t) = \sum_{s} OpexDis(s) * \left(\sum_{w|w\in lws} FlowWS(w,s,t) + \sum_{h|h\in lhs} FlowHS(h,s,t) \right) \quad \forall\, t \tag{4.72}$$

4.3.10 Model summary

There are two particular cases where the shale gas supply chain optimisation model described above becomes a Mixed Integer Programming (MILP) problem. First, when shale gas composition is considered constant across the shale formation and over the planning time, then the bilinear terms associated with the estimation of compositions in the outlet stream of the compressors are not required in the model formulation. Therefore, the optimisation model becomes MILP. Secondly, in the case where no more than one gas processing plant is allowed, the estimation of the output compositions in the compressors is not necessary. Instead, component flows are used in the material balances associated with the gas processing units. Consequently, despite of the fact that the gas composition could be variable, the optimisation model will remain as an MILP.

It was pointed out in the previous sections, that the shale gas composition could depend on well-pad location and/or well-pad age. In this case, the shale gas composition in outlet streams from well-pads and compressor stations are variables.

Additionally, the TDS concentration on wastewater can vary not only spatially but also temporally. In this case, TDS concentration associated with wastewater from well-pads is a variable rather than a parameter. In other words, parameter $TDSw(w)$ becomes variable $TDSw(w,t)$, which can be estimated as function of the binary variable $WellDes(d,w,t)$ using an expression similar to equation (4.18). In the general case, the model would be classified as a Mixed Integer Nonlinear Programming (MINLP) problem given that bilinear terms are present in the mathematical model. These bilinear terms, which are nonconvex, are due to the product of two continuous variables, flow rates and either gas composition or TDS concentration. Therefore, the model can be classified as a Mixed Integer Bilinear Programing problem, which is a subclass of Mixed Integer Quadratically Constrained Programing (MIQCP) problems. These types of optimisation problems can be transformed into an MILP problem by the convexification of bilinear products, for instance, through convex hull approximation of the bilinear terms [241–244]. The solution to this sub-problem provides an upper bound to the original MIQCP problem and an iterative solution approach is needed in order to get a solution close enough to the global optima. Although solvers like DICOPT [245] and SBB [246] can be used to solve the original MIQCP problem, those solvers can lead to local optimal solutions in most cases. Finally, global optimisation solvers like ANTIGONE (actually GloMIQO) [247,248], BARON [249,250], and LindoGlobal [251] can be used at the expense of high computational times. Since there is a trade-off between solution quality and computational cost, it is appropriate to test all those options in order to define the more effective approach to solve the MIQCP optimisation problem. Further details regarding the spatial and temporal variation in gas composition can be found in Guerra et al. [45]. Finally, all of the possible models that can result from the mathematical formulation for shale gas supply chain optimisation are summarised in Table 4.1.

Table 4.1. Model summary: Shale Gas Supply Chain.

Case	Set of Equations	Model Classification
Constant gas composition	(4.1)-(4.17), (4.20)-(4.30), (4.32)-(4.45), (4.48)-(4.57), (4.60), (4.62), and (4.64)-(4.72)	MILP
Up to 1 gas plant	(4.1)-(4.17), (4.19)-(4.30), (4.32)-(4.45), (4.48)-(4.56), (4.58), (4.59), (4.61), and (4.63)-(4.72)	MILP
General case	(4.1)-(4.18), (4.20)-(4.44),(4.46)-(4.57), (4.60), (4.62), and (4.64)-(4.72)	MIQCP

4.4 Case study definition[5]

The infrastructure for the case studies was designed based on the Middle Magdalena Valley Basin, which is a prospective shale play in Colombia. All case studies are based on the same potential infrastructure for gas and water transportation and processing. Three different instances are considered: Case A1, A2 and A3. For this case study, the designs "14w_9000L_200s" and "6w_5000L_200s" were selected. These designs were chosen based on their economic performance and environmental impact (see Chapter 2), and will be referred to as "MaxNPV" and "MinWI". The potential infrastructure for gas and water supply chain for Case A1 (see Figure 4.3) was designed in ArcGIS 10.2 as follows: The well-pads denoted as W1 and W4 are connected to the compressor station 1. The well-pads W2 and W3 are connected to the compressor station 2. The well-pad W6 can send the produced gas to the compressor station 1 and/or 2. Only the well-pad W5 is connected directly to a gas treatment plant, in this case, gas plant 2. According to geochemistry information of the area, the location of the well-pads coincides with a wet-gas bearing shale formation. Moreover, it was assumed that the composition of shale gas was constant with time and location of the well-pads. After the raw gas is processed, the final products are sent to the demand centres. In this case, three injection points located along the National pipeline network in Colombia are considered as demand centres. The methane fraction produced in gas plant 1 and 2, can be delivered to two

[5] This section is based on manuscript II of the list of publications presented at the end of this thesis

different injection points in the southwest or southeast, respectively. These injection points are subsequently connected to several gas-based power plants. Only one common point placed in north of the shale play is included for ethane injection. This point is indirectly connected to a petrochemical plant. The prices of the final products were based on information from the Colombian Mining and Energy Planning Unit-UPME (http://www1.upme.gov.co/). The fresh water requirements for drilling and fracturing operation in well-pad locations can be supplied from three rivers. River III supplies water to well-pads W1, W2 and W4; river II is the water source for well-pad W3; and river I supplies fresh water to well-pads W5 and W6. The produced water can be sent by truck to any of the two water treatment facilities. Alternatively, the wastewater can also be sent for deep injection into an adequate well located towards the north of the shale play. The treated water can be recycled and used for drilling and fracturing new well-pads or discharged into rivers I and II. Water trucking is the only transportation mode considered, although additional modes can be included if appropriate.

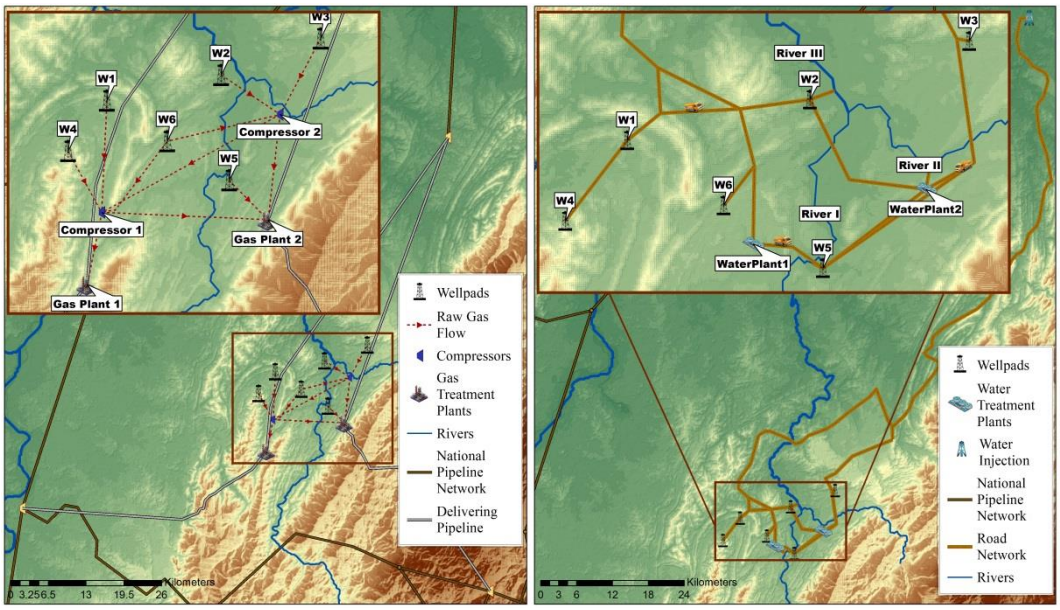

Figure 4.3. Gas supply chain (Left-hand side) and water supply chain (Right-hand side) for a case study with 6 potential well-pads.

The potential infrastructure for gas and water transportation and processing was based a road network connecting the different water sources with the demand points and the treatment facility locations. Regarding the gas transportation network, the

gas pipelines were discretised in three different capacities, where each capacity corresponds to a given commercial diameter depending on the distances between the two connected nodes, for example, the distance between a given well-pad and a given compressor station. The commercial diameters were estimated based on simulations implemented in Aspen Hysys®. The total distances for the different pipeline connections were calculated in ArcGIS 10.2 [240]. This information is used to calculate the installation costs. Two compressor capacities of 150 and 300 MMSCFD were included in the case study. The cost information regarding the installation of a compressor in Colombia was supplied by a local company, under confidential agreement. The energy consumption of the compressors, calculated in Aspen Hysys®, was the basis for estimating the operational costs. Three capacities of 100, 200 and 350 MMSCFD were chosen for the gas treatment plants. The installation costs and the operating costs were based on Aspen Hysys®, Aspen Capital Cost Estimator®, and information provided by local companies in Colombia.

For the water supply chain, the water transportation costs were calculated based on the road network distances. The rivers I, II and III were assumed to have enough available water to drill and fracture 14 wells in the rainy season, which for the specific area under study corresponds to the third quarter of the year. For the dry season, the first quarter of the year, the available water was estimated to be about 50% of the available water in the rainy season. For the second and fourth quarter, this percentage was set at 75%. The total dissolved solids (TDS) concentration on water for the rivers I, II and III were set at 0.13, 0.15 and 0.14 g/L, respectively. The TDS in the produced water was assumed to be different in each well-pad ranging between 34.3 and 106.7 g/L. The capacities of the water treatment plants were discretised in 94,500, 220,500 and 441,000 gallon/day. The water plant 1 operates with primary treatment and can process water with maximum TDS concentration of 50 g/L. The water plant 2 operates with secondary treatment technology which can treat water with TDS concentrations of up to 120 g/L and produces a treated water stream with TDS concentration of 0.1 g/L. The installation and operating costs correspond to the Colombian context and were supplied by local companies under confidential agreement. The maximum discharge flow rate into rivers I and II was set

at 40,000 and 200,000 gallon/day. For the deep well injection technology, the well capacity is limited up to 336,000 gallon/day, with operating costs of 0.75 USD/gallon.

The infrastructure for the 6 well-pad case was extended in Case A2 to an 8-well-pad infrastructure by adding two well-pads, W7 and W8, which are connected to the compressor 2 as shown in Figure 4.4.

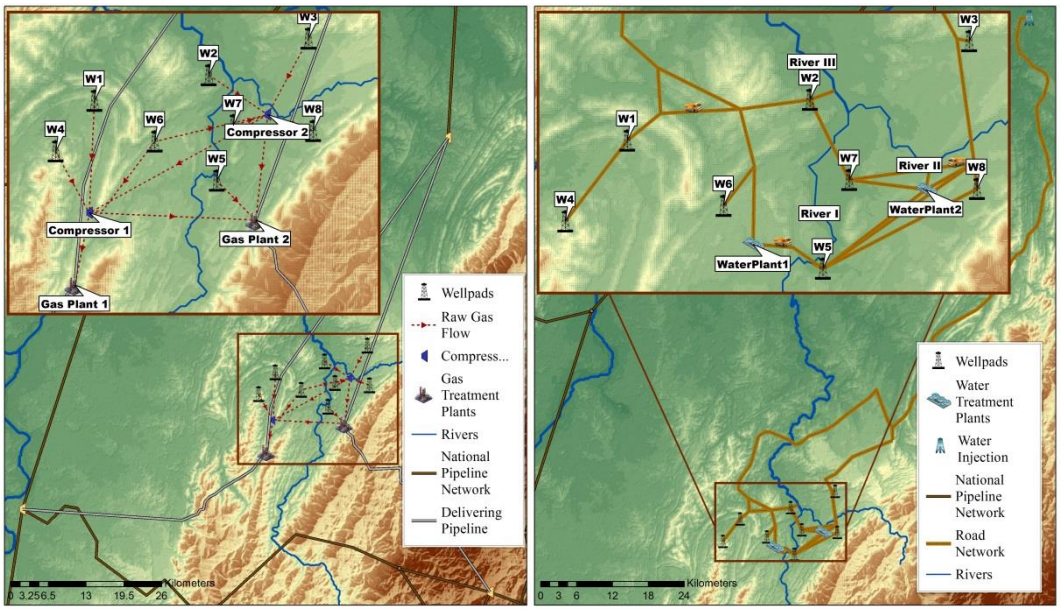

Figure 4.4. Gas supply chain (Left-hand side) and water supply chain (Right-hand side) for a case study with 8 potential well-pads.

The fresh water for the well-pads W7 and W8 is collected from river I and river II, respectively. The wastewater can be disposed into a deep-injection well or sent by truck to be treated in either water plant 1 or 2. The 10-well-pad infrastructure of Case A3 builds upon the previous infrastructure with two new well-pads, W9 and W10 as shown in Figure 4.5.

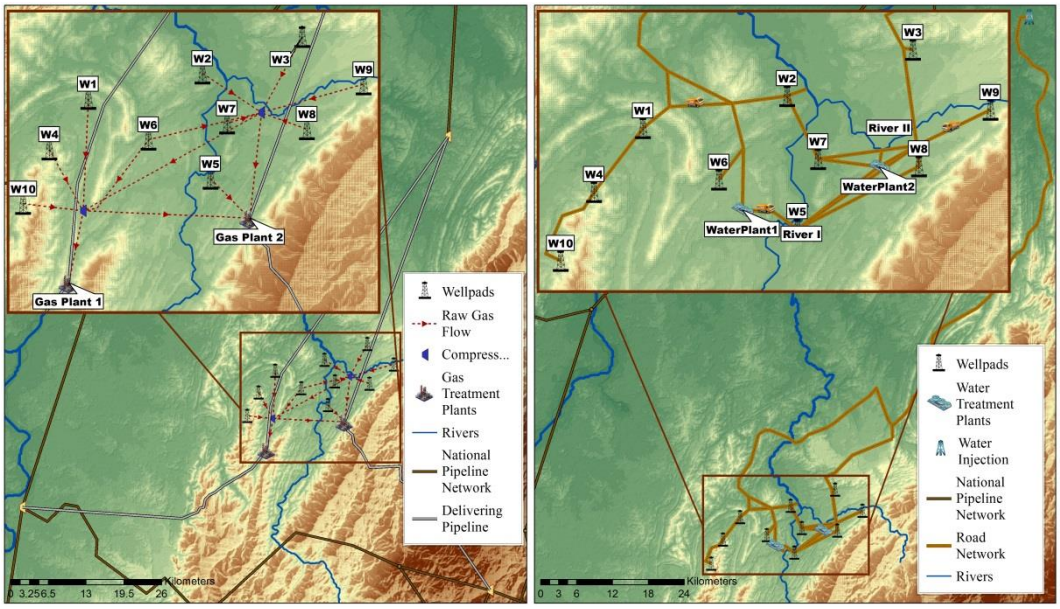

Figure 4.5. Gas supply chain (Left-hand side) and water supply chain (Right-hand side) for a case study with 10 potential well-pads.

The well-pad W9 and W10 are connected to compressors 2 and 1, respectively. The source of fresh water for well-pad W9 is river I whereas the water for the well-pad W10 is supplied by river II. The deep-injection technology for disposing the wastewater is available for the new well-pads. Water plant 1 and 2 can process the wastewater from well-pad W9, and only water plant 1 can process the produced water from well-pad W10. The dataset used in the case studies is presented in Appendix A.

Finally, the MILP problems were solved using GAMS 24.4.1 with CPLEX 12.6.1 on a server with Dual Intel® Xeon® E5620 @2.4Ghz with 4 Cores and 16 GB RAM running Debian Linux. The optimality gap was set to less or equal to 1% for all cases. The model statistics for all of the instances are presented in Table 4.2. As expected, the size of the model increases as the number of well-pads increases.

Table 4.2. Model statistics and computational results for Case Studies A, A2, and A3

	A1 (6 well-pads)	A2 (8 well-pads)	A3 (10 well-pads)
Total number of variables	7,779	8,845	9,831
Continuous variables	5,201	5,921	6,561
Binary variables	2,578	2,924	3,270
Total number of constraints	6,661	7,295	7,929
Non zero constraint matrix elements	87,171	100,233	112,935
CPU time [s]	123.3	518.0	6,666.2
Nodes explored	34,991	151,145	2,590,842
Optimal NPV [Million $]	114.26	333.47	584.39

This increase in the size of the model, especially the increase in the total number of binary variables, has a direct impact on the total number of nodes explored to find a solution that meets the optimality criteria, and therefore on computation times. As observed in Table 4.2, the number of nodes explored and the CPU time increases exponentially with the number of binary variables. Also, the CPU time increases almost linearly with the total number of nodes that are explored, as expected. The dataset used in the case studies is presented in Appendix A

4.5 Results and discussion

4.5.1 Implications of water scarcity (water-energy nexus)

The implications of water scarcity are addressed through a parametric analysis on water availability for Case A3 (10 potential well-pads). The corresponding cumulative cash flows are presented in Figure 4.6.

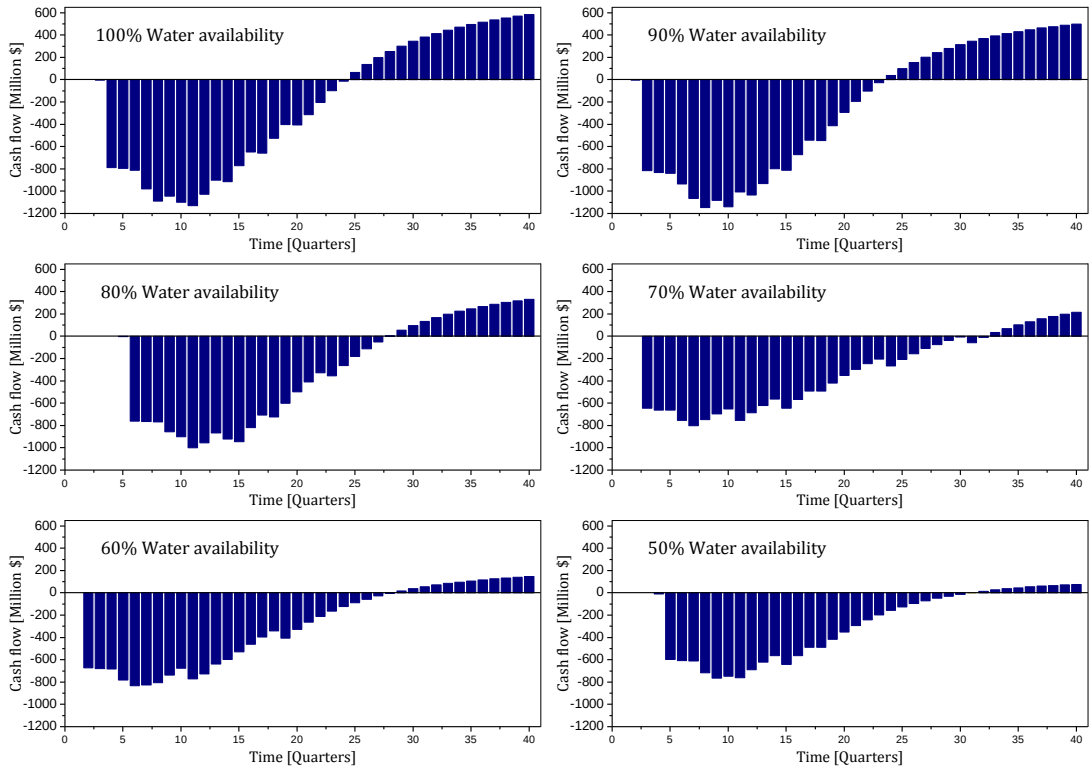

Figure 4.6 Discounted cash flow for Case A3.

Initially, it should be noticed that the initial investments do not occur in the first period and sometimes they happen as late as 6 periods, namely, 1.5 years before the infrastructure development starts. The reason for this behaviour is that the optimisation framework does not consider shutting of wells. Therefore, once a well-pad is installed, it continues producing gas even if the production rate is not favourable. This forces the model to select carefully the periods where the well-pads are installed so that when the production rate has declined this does not affect the economic performance of the supply chain. This causes that sometimes the installation of the well-pads are delayed so that the production rate at the end of the planning horizon does not decrease substantially. As a consequence, since the planning horizon is fixed to 10 years, the timing for investments can be reinterpreted. For instance, if the initial investment was made after 4 periods (1 year), this can be thought of as a project of a total duration of 9 years. The delays in investments for each case will be pointed out in the following discussion.

For the base case (100% Water availability) the initial investment was made in the fourth period, the breakeven point of the project was reached after 22 periods

(5.5 years) and the final NPV is $584.4 million. When the water availability was reduced by 10% (90% Water availability) the initial investment is shifted backwards one period although the time but the breakeven point remains the same as before (5.5 years). Nonetheless, the NPV for this case is $499.6 million, which is a reduction of 14.5% compared to the base case. A further reduction of 20% of fresh water (80% Water availability) causes the breakeven time to increase to 6 years after the initial investment. The NPV is substantially reduced to $332.4 million; 43.1% with respect to the base case. For the 70% Water available case, the project achieves a profit after 31 periods (7.75 years) of the initial investment. The NPV of the project is $218.1 million, which corresponds to a reduction of 62.7% from the base case. For 40% and 50% of water reduction (60% and 50% Water available cases), the breakeven time is 7 years. The NPV for both projects is $148.3 and $78.1 million, which correspond to a reduction of 74.6% and 68.6% from the base case, respectively. Capex, Opex, royalties, and taxes, which are discounted to the first period, and the total cost breakdown for the parametric analysis is depicted in Figure 4.7. The total cost decreased from $3,039.2 million for the base case to $1,575.5 million for the case with 50% reduction of water availability, which is around 48.2% decrease in expenses.

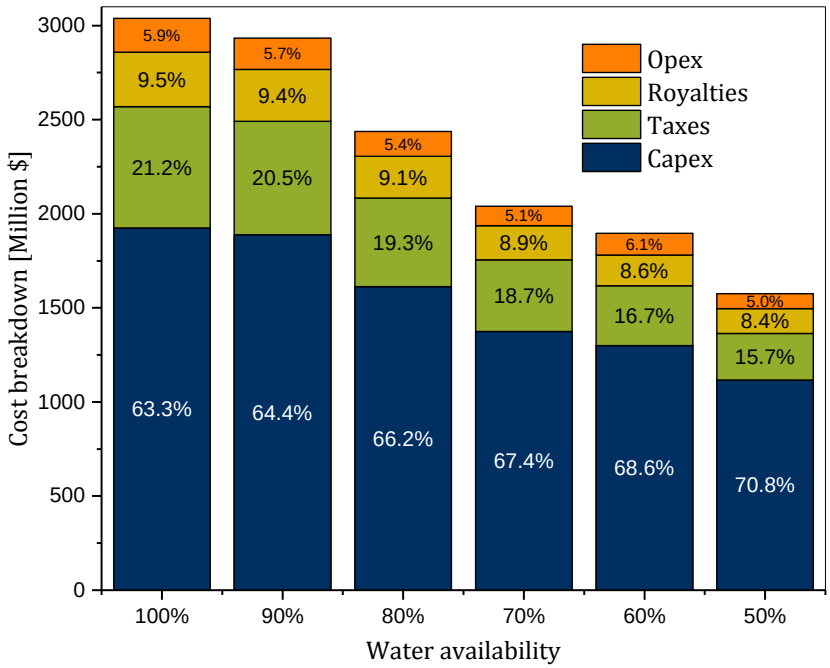

Figure 4.7. Cost breakdown for Case Study A3.

The breakeven price varies from 3.39 $/MMBtu to 4.28 $/MMBtu for the cases of 100% and 50% water availability, respectively. The limitation on fresh water availability is reflected in an increment of 26.4% of the gas breakeven price. These trends suggest a sustained decline in the production, transportation and processing of raw gas. The drop in gas production is evidenced by the tendency for selecting less intensive water designs as the limitations of fresh water become critical.

The well-pad designs selected for every case are summarised in Figure 4.8. Initially, 7 well-pads were installed with MaxNPV configuration, and 3 well-pads with MinWI configuration.

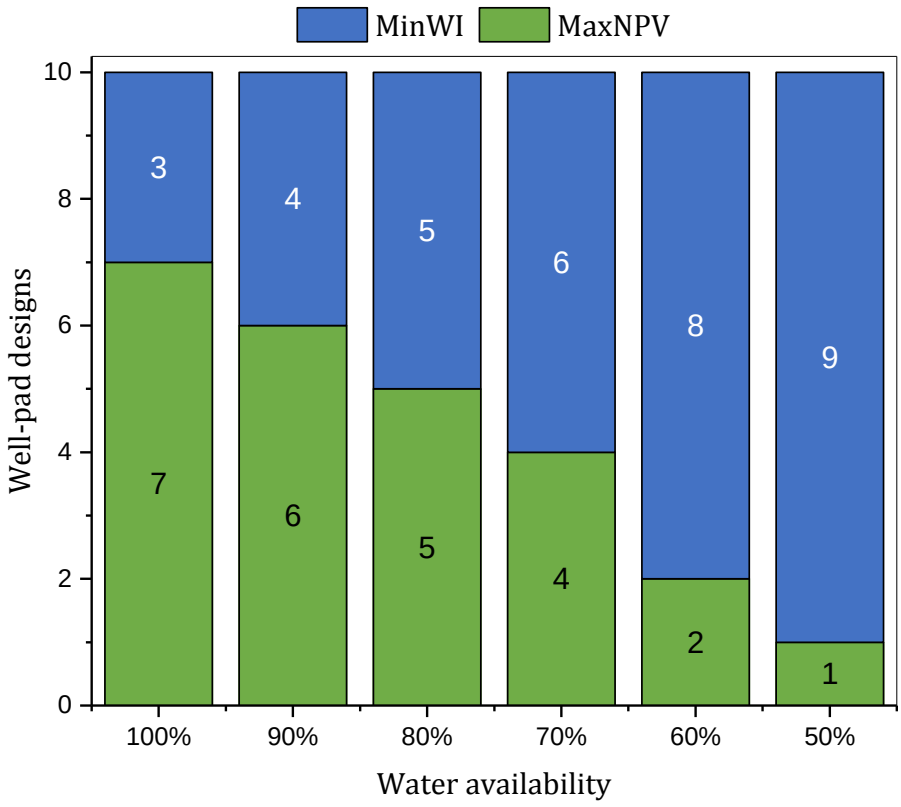

Figure 4.8. Selected well-pad designs for Case Study A3.

For the second case, the configuration of well-pad W10 is shifted from MaxNPV to MinWI. This well-pad is located relatively far from the water sources and from the water treatment facilities; the change of its configuration not only overcomes the limitations of fresh water but also has major impact on reducing the water transportation costs. For the next case, the model opts for a similar decision based on the transportation costs. In this case, the well-pad W3 is drilled and

fractured following a MinWI configuration. In the following cases the MinWI designs become predominant. Finally, for the last case only the well-pad W5 has MaxNPV design, as this well-pad is located close to the water source and water treatment facilities, which results in low transportation costs of water. The drilling scheme for the scenarios is presented in Figure 4.9.

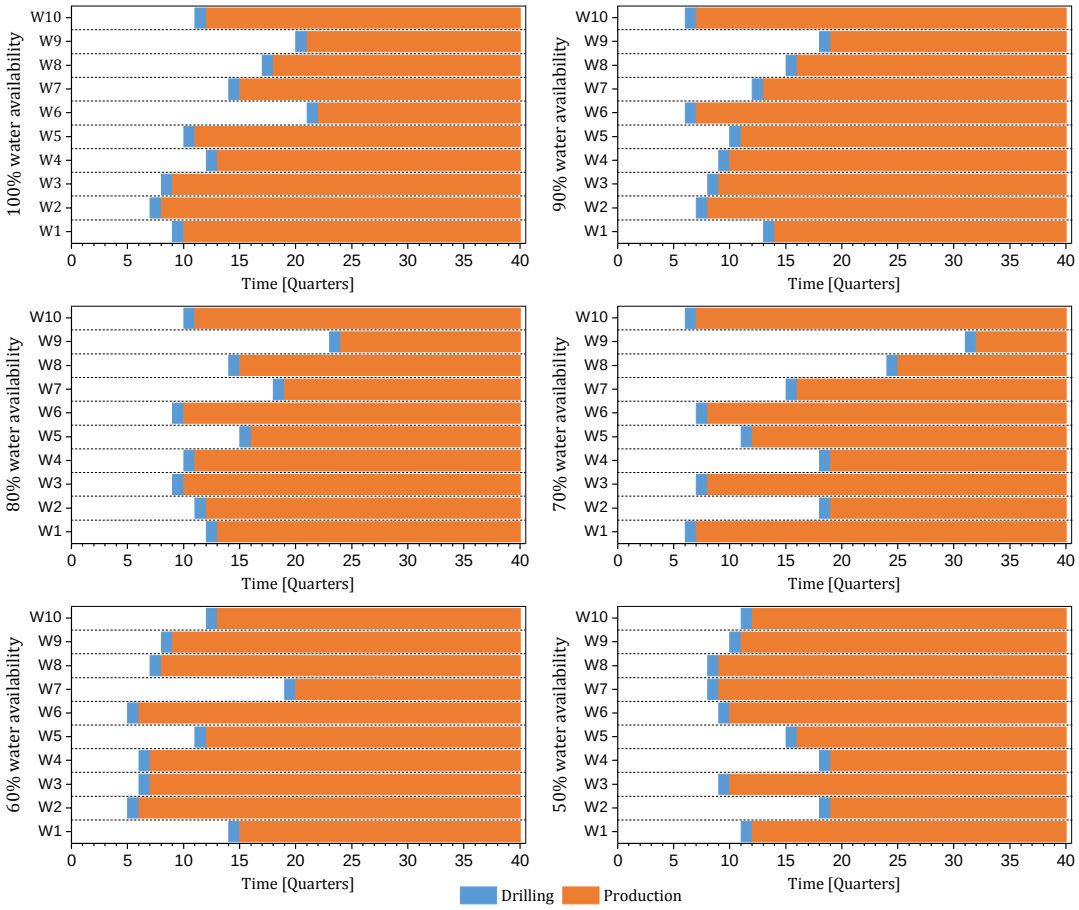

Figure 4.9. Drilling schedule for Case Study A3.

Initially, only one well-pad per period is drilled, however, as the availability of water decreases and more well-pads with MinWI configuration are selected, it is possible to drill two well-pads in the same period. For example, for the case 90% water availability, the well-pads W6 and W10 are drilled simultaneously in period 6. For the next case, 80% water availability, the drilling scheme suggests drilling the well-pads W3 and W6 in period 9 and then W4 and W10 in period 10. Analogous patterns are found for the rest of the cases, although there are not explicit trends in the drilling schedule of the different well-pads. However, there is an interesting tendency in the way pairs of well-pads are chosen to be drilled; they are

complementary in regard to the TDS concentration of the produced water. In our case study, the maximum TDS concentration of the input stream is set to 50 g/L for primary treatment. A pair of well-pads is drilled in such a way that one well-pad has lower TDS concentration in its wastewater and this can be processed with primary treatment, whereas for the second well-pad, the TDS concentration is high and therefore secondary treatment is required or dilution for primary treatment. For example, the well-pads W6 and W10, in the case 90% water availability, have TDS concentrations of 61.05 g/L and 39.9 g/L. This means that 50% of the produced water in that period will be processed with primary treatment, whereas the rest will be treated in a second facility with secondary treatment. A similar behaviour was found for the case with 80% water availability, where the first pair, W3 and W6, has TDS concentrations of 36.7 g/L and 61.0 g/L, respectively. The second pair, W4 and W10, has TDS concentrations of 106.8 g/L and 39.9 g/L, respectively. The same pattern can be found for the rest of the case studies. The reduction in fresh water availability is expected to affect the decisions regarding the water management as shown in Figure 4.10.

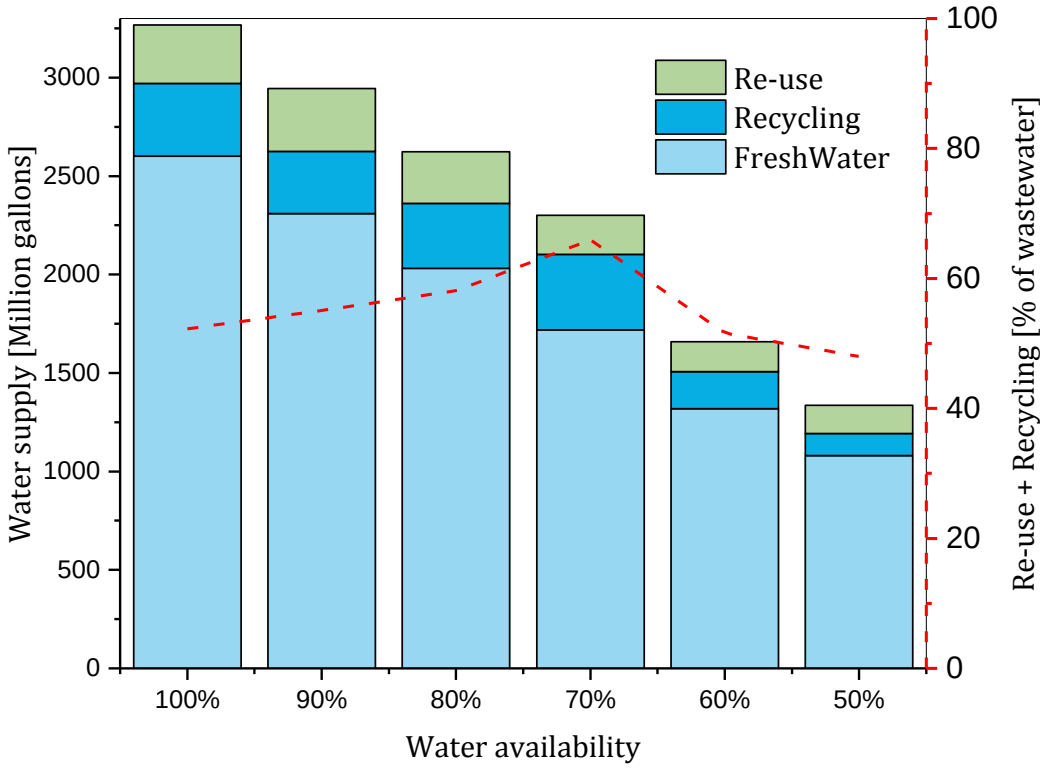

Figure 4.10. Water management strategy for Case Study A3

For the base case, the total water consumption was 3,266.5 million gallons; 2,601.5 million gallons (79.6%) are supplied by the rivers I, II and III, whereas 665.0 million gallons (20.4%) are supplied by water treatment facilities. The total water consumption varies along with the reduction of fresh water. For the final case, 1,080.3 million gallons (80.9%) of fresh water were used for drilling and fracturing operations; 255.8 million gallons (19.1%) are supplied by the water treatment facilities. The total amount of re-used water for the first 4 cases, 100% - 70% water availability, is virtually the same with an average of 618.6 million gallons. The pattern changes for the cases of 60% and 50% water availability, in which 338.5 million gallons and 255.8 million gallons were treated, respectively. This can be explained by the fact that in the last two cases, not only did the fresh water supply decrease, but also the water demand decreases as the MinWI designs become prevalent; as a consequence, the water supply relies less on treated water and the share of fresh water can be higher, reducing capital and operating cost associated with water treatment plants. In general, the results suggest that under water scarcity scenarios, it is preferable to adjust the design of the well-pads to require less water rather than expanding the infrastructure for water treatment.

4.5.2 The role of economies of scale in water-stressed scenarios

High water withdrawal and consumption is one of the major concerns regarding the production of shale gas. On the other hand, the forecast of water availability is subject to uncertainty due mainly to climate and weather variability. The analysis of the water-energy-economy of scale nexus in the context of shale gas development discloses synergies regarding water availability, the configuration of the well-pad, the water management strategy, and the economics of the shale gas development. Thus, a deeper understanding of the repercussions of water availability on the design of the shale gas supply chain is warranted. This goal is addressed, next, by extending the analysis presented in section 4.5.1 to include economies of scale represented by the number of potential well-pads. Four metrics, two related to economics (cumulative production and breakeven price) and two to water management (water consumption and water re-use/recycle), are used to evaluate the impact of water

scarcity on both the economics and the water impacts. The results are summarised in Figure 4.11.

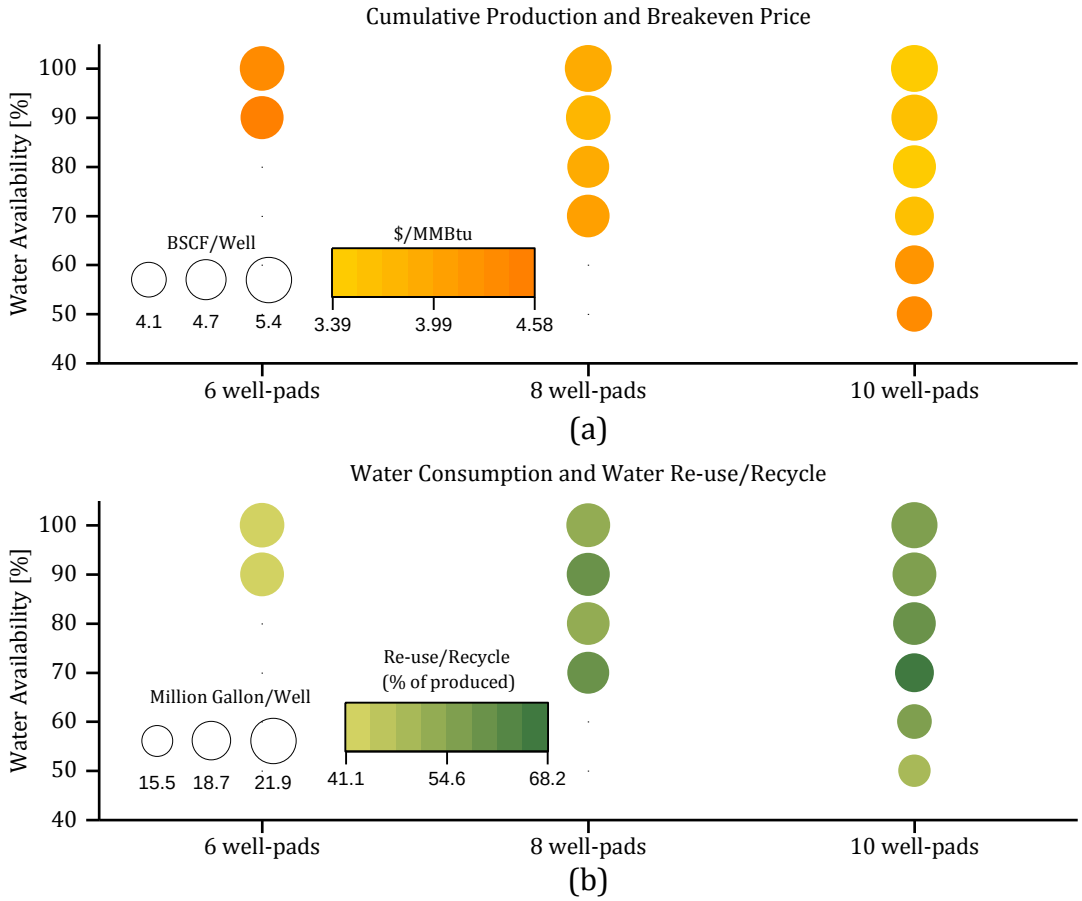

Figure 4.11. Economics and water management strategy as function of freshwater availability: (a) EUR and breakeven price and (b) Water management strategy.

As the results show, a reduction of 20% in the water availability would make Case A1 (6 well-pads) economically infeasible. Moreover, Case A2 (8 well-pads) is not profitable if the availability of freshwater resources is reduced by 40% or more. The optimal NPV decreases monotonically with the increasing water scarcity and increases with the number of well-pads, as shown previously. For instance, for a 10% of reduction in the available freshwater sources, the NPV drops on average $113.1 million, $71.9 million, and $101.3 million for Cases A1, A2, and A3, respectively. This is due to a reduction of installation of well-pads with high productivity configuration. Moreover, water scarcity impacts both the estimate ultimate recovery EUR per well (bubbles size in Figure 4.11a) and the gas breakeven price (colour intensity in Figure 4.11a) of shale gas development. The EUR varies

from 4.1 BSCF/well to 5.4 BSCF/well when the availability of freshwater sources varies up to 50%, with low and high EUR values corresponding to scarcity and abundance of freshwater sources, respectively. The variation in the number of well-pads does not significantly affect the EUR, but water availability has a more prominent effect on EUR. This is more evident for Case A3 (10 well-pads), where a reduction of 50% in fresh water sources generates a cutback of 23.4%, on average, in the productivity of a single well due to the use of less water intensive configurations but which at the same time are less productive. The breakeven price ranges from 3.39 $/MMBtu to 4.58 $/MMBtu. In general, at constant water availability, the breakeven price decreases as the number of potential well-pads increases. For instance, as shown previously, at 100% of water availability, the breakeven price was reduced by 20.9% from Case A1 to Case A3, which is an effect of economies of scale. Furthermore, at constant number of potential well-pads, the breakeven price, in most cases, tends to increase as the scenarios are more water constrained. For Case A2, the breakeven price increased 4.7% for a reduction of 40% in fresh water resources. This variation is more appreciable in Case A3 where the breakeven price increased up to 26.4% when the fresh water sources were reduced by 50%. These trends are due to a sustained decline in the production, which leads to a less efficient use of the transportation and processing infrastructure. Nonetheless, this cannot be generalised as there are two exemptions, such as Case A2, for water availability variation from 100% to 90%, and Case A3, when available freshwater resources changed from 90% to 80%, in which the breakeven price presented a reduction of 2.8% and 1.7%, respectively. For these two cases, the re-scheduling of drilling operations leads to a higher efficiency in the shale gas production, transportation, and processing infrastructure. The breakeven price in Case A3 presented a sharp increment when water availability changed from 70% to 60% in Case A3 which is abrupt when compared to the trend shown from 100% to 70%. This can be explained by the variation of the total number of wells along with the reduction in available fresh water. For instance, when water availability ranges from 100% to 70%, a variation of 10% results, on average, in a reduction of 8% in the total number of installed wells. However, once the water resources were constrained from 70% to 60%, the total installed wells dropped by 21%. The results presented in Figure 4.11a

highlight the water resources as a critical aspect in the design of shale gas supply chains and how limited access to water can have negative effects on well-pads productivity and global economic performance.

The reduction in fresh water availability is also expected to affect decisions regarding the selection of the well-pads configuration and the water management, as shown in Figure 4.11b. Two alternatives can be implemented in order to tackle production of shale gas under scenarios of water scarcity, these are: selection of less water intensive well-pads designs, and intensification of wastewater treatment processes for increasing water re-use and recycle rates. Each alternative, or their combination, can reduce water consumption in the event of water scarcity. Accordingly, Figure 4.11b presents the variations of water consumption per well (bubbles size) and % of water re-use plus recycle (colour intensity) as function of water availability and number of potential well-pads in the shale gas supply chain. The water consumption, defined here as total fresh water withdrawal minus total treated wastewater that is returned to the freshwater sources, ranges from 15.5 million gallon/well to 21.9 million gallon/well. The water consumption decreases monotonically with the scarcity of fresh water sources driven mostly by an increase in the proportion of less water intensive wells and/or an increase in water re-use and recycle. For instance, for Case A3, in which all the 10 well-pads were always selected regardless of water scarcity, the proportion of less water intensive wells increases monotonically from ~15.5% to ~79.4%, reducing water consumption, as the availability of fresh water decreases from 100% to 50%. On the other hand, for Case A2 (8 well-pads), the decrease in water consumption when water availability is reduced from 80% to 70% is due only to an increase in water re-use and recycle, since the proportion of less water intensive wells remains constant at ~36.4%. However, when water availability is reduced from 90% to 80%, both water consumption as well as and water re-use and recycle decrease. This reduction in water consumption is only driven by an increase of ~12.0% in the number of less water intensive wells, which also compensates for the reduction in water re-use and recycle. In Case A2 only 7 well-pads are activated if available fresh water is decreased by 10% or more. Likewise, in Case A1 (6 well-pads) only 5 well-pads are

chosen when the available fresh water is reduced from 100% to 90%. In this case, water consumption decreases as a consequence of an increase from 30.0% to 39.1% in number of less water intensive wells that are selected. This increase also compensates for a reduction of ~2.6% in re-used and recycled water. The previous situation is also observed in Case A3, when the reduction in the available fresh water decreases by 40% or more. Regarding water re-use and recycle, it ranges from 41.1% to 68.2% and in some cases it increases to reduce water withdrawal intensity and mitigate the water scarcity. Nevertheless, there is not a common trend for water re-use and recycle as function of water scarcity.

4.5.3 Wastewater quality and the economics of shale gas development

In a previous work by Guerra et al. [45], the concentration of TDS in wastewater and its impact on the drilling strategy, i.e. well-pad configuration and scheduling of drilling and fracturing operations, for the development of shale gas resources was investigated for a case study composed of 5 potential well-pads. In this work, this is extended to further explore the effect of wastewater TDS concentration in the economics and water management via parametric analysis for the case study addressed in the previous work (5 well-pads), and Case A1 (6 well-pads), Case A2 (8 well-pads), and Case A3 (10 well-pads). The parametric analysis considers 5% step variations from 0 to +/- 10% in the wastewater TDS concentration from the base case (0% variation of TDS or original TDS concentrations). Furthermore, the importance of considering the design of well-pads as a key decision variable in the development of shale gas supply chains was addressed. In this case, the optimal well-pad configuration for each base case (0 % variation of TDS) is kept fixed as the TDS concentration changes from -10 % to 10 %. The corresponding results are summarised in Figure 4.12.

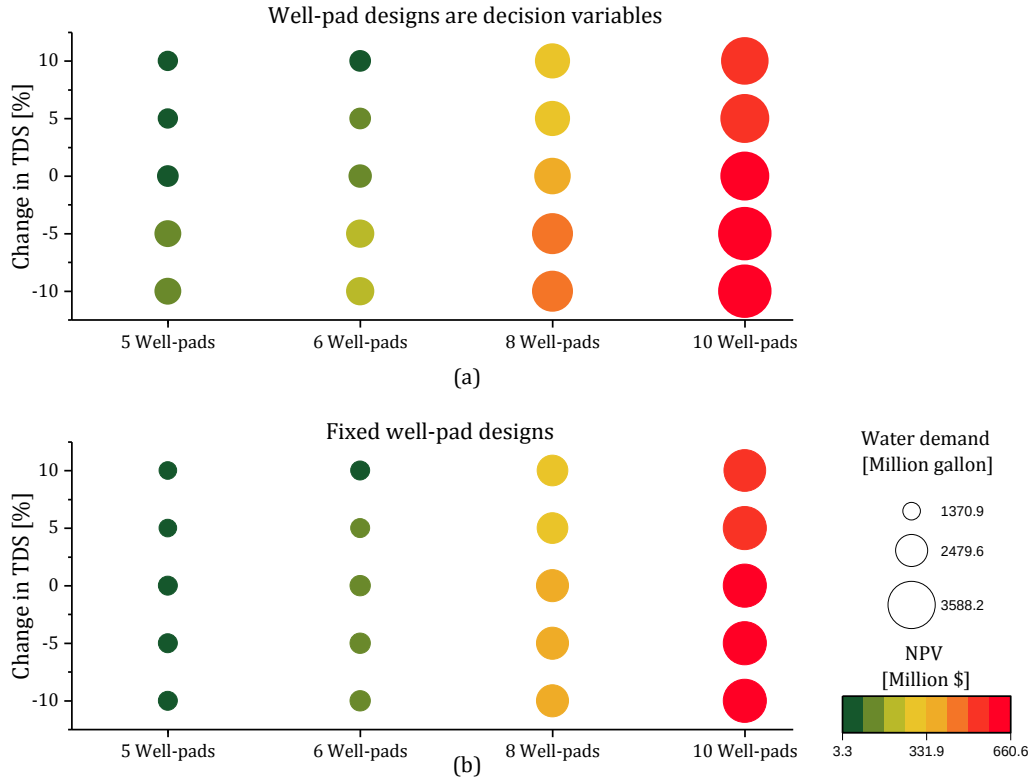

Figure 4.12. Role of TDS wastewater concentration in shale gas supply chains: (a) well-pad designs are considered decisions variables, and (b) well-pad designs are fixed with variation in TDS concentration.

From the results, it is worth to highlight three key aspects: (1) there is an inverse relationship between the TDS concentration in wastewater and the corresponding NPV of the cases presented, (2) the water demand for drilling and fracturing operations decreases as the concentration of TDS in wastewater increases, and (3) as the number of potential well-pads increases, the design of the shale gas supply chain becomes more resilient to changes in the wastewater quality.

The impact of the TDS concentration on the NPV is due to the fact that higher contamination in wastewater requires intensification of water treatment processes, which increases capital and operating costs. This leads to the selection of less water insensitive configurations for well-pads with relatively high concentrations of TDS or to the deactivation of well-pads where TDS concentration is relatively higher. A reduction of TDS achieves the opposite effect; lower TDS allows processing of larger amounts of wastewater which brings about selection of more water insensitive configurations associated with higher gas productivity, thus increasing the NPV. On

average, for adjustable well-pad configurations, a decrease of 10% in TDS concentration in wastewater allows the wastewater treatment facilities to process more wastewater which relates to higher shale gas production, leading to increments of about $68.9 million, $78.3 million, $105.2 million, and $76.2 million on the NPV, for 5 well-pads, 6 well-pads, 8 well-pads, and 10 well-pads, respectively (Figure 4.12a). On the other hand, for fixed well-pad configurations, the NPV increases only $7.2 million, $10.5 million, $14.0 million, and $10.8 million due to the same 10% of decrease in TDS concentration, for the same cases, respectively (Figure 4.12b). Besides quantifying the effects of TDS concentration on the NPV, these results illustrate the additional benefit of including the well-pad configuration as a decision variable in the strategic design and planning of shale gas supply chains. For the cases previously discussed, the NPV could be improved between $61.7 million and $91.2 million by optimising the configuration of the well-pad according to the TDS concentration in wastewater. Another consequence of higher TDS concentration is that the percentage of fresh water utilisation in the optimal water supply mix increases. This is also related to the increment of wastewater treatment cost which impacts the amount of total wastewater send to water treatment plants, therefore, more fresh water is required in order to meet water demand and TDS specifications for drilling and fracturing operations associated with the installation of the well-pads. The previous tendencies can be achieved by decreasing the number of installed well-pads or by a better configuration of the well-pads to exploit more efficiently the gas resources. This is intrinsically related to aspect 2, since well-pads with higher productivity are associated with higher number of wells per well-pad, longer horizontal wells, and more fracturing stages. The installation of well-pads with these characteristics boosts the demand for water. For instance, for adjustable well-pad configurations and for the base case of 5 well-pads, 3 out of 5 well-pads were installed with a high productivity configuration. When TDS increased by 10%, the same number of well-pads were chosen to have high gas production, however, in total only 4 well-pads were selected. As a consequence, the total water demand dropped by 6.9%. By contrast, by reducing the TDS in 10%, 4 out of 5 well-pads were installed with high gas productivity configuration. Accordingly, the water demand was increased by 21.8%. Similar trends were observed for Case A1, Case

A2, and Case A3 in which the variation of TDS in ±10% affected the number and configuration of the well-pads causing fluctuations in the water demand. For Case A1, the water demand varied from -6.4% to 20.4%, for Case A2, these percentages ranged from -4.2% to 13.3%, and for Case A3, the water demand varied from -3.1% to 9.8%. For fixed well-pad configurations, the fluctuations in water demand are less drastic, in fact, the water demand for all the cases is kept constant as the TDS concentration decreases down to -10%. A slight reduction in the water demand was observed when the TDS increased up to 10%. In this case, the water demand for 5, 6, 8, and 10 well-pad cases decreased by 6.8%, 6.4%, 4.2%, and 3.1% in comparison to the base case, respectively. These variations are due exclusively to installation of fewer well-pads. Although less noticeable, the wastewater quality associated with the exploitation of shale gas resources also affects decisions concerning the water management strategies in scenarios where the design of the well-pads are not subject to optimisation. Regarding aspect 3, the influence of the TDS concentration on the NPV and water demand subsides as the number of potential well-pads increases. For cases with adjustable well-pad configurations, the NPV decreases by 96.5%, 55.9%, 32.1%, and 16.7% when TDS concentration ranges from -10% to +10%, for 5, 6, 8, and 10 well-pads, respectively. Similarly, the water demand drops by 23.6%, 22.6%, 15.4%, and 11.8%, for the same cases, respectively. Likewise, for cases in which the configuration of the well-pads is not a decision variable, the NPV presents comparable variations of 90.2%, 32.0%, 14.3%, and 7.6%, whereas for water demand the variations are 6.9%, 6.4%, 4.2%, and 3.1% for 5, 6, 8, and 10 well-pads, respectively. This behaviour can be linked to the fact that as the number of potential well-pads increases so does the number of alternatives for reconfiguration of the well-pads designs and/or the optimal drilling and fracturing schemes, which allows favours solutions that mitigate to a certain extent the variations in the water and wastewater quality. In addition, it is worth mentioning that although the wastewater management component seems more stable for cases with fixed well-pads designs, their economic performance is, in general, severely affected. Hence, a comprehensive planning and design of shale gas supply chains should exploit the advantages of optimising the configuration of well-pads.

4.6 Conclusions

A comprehensive mathematical model has been proposed to address the optimisation of integrated shale gas supply chains with water management. The optimisation framework was implemented to address the impact of water availability on shale gas development and investigate the interplay between water management, well-pad and supply chain design and economy of scale in shale gas development.

A scenario with 10 potential well-pads was used in order to investigate the effects of water resources availability of the economic s of shale gas development. Through a parametric analysis it was possible to show that the economics is considerably affected under water scarcity scenarios. For the specific case presented in this work, the NPV dropped 68.6% when the water resources were reduced by 50%. In addition, the well-pad designs shifts from 7 MaxNPV and 3 MinWI, to 1 MaxNPV and 9 MinWI as the water resources are reduced. The drilling strategy shows a tendency of installing pair of well-pads that are complementary with respect to the TDS concentration of their associated wastewater. Regarding water management strategy, besides adjusting well-pad designs, the recycle and re-use of water increase as the water resources decrease, however, a critical point was found in 70% of water availability in which this trend switches and the water consumption is controlled only by adjusting the well-pad designs.

The previous analysis was further extended to account for economies of scale. Three cases with different number of well-pads (6, 8, and 10 potential well-pads) were used to address the impact of economies of scale on shale gas development. It was found that shale gas development benefits from economies of scale. For instance, the breakeven price decreases by 20.9% as the number of potential well-pads increases from 6 to 10 well-pads. In addition, it was shown that the economic feasibility of a small shale gas development is highly vulnerable to variations in availability of water resources. Moreover, the results from the parametric analysis involving the TDS concentration in wastewater reaffirm our findings regarding the role of well-pad configurations in the resilience of the shale gas supply chain. For instance, as TDS concentration increases, the configuration of well-pads shifts to less

water intensive designs, which leads to a decrease in wastewater flowrates as well as in gas production affecting the profitability of the shale gas development. Therefore, an adequate assessment of water resources is crucial at designing and planning shale gas supply chains.

Finally, it was possible to address quantitatively the interdependency of important aspects of shale gas supply chains, which demonstrates the advantages of implementing mathematical optimisation frameworks to disclose synergies that otherwise are difficult to elucidate.

Chapter 5. BioSNG supply chains[6]

In this chapter, a mathematical framework is presented for the strategic optimisation of BioSNG supply chains at a national and regional scale. The proposed model corresponds to a spatially-explicit multiperiod mixed integer linear programming (MILP). The framework is implemented to address the production of BioSNG from domestic resources as a possible substitute of natural gas in UK. First, the economic feasibility of BioSNG is addressed. Then, the economic impact of energy integration is addressed through a scenario in which power is cogenerated and sold to the grid. Two main subsidisation schemes are considered in this study: Feed-in tariff for the injection of BioSNG into the gas pipeline network, and renewable obligation certificates (ROCs) for the cogeneration of power. Finally, different levels of percentage of subsidisation with respect to the total incurred costs (Capex and Opex) are addressed maintaining a fixed feed-in tariff of £70/MWh.

5.1 Literature review

A successful implementation of renewable technologies in a regional and/or national context would require a thorough integration of three main components: feedstock procurement rates, production optimisation, and product transportation. This must be addressed while taking into account regional targets and government policies. Mathematical modelling and optimisation techniques are powerful tools that provide a systematic methodology to tackle these problems [252,253]. A substantial amount of research has been dedicated to the development of methodologies for the assessment of supply chain networks for the production of biofuels. Several optimisation frameworks have been developed to address the design and optimisation of ethanol supply chains in which decisions such as feedstock transportation routes, location and installed capacity of processing facilities, technology selection, and ethanol transportation are optimised with respect to an

[6] This chapter is based on manuscript IV of the list of publications presented at the end of this thesis

economic objective [254–257]. Some optimisation frameworks have been developed based on spatially-explicit formulations to better account for regional discretisation which provides flexibility to design the optimal transportation network for feedstocks and final products across a country [30,258–260]. The effects of economies of scale have been subject of research [261,262], as well as coproduction of heat and power by considering energy integration in processing facilities [263,264], which can significantly improve the economic performance and environmental benefits of sustainable processes [265]. Other authors have investigated the impact of market conditions and the government role in the development of biofuel supply chains [266,267]. Furthermore, multiobjective optimisation techniques have been implemented for the optimal design and planning of biofuel supply chains while considering not only economic performance but also environmental and social aspects [32,268–272]. Finally, several optimisation frameworks have been proposed to deal with uncertainty in parameters such as feedstocks costs, price of final products, and future demand which can greatly affect the optimal decisions when compared to deterministic models [33,273,274]. Regarding BioSNG supply chains, Steubing et al. [275] proposed a snapshot model for the optimal design of a supply chain for the production of BioSNG, heat and electricity from wood while maximising profit and minimising environmental impact. The authors reported that the environmental impact benefits from installation of plants with capacities ranging between 5 MW and 40 MW, whereas the economic performance increases when plants with capacities between 100 MW and 200 MW are installed.

In the light of the previous survey, available literature addressing the optimal development of nationwide supply chains for the production of BioSNG from biomass and/or waste streams is scarce. The purpose of this work is to present a systematic methodology based on a mathematical framework that contributes to the knowledge of the design and optimisation of BioSNG supply chains in a regional and nationwide context [276]. Moreover, available studies in the UK address the economic feasibility only for single-site BioSNG projects. However, as the support of the UK government and private sectors for developing this technology increases,

an integrated framework is needed in order to evaluate the potential of BioSNG as an alternative energy source in the UK and its role in meeting national targets. This work aims to fill in that gap by providing a comprehensive decision-making support tool for the evaluation of a future BioSNG supply chain development based on domestic renewable resources and waste streams in the UK. In order to address the problem, a spatially-explicit multiperiod mixed integer linear programming (MILP) model is proposed for the strategic design and economic optimisation of a second generation nationwide BioSNG supply chain. The optimisation framework considers cogeneration of heat & power, location and selection of optimal capacities for processing facilities, economies of scale, different types of feedstocks as well as their geographic distribution, land utilisation and optimal cultivation rates for new specialised energy crops, and design of the transportation network from feedstocks suppliers to processing facilities and final products to demand centres. In addition, government incentives for production and injection of BioSNG into the national grid (Feed-in tariffs) and for generation of renewable energy (ROCs) are considered.

5.2 Problem statement

The development of a supply chain for the production of BioSNG involves several strategic, logistic and operational decisions, including feedstock utilisation rate, cultivation rate of new energy crops, feedstock transportation modes, location and capacity for processing facilities, and production rates of final products. A generic BioSNG supply chain is presented in Figure 5.1.

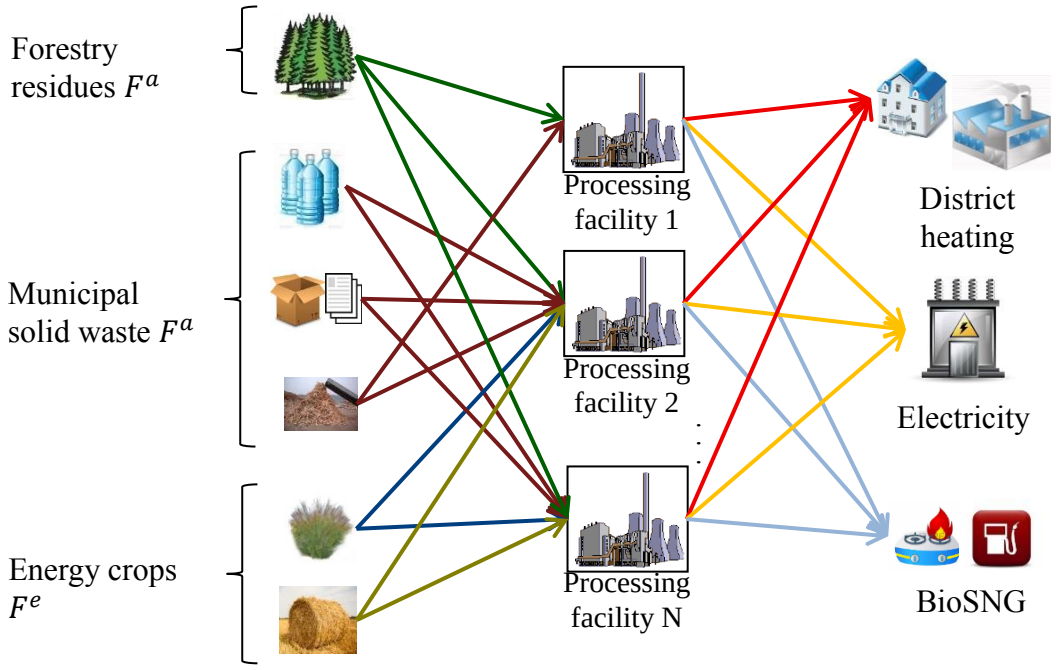

Figure 5.1. Generic BioSNG supply chain.

The BioSNG supply chain considers a set of feedstocks suitable for BioSNG production ($f \in F$) which are divided into a set of on-site available feedstocks ($f \in F^a$), such as woody biomass, straw, and residual waste, and a set of new potential feedstocks ($f \in F^e$) that require initial investments before they can be used in BioSNG production, such as miscanthus. The availability of these resources distributed along a set of regions ($g \in G$) is considered to be given. These regions also serve as potential locations for installation of new processing facilities ($k \in K$) where raw feedstock is converted into final products ($p \in P$), i.e., BioSNG, heat and/or power. In order to include economies of scale, the relationship between plant capacities and capital expenditures is discretised in linear segments ($s \in S$) by implementing a piecewise linearisation approach. Different transportation modes ($l \in L$) are available for raw feedstocks and BioSNG. The available transportation modes for feedstocks or final products between regions are defined by the set $\eta_{iggʹl}$ where ($i \in I$) contains all the resources, i.e., feedstocks and final products, considered in the BioSNG supply chain. Biomass and residual waste can be transported either by truck or railroad. BioSNG can be transported as compressed natural gas by trailer from the processing plants to the gas network. It is worth to mention that power and heat have their own transmission systems whose

incorporation in the mathematical formulation would require additional complex technical and operational considerations [277–280]. Therefore, for the sake of simplicity, these systems are not considered in the present formulation; instead, it is assumed that they are sold locally. In general, the BioSNG Supply Chain design problem can be defined as follows:

Given the input data:

- Geographical distribution of demand centres
- Gas, power and heat demand over the entire planning horizon
- Feedstock types and their geographical availability
- Geographical distribution of land availability for new crops
- Feedstock production costs
- Capital and operating costs for transportation modes
- Transport logistics (modes, capacities, distances, availability)
- Technical (yields) and economic (capital and operating costs) parameters as a function of feedstock types and production technology
- Gas, power and heat market prices
- Government incentives (Feed-in tariff and ROCs)

The key variables to be optimised over the planning horizon are:

- Feedstock procurement rate for each feedstock type
- BioSNG production rates
- Technology selection, locations and scales of BioSNG production facilities
- Biomass cultivation sites
- Flows of each feedstock type and BioSNG between regions
- Modes of transport of delivery for biomass and biofuel

The BioSNG supply chain is formulated as a spatially-explicit multiperiod and single objective MILP model. The goal is the maximisation of Net Present Value (NPV) subject to logistical, operational and economic constraints. The mathematical framework is presented in section 5.3.

5.3 BioSNG supply chain optimisation framework

This section presents a deterministic optimisation model for the strategic design and planning of BioSNG supply chains. The proposed model is defined by material balances, production and demand constraints, logistic constraints and economic constraints. The features of the model are discussed in detail in the following sections.

5.3.1 Nomenclature

Indices

f	Feedstocks
g, g'	Regions
i	Resources
k	Technologies
l	Transportation modes
p	Final products
s	Segments for cost linearisation
t, t'	Time periods
z	Local distribution zone (LDZ)

Sets

F	Set of feedstocks, $F = F^a \cup F^e$
F^a	Set of available feedstocks
F^e	Set of new energy crops
G	Set of regions
I	Set of resources (feedstocks and final products), $I = F \cup P$
K	Set of technologies for integrated facilities
P	Set of final products
S	Set of segments for cost linearisation
T	Set of time periods
Z	Set of Local distribution zones (LDZs)
F_k	Set of feedstocks f that can be processed by technologies k
G_z	Set of regions g with injection points corresponding to a local

	distribution zone z
$\eta_{igg'l}$	Set of feasible transport links for each resource i between region g and g' via transport mode l

Scalars

Avf	Availability factor for renewable energy plants
Cf	Capacity factor for renewable energy plants
$LimP$	Upper bound for production in regions [GWh y^{-1}]
$LimD$	Upper bound for demand in regions [GWh y^{-1}]
Tr	Tax rate
α	Operating period in a year [h y^{-1}]
μ	Steam to power generation efficiency
γ, ψ, λ	Conversion factors

Parameters

$AD_{gg'l}$	Actual delivery distance between regions g and g' via transport mode l [km]
aIN_{fks}	Independent term of the linearised capex curve for an integrated plant processing feedstock f with technology k at each segment s [£M]
bIN_{fks}	Slope of the linearised capex curve for an integrated plant processing feedstock f with technology k at each segment s [M£ MW^{-1}]
$CMax_{ks}$	Maximum capacity of technology k at each linearisation segment s of the Capex curve [MW]
$CMin_{ks}$	Minimum capacity of technology k at each linearisation segment s of the Capex curve [MW]
Dem_{pzt}	Demand of product p in local distribution zone z in time period t [GWh y^{-1}]
$DepF_{tt'}$	Depreciation factor for investments in t during periods t'
$DfCA_t$	Discount factor for capital costs in time period t
$DfCF_t$	Discount factor for cash flow in time period t
DW_l	Driver wage for transportation mode l [£k h^{-1}]
$EstCost_{ft}$	Establishment costs for energy crops ($f \in F^e$) in time period t [M£ ha^{-1}]

FE_l	Fuel efficiency for transportation mode l [km L^{-1}]
$FMax_{fgt}$	Maximum feedstock ($f \in F^a$) availability in region g and time period t [ton y^{-1}]
$FMin_{fgt}$	Minimum feedstock ($f \in F^a$) availability in region g and time period t [ton y^{-1}]
FP_l	Fuel price for transportation mode l [£k L^{-1}]
$FxOpIN_{fkt}$	Fixed costs for operation and maintenance for an integrated plant processing feedstock f via technology k in time period t [£M y^{-1}]
$FxTC_i^{Loc}$	Fixed local transport costs for resources i [£ Ton^{-1}]
$FxTC_{il}^{Reg}$	Fixed regional transport costs for resources i via mode l [£ Ton^{-1}]
GE_l	General expenses of transportation mode l [£k d^{-1}]
Inc_{pt}	Renewable heat incentive for p injection in time period t [£ kWh^{-1}]
$Land_{gt}$	Arable land available in region g and time period t [ha]
LD_g	Actual local delivery distance within a region g [km]
LHV_i	Low heating value for resource i [GJ ton^{-1}]
LUT_l	Load-unload time of transportation mode l [h]
$MaxLand_t$	Maximum total land available for energy crops in time period t [ha]
ME_l	Maintenance expenses for transportation mode l [£k km^{-1}]
$OpCost_{ft}$	Operation costs related to energy crops ($f \in F^e$) in time period t. It includes fixed overheads, agrochemicals, harvesting costs, and storage costs [£M ha^{-1} y^{-1}]
$PlanRem_{ft}$	Plantation removal costs for energy crops ($f \in F^e$) in time period t [£M ha^{-1}]
$Price_{pt}$	Price of products p in time period t [£ kWh^{-1}]
$Rent_{gt}$	Rent costs for land in region g in time period t [£M ha^{-1} y^{-1}]
SP_l	Average speed of transportation mode l [km h^{-1}]
$TCap_l$	Capacity of transportation mode l [kg]
TMA_l^{Loc}	Local availability of transportation mode l [h d^{-1}]
TMA_l^{Reg}	Regional availability of transportation mode l [h d^{-1}]
TMC_l	Capital cost for establishing a transportation mode l for

	BioSNG [£M]
UFC_{fgt}	Unit feedstock costs of available feedstocks ($f \in F^a$) per region g in time period t [£ Ton^{-1}]
$VrOpIN_{fkt}$	Variable costs of operation and maintenance for an integrated plant processing feedstock f using technology k in time period t [£M GWh^{-1}]
$VrTC_i^{Loc}$	Variable local transport costs for resources i [£ Ton^{-1} km^{-1}]
$VrTC_{il}^{Reg}$	Variable regional transport costs for resources i via mode l [£ Ton^{-1} km^{-1}]
$Yield_{fgt}$	Cultivation yield for energy crops ($f \in F^e$) within region g in time period t [ton y^{-1} ha^{-1}]
βIN_{fkt}	Efficiency of an integrated plant processing feedstock f with technology k to produce p

Positive continuous variables

A_{fgt}	Area occupied by second generation crop ($f \in F^e$) in region g and time period t [ha]
$CAPEX_t$	Total investment cost for the supply chain in time period t [£M]
$CAPEX\_EC_t$	Total investment cost for new energy crops in time period t [£M]
$CAPEX\_IN_t$	Total investment cost of integrated plants in time period t [£M]
$CAPEX\_TR_t$	Total investment cost for new BioSNG transport facilities time period t [£M]
$CAPIN_{fkgts}$	Initial installed capacity for an integrated plant processing feedstock f using technology k in region g and and is available in time period t at segment s [MW]
D_{igt}	Demand for resource i in region g in time period t [GWh y^{-1}]
$DEP_{tt'}$	Depreciation for investments in t during periods t' [£M y^{-1}]
DGZ_{pgzt}	Variable relating the supply of a final product p in region g and the demand of a local distribution zone z for in time period t [GWh y^{-1}]
DIN_{fkgt}	Demand of an integrated plant processing feedstock f with technology k in region g in time period t [GWh y^{-1}]
FC_t	Total feedstock cost in time period t [£M y^{-1}]

$IncentiveGOV_t$	Incentives associated with government subsidies for BioSNG production in time period t
$IncentiveROC_t$	Incentives associated with Renewable Obligation Certificates for power generation in time period t
$INCOME_t$	Total revenues in time period t [£M y^{-1}]
$LocSup_{gt}$	Variable that accounts for the demand of BioSNG met locally in region g and time period t [GWh y^{-1}]
$OPEX_t$	Total operational cost in time period t [£M y^{-1}]
P_{igt}	Production rate of product i in region g in time period t [GWh y^{-1}]
PC_t	Total production cost in time period t [£M y^{-1}]
PIN_{fkpgt}	Production rate at an integrated plant processing feedstock f with technology k to produce p in region g in time period t [GWh y^{-1}]
$Q_{igg't}$	Flow rate of product i via mode l from region g to g' in time period t [GWh y^{-1}]
$TArea_{fgt}$	Total area occupied by second generation crops ($f \in F^e$) in region g and time period t [ha]
TAX_t	Total taxes in time period t [£M y^{-1}]
TC_F_t	Total transportation cost for feedstocks in time period t [£M y^{-1}]
$TC\_SNG_t^{Reg}$	Regional transportation cost for new BioSNG transport facilities in time period t [£M y^{-1}]
$TC\_SNG_t^{Loc}$	Local transportation cost for new BioSNG transport facilities in time period t [£M y^{-1}]
$ToCAPIN_{fkgt}$	Total capacity of an integrated plant processing feedstock f in region g and using technology k that is available in time period t [MW]

Free continuous variables

Cf_t	Cash flow after taxes in time period t [£M y^{-1}]
NPV_t	Net present value [£M]
$PROFIT_t$	Profit after depreciation and operational costs in time period t [£M y^{-1}]

Binary variables

$AvIN_{fkgts}$	1 if an integrated plant processing feedstock f using technology k and located in region g is operating in time period t with a capacity delimited by a segment s, 0 otherwise.
PD_{gt}	1 if BioSNG production in region g and time period t is less than the demand in region g and time period t, 0 otherwise.
δIN_{fkgts}	1 if an integrated plant processing feedstock f using technology k in region g is installed in time period t with a capacity delimited by a segment s, 0 otherwise.

5.3.2 Objective function

The objective function of the model is the maximisation of the net present value, NPV, subject to operational and logistic constraints. The net present value is expressed as the cash flow, CF_t, minus the capital expenditures, $CAPEX_t$, as shown in Equation (5.1). The parameters $DfCF_t$ and $DfCA_t$ are the corresponding discount factors.

$$max \quad NPV = \sum_t (DfCF_t * CF_t - DfCA_t * CAPEX_t) \tag{5.1}$$

5.3.2.1 Capital investments

Capital expenditures, $CAPEX_t$, are calculated as the summation of the investment in integrated facilities, $CAPEX\_IN_t$, investment in infrastructure for BioSNG transportation, $CAPEX\_TR_t$, and investment in new energy crops for BioSNG production, $CAPEX\_EC_t$, as shown in Equation (5.2).

$$CAPEX_t = CAPEX\_IN_t + CAPEX\_TR_t + CAPEX\_EC_t \quad \forall\, t \tag{5.2}$$

5.3.2.2 Cash flow and depreciation

Cash flow is defined as the profit before taxes, $PROFIT_t$, plus depreciation of assets, $DEP_{t't}$, minus taxes, TAX_t, as presented in Equation (5.3).

$$CF_t = PROFIT_t + \sum_{t'} DEP_{t't} - TAX_t \quad \forall\, t \tag{5.3}$$

The linear method is used to calculate the depreciation, $DEP_{tt'}$, as a function of capital expenditures using a given depreciation rate, $DepF_{tt'}$, as expressed in Equation (5.4). $DEP_{tt'}$ represents the depreciation during period t' for investments made in a previous period t:

$$DEP_{tt'} = DepF_{tt'}(CAPEX\_IN_t + CAPEX\_TR_t) \quad \forall\, t, t' \tag{5.4}$$

where $CAPEX\_IN_t$ and $CAPEX\_TR_t$ correspond to capital expenditures for integrated facilities and new infrastructure for BioSNG transportation, respectively. Investment costs related to energy crops (pre-planting and establishment costs), $CAPEX\_EC_t$, are considered non-depreciable.

5.3.2.3 Income

The income for each period, $INCOME_t$, is calculated based on the total production, P_{pgt}, where $(p \in P)$ corresponds to final products, i.e., BioSNG, heat, and, power. Similarly, set $(g \in G)$ relates to regions considered in the BioSNG supply chain. Additionally, final products prices, $Price_{pt}$, and possible government incentives, Inc_{pt}, are included as described in Equation (5.5):

$$INCOME_t = \sum_{pg} \left(Price_{pt} + Inc_{pt}\right) * P_{pgt} \quad \forall\, t \tag{5.5}$$

5.3.2.4 Profit and taxes

The net profit associated with the BioSNG supply chain operation is calculated as the income, $INCOME_t$, minus operating expenditures, $OPEX_t$, and minus depreciation, as defined in Equation (5.6).

$$PROFIT_t = INCOME_t - OPEX_t - \sum_{t'} DEP_{t't} \quad \forall\, t \tag{5.6}$$

This formulation considers that taxes apply only when profit is positive, taxes are set to zero otherwise. The taxation charge is estimated based on a tax rate, Tr, and profit. These conditions are modelled by Equations (5.7) and (5.8). In case of a different tax system for a particular case study, Equations (5.7) and (5.8) should be modified accordingly.

$$TAX_t \geq Tr * PROFIT_t \quad \forall\, t \tag{5.7}$$

$$TAX_t \geq 0 \quad \forall\, t \tag{5.8}$$

5.3.2.5 Operating expenditures

Operating expenditures are estimated as the sum of feedstock costs, FC_t, production costs, PC_t, and transportation costs, TC_t, as shown in Equation (5.9).

$$OPEX_t = FC_t + PC_t + TC_t \quad \forall\, t \tag{5.9}$$

The feedstock costs include payments for acquisition of available feedstocks and operation of new cultivated areas for production of energy crops. Productions costs refer to expenses incurred for operating processing facilities. Finally, transportation costs take into account expenses related to biomass, residual waste, and BioSNG transportation.

5.3.3 Production constraints

Initially, a global balance is included to account for the production, demand, and transfers of resources i, i.e., feedstocks and final products, between regions g and g' in time period t, as depicted in Equation (5.10):

$$P_{igt} + \sum_{l} \sum_{g' \in \eta_{ig'gl}} Q_{ig'glt} = D_{igt} + \sum_{l} \sum_{g' \in \eta_{igg'l}} Q_{igg'lt} \quad \forall\, i, g, t \tag{5.10}$$

P_{igt} and D_{igt} correspond to the production and demand of resources i in region g and in time period t, respectively. Variable $Q_{ig'glt}$ represents transfers of resources i between regions g and g' via transport mode l during time period t. The feasible connections between resources, regions, and available transportation modes are predefined by the set $\eta_{igg'l}$. The production P_{igt} encompasses production of new energy crops, procurement of available feedstocks, and final products. Moreover, D_{igt} comprises demand of both new and available feedstocks required by potential processing facilities, and demand of final products, which is subsequently related to specific demand data according to the case study.

5.3.3.1 Available feedstocks

The procurement rate P_{fgt} of feedstock available on site ($f \in F^a$) is modelled through Equation (5.11). In this case, feedstocks are assumed to be readily available on site, therefore, new areas for cultivation are not required.

$$\gamma * LHV_f * Fmin_{fgt} \leq P_{fgt} \leq \gamma * LHV_f * Fmax_{fgt} \quad \forall f \in F^a, g, t \tag{5.11}$$

The procurement rate is limited by parameters $Fmax_{fgt}$ and $Fmin_{fgt}$ which refer to the maximum local availability and minimum flow rates. Parameter LHV_f corresponds to the low heating value of the feedstocks. Scalar γ is a conversion factor introduced for consistency of units.

5.3.3.2 Energy crops

In addition to currently available feedstocks, cultivation of new energy crops, e.g. Miscanthus, short-rotation coppice, switchgrass, for the production of BioSNG is considered. The cultivation rate of new feedstocks is estimated based on the feedstock productivity, $Yield_{fgt}$, which varies according to land quality and type of feedstock, and the total cultivation area, $TArea_{fgt}$, required for feedstocks ($f \in F^e$) in region g and time period t. The corresponding formulation is presented in Equation (5.12).

$$P_{fgt} = \gamma * LHV_f * Yield_{fgt} * TArea_{fgt} \quad \forall f \in F^e, g, t \tag{5.12}$$

The total cultivation area $TArea_{fgt}$ required for new plantations along the planning horizon is expressed by Equation (5.13):

$$TArea_{fgt} = TArea_{fg,t-1} + A_{fgt} \quad \forall f \in F^e, g, t \tag{5.13}$$

where A_{fgt} is the new added area for cultivations of feedstocks ($f \in F^e$) in region g during time period t. The cultivation of energy crops in new areas can take several years before harvesting, e.g., ~3 years for Miscanthus [281], which makes the role of the government crucial to encourage their cultivation, possibly, through long-term agreements with farmers. Accordingly, Equation (5.13) ensures that an area that has been chosen for energy crops cultivation will not be reduced or completely abolished in the next period which could be negative for the economy of

farmers. The total cultivation area is limited by the local available land which is estimated as the total area of a region g, represented by parameter $Land_{gt}$, multiplied by a factor of land usage δ_{gt} which represents the fraction of suitable land that can be used in region g and time period t for growing energy crops, as shown in Equation (5.14).

$$\sum_{f \in F^e} TArea_{fgt} \leq \delta_{gt} Land_{gt} \quad \forall\, g, t \tag{5.14}$$

Finally, the suitable land for new plantations cannot be used entirely for energy crops due to sustainability issues and risks associated with land competition [282], thus, Equation (5.15) is introduced to constraint the maximum total area that can be used for new energy crops, represented by parameter $MaxLand_t$.

$$\sum_{f \in F^e, g} TArea_{fgt} \leq MaxLand_t \quad \forall\, t \tag{5.15}$$

5.3.3.3 Final products

In this framework, integrated plants will be considered as potential facilities for the production of BioSNG and coproducts, e.g. heat and power, from raw feedstocks. In this case, the feedstocks are pre-processed and converted into final products in the same facilities. The production from integrated plants can be related to the regional production by means of Equation (5.16).

$$P_{pgt} = \sum_{k} \sum_{f \in F_k} PIN_{fkpgt} \quad \forall\, p, g, t \tag{5.16}$$

P_{pgt} refers to the production of p in region g and time period t. PIN_{fkpgt} indicates the production of a potential integrated plant processing feedstock f with technology k to produce p in region g during time period t. Set F_k contains connections between feedstocks f that can be processed with technologies k. A global balance for integrated plants relating their production of BioSNG, $PIN_{fk,biosng,gt}$, with the corresponding demand of feedstocks, DIN_{fkgt}, can be expressed as shown in Equation (5.17).

$$PIN_{fk,biosng,gt} = \beta IN_{fk,biosng} * DIN_{fkgt} \quad \forall\, k, f \in F_k, g, t \tag{5.17}$$

Parameter $\beta IN_{fk,biosng}$ accounts for the efficiency of an integrated plant using feedstock f to produce BioSNG via technology k. Equation (5.17) is valid only for all the feasible connections predefined in set F_k. Besides BioSNG, heat & power are important coproducts derived from energy integration which increases the global efficiency of the BioSNG production and therefore would benefit the economic performance [24]. A general scheme showing energy integration in BioSNG facilities is depicted in Figure 5.2.

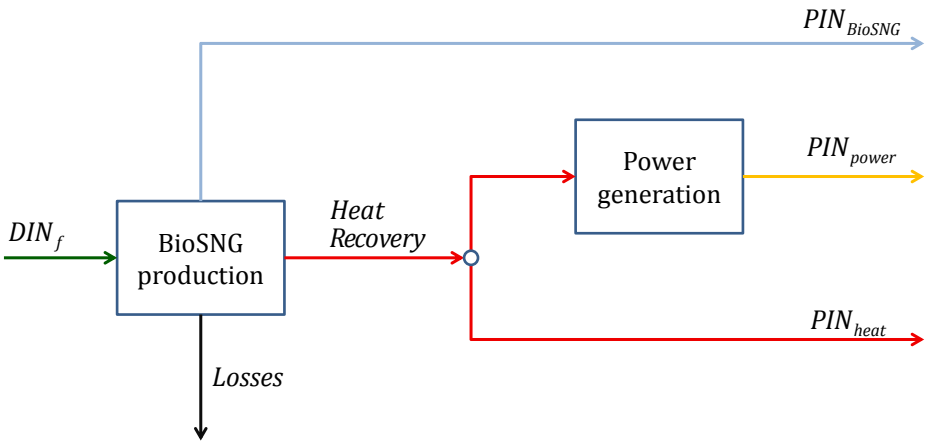

Figure 5.2. Optional energy integration for BioSNG production

As the production of BioSNG is the main objective, it is considered that the efficiency from feedstocks to BioSNG is fixed and will not be affected by the co-generation of heat and/or power. That is, the production of syngas will be used exclusively for BioSNG production and will not be diverted for cogeneration of heat & power. On the other hand, the production of power will be affected by the production of heat and vice versa. In addition, the generation of power from heat is subject to an efficiency denoted by μ. This is taken into account in the mathematical formulation by including a global balance across integrated facilities as depicted in Equation (5.18).

$$\frac{PIN_{fk,power,gt}}{\mu} + PIN_{fk,heat,gt} \leq \beta IN_{fk,heat} * DIN_{fkgt} \quad \forall\, k, f \in F_k, g, t \tag{5.18}$$

This equation relates the demand of an integrated plant, DIN_{fkgt}, with the production of heat, $PIN_{fk,heat,gt}$, and power, $PIN_{fk,power,gt}$, by introducing the efficiency of heat recovery, $\beta IN_{fk,heat}$, and the efficiency of power generation, μ. This formulation determines the optimal proportion of heat and power generated in a certain processing plant.

5.3.4 Demand constraints

The demand D_{igt} (see Equation (5.10)) refers not only to the demand of final products, i.e. BioSNG, heat, and power, but also to the demand of feedstocks in integrated plants in a certain region as described in section 5.3.3. The corresponding equations relating these variables are presented next.

5.3.4.1 Feedstocks demand

Demand of feedstocks in each potential new facility must be related to the regional demand of such feedstocks. In this case, it is not necessary to include different demand constraints for available and new feedstocks, unlike the production constraints (see sections 5.3.3.1 and 5.3.3.2). Therefore, the demand for both types of feedstocks can be expressed in just one constraint as shown in Equation (5.19).

$$D_{fgt} = \sum_{k:f \in F_k} DIN_{fkgt} \quad \forall f, g, t \tag{5.19}$$

Variable D_{fgt} refers to the total regional demand of feedstocks $(f \in F)$ during time period t.

5.3.4.2 Final products demand

One of the major advantages of BioSNG is its compatibility with conventional natural gas which makes possible the transportation of BioSNG through conventional gas pipeline transportation networks. Accordingly, in this model it is assumed that the BioSNG will be injected into the existing National Grid Transmission System, specifically in points that are connected to the Gas Distribution Network (GDN). In the UK, the GDN is divided into Local Distribution Zones (LDZs) which are in charge of transporting natural gas from the injection points to final customers. In this work, it is considered that the BioSNG is used to

supply customers that require medium to low gas pressure supply. Therefore, the demand will be set based on the LDZs. In order to maintain a general mathematical framework, it is assumed that the geographical distribution of the LDZs do not match the distribution of regions g. This is taken into account by including Equations (5.20) and (5.21):

$$D_{pgt} = \sum_{z:g\in G_z} DGZ_{pgzt} \quad \forall\, p, g, t \tag{5.20}$$

$$\sum_{g\in G_z} DGZ_{pgzt} \leq Dem_{pzt} \quad \forall\, p, z, t \tag{5.21}$$

The previous equations allow to link the demand of products p in regions g, represented by variable D_{pgt}, with the demand of products p in LDZ regions z, represented by parameter Dem_{pzt}. The set G_z contains the regions g that have at least one injection point belonging to a Local Distribution Zone z. As the final goal is maximisation of net present value, the demand constraint is written as an upper bound. In case of power and heat cogeneration, it is assumed that they are sold locally and therefore no transportation cost is incurred.

5.3.5 Capital investments

The estimation of capital investments depend on three components: (1) investments in new processing facilities, (2) investment in new infrastructure for BioSNG transportation from processing facilities to injection points, and (3) investments associated with cultivation of new energy crops. The corresponding mathematical formulation is presented as follows.

5.3.5.1 Processing facilities

As the capacity of a plant increases, the investment costs per unit of installed capacity are reduced. This is known as economies of scale and follows a non-linear curve pattern that resembles a power curve. The effect of economies of scale is taken into account in the mathematical formulation, however, the capital investment costs for integrated plants are linearised by implementing a piecewise linear approximation approach. The concave curve is split up into several linear segments s as depicted in Equation (5.22).

$$CMin_{ks} * \delta IN_{fkgts} \leq CAPIN_{fkgts} \leq CMax_{ks} * \delta IN_{fkgts} \quad \forall\, k, f \in F_k, g, t, s \tag{5.22}$$

The variable $CAPIN_{fkgts}$ refers to new installed capacity of integrated plants in region g and time period t. Parameters $CMin_{ks}$ and $CMax_{ks}$ limit the minimum and maximum capacity that can be installed for an integrated plant with technology k if segment s is chosen. δIN_{fkgts} is a binary variable taking the value of 1 if an integrated plant is installed for processing feedstock f with technology k in region g and time t with a capacity limited by the segment s; otherwise is 0. Only one segment can be activated, and only one integrated plant for each type of feedstock is allowed to be installed in region g. These conditions are modelled through Equations (5.23) and (5.24), respectively.

$$\sum_{s} \delta IN_{fkgts} \leq 1 \quad \forall\, k, f \in F_k, g, t \tag{5.23}$$

$$\sum_{s} \sum_{k:f \in F_k} \delta IN_{fkgts} \leq 1 \quad \forall\, f, g, t \tag{5.24}$$

Equation (5.25) accounts for the total installed capacity of an integrated plant processing feedstock f with technology k in region g during time t.

$$ToCAPIN_{fkgt} = ToCAPIN_{fkg,t-1} + \sum_{s} CAPIN_{fkgts} \quad \forall\, k, f \in F_k, g, t \tag{5.25}$$

The maximum amount of feedstock f that can be processed in an integrated plant, DIN_{fkgt}, is limited by its total installed capacity, $ToCAPIN_{fkgt}$, the capacity factor, Cf, and the availability factor, Avf. The capacity factor refers to the ratio between the actual production in a certain period and the nameplate capacity of the plant. The availability factor is the fraction of time that a plant can operate before maintenance is required. In general, these values correspond to the fraction of the capacity that can actually be used as described in Equation (5.26).

$$DIN_{fkgt} \leq Cf * Avf * \alpha * ToCAPIN_{fkgt} \quad \forall\, k, f \in F_k, g, t \tag{5.26}$$

Scalar α corresponds to the number of hours in a year. Finally, the total investment cost, $CAPEX\_IN_t$, is calculated by means of Equation (5.27):

$$CAPEX\_IN_t = \sum_{kgs} \sum_{f \in F_k} \left(bIN_{fks} * \delta IN_{fkgts} + aIN_{fks} * CAPIN_{fkgts} \right) \quad \forall\, t \tag{5.27}$$

where aIN_{fks} and bIN_{fks} are parameters that represent variable and fixed investment costs. This information results from the linearisation of the corresponding investment cost curve.

5.3.5.2 BioSNG transportation infrastructure

It is assumed that new facilities are required for BioSNG transportation. In this case, only Compressed Natural Gas (CNG) for BioSNG transportation is included. A modified mathematical formulation from previous works [34,283] is incorporated to account for investments in new facilities for BioSNG transportation as shown in Equation (5.28):

$$\begin{aligned} CAPEX\_TR_t = & \sum_{(gg'l)|\in \eta_{biosng,gg'l}} \frac{\psi * TMC_l * Q_{igg'lt}}{TMA_l^{Reg} * TCap_l * LHV_i} \left(\frac{2 * AD_{gg'l}}{SP_l} + LUT_l \right) \\ & + \sum_{(gl)|l=\{trailer\}} \frac{\psi * TMC_l * LocSup_{gt}}{TMA_l^{Loc} * TCap_l * LHV_i} \left(\frac{2 * LD_g}{SP_l} + LUT_l \right) \quad \forall\, t \end{aligned} \tag{5.28}$$

Equation (5.28) is composed by two terms that correspond to capital investments for regional and local transportation of BioSNG, respectively. TMC_l refers to the capital cost for establishing a new transportation mode l. LUT_l is the load-unload time of the transportation units, e.g. trailers, trucks. $TCap_l$ is the capacity of a new transportation unit. TMA_l^{Reg} and TMA_l^{Loc} are the regional and local availability of transportation mode l expressed in hours per day. SP_l is the average speed of transportation mode l. LD_g and $AD_{gg'l}$ are the local and regional delivery distances. The calculation of costs is driven by the amount of BioSNG that is being transported either locally or regionally. This is represented by the variable $Q_{biosng,gg'lt}$ which is the flow rate of product BioSNG between regions g and g' via mode l, and the variable $LocSup_{gt}$ which refers to the amount of BioSNG that is produced and supplied within the same region. In order to calculate the local supply, it is assumed that $LocSup_{gt}$ is limited either by the local production $P_{biosng,gt}$ or the

local demand $D_{biosng,gt}$. That is, if the local production is higher than the local demand, then $LocSup_{gt}$ is set to be equal to the local demand. Likewise, if the local production is lower than the local demand, then $LocSup_{gt}$ is set to be equal to the local production. These conditions are modelled through Equations (5.29) and (5.30):

$$LocSup_{gt} \geq P_{biosng,gt} - LimP * \left(1 - PD_{gt}\right) \quad \forall\, g, t \tag{5.29}$$

$$LocSup_{gt} \geq D_{biosng,gt} - LimD * PD_{gt} \quad \forall\, g, t \tag{5.30}$$

where, $LimP$ is an upper bound for production and $LimD$ an upper bound for demand. PD_{gt} is a binary variable that equals 1 if BioSNG production in region g and time period t is less than the demand in same region and time period. If that is the case, $LocSup_{gt}$is set at the value of $P_{biosng,gt}$, otherwise if $P_{biosng,gt}$ is greater than $D_{biosng,gt}$, the binary variable is equal to 0 and the variable $LocSup_{gt}$ is set at the value of $D_{biosng,gt}$. It is worthwhile to mention that this is an approximation in order to reduce the complexity of the model.

5.3.5.3 New feedstocks

If plantation of new feedstocks is required, then investments in cultivating areas with new crops should be made. The total capital expenditures, $CAPEX\_EC_t$, in new crops is expressed in Equation (5.31):

$$CAPEX\_EC_t = \sum_{f \in F^e, g} \left(EstCost_{ft} + PlanRem_{ft}\right) * A_{fgt} \quad \forall\, t \tag{5.31}$$

$EstCost_{ft}$ and $PlanRem_{ft}$ are parameters that account for costs associated with the establishment of new plantations and plantation removal costs, respectively.

5.3.6 Operating expenditures

Operational costs consist of cost associated with feedstock production, cost of production in integrated facilities, and corresponding transportation costs.

5.3.6.1 Feedstocks costs

Equation (5.32) presents the estimation of total costs, FC_t, related to procurement of feedstock:

$$FC_t = \sum_{f \in F^a, g} \frac{\lambda * UFC_{fgt} * P_{fgt}}{LHV_f} + \sum_{f \in F^e, g} \lambda * \left(Rent_{gt} + OpCost_{ft}\right) * TArea_{fgt} \quad \forall\, t \tag{5.32}$$

The first term of the right-hand side of Equation (5.32) accounts for costs associated with purchasing available feedstocks, e.g., forestry residues and agricultural waste. The second term refers to costs associated with cultivation of new feedstocks. The parameter UFC_{fgt} represents the unit acquisition cost for available feedstocks ($f \in F^a$). Parameters $Rent_{gt}$ and $OpCost_{ft}$ are the renting costs of land for new plantations and general operational costs, respectively. The latter includes fixed overheads, agrochemicals, harvesting costs, and storage costs.

5.3.6.2 Production costs

Total production costs, PC_t, are split into fixed and variable costs. Fixed costs are independent of the output level of a plant and often include insurance, rent, salaries, etc. On the other hand, variable costs such as inventory, utilities, packaging, etc. depend proportionally on the actual production of a plant. This is expressed mathematically in Equation (5.33).

$$PC_t = \sum_{kg} \sum_{f \in F_k} \left(FxOpIN_{fkt} * AvIN_{fkgt} + VrOpIN_{fks} * PIN_{fkg,biosng,t}\right) \quad \forall\, t \tag{5.33}$$

Parameters $FxOpIN_{fkt}$ and $VrOpIN_{fks}$ correspond to fixed and variable costs of integrated plants. The binary variable that accounts for installation and subsequent capacity expansions, δIN_{fkgts}, is not adequate to calculate the fixed operational costs. Therefore, a new binary variable, $AvIN_{fkgt}$, is introduced which becomes active once a plant is installed. This condition is modelled by means of Equations (5.34) and (5.35).

$$AvIN_{fkgt} \geq \sum_{s} \delta IN_{fkgts} \quad \forall\, k, f \in F_k, g, t \tag{5.34}$$

$$AvIN_{fkgt} \geq AvIN_{fkg,t-1} \quad \forall\, k, f \in F_k, g, t \tag{5.35}$$

5.3.6.3 Transportation costs

The total transportation cost, TC_t, is calculated as the sum of local and regional transportation costs for delivery of feedstocks, and BioSNG as shown in Equation (5.36):

$$TC_t = TC\_F_t + TC\_SNG_t^{Reg} + TC\_SNG_t^{Loc} \quad \forall\, t \tag{5.36}$$

Calculation of feedstock transportation costs includes local and regional components. Furthermore, the local and regional costs are divided into two terms, fixed and variable expenses as depicted in Equation (5.37). The unit fixed cost for local transportation of feedstocks is represented by parameter $FxTC_f^{Loc}$. The total fixed cost is proportional to the production of feedstocks which is denoted by the variable P_{fgt}. On the other hand, the local variable cost is estimated based on the unit local variable cost, $VrTC_f^{Loc}$, the local production of feedstocks, P_{fgt}, and local transportation distance, LD_g.

$$\begin{aligned} TC\_F_t = \sum_{fg} \left(\frac{\lambda * FxTC_f^{Loc} * P_{fgt}}{LHV_f} + \frac{\lambda * VrTC_f^{Loc} * LD_g * P_{fgt}}{LHV_f} \right) \\ + \sum_{(fgg'l) \in \eta_{igg'l}} \left(\frac{\lambda * FxTC_{fl}^{Reg} * Q_{fgg'lt}}{LHV_f} \right. \\ \left. + \frac{\lambda * VrTC_{fl}^{Reg} * AD_{gg'l} * Q_{fgg'lt}}{LHV_f} \right) \quad \forall\, t \end{aligned} \tag{5.37}$$

An equivalent formulation is included to account for regional transportation costs in which parameters $FxTC_{fl}^{Reg}$ and $VrTC_{fl}^{Reg}$ refer to fixed and variable unit regional costs for transporting feedstock f via mode l. The regional distances are represented by parameter $AD_{gg'l}$. Scalar λ is a conversion factor included for consistency of units. Additionally, local transportation costs of BioSNG, $TC\_SNG_t^{Loc}$, associated with new installed facilities are calculated through Equation (5.38):

$$TC\_SNG_t^{Loc} = \sum_{gl} \Bigg[FP_l \frac{2 * \lambda * LD_g * LocSup_{gt}}{FE_l * TCap_l * LHV_i} + DW_l \frac{\lambda * LocSup_{gt}}{TCap_l * LHV_i} \left(\frac{2 * LD_g}{SP_l} + LUT_l \right) + ME_l \frac{2 * \lambda * LD_g * LocSup_{gt}}{TCap_l * LHV_i} + GE_l \frac{\lambda * LocSup_{gt}}{TMA_l^{Loc} TCap_l * LHV_i} \left(\frac{2 * LD_g}{SP_l} + LUT_l \right) \Bigg] \quad \forall\, t, i = \{biosng\} \tag{5.38}$$

Four main components constitute the local costs due to BioSNG transportation: fuel price, FP_l, driver wage, DW_l, maintenance expenses, ME_l, and general expenses, GE_l. Parameter FE_l refers to the fuel efficiency. Finally, an analogous formulation is included to calculate the regional costs for BioSNG transportation, $TC\_SNG_t^{Reg}$, as depicted in Equation (5.39):

$$TC\_SNG_t^{Reg} = \sum_{(igg'l) | \in \eta_{igg'l}} \Bigg[FP_l \frac{2 * \lambda * AD_{gg'l} * Q_{igg'lt}}{FE_l * TCap_l * LHV_i} + DW_l \frac{\lambda * Q_{igg'lt}}{TCap_l * LHV_i} \left(\frac{2 * AD_{gg'l}}{SP_l} + LUT_l \right) + ME_l \frac{2 * \lambda * AD_{gg'l} * Q_{igg'lt}}{TCap_l * LHV_i} + GE_l \frac{\lambda * Q_{igg'lt}}{TMA_l^{Reg} TCap_l * LHV_i} \left(\frac{2 * AD_{gg'l}}{SP_l} + LUT_l \right) \Bigg] \quad \forall\, t, i = \{biosng\} \tag{5.39}$$

5.3.7 Model summary

The proposed optimisation framework previously described addresses the long-term strategic design of BioSNG supply chains at regional and national levels. The proposed model relies on an economic component, Equations (5.1) to (5.9), that

is common to other methodologies presented for different systems. However, there are important considerations particularly relevant to the design of BioSNG supply chains worth of highlighting. One of them is the computation of land used for sustainable energy applications, modelled through Equations (5.12) and (5.13), since they allow to contemplate regional and nationwide environmental limits for a sustainable production of BioSNG from energy crops, which is modelled by means of Equations (5.14) and (5.15). Energy integration for the cogeneration of heat and power is another important aspect for the economics of BioSNG supply chains. This has been included as part of the optimisation process by means of Equation (5.18). The compatibility of BioSNG with natural gas makes possible its injection into the gas transmission or distribution system. Certainly, this is remarkably beneficial for the economics of BioSNG production. Accordingly, Equations (5.20) and (5.21) account for any existing natural gas transportation network that can supply BioSNG to final consumers. Finally, costs related to the development of new infrastructure for local and regional deliveries of BioSNG from processing plants to injection points should be considered. This is accounted for by Equations (5.28) to (5.30) which are included to calculate the capital investments of BioSNG transportation infrastructure, and Equations (5.38) and (5.39) which are included to account for the associated operational costs.

5.4 Case study definition: a UK-based case study

The applicability of the proposed optimisation model is demonstrated through the implementation of a UK case study. The optimisation framework requires technical and economic information regarding feedstock cultivation, processing facilities, and transportation modes. In addition, geographically distributed data is necessary in order to quantify demand distribution and location of available and new resources for energy generation. A Geographical Information System (GIS) was used to process this type of information. In general, the information comes in shapefile or raster format; these layers are uploaded in ArcGIS 10.2® [240] in which a pre-processing stage is carried out to generate data that fits the particular features of the case study such as the time horizon and the discretisation of the territory under study. This case study considers a time horizon of 20 years from 2020 to 2040 divided into

four 5-year periods. Additionally, the UK map was discretised accordingly to level 2 of the Nomenclature of Territorial Units for Statistics (NUTS2) [284]. A map showing NUTS1 and NUTS2 classification as well as equivalence between NUTS2 codes and the corresponding actual names of the regions is provided Appendix A. In total, 35 regions are included in the case study.

5.4.1 Resources

In this study, 4 types of resources are included as potential feedstocks for BioSNG production: (1) woody biomass, (2) cereal straw, (3) miscanthus, as a new energy crop, and (4) residual waste. The potential availability of each feedstock is estimated based on domestic resources.

5.4.1.1 Woody biomass

Currently, woody biomass is regarded as the most likely feedstock to be used in first commercial plants for production of BioSNG [116]. In this study, the potential of woody biomass available for renewable energy generation is estimated based on 4 sources: (1) forestry residues and stemwood, (2) arboricultural arisings, and (3) sawmill coproducts.

Forestry residues are mainly composed by tips and branches (56%), poor quality stemwood (30%), and foliage (14%) [285]. The European Environmental Agency (EEA) estimated that in the UK the total potential that can be used without impacting the environment is 3450 kTon/y for 2020 and 2532 kTon/y for 2030 [286]. As the information is reported at national level, a map for the geographic distribution of forestry lands across UK [287] (see Appendix A) is used as proxy for the calculation of available forestry residues at NUTS2 level. Arboricultural arisings include stemwood, branches, wood chips, and foliage from harvesting, pruning and safety operations in urban and semi-rural areas. The contribution of arboricultural arisings for energy generation is 332 kTon/y [288]. In order to distribute this potential into the 35 regions (NUTS2), a Land Cover Map of Great Britain published in 2007 (LCM2007) was used [289]. With respect to sawmill coproducts, the fraction available for energy generation is set to 10% of the total sawmill coproducts since most of the production is sold to wood processing industries [288]. The total

production of sawmill coproducts in the UK for 2020 was projected to be 120 kTon/y [285]. The sawmill coproducts potential at NUTS2 level was estimated based on a map of active sawmills in the UK (see Appendix A).

In total, the resources of woody biomass that can be used for energy generation are estimated in 3902 kTon/y by 2020. As the woody resources are composed by different types of biomass, an average cost of 65 £/Ton was used for all the regions [290]. This cost was kept constant for all the planning periods.

5.4.1.2 Cereal straw

Agricultural residues are an additional source of biomass for renewable energy generation. For this case study, cereal straw, from wheat and barley, is considered to be a suitable feedstock for future projects in BioSNG production. The Department for Environment Food and Rural Affairs (Defra) estimated that the total straw production in the UK in 2007 ranged between 9 and 10 MTon/y. Nonetheless, a significant fraction of these resources are recycled for activities such as animal bedding (56%), animal feed (19%), and used as fertilisers and organic matter supplements [291]. After considering these figures, Defra estimated the total production of cereal straw available for bioenergy production to be 3000 kTon/y [292]. The price of cereal straw was fixed at 60 £/Ton which is the average of the monthly price reported by Defra for pickup baled wheat straw in 2014 [293].

5.4.1.3 Miscanthus

Specialised energy crops can play an important role in the development of renewable supply chains. Miscanthus is a perennial energy crop with great potential for sustainable energy generation, which could have environmental advantages if its cultivation is carried out in marginal land areas avoiding land competition and woodland or grassland replacement [294]. In this study, miscanthus is included as a potential new feedstock. In this case, the availability is defined in terms of the crop productivity and available marginal land for energy crops cultivation across the UK. The miscanthus yield potential for current and future climate conditions across Great Britain was investigated by Hastings et al. [295]. Miscanthus yield maps were generated for 2020, 2030 and 2050 in which three scenarios were considered; low,

medium and high productivity. In this study, the high productivity scenario was used as it seems to be the path the UK is committed to for the foreseeable future (The School of Biological Sciences, The University of Aberdeen. Personal communication). Additionally, Lovett et al. [296] studied the potential available land for cultivation of new perennial crops for energy generation. A rigorous land classification was implemented in order to exclude territories from the estimation of the final land availability such as: Urban areas, main roads, rivers, lakes, natural and seminatural areas, areas with slope greater than 15%, high organic carbon soils, existing woodland, cultural heritage, natural parks, and areas of outstanding natural beauty. Finally, a potential availability of 8.1 Mha was estimated for new specialised energy crops, which is equivalent to 35% of the Great Britain territory. The interception of the potential miscanthus yield map and the available land map is shown in Figure 5.3.

The European Environmental Agency (ECA) published the report "Estimating the environmentally compatible bioenergy potential from agriculture" [282] where they established feasible limits of land usage for energy crops without risking aspects such as sustainability, and food security due to possible land competition. The maximum limits were estimated to be 824 kha in 2010 and 1584 kha for 2030. Although these limits refer to arable land, they were implemented in the current case study in order to prevent possible over utilisation of available land exclusively for miscanthus cultivation.

Regarding the economic aspects, plantation of new energy crops requires initial investment related to establishment and removal activities; additional operational costs are also considered which correspond to activities such as fixed overheads, agrochemicals, harvesting costs, and storage. This information was taken from the work published by Bauen et al. [281].

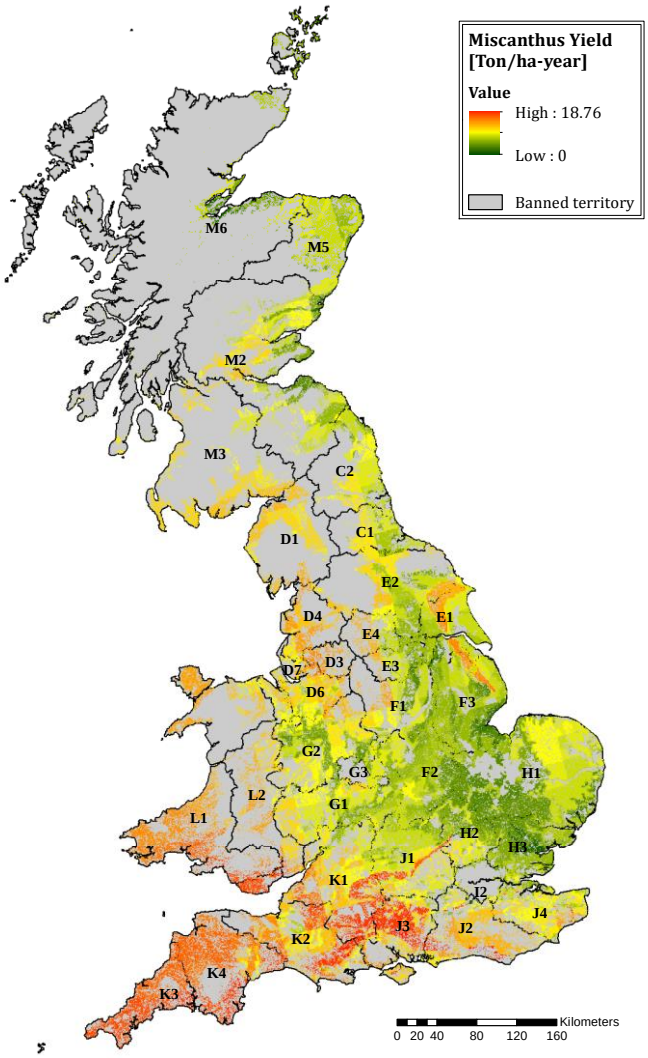

Figure 5.3. Miscanthus yield estimation for high productivity scenario in 2020. (Map generated with data from [295] and [296])

5.4.1.4 Residual waste

The waste management hierarchy places waste prevention at the top, followed by reuse, recycle/compost, then energy recovery, and finally disposal as the last option [297]. The UK has adopted a policy framework that gives priority to recycling, while limiting the percentage of waste that can be treated in waste-to-energy facilities. Three categories were included for the estimation of available waste for energy production: MSW, commercial sector, and industrial sector.

In Wales, MSW availability is estimated to be 531 kTon/y and 128 kTon/y available for 2020 and 2040, respectively [298,299]. The available resources from commercial and industry sectors for energy generation are 497 kTon/y and 596

kTon/y in 2020, and decrease to 132 kTon/y and 148 kTon/y in 2040, respectively [300,301]. In Scotland, the available resources for energy generation by 2020 from MSW, commercial, and industrial sectors are estimated in 706 kTon/y, 1058 kTon/y, and 405 kTon/y, respectively [302]. The resource availability decreases around 69% by 2040. In England, the total available resources are estimated in 7,344 kTon/y, 5911 kTon/y, and 5971 kTon/y for MWS, commercial sector, and industrial sector, respectively [303–306].

In total, available residual waste for energy generation the UK is around 23,020 kTon/y in 2020 and decreases to 7544 kTon/y by 2040, around 67% less availability than at the beginning of the planning horizon. Figure 5.4 presents information regarding the distribution of MSW, commercial waste, and industrial waste for 2009 and the steps involved to estimate available residual waste resources for energy generation in 2020. These figures were subsequently distributed across the UK at NUTS2 using as proxy projections of population per region [307].

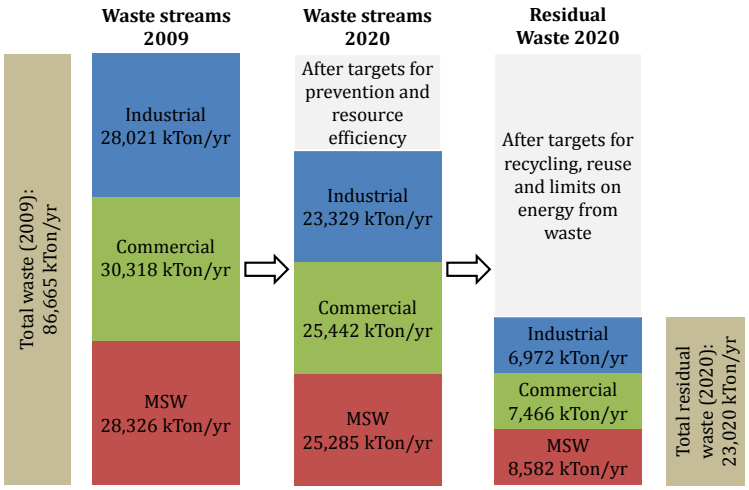

Figure 5.4. Estimation of available residual waste resources in the UK for 2020

In 2014, the landfill tax was set at 80 £/Ton, this means that local authorities have to pay £80 for every ton of waste sent to landfill. Alternative technologies that can process waste for lower costs would gain rapid acceptance since they can represent a cheaper option to treat waste. Different gate fees have been reported for waste [29,308], in this work an average for the cost of waste was initially set at -35

£/Ton for the first planning period. This represents an important incentive for companies involved, especially considering that the use of waste as feedstock is comparatively more challenging than woody biomass or perennial crops. However, as the usage of waste for energy generation increase, it is expected major competition for residual waste which will likely increase gate fees [29]. Unfortunately, the prediction of gate fees for residual waste has not been reported for the UK, therefore, in order to take this into account to some extent, a steady increment of gate fees was carried out along the planning horizon.

The regional distribution of woody biomass, cereal straw, miscanthus, and residual waste is presented in Figure 5.5. Regions H1 (East Anglia), M2 (Eastern Scotland), and L1 (West Wales and The Valleys) present high availability of woody biomass resources. Cereal straw resources are predominantly located in regions H1 and M2, the eastern part of mid England and regions G1 (Herefordshire, Worcestershire and Warwickshire), and K1 (Gloucestershire, Wiltshire and Bristol/Bath area). The potential for miscanthus cultivation is comparatively higher in regions H1, L1, and K1. It is worth to mention that the distribution shown in the map is calculated with data presented in Figure 5.3 and no global limit on land utilisation was considered.

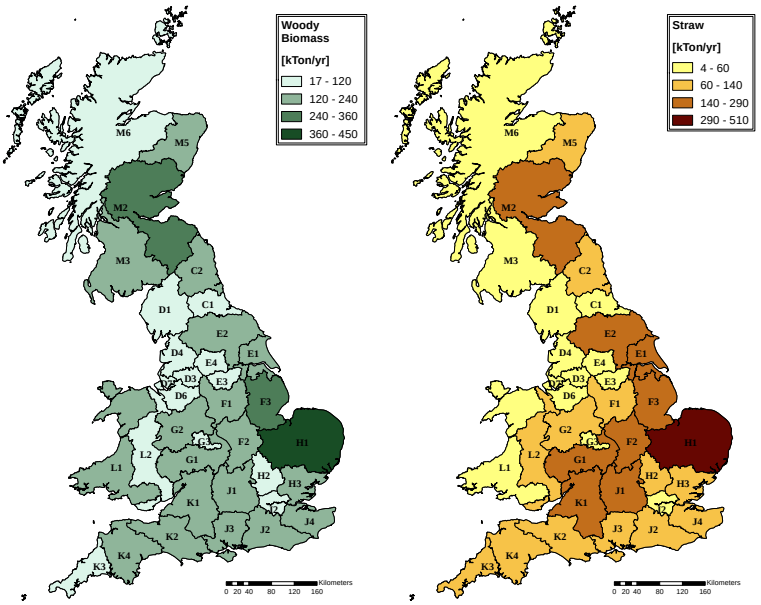

(a) (b)

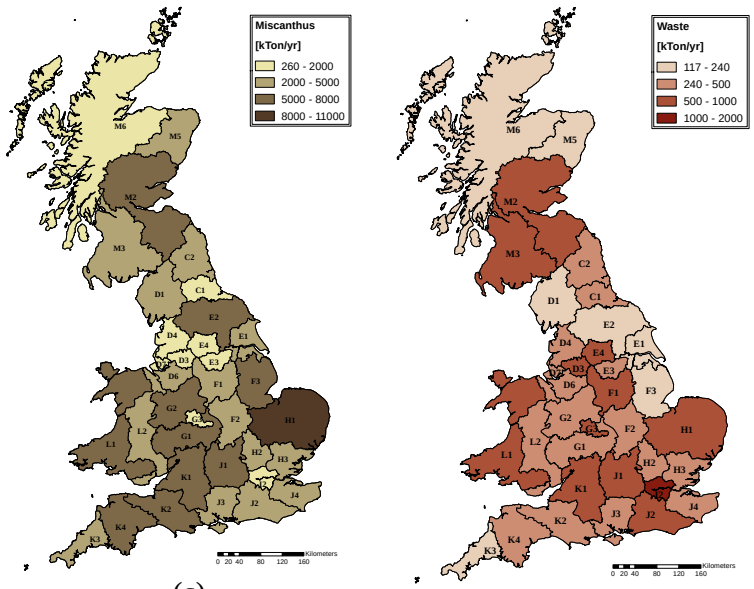

(c) (d)

Figure 5.5. Forecasted resource availability distribution in UK for period 2020-2024 for different feedstocks: (a) Woody Biomass. (b) Straw. (c) Miscanthus. (d) Waste.

Finally, residual waste distribution is substantially high in regions corresponding to the main cities in the UK, such as London (I2), Birmingham (G3), Leeds and Bradford (E4), Edinburgh (M2), Glasgow (M3).

5.4.2 Conversion technologies

In this work gasification technology is considered as the main route for BioSNG production in integrated plants. Several gasification technologies exist, Entrained Flow, Circulating Fluidised Bed, and allothermal (Indirect) gasification. The overall efficiency to BioSNG is usually higher for allothermal gasification [25]. Before the gasification step, feedstocks may need to be dried depending on the moisture content, since moisture decreases the gasifier performance. The net overall efficiencies on LHV basis, including electricity consumption and methanation process, are 54% for Entrained Flow, 58% for CFB, and up to 67% for allothermal gasification [25]. In this study, the design called MILENA, which is based on allothermal gasification and still under development by the Energy research Centre of the Netherlands (ECN), was chosen as the conversion technology for integrated plants. The global efficiency of the process can reach up to 91% if energy integration is considered [24]. The data is reported for woody biomass feedstock; however, due to lack of information the same efficiencies are used for cereal straw and miscanthus. For facilities treating residual waste, plasma gasification was selected since it is

more flexible and robust to handle this type of feedstock in comparison to allothermal gasification. The global efficiency for BioSNG production using plasma gasification was reported to be 52% with a potential increase of 10% if heat recovery is implemented [309].

Regarding capital investments, Batidzirai [310] estimated that a "nth-plant" using the MILENA concept with capacity to process 100 MW of woody biomass will require an initial investment of £116M. Taking these figures as a reference and using a scale factor of 0.67, it is possible to generate a curve that relates capital investment with installed capacity that reflects economies of scale. The scale factor was estimated based on data published in [29]. The maximum capacity of an integrated plant that can be installed in a region was limited to 1000 MW for every period of the planning horizon [311]. It is worth mentioning that this capacity is considerably large and it can make challenging the daily logistics for transportation of the necessary raw material. Therefore, this is a limitation of the proposed model since it does not address daily logistics for the transportation network. Based on this information, the capex curves for straw and miscanthus were obtained by correcting the data with the corresponding LHVs. This is an attempt for considering variations of investments for a specific type of biomass. However, this assumption does not take into account particular technical variations in the process, therefore, more detailed studies are needed to fill this gap. For facilities using plasma gasification, the capital expenditure was estimated to be £95M for an plant with installed capacity of 57 MW [310]. A scale factor of 0.8 was used to generate additional data for different capacities.

The operating costs are composed by two terms, fixed and variable costs. The fixed costs are independent of the operation of the plant whereas the variables costs depend on the throughput of the plant. The fixed cost for processing woody biomass, miscanthus, and cereal straw is set at 3 M£/y. The variable cost for woody biomass was estimated to be 0.0037 M£/GWh. This value was used to infer the corresponding variable costs for miscanthus and cereal straw by means of a correction based on LHVs. For facilities operating with plasma technology, the fixed cost was set to 2.8 M£/y with a variable cost of 0.0236 M£/GWh. The previous data was inferred from

available information in literature [29,309]. The data for global efficiencies of the process, capital investments, and operating costs take into account the entire process from raw feedstocks to BioSNG, which involves: (1) biomass reception, preparation and handling, (2) gasification, (3) syngas processing (which includes contaminants removal and hydrogen/carbon monoxide ratio adjustment), (4) syngas methanation, and (5) gas conditioning and compression. A summary is presented in Table 5.1.

Table 5.1. Capex, Opex and technical specifications of processing facilities.

	Allothermal gasification (MILENA)	Plasma gasification
Capacity [MW]	100	100
Capex [£M]	116	149
Fixed cost [M£/y]	3.0	2.8
Variable cost [M£/GWh]	$3.7x10^{-3}$	$2.4x10^{-2}$
Feedstock-to-BioSNG efficiency	63.8%	52.0%
Heat recovery efficiency	22.2%	10.0%
References	[29,310]	[309]

5.4.3 Transportation infrastructure

Three modes for regional transportation are included in the case study: truck, trailer and railroad. In the case of local transportation only truck and trailer are considered. The transportation costs are divided into fixed and variable costs. The term that accounts for the fixed costs depends on the amount of feedstock transported; similarly, the term for variable costs depends on the mass transported but also on the transportation distance. The transportation cost data for woody biomass and miscanthus for truck and rail modes was taken from Searcy et al. [312]. On the other hand, BioSNG is transported only by trailers as compressed natural gas (CNG). The fixed and variable costs for truck and rail mode for each feedstock are summarised in Table 5.2.

Table 5.2. Fixed and variable costs for feedstock transportation.

	Fixed costs [£/GWh]		Variable costs [£/km-GWh]	
	Truck	Rail	Truck	Rail
Woody biomass	821.9	1,496.3	19.1	4.6
Residual waste	1,451.7	4,679.2	39.9	7.6
Miscanthus	1,097.9	3,538.9	30.0	5.8
Cereal straw	1,088.8	3,509.4	29.8	5.7

From the data it can be noticed that fixed costs for truck transportation are lower than for rail transportation, by contrast, variable costs for truck transportation are higher than for rail. This makes transportation by rail more convenient over longer distances, whereas transportation by truck is more appropriate for short distances. Additionally to local and regional transportation costs, it is considered that further investments are required for establishing an adequate transportation network for BioSNG from production plants to injection points. The corresponding information was taken from Almansoori and Shah [313] and Agnolucci et al. [283].

The estimation of distances between the different regions for truck and rail transportation modes was based on two georeferenced maps (see Figure 5.6) corresponding to the UK Road network and the UK Railroad network [314].

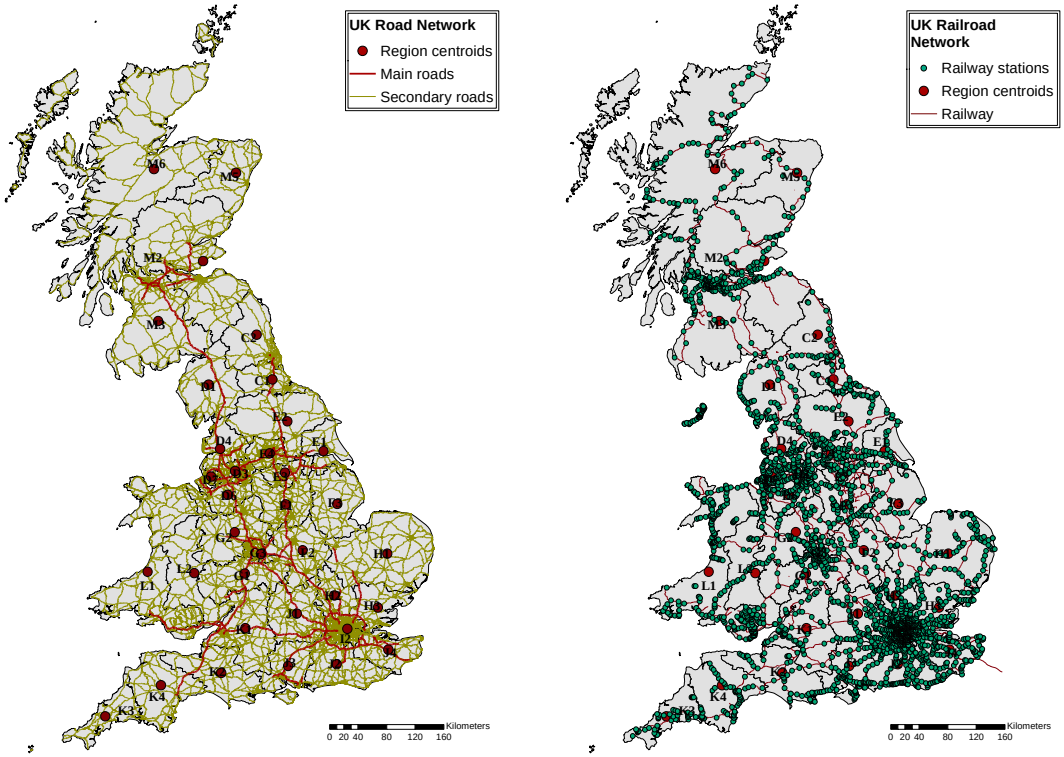

(a) (b)

Figure 5.6. Transportation infrastructure in the UK. (a) Road network and (b) Railroad network. Contains Ordnance Survey data © Crown copyright and database right 2015 [314].

It is assumed that future plants will be located in the centroids of the regions; the coordinates of each point are calculated with ArcGis 10.2. The distance by road between pair of regions was estimated through a network data set created in ArcGis

10.2 by joining layers containing main roads, secondary roads, roundabouts and interceptions; not shown in the map for convenience. Using the tool "Network Analysis" it is possible to intercept this network with the region centroids, creating an origin-destination matrix (OD Matrix) containing the minimum distance between two regions. The OD Matrix is then filtered to get the connectivity of the regions sharing a common border (neighbourhood). Additionally, a visual inspection was carried out to detect possible connections between regions without a common border whose connectivity is possible due to the dense road and/or rail network. For example, region I2 can be connected to J1, and J1 can be connected to region K1, however, there is a main road between I2 and K1 that makes possible a connection between them despite that the region J1 is in-between. This consideration will allow more flexibility in the final decisions regarding the transportation of feedstocks. An analogous procedure was followed for obtaining the distances by railroad. The local transportation distances were estimated by drawing a circumference around the centroid of a region whose radio represents the average travel distance for taking biomass from any area within the region to its centroid. This approach takes into account the spread distribution of the biomass around the centroid of a region. The same methodology was applied for obtaining the transportation distances between a plant and the injection points available locally.

5.4.4 Demand data

The Gas Ten Year Statement 2013 (GTYS) published by the National Grid [315] reports the gas and power annual demand forecasted until 2027. The GTYS deals with the associated uncertainty by analysing 2 different scenarios; GoneGreen and SlowProgression. In GoneGreen scenario, it is assumed that the environmental targets set for 2020, 2030 and 2050 are met. By contrast, in SlowProgression scenario the progress in renewables is slow, therefore, the target for 2020 is actually met between 2020 and 2025, and the target for 2030 is not achieved. This is reflected on a higher future demand for electricity and gas in SlowProgression scenario in comparison to GoneGreen scenario. For this study, the gas demand is fixed based on the GoneGreen scenario. No demand for heating is considered, therefore, all the heat recovered from the BioSNG production can be converted into power assuming an

efficiency of 40%. The future gas and power demand as well as their corresponding forecasted prices are shown in Figure 5.7.

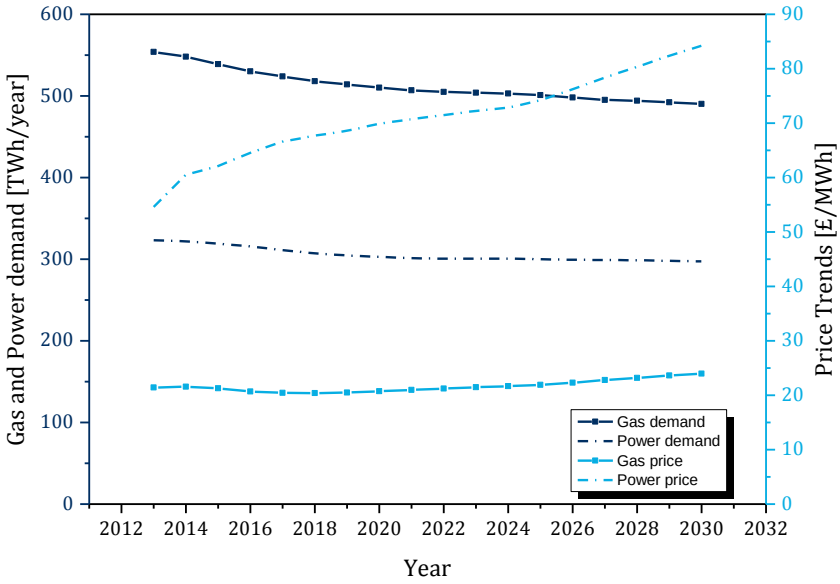

Figure 5.7. Forecasted gas demand for GoneGreen scenario [315,316]

Future gas and power prices were assigned based on the report UK Future Energy Scenarios published by the National Grid [316]. Gas prices vary from 20.7 £/MWh in 2020 up to 24.0 £/MWh in 2030. In the case of power, the prices are considerable higher starting from 69.9 £/MWh in 2020 and increasing up to 84.1 £/MWh in 2035. As a mean to supply the BioSNG to the demand centres, the BioSNG is sent to the gas transmission system (GTS), specifically to offtake points that connect the GTS with the GDN. The GDN is divided into 13 LDZs with the objective of delivering natural gas taken from the GTS to the final consumers. On average, the LDZs supply around 65% of the total gas demand in the UK. The LDZs supply 100% of the domestic demand and part of the demand from industrial and commercial customers. The rest of the demand (35%) is supplied through the GTS since some customers require operate at high pressure, such as power generation plants and some industries. The GDN is operated by 4 companies:

- Southern Gas Networks is in charge of Scotland (SC), Southern England (SO) and South East England (SE).

- Northern Gas Networks operates Northern England (NO) and North East England (NE).
- National Grid Gas operates North West England (NW), West Midlands (WM), East Midlands (EM), East Anglia (EA) and North Thames (NT).
- Wales & West Utilities is in charge of Wales North (WN), Wales South (WS) and South West (SW).

The GTS map published by the National Grid, and the LDZ distribution is shown in Figure 5.8. This map was updated by including 97 offtake points based on the information published in [315]. The dotted regions correspond to NUTS2 classification.

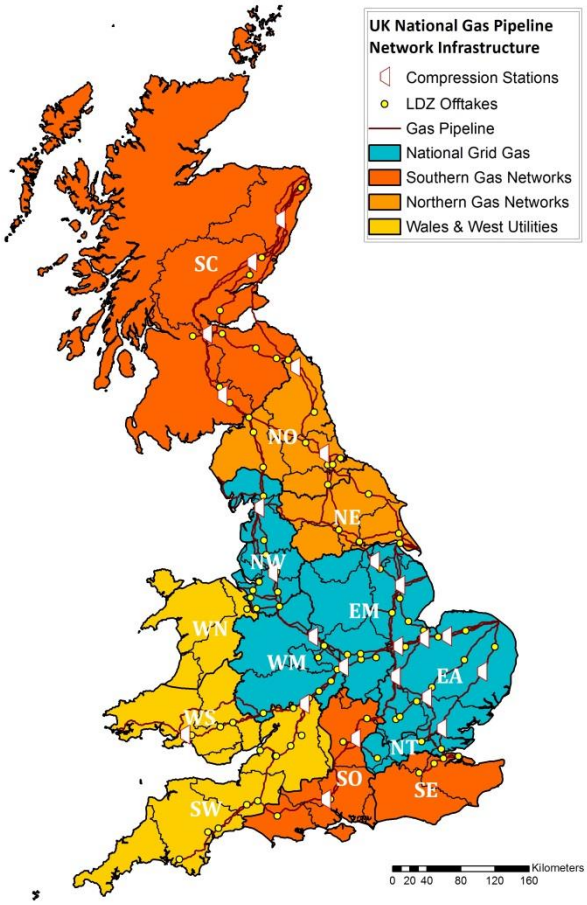

Figure 5.8. UK Gas pipeline network and Local Distribution Zones (LDZs) (map generated based on [317] and [318])

As the forecast demand correspond to the entire country, the demand per LDZ is assigned by calculating the demand fraction for each of the 13 LDZs based on

historical information [319]. It is worth to mention that in some cases, a region of the NUTS2 can supply BioSNG to two or more LDZs, for example region L2 can supply West North (WN) and Wales South (WS). Finally, it was assumed that all of the electricity generation is sold locally; therefore no power transmission system is included in this case study.

5.4.5 Economic parameters

Two different factors are used to discount the cash flow, CF_t, and capital expenditures, $CAPEX_t$, terms in the objective function. It is considered that the investments are made at the beginning of every 5-year period. The capital expenditures are discounted on a 5-year basis which corresponds to the time resolution chosen for the case study. Accordingly, the discount factor is calculated as follows:

$$DfCA_t = \left(\frac{1}{1+i}\right)^{5*(t-1)}$$

where i refers to the interest rate. The cash flow depends on terms such as operating costs, income, taxes, etc. These costs should be discounted periodically; therefore it is considered that the cash flow is discounted annually. Taking into account that the period t corresponds to a 5-year period, the equation is modified as follows:

$$DfCF_t = \frac{\sum_{j=1}^{5}(1+i)^{(j-1)}}{(1+i)^{5t}}$$

An average value of 10% was used for the interest rate i. For estimating the depreciation of the investments, it is assumed a 100% of depreciation in the first 7 years of the time horizon [320]. For the tax rate, Tr, a typical value of 35% was chosen. In addition, the rate for possible incentives for BioSNG production, denoted by parameter Inc_{pt}, is fixed based on the Renewable Heat Incentive programme. This incentive applies only for gas production, its average value is around 70 £/MWh. In case of power generation, Renewable Obligation Certificates (ROCs) are included as part of the income. For this case study, ROCs were set to 45 £/MWh.

The complete data set of the case studies can be found as supporting information in [276].

5.5 Results and discussion

This section presents the computational results for the case study described previously in section 5.4. Two instances of the same case study are considered: Case A, and Case B. The instances differ in the number of commodities (BioSNG and/or power) that are allowed as final products. Case A investigates the economic performance of the BioSNG supply chain in UK in which only BioSNG is allowed as final product. Case B aims to quantify the economic impact of cogenerating power along with BioSNG. The relevance of Case B stems from the fact that it is uncertain if the current regulation regarding the generation of renewable electricity could apply to gasification-based processing facilities. A regulation framework would not only facilitate the interconnection with the National Grid, making power sales to the system achievable, but also it would provide access to government incentives such as the Renewable Obligation Certificates (ROCs) programme. Unlike the gas transportation system and the electricity network in the UK, the heat district network capacity is not fully developed, which greatly restricts the centralised generation and distribution of heat to the demand centres. In consequence, the percentage of heat demand supplied by heat district networks is marginal and largely surpassed by the supply of electricity and natural gas. Therefore, it is considered that residual heat is used completely in electricity cogeneration, and not as an additional commodity. Finally, a parametric analysis based on Case B is carried out in which the economic performance of the BioSNG supply chain is addressed with respect to the percentage of total incurred costs subsidised by the government.

The optimisation problems were solved using GAMS 24.4.1. The MILP problem was solved with CPLEX 12.6.1. All runs were performed on a Dell OptiPlex 9010 with Intel® Core™ i7-3770 CPU @3.40 GHz and 16 GB RAM running Windows 7® Enterprise (64-bit operating system). The optimality gap was set to less or equal to 1% for all cases. The corresponding statistics for Case A and Case B are presented in Table 5.3.

Table 5.3. Model statistics and computational results for Case Study A and Case Study B.

	Case study A	Case study B
Total number of variables	15,713	16,553
Continuous variables	12,773	13,613
Binary variables	2,940	2,940
Total number of constraints	11,933	12,245
Non zero constraint matrix elements	54,629	56,589
CPU time [s]	2,483	2,620
Optimal NPV [£bn]	10.27	20.71

5.5.1 Production of BioSNG

The total cost breakdown for Case A is shown in Figure 5.9a. The values for Capex, Opex, and taxes are discounted to the first period.

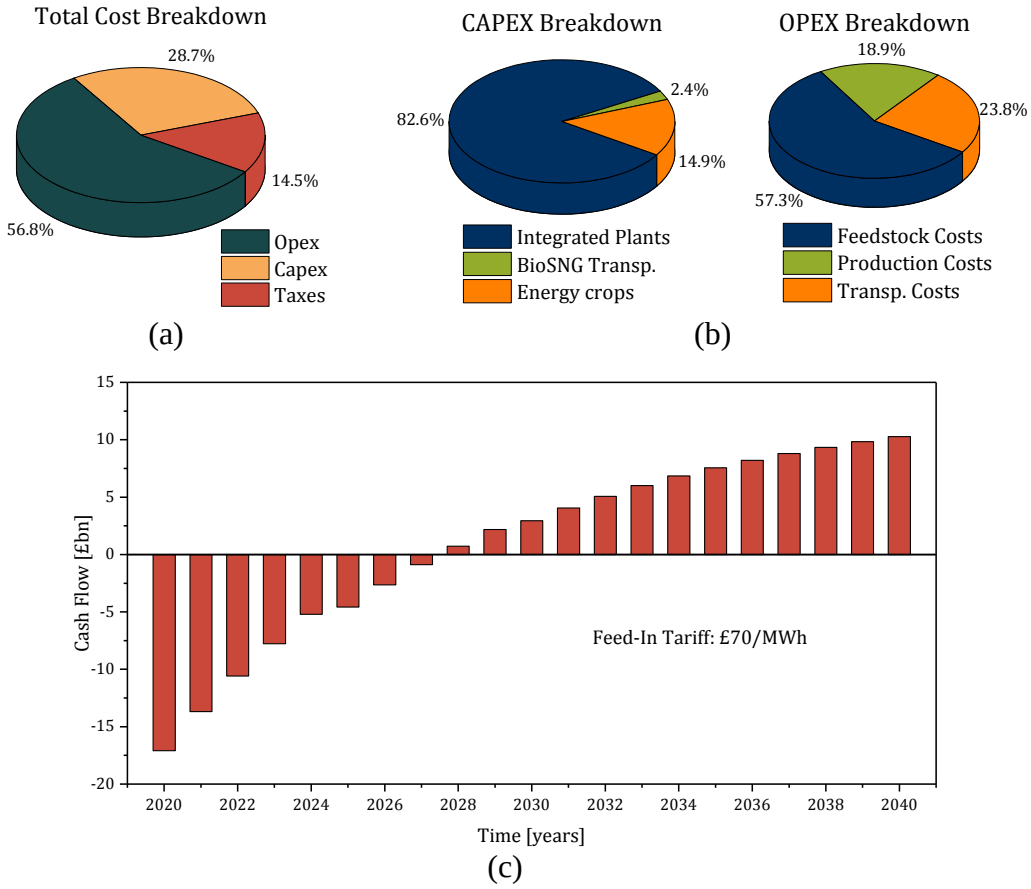

Figure 5.9. Summary of the economic performance for Case A: (a) total cost breakdown. (b). Capex and Opex Breakdown. (c) Cumulative net cash flow

The main component in the total costs is the operating expenditures with a share of 56.8%, followed by the capital expenditures with a share of 28.7%, and finally

14.5% of the total costs correspond to tax payments. The results indicate that the operational expenditures are the dominant component in the development of a BioSNG supply chain. Therefore, uncertainties in economic, technology, and crop parameters would likely impact the operation of the BioSNG supply chain.

The corresponding breakdown for Capex and Opex is shown in Figure 5.9b. The results show that the economics of the BioSNG supply chain is mainly dominated by feedstock purchases followed by installation of processing facilities. These two components account for 56.2% of the total expenses. Expenses related to transportation of feedstocks come in third place. Comparatively, investment in new infrastructure for BioSNG transportation is marginal. The cumulative cash flow was recalculated in a yearly basis as shown in Figure 5.9c. The optimal net present value was about £10.27bn and the breakeven time is reached after approximately 8 years. The breakeven gas price, defined here as the ratio between total expenditures (Capex plus Opex) and total gas production, was found to be 28.5 £/MWh.

The optimal feedstock production distribution across the UK is presented in Figure 5.10a. The classification shown in the map is based on the summation of average annual tons produced for every feedstock in a specific region. Six regions stand out in terms of feedstock generation for BioSNG production: M3 in Scotland, L1 and L2 which comprise Wales, and K3, K4 and J3 in England.

The use of residual waste for BioSNG production is dominant in most of the regions in England, especially in I2, D7, and G3 in which the cities of London, Liverpool, and Birmingham are located, respectively. The contribution of cereal straw in BioSNG production is comparatively low and fairly sparse between Scotland and England. In the case of woody biomass, its procurement rate for BioSNG production is about the same as the cereal straw. The cultivation of miscanthus has taken place predominantly towards the west part of UK.

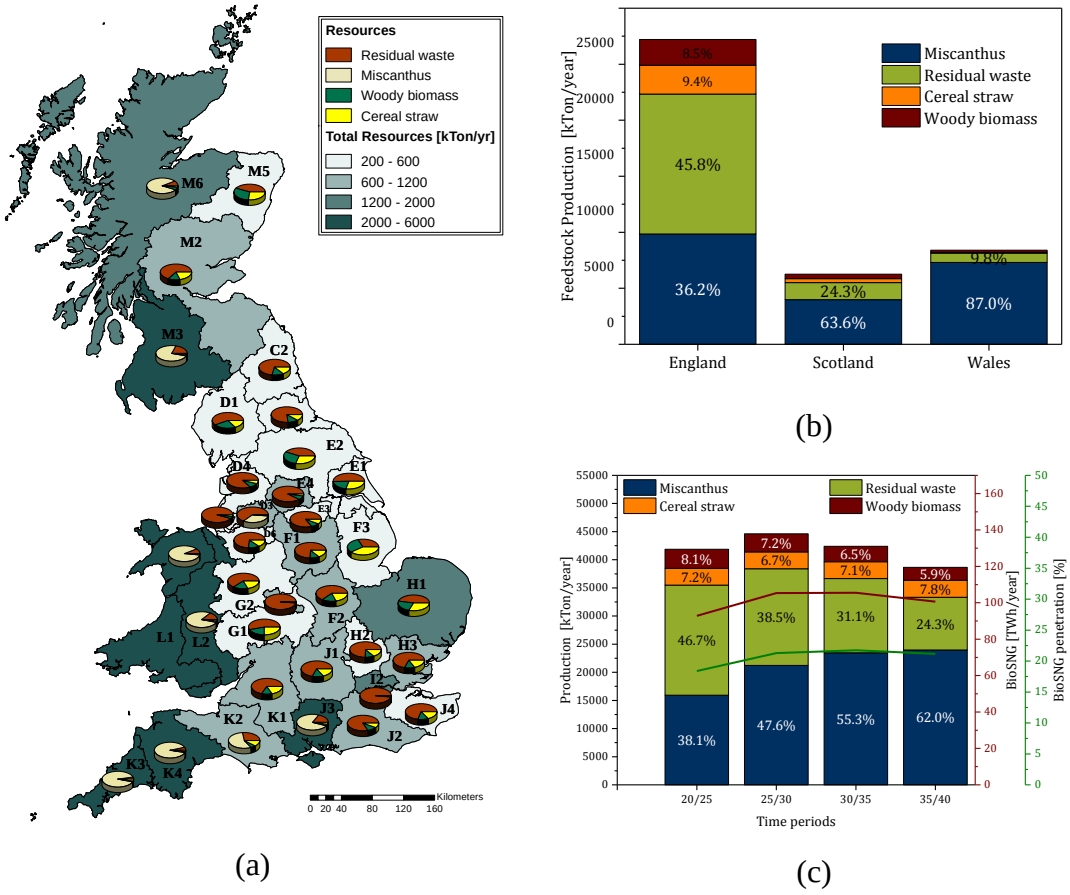

Figure 5.10. Optimal feedstock production: (a) Regional feedstock distribution and composition across the UK. (b) Average feedstock production for England, Scotland, and Wales. (c) Feedstock production and BioSNG penetration along the planning horizon

The regions with the highest feedstock throughput have in common cultivation of miscanthus. Surprisingly, region H1, which has the highest initial potential for miscanthus, was not selected. The combination of two facts can explain this result. First, due to sustainability reasons, the total land available for miscanthus cultivation is restricted, and second, the yields reported for this region are around the average or below (see Figure 5.3) which means that the high potential of region H1 comes from the extension of land rather than from the land productivity. Under these circumstances, the optimisation model chooses efficiency of land utilisation over potential, which is confirmed by the fact that the regions selected for miscanthus cultivation coincide with areas with high productivity.

The distribution of feedstock procurement across the countries is summarised in Figure 5.10b. In average, 65% of the total feedstock production comes from

England; Wales contributes with 20%, and finally Scotland with 15%. Miscanthus is the main source of biomass in Scotland and Wales, whereas in England, the predominant feedstock is residual waste. The utilisation of feedstocks along the planning horizon is summarised in Figure 5.10c. The share of woody biomass and cereal straw is nearly constant along the time periods. The utilisation of residual waste decreases along the planning horizon as a repercussion of the policies implemented aiming to a zero waste economy. On the other hand, the importance of miscanthus increases along with time compensating for the reduction of available residual waste. In terms of BioSNG penetration, it is possible to supply 18.4% of the gas demand in the period 2020-2025, and up to 21.2% of the demand in 2035-2040. The feedstock transfers between regions and the final installed capacity for every type of feedstock is presented in Figure 5.11.

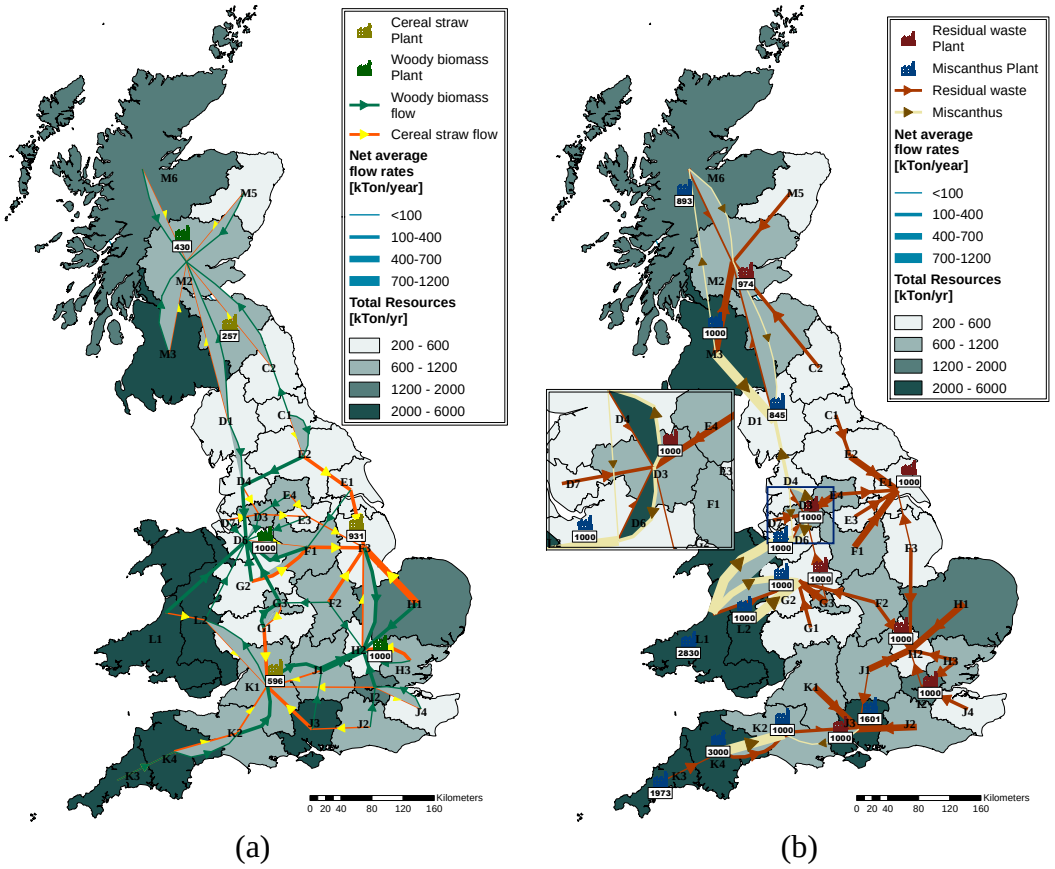

(a) (b)

Figure 5.11. Regional feedstock transfers and final installed capacity: (a) Net average flows for cereal straw and woody biomass. (b) Net average flows for miscanthus and residual waste

The final installed capacity for processing woody biomass is 2430 MW. The facilities are located in the north, centre, and south of UK, exhibiting a centralised production scheme. In the case of Cereal straw, the total install capacity is 2054 MW. Similarly to woody biomass, the distribution of the cereal straw plants across the UK feature a centralised scheme. Despite the high availability of cereal straw in region H1, the optimisation model does not opt for installing a plant in that region; instead, a plant is installed in the contiguous region F3. The reason for this decision lies in the transportation costs. It can be seen that this facility processes cereal from several regions around mid-England, therefore a more central location is preferred in order to reduce the transportation expenses.

A final installed capacity of 6974 MW is required in order to process residual waste, with 86% of the capacity located in England. In the case of miscanthus, 16142 MW of processing capacity are installed across the UK. The processing of miscanthus is carried out in two facilities in Scotland, seven facilities in England, and two facilities in Wales. Most of the plants are installed in a region where miscanthus has been planted, except in region D6, minimising the transportation distances and therefore the associated costs. A quick inspection of Figure 5.11b confirms that the transportation network for miscanthus is less complex than for the other feedstocks. It is clear from the results that miscanthus plays a crucial role in the production of BioSNG, especially in Wales and south west of England. Moreover, the production of BioSNG from miscanthus follows a distributed scheme when compared to woody biomass and cereal straw. The final total installed capacity was 27.3 GW, from which facilities for processing cereal straw corresponds to 6.5%, followed by woody biomass (8.9%), residual waste (25.5%), and miscanthus (59.1%). In terms of utilisation of transportation modes between regions, rail is usually the preferred mode although closely followed by truck transportation. For cereal straw, however, truck transportation is the preferred mode. In general, for feedstocks highly distributed and with low availability, the optimisation model prefers installing centralised plants with high capacity rather than small distributed plants. This suggests that the effect of economies of scale is, until certain extent, prevalent over the extra expenses associated with feedstock transportation.

A summary of the regional production of BioSNG, average supply in every LDZ, and net income is presented in Figure 5.12. In total 18 out of 35 regions are selected for BioSNG production. Figure 5.12a shows that most of the BioSNG transportation takes place within the regions, from processing facilities to injection points. This is a direct result of considering existing gas networks for injection of BioSNG, which reflects in low investments for BioSNG transportation infrastructure. Only three regional transfers are required due to the absence of injection points. The fact that the installation of facilities takes place in regions with no injection points, suggest that the additional expenses for transporting BioSNG between regions are offset by potential extra expenses of transporting feedstocks if the facilities were installed in contiguous regions with access to the GDN.

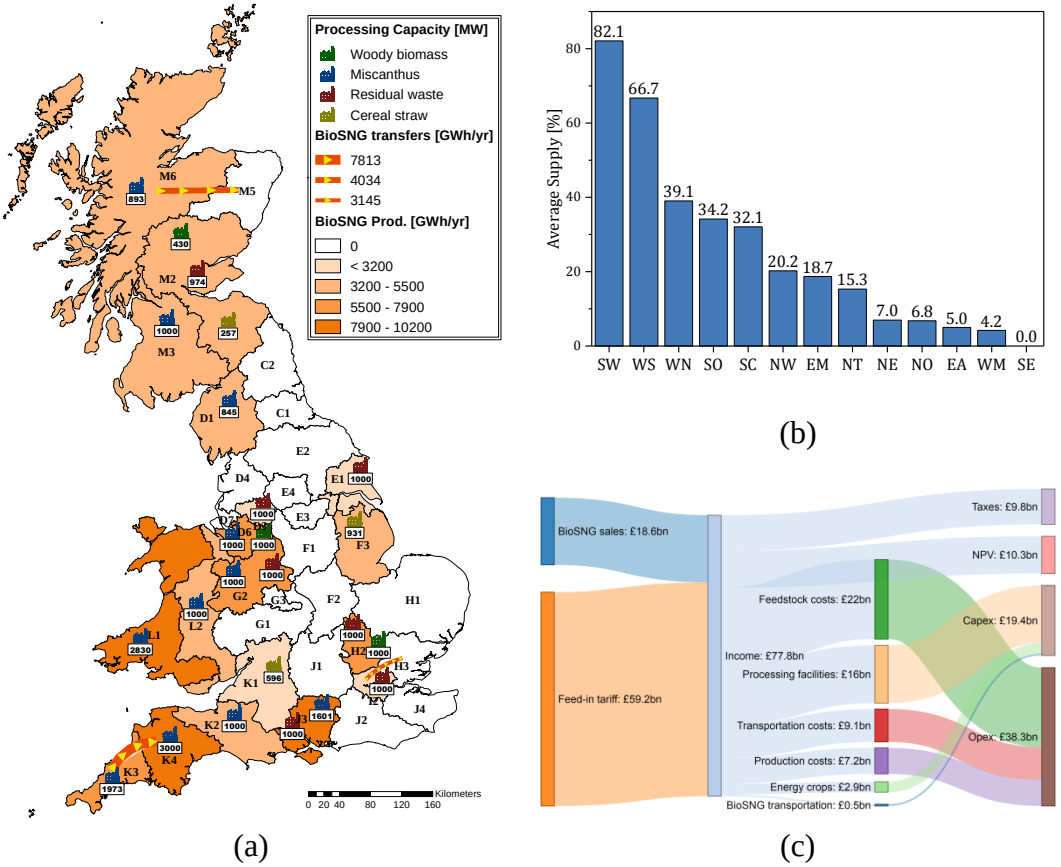

Figure 5.12. BioSNG supply and economic performance: (a) BioSNG production and regional transfers. (b) Average supply per LDZ. (c) Sankey diagram for the global economic performance

The average supply for each LDZ is presented in Figure 5.12b. South West (SW) and Wales South (WS) can potentially achieve a BioSNG penetration of 82.1%

and 66.7%, respectively. A significant supply is also achieved for Wales North (WN), Southern England (SO), and Scotland (SC), varying between 32.1% and 39.1%. The high supply percentages are mainly driven by the cultivation of Miscanthus in the respective areas. 15.3% of the demand in North Themes (including the City of London) can be supplied by BioSNG produced from residual waste and woody biomass. No injection of BioSNG takes place in South East England (SE). Finally, Figure 5.12c presents a comparison between the main components of the total costs and income from government incentives and BioSNG sales. Notably, tax payments equal the transportation costs and are higher than the production costs. At the tariff of 70 £/MWh, the incentives from the government during 20 years are £59.2bn, which corresponds to 76.1% of the total income. Moreover, the income related to BioSNG production is £18.6bn, which is 23.9% of the total income. The incentives are essentially used to cover operating and capital expenditures, whereas the BioSNG income offsets tax payments, and the surplus corresponds to the optimal NPV of £10.7bn. The fact that the totality of investments and operating costs required to be subsidised, makes less attractive the developing of a BioSNG supply chain from the government perspective. This will be further investigated in section 5.5.3.

5.5.2 Economic impact of power cogeneration

As previously discussed, it is unclear how the current regulation in the UK, regarding production of renewable energy, applies to electricity generated as a coproduct of the gasification process. Great efforts have been devoted for the continuous development of an inclusive regulatory framework that contemplates the great variety of sustainable technologies. It is reasonable, then, to consider that coproduction of electricity from gasification will benefit from schemes such as the Renewable Obligation Certificates (ROCs). This section the cogeneration of power and its potential benefits on the economic feasibility of the BioSNG supply chain. A comparison of the cumulative cash flow for Case A and Case B is presented in Figure 5.13.

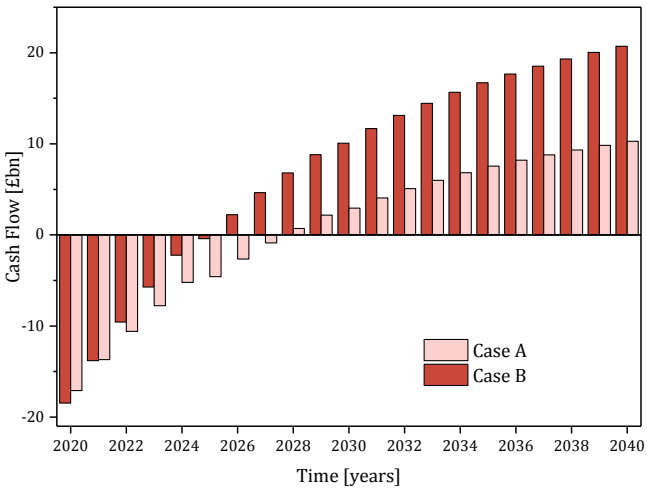

Figure 5.13. Cumulative cash flow comparison for Case A and Case B

When power sales are included, the breakeven time is 6 years, 2 years less than in Case A. The optimal NPV is £21.4bn, 48.3% higher than in the previous case. The initial investments are fairly higher in Case B than in Case A, this is related to investments in additional processing capacity as shown in Figure 5.14a.

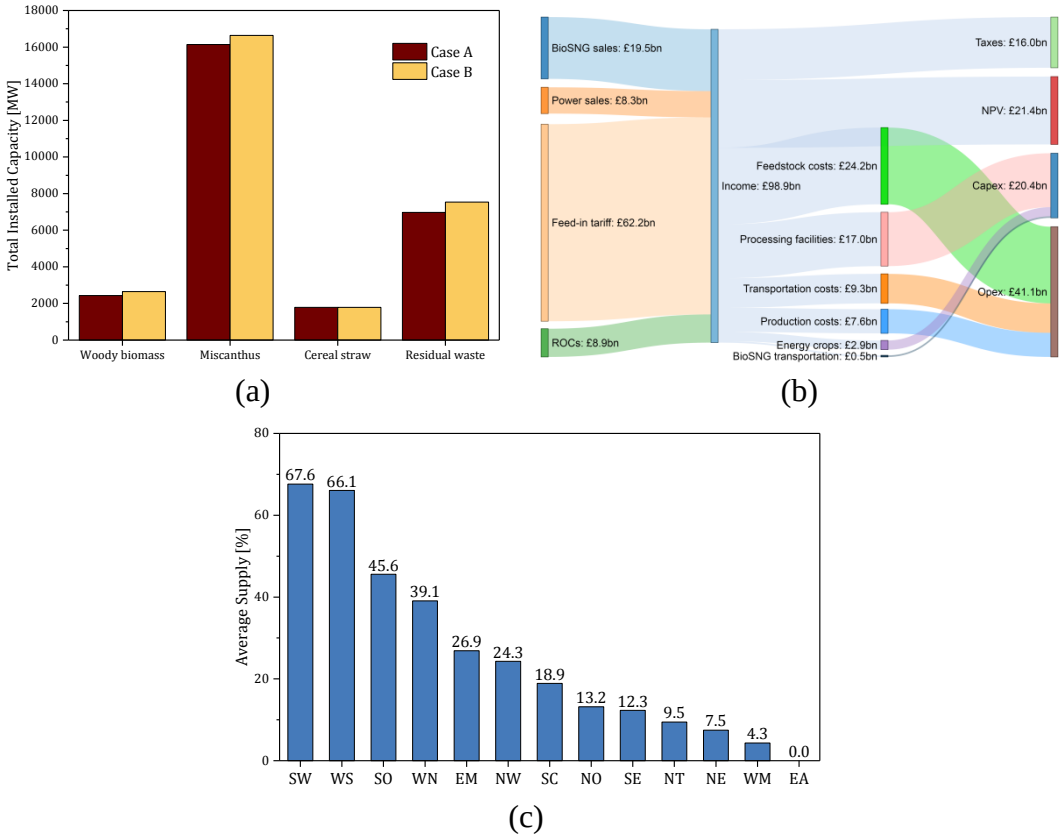

Figure 5.14. Summary of optimisation results for Case B: (a) Final installed capacity. (b) Sankey diagram for the global economic performance. (c) BioSNG supply per LDZ

The coproduction of power as extra commodity enables the supply chain to increase the processing of feedstock in order to take advantage of the new source of income. Consequently, the production of woody biomass, miscanthus and residual waste increased 2.6%, 4.6% and 2.6%, respectively.

Nonetheless, the production of cereal straw was the same as in Case A, which indicates that this feedstock is being used at its maximum availability. Additional 215 MW were installed for woody biomass processing in comparison to Case A. For miscanthus and residual waste, the additional capacity was 500 MW and 561 MW, respectively. In the case of cereal straw, the installed capacity was the same as in Case A. The regions selected for installation of facilities in Case B is compared with the results for Case A in Table 5.4.

Table 5.4. Comparison for plant installations for Case A and Case B

	Case A	Case B
Woody biomass	D6, H2, M2	D1, F2, J3
Cereal straw	F3, K1, M2	F3, K1, M2
Miscanthus	D1, D6, G2, J3, K2, K3, K4, L1, L2, M3, M6	D1, D4, D6, G2, J2, J3, K1, K2, K4, L1, L2, M3
Residual waste	D3, E1, G2, H2, I2, J3, M2	D3, E1, G2, H3, J1, J2, K2, M2

The decision for location of facilities processing cereal straw remained the same as in Case A. However, some of the regions for processing woody biomass, miscanthus, and waste are different to the previous case. Notably, this coincides with the feedstocks that required additional capacity due to an increment in their production, as discussed previously. The additional production of miscanthus, woody biomass, and residual waste, involves higher transportation activity driving associated costs up. This situation can be mitigated by readjusting the location of the corresponding facilities. A summary of the economic performance of Case B is presented in Figure 5.14b. The proportions of the different components of the total costs are similar to Case A. Regarding the total income, the feed-in tariff increased slightly and continues to be the main source of profit with a share of 62.8%. The BioSNG income increased 4.7% with respect to Case A, reaching £19.5bn (19.7%).

Power sales and ROCs contribute with £8.3bn (8.4%) and £8.9bn (9.1%), respectively. Finally, the supply of BioSNG presented a small increment of 0.8%, in comparison to Case A, reaching 21.4%. The coproduction of power is enough to supply 4.4% of the total demand along the planning horizon. The comparison of results for Case A and Case B is summarised in Table 5.5.

Table 5.5. Results comparison for Case A and Case B

	Case A	Case B	Variation [%]
NPV [£bn]	10.7	21.4	100.0
Total Capex [£bn]	19.3	20.4	5.7
Total Opex [£bn]	38.3	41.1	7.3
Taxes [£bn]	9.8	16.0	63.3
Total Income [£bn]	18.6	27.8	49.5
Total Incentives [£bn]	59.2	71.2	20.3
BioSNG production [GWh/y]	101,109	105,070	3.9
Power production [GWh/y]	-	13,234	-
BioSNG penetration [%]	20.6	21.4	3.9
Power penetration [%]	-	4.4	-
Breakeven cost [£/MMBTU]	28.5	26.5	-7.0

The average BioSNG supply in every LDZ is presented in Figure 5.14c. Although the supply in SW was reduced in 14.5%, this region continues to be the most relevant in terms of BioSNG supply, narrowly followed by WS. By contrast, regions such as SO and SC increased its share of BioSNG supply. These alterations are closely linked to the rearrangement of the facilities across the UK as explained before.

5.5.3 Parametric analysis of government incentives

This section presents a parametric analysis in which the role of the government in developing a BioSNG supply chain is addressed. Results for Case A and Case B show that the incentives associated with the feed-in tariff scheme surpass largely the income of BioSNG sales and are virtually equal to the capital investments and operating expenses. Consequently, a new constraint was included in the optimisation model in order to limit the fraction of Capex and Opex that can be funded through the feed-in tariff scheme as depicted in Equation (5.40).

$$\sum_t (DfCF_t * IncentiveGOV_t) \leq \theta * \sum_t (DfCF_t * OPEX_t + DfCA_t * CAPEX_t) \quad (5.40)$$

$IncentiveGOV_t$ is a variable that accounts for economic incentives provided by the government through the Feed-in tariff scheme. The parameter θ corresponds to the fraction of operating and capital expenditures subsidised by the government. Both terms on each side of the constraint are discounted to present value. In addition, variable $IncentiveGOV_t$ will be restricted by the production of BioSNG in every period times the tariff, which for this study is 70 MWh/y. This condition is modelled by Equation (5.41):

$$IncentiveGOV_t \leq \sum_{pg} Inc_{pt} * P_{pgt} \quad \forall\, t, p = \{biosng\} \quad (5.41)$$

Incentives related to power generation are modelled through the Equation (5.42).

$$IncentiveROC_t = \sum_{pg} Inc_{pt} * P_{pgt} \quad \forall\, t, p = \{power\} \quad (5.42)$$

where $IncentiveROC_t$ is a variable that accounts for economic incentives through ROCs due to power generation. Finally, the equation for income is modified accordingly in order to take into account the new variables as shown in Equation (5.43):

$$INCOME_t = \sum_{pg} \left(Price_{pt} * P_{pgt}\right) + IncentiveGOV_t + IncentiveROC_t \quad \forall\, t \quad (5.43)$$

The parameter θ was varied systematically from 100% (Capex and Opex can be completely subsidised by the government), down to 0%. The impact of θ on NPV, capital and operating expenditures, and feedstocks procurement rate is presented in Figure 5.15.

The results show that the development of a BioSNG supply chain is economically feasible if the government supports minimum 30% of the total associated expenses. Nonetheless, this level of subsidisation only achieves a BioSNG penetration of 0.9%. The investments are focused on developing cereal straw as the only feedstock for BioSNG production. The operating costs are almost

three-fold of the corresponding Capex. The subsidisation is not enough to develop cultivation of miscanthus.

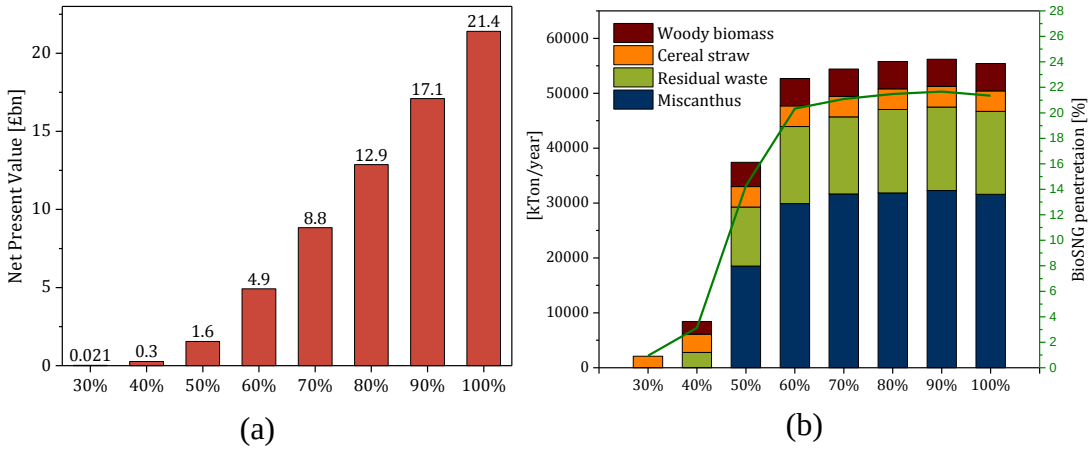

Figure 5.15. Role of government incentives on the BioSNG supply chain: (a) Net present value. (c) Feedstocks production and BioSNG penetration

At $\theta = 40\%$, woody biomass and residual waste are added to the mix of feedstocks. Consequently, the production of BioSNG can supply 3.1% of the total gas demand. Investments in cultivation of miscanthus start once the government subsidies up to 50% of the total costs. At this point, the NPV is £1.6bn; the investments in facilities as well as the operating costs increased significantly in comparison to the previous case. The cultivation of miscanthus is now the main source of feedstocks. The supply of BioSNG increased remarkably to 14.3%.

An additional increment of 10% in θ drives the investments and operating expenses up in 49.8% and 52.7%, respectively. This is due mostly to installation of new facilities for processing miscanthus. The NPV increased three-fold reaching £4.9bn. The BioSNG supply also increased considerably achieving 20.3% of the total gas demand. After this point, the investments, operating costs, and BioSNG penetration are moderately stable, therefore, the parameter θ has only effect on the NPV. It is worth of mention that there is a slight decrement of investments, and consequently the BioSNG penetration, when θ goes from 90% to 100%. Tax payments are causing this effect. It is expected that the production of BioSNG, and therefore the income, increases along with θ. However, at 100%, the optimal solution led to decreasing slightly the production of BioSNG in order to compensate for the increment of taxes. Additional runs confirmed this. The results revealed that

varying the tax rate ±10%, from the base case (tax rate = 35%), the production of BioSNG in the last period increased 0.15% with respect to the base case for a tax rate of 25%. Similarly, for a tax rate of 45%, the production of BioSNG in the last period decreased 0.32% in comparison to the base case. This reaffirms the importance of developing systematic frameworks that assist in disclosing trends that are not evident. Finally, the corresponding breakdown of total cost and income for every θ is presented in Figure 5.16.

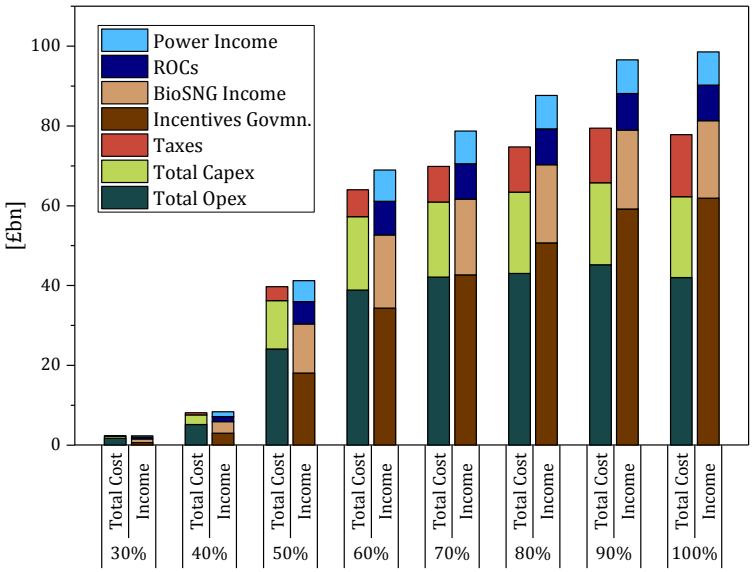

Figure 5.16. Total cost and income breakdown variation with government incentives

In general, the incentive from the government is the most important source of profit. A supply of 1% of the total demand (θ=30%), requires an investment from the government of £674 million. This contribution has to increase up to £18.1bn to achieve a BioSNG penetration of 14.3%. It was found that a support of 60% is a critical point in which a significantly high supply (20.3%) of the total gas demand can be achieved with a financial aid of £34.4bn. In order to increase the supply in 1% (21.3%) it is necessary a financial aid of £61.9bn, around 44.5% more.

5.6 Conclusions

A spatially-explicit multiperiod mixed integer linear programming model is proposed to address the optimal strategic design of BioSNG supply chain in a regional and national context. In order to demonstrate the capabilities of the

optimisation framework, a UK case study was implemented. Domestic resources such as woody biomass, cereal straw, residual waste, and miscanthus were included as potential feedstocks for BioSNG production. The availability of these resources considers sustainability criteria and national policies regarding their current and future management strategy. Allothermal gasification and plasma gasification are considered as the main processing routes. The results indicate that feedstock purchases account for 32.5% of the total cost, above investments in integrated facilities which accounted for 23.7% of the total costs.

In addition, it was found that among four feedstocks, miscanthus is crucial for the production of BioSNG in the UK. This feedstock is mainly developed along the west part of the UK where the productivity is comparatively higher than in the rest of the region. On average, England is the highest feedstock supplier with 65% of the total feedstock production; followed by Wales with 20%, and finally Scotland with 15%. The optimisation results show that for the planning horizon (20 years) the production of BioSNG can supply up to 20.6% of the total gas demand. Moreover, the results suggest that the installation of facilities does not necessarily coincide with regions of high potential for feedstocks production. Instead, the transportation cost is a crucial component that can influence the optimal location of a facility.

Furthermore, the cogeneration of power was investigated as an option of improving the economic performance of a BioSNG supply chain. It was found that cogeneration of power nearly doubles the NPV in comparison with a case in which only BioSNG is produced. Moreover, the breakeven time is reduced in two years. In this scenario, the production of BioSNG achieved a supply of 21.4% and the coproduction of power can supply 4.4% of the total demand during the planning horizon. In terms of economics, the financial contribution from the government due to BioSNG production is the main source of profit as it is three-fold the income from BioSNG sales. In addition, by means of a parametric analysis it was possible to establish that the development of a BioSNG supply chain is economically feasible if the government supports minimum 30% of the total associated expenses with a subsidisation tariff of £70/MWh. Nonetheless, the BioSNG penetration is marginal and the NPV is significantly low. Therefore, this scenario is not economically

attractive for investment from private sectors. It was possible to determine that a contribution from the government of 60% is a critical point in which a BioSNG penetration of 20.3% can be achieved. Further increments in subsidisation do not have a significant impact on the supply.

Chapter 6. Important aspects in BioSNG supply chains

The optimisation framework proposed for the strategic design of BioSNG supply chains in Chapter 5 considers only one route for BioSNG production. In this section, the optimisation framework is extended to account for a second optional route which consists of pretreatment technologies and upgrading facilities. The main objective is to investigate the trade-off between capital investment and reduction of transportation costs, and their impact in the economic performance of a BioSNG supply chain. Moreover, the impact of government subsidisation is further investigated through a parametric analysis in which the tariff is varied from £0/MWh up to £100/MWh. Finally, the major contributing factors in the design of BioSNG supply chains are identified through the implementation of a rigorous global sensitivity analysis.

6.1 Problem statement

The problem statement introduced in section 5.2 has been revisited in order to consider two different conversion routes to account for distributed or centralised production schemes as shown in Figure 6.1.

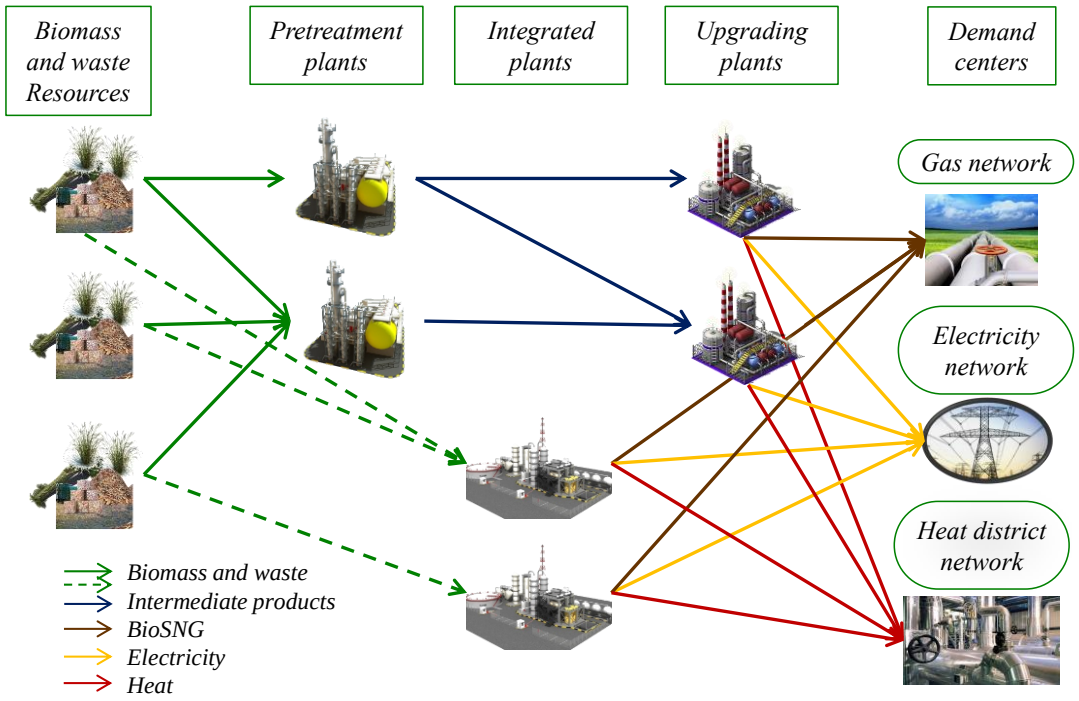

Figure 6.1. Generic BioSNG supply chain

For the centralised scheme, integrated plants process raw feedstock and convert it into final products, BioSNG, heat and/or power. For the distributed arrangement, the raw feedstock is sent first to a pretreatment plant where it is processed to obtain intermediate products with higher energy density and then fed into upgrading plants for their conversion into final products. The technologies included for pretreatment plants are pelletisation, torrefaction-pelletisation (TOP), and pyrolysis which can produce intermediate products such as bioOil, bioSlurry, torrefied biomass, and pellets, respectively. For integrated plants and upgrading plants the chosen technology is gasification. The corresponding mathematical formulation is presented in 6.2.

6.2 Mathematical formulation of pretreatment technologies

6.2.1 Nomenclature

Only new nomenclature is listed next

Sets

K^I	Set of technologies for integrated facilities
K^P	Set of technologies for pretreatment facilities
K^U	Set of technologies for upgrading facilities

Parameters

aPR_{fks} Independent term of the linearised capex curve for pretreatment plants processing feedstock f with technology k at each segment s [£M]

aUP_{hks} Independent term of the linearised capex curve for upgrading plants processing intermediate product h with technology k at each segment s [£M]

bPR_{fks} Slope of the linearised capex curve for pretreatment plants processing feedstock f with technology k at each segment s [£M MW^{-1}]

bUP_{hks} Slope of the linearised capex curve for upgrading plants processing intermediate product h with technology k at each segment s [£M MW^{-1}]

$FxOpPR_{fkt}$ Fixed costs for operation and maintenance for pretreatment plants processing feedstock f via technology k in time period t [£M y^{-1}]

$FxOpUP_{hkt}$ Fixed costs for operation and maintenance for upgrading plants processing intermediate product h via technology k in time period t [£M y^{-1}]

$VrOpPR_{fkt}$ Variable costs of operation and maintenance for pretreatment plants processing feedstock f using technology k in time period t [£M GWh^{-1}]

$VrOpUP_{hkt}$ Variable costs of operation and maintenance for upgrading plants processing intermediate product h using technology k in time period t [£M GWh^{-1}]

βPR_{fkt} Efficiency of pretreatment plants processing feedstock f with technology k to produce p

βUP_{hkt} Efficiency of upgrading plants processing intermediate product h with technology k to produce p

Positive continuous variables

$CAPEX\_PR_t$ Total investment cost of pretreatment plants in time period t [£M]

$CAPEX\_UP_t$ Total investment cost of upgrading plants in time period t [£M]

$CAPPR_{fkgts}$ Initial installed capacity for a pretreatment plant processing feedstock f using technology k in region g and and is available in time period t at segment s [MW]

$CAPUP_{hkgts}$ Initial installed capacity for an upgrading plant processing intermediate product h using technology k in region g and and is available in time period t at segment s [MW]

DPR_{fkgt} Demand of a pretreatment plant processing feedstock f with technology k in region g in time period t [GWh y^{-1}]

DUP_{hkgt} Demand of an upgrading plant processing intermediate product h with technology k in region g in time period t [GWh y^{-1}]

PPR_{fkpgt} Production rate at a pretreatment plant processing feedstock f with technology k to produce p in region g in time period t [GWh y^{-1}]

PUP_{hkpgt} Production rate at an upgrading plant processing intermediate product h with technology k to produce p in region g in time period t [GWh y^{-1}]

$ToCAPPR_{fkgt}$ Total capacity of a pretreatment plant processing feedstock f in region g and using technology k that is available in time period t [MW]

$ToCAPUP_{hkgt}$ Total capacity of an upgrading plant processing intermediate product h in region g and using technology k that is available in time period t [MW]

Binary variables

$AvPR_{fkgts}$ 1 if a pretreatment plant processing feedstock f using technology k and located in region g is operating in time period t with a capacity delimited by a segment s, 0 otherwise.

$AvUP_{hkgts}$ 1 if an upgrading plant processing intermediate product h using technology k and located in region g is operating in time period t with a capacity delimited by a segment s, 0 otherwise.

δPR_{fkgts} 1 if a pretreatment plant processing feedstock f using technology k in region g is installed in time period t with a capacity delimited by a segment s, 0 otherwise.

δUP_{hkgts} 1 if an upgrading plant processing intermediate product h using technology k in region g is installed in time period t with a capacity delimited by a segment s, 0 otherwise.

6.2.2 Objective function

6.2.2.1 Capital investments

Capital expenditures, $\mathrm{CAPEX_t}$, are calculated as the summation of the investment in integrated facilities, $\mathrm{CAPEX\_IN_t}$, investment in upgrading facilities, $\mathrm{CAPEX\_UP_t}$, investment in pretreatment facilities, $\mathrm{CAPEX\_PR_t}$, investment in infrastructure for BioSNG transportation, $\mathrm{CAPEX\_TR_t}$, and investment in new energy crops for BioSNG production, $\mathrm{CAPEX\_EC_t}$, as shown in Equation (6.1).

$$CAPEX_t = CAPEX\_IN_t + CAPEX\_UP_t + CAPEX\_PR_t + CAPEX\_TR_t + CAPEX\_EC_t \quad \forall\, t \tag{6.1}$$

6.2.2.2 Cash flow and depreciation

Cash flow is defined as the profit before taxes, $PROFIT_t$, plus depreciation of assets, $DEP_{t't}$, minus taxes, TAX_t, as presented in Equation (6.2).

$$CF_t = PROFIT_t + \sum_{t'} DEP_{t't} - TAX_t \quad \forall\, t \tag{6.2}$$

The linear method is used to calculate the depreciation, $DEP_{tt'}$ as a function of capital expenditures using a given depreciation rate, $DepF_{tt'}$ as expressed in Equation (6.3). $DEP_{tt'}$ represents the depreciation during period t' for investments made in a previous period t:

$$DEP_{tt'} = DepF_{tt'}(CAPEX\_IN_t + CAPEX\_UP_t + CAPEX\_PR_t + CAPEX\_TR_t) \quad \forall\, t, t' \tag{6.3}$$

The investment costs related to energy crops (pre-planting and establishment costs), $\mathrm{CAPEX\_EC_t}$, are considered non-depreciable.

6.2.3 Production of intermediate and final products

For the production of intermediate and final products, three different conversion technologies are considered: Integrated technologies, pre-treatment technologies and upgrading technologies. The integrated technologies represent a possible route for the production of final products. In this case, the biomass is pre-processed and converted to final products in the same facilities; this implies higher

costs related to the transportation of raw biomass. A second optional route is to decouple the integrated process into two processes where the biomass is sent first to pretreatment conversion plants to generate intermediate products with higher energy density. The intermediate products are sent to upgrading conversion plants where the final products are obtained. This route allows to reduce transportation costs, however higher capital investments are required. The production of final products, P_{pgt}, is equal to the production from integrated plants plus the production from upgrading plants, as depicted in Equation (6.4).

$$P_{pgt} = \sum_{k \in K^I} \sum_{f \in F_k} PIN_{fkpgt} + \sum_{k \in K^U} \sum_{h} PUP_{hkpgt} \quad \forall\, p, g, t \tag{6.4}$$

PIN_{fkpgt} indicates the production of a potential integrated plant processing feedstock f with technology $k \in K^I$ to produce p in region g during time period t. Set F_k contains connections between feedstocks f that can be processed with technologies k. PUP_{hkpgt} refers to the production of a potential upgrading plant processing intermediate product h with technology $k \in K^U$ to produce p in region g during time period t. K^I and K^U are sets for integrated and upgrading technologies, respectively. It is assumed that intermediate products can be processed by any upgrading technology.

The regional production of intermediate products, P_{hgt}, is related to the production in pretreatment facilities, PPR_{fkhgt}, by means of Equation (6.5):

$$P_{hgt} = \sum_{k \in K^P \cap\, k:h \in H_k} \sum_{f \in F_k} PPR_{fkhgt} \quad \forall\, h, g, t \tag{6.5}$$

Set H_k contains connections between intermediate products h that can be processed with technologies k. No energy integration is considered for pretreatment plants. Therefore, only one balance is enough to model the process as described in Equation (6.6):

$$PPR_{fkhgt} = \beta PR_{fkh} DPR_{fkgt} \quad \forall\, k \in K^P, f \in F_k, h \in H_k, g, t \tag{6.6}$$

where βPR_{fkh} corresponds to the efficiency of producing h from f using technology k, and DPR_{fkgt} is the local demand of a pretreatment plant. Finally, energy integration is considered for upgrading plants for the production of heat and power. Consequently, two equations are formulated corresponding to the BioSNG production and the global balance of the plant. The BioSNG production rate, $PUP_{hk,biosng,gt}$, is calculated as stated in Equation (6.7):

$$PUP_{hk,biosng,gt} = \beta UP_{hk,biosng} DUP_{hkgt} \quad \forall\, h,k \in K^U, g, t \tag{6.7}$$

where $\beta UP_{hk,biosng}$ is the efficiency of conversion of intermediate products to BioSNG, and DUP_{hkgt} is the local demand for intermediate products. The global balance of upgrading plants is equivalent to the balance for integrated plants as shown in Equation (6.8).

$$\frac{PUP_{hk,power,gt}}{\mu} + PUP_{hk,heat,gt} \leq \beta UP_{hk,heat} * DUP_{hkgt} \quad \forall\, h,k \in K^U, g, t \tag{6.8}$$

6.2.4 Demand Constraints

6.2.4.1 Demand of feedstocks

The regional demand of feedstocks, D_{fgt}, is calculated as shown in Equation (6.9):

$$D_{fgt} = \sum_{k \in K^I \cap\, k:f \in F_k} DIN_{fkgt} + \sum_{k \in K^P \cap\, k:f \in F_k} DPR_{fkgt} \quad \forall\, f, g, t \tag{6.9}$$

where the DIN_{fkgt} and DPR_{fkgt} refer to the demand of feedstocks in integrated and pretreatment facilities, respectively.

6.2.4.2 Demand of intermediate products

The total regional demand for intermediate products; D_{hgt}, is calculated based on the summation of the demand by upgrading plants in order to generate final products. This is expressed as shown in Equation (6.10).

$$D_{hgt} = \sum_{k \in K^U} DUP_{hkgt} \quad \forall\, h, g, t \tag{6.10}$$

6.2.5 Capital investments

6.2.5.1 Piecewise Linearisation for Pretreatment Plants

The same strategy for linearisation is used for pretreatment plants. The segments are limited by $CMin_{ks}$ and $CMax_{ks}$. $CAPPR_{fkgts}$ is the new installed capacity of pretreatment plants in region g, using technology k during period t.

$$CMin_{ks} * \delta PR_{fkgts} \leq CAPPR_{fkgts} \leq CMax_{ks} * \delta PR_{fkgts} \quad \forall\, k \in K^P, f \in F_k, g, t, s \tag{6.11}$$

δPR_{fkgts} is a binary variable that equals 1 if a plant is installed using technology k for processing feedstock f in period t with a capacity defined by the segment S. Only one segment can be activated, and only one pretreatment plant is allowed to be installed for each type of feedstock in region g. These conditions are modelled through Equations (6.12) and (6.13), respectively.

$$\sum_{s} \delta PR_{fkgts} \leq 1 \quad \forall\, k \in K^P, f \in F_k, g, t \tag{6.12}$$

$$\sum_{s} \sum_{k \in K^P \cap\, k: f \in F_k} \delta PR_{fkgts} \leq 1 \quad \forall\, f, g, t \tag{6.13}$$

The total current capacity, $ToCAPPR_{fkgt}$, is equal to the newly installed capacity, $CAPPR_{fkgts}$, plus the previous capacity, $ToCAPPR_{fkg,t-1}$. This condition is represented by Equation (6.14):

$$ToCAPPR_{fkgt} = ToCAPPR_{fkg,t-1} + \sum_{s} CAPPR_{fkgts} \quad \forall\, k \in K^P, f \in F_k, g, t \tag{6.14}$$

The demand of a pretreatment plant, DPR_{fkgt}, is limited by the current installed capacity, $ToCAPPR_{fkgt}$, the capacity factor, Cf, and the availability factor, Avf, as shown in in Equation (6.15).

$$DPR_{fkgt} \leq Cf * Avf * \alpha * ToCAPPR_{fkgt} \quad \forall\, k \in K^P, f \in F_k, g, t \tag{6.15}$$

Finally, the total investment cost, $CAPEX\_PR_t$, is calculated as shown in Equation (6.16):

$$CAPEX\_PR_t = \sum_{k \in K^P, gs} \sum_{f \in F_k} \left(bPR_{fks} * \delta PR_{fkgts} + aPR_{fks} * CAPPR_{fkgts} \right) \quad \forall\, t \tag{6.16}$$

where aPR_{fks} and bPR_{fks} are parameters that represent variable and fixed investment costs. This information is obtained from the linearisation of the corresponding investment cost curve.

6.2.5.2 Piecewise Linearisation for Upgrading Plants

The capital investment costs linearisation for upgrading plants is shown in Equation (6.17). $CAPUP_{hkgts}$ refers to the newly installed capacity during period t in region g, using technology k available in time period t.

$$CMin_{ks} * \delta UP_{hkgts} \leq CAPUP_{hkgts} \leq CMax_{ks} * \delta UP_{hkgts} \quad \forall\, k \in K^U, h, g, t, s \tag{6.17}$$

δUP_{hkgts} is a binary variable that equals 1 in case an upgrading plant with technology k is available for processing intermediate products h in time t and with a capacity limited by a segment s. Only one segment can be activated and only one upgrading plant is allowed to be installed in region g, as shown in Equations (6.18) and (6.19), respectively.

$$\sum_{s} \delta UP_{hkgts} \leq 1 \quad \forall\, k \in K^U, h, g, t \tag{6.18}$$

$$\sum_{s} \sum_{k \in K^U} \delta UP_{hkgts} \leq 1 \quad \forall\, h, g, t \tag{6.19}$$

The total current capacity, $ToCAPUP_{hkgt}$, is equal to the newly installed capacity, $CAPUP_{hkgts}$, plus the previous capacity, $ToCAPUP_{hkg,t-1}$. This condition is represented by Equation (6.20):

$$ToCAPUP_{hkgt} = ToCAPUP_{hkg,t-1} + \sum_{s} CAPUP_{hkgts} \quad \forall\, k \in K^U, h, g, t \tag{6.20}$$

Similarly, the demand of intermediate products in an upgrading plant, DUP_{hkgt}, is limited by the current installed capacity, $ToCAPUP_{hkgt}$, the capacity factor, Cf, and the availability factor, Avf, as shown in in Equation (6.15).

$$DUP_{hkgt} \leq Cf * Avf * \alpha * ToCAPUP_{hkgt} \quad \forall\, k \in K^U, h, g, t \tag{6.21}$$

Finally, the total investment cost, $CAPEX\_UP_t$, is calculated as shown in Equation (6.22):

$$CAPEX\_UP_t = \sum_{k \in K^U, gs} \sum_{h} \big(bUP_{hks} * \delta UP_{hkgts} + aUP_{hks} * CAPUP_{hkgts} \big) \quad \forall\, t \tag{6.22}$$

where aUP_{hks} and bUP_{hks} are parameters related to the linearisation of the investment costs curve.

6.2.6 Production Costs

The total production cost, PC_t, is divided into fixed and variable costs. Fixed costs are independent of the output level of a plant and often include insurance, rent, salaries, etc. On the other hand, variable costs such as inventory, utilities, packaging, etc. depend proportionally on the actual production of a plant. This is expressed mathematically in Equation (6.23):

$$
\begin{aligned}
PC_t = & \sum_{k\in K^I,g} \sum_{f\in F_k} \left(FxOpIN_{fkt} * AvIN_{fkgt} + VrOpIN_{fks} * PIN_{fkg,biosng,t}\right) \\
& + \sum_{k\in K^P,g} \sum_{f\in F_k} \sum_{h\in H_k} \left(FxOpPR_{fkt} * AvPR_{fkgt} + VrOpPR_{fks}\right. \\
& \left. * PPR_{fkght}\right) \\
& + \sum_{k\in K^U,g} \sum_{h} \left(FxOpUP_{hkt} * AvUP_{hkgt} + VrOpUP_{hks}\right. \\
& \left. * PUP_{hkg,biosng,t}\right) \quad \forall\, t
\end{aligned}
\tag{6.23}
$$

The parameters $FxOpIN_{fkt}$, $FxOpPR_{fkt}$, and $FxOpUP_{hkt}$ refer to fixed costs for integrated plants, pretreatment plants, and upgrading plants, respectively. The fixed costs are activated accordingly by the availability variables $AvIN_{fkgt}$, $AvPR_{fkgt}$, and $AvUP_{hkgt}$, which correspond to binary variables. Finally, $VrOpIN_{fks}$, $VrOpPR_{fks}$, and $VrOpUP_{hks}$ designate the respective variable costs for integrated, pretreatment plants, and upgrading plants, respectively. The availability variables are related to installation variables by means of Equations (6.24) and (6.25) for integrated plants:

$$AvIN_{fkgt} \geq \sum_{s} \delta IN_{fkgts} \quad \forall\, k \in K^I, f \in F_k, g, t \tag{6.24}$$

$$AvIN_{fkgt} \geq AvIN_{fkg,t-1} \quad \forall\, k \in K^I, f \in F_k, g, t \tag{6.25}$$

Analogous equations are included for pretreatment plants (see Equations (6.26)-(6.27)) and upgrading plants (see Equations (6.28)-(6.29)):

$$AvPR_{fkgt} \geq \sum_{s} \delta PR_{fkgts} \quad \forall\, k \in K^P, f \in F_k, g, t \tag{6.26}$$

$$AvPR_{fkgt} \geq AvPR_{fkg,t-1} \quad \forall\, k \in K^P, f \in F_k, g, t \tag{6.27}$$

$$AvUP_{hkgt} \geq \sum_{s} \delta UP_{hkgts} \quad \forall\, k \in K^U, h \in H_k, g, t \tag{6.28}$$

$$AvUP_{hkgt} \geq AvUP_{hkg,t-1} \quad \forall\, k \in K^{U}, h \in H_k, g, t \tag{6.29}$$

6.3 Case study definition

Besides integrated facilities for biomass gasification, discussed in section 5.4.2, two more types of facilities are considered for two possible paths for production of BioSNG: (1) upgrading facilities, and (2) pretreatment facilities. In general, integrated facilities consist of a phase of feedstock conditioning, which could include chipping and moisture reduction, gasification, methanation, and gas cleaning. In upgrading facilities, on the other hand, the conditioning step is not necessary since the feedstocks have already been preprocessed in pretreatment facilities into higher energy density intermediate products. The preprocessing of feedstocks could bring two benefits: (1) installation of smaller upgrading facilities in comparison to integrated facilities, and (2) savings associated with transportation costs. However, this comes at the expense of installing pretreatment facilities. This trade-off will be further discussed in section 6.4.1.

Four technologies are investigated for feedstock pretreatment: (1) pelletisation, (2) rotating cone reactor pyrolysis (RCRP), (3) fluidised bed reactor pyrolysis (FBRP), and (4) torrefaction – pelletisation (TOP). It was considered that pelletisation can process woody biomass, straw, residual waste, and miscanthus. Woody biomass, straw, and miscanthus can be used for production of bio-oil through RCRP, bioslurry via FBRP, or torrefied biomass via TOP. Since the production of BioSNG is the main objective, it was assumed that the operation of the pretreatment plants is optimised to maximise the output of intermediate products. Accordingly, heat recovery for power cogeneration is only possible for integrated and upgrading plants. Information regarding efficiencies of pretreatment technologies is usually only available for woody biomass. Therefore, the efficiencies for the other feedstocks were estimated by implementing a correction factor based on the corresponding LHVs. This, however, is only an approximation to take into account that different feedstocks have different conversion efficiencies. Accordingly, the efficiency of pelletisation varies from 80% to 95% [321,322], being the efficiency of

pelletisation of residual waste the lowest. Despite the low efficiency, it is worth mentioning that pelletisation of residual waste presents great benefits in terms of energy density increment which contributes to efficient transportation (lower costs), and smaller upgrading facilities, e.g. the production of 1 MWh of BioSNG requires 770 kg of residual waste or 330 kg of pellets. Regarding pyrolysis, the efficiency of conversion for RCRP ranges between 69% and 74% whereas efficiencies for FBRP vary from 87% to 92% [113]. Finally, TOP has, on average, the highest efficiency, between 94% and 96% [113].

The capital investments for pretreatment technologies are considerably low in comparison to integrated facilities. They go from £17 million for RCRP up to £31M for FBRP. The fixed operating costs are on average 3 M£/y, for integrated facilities, whereas for pretreatment facilities they range from 1 million per year for TOP and 2 M£/y for RCRP. The variable costs were inferred from data available in literature [29,309]. For pretreatment technologies, the variable costs vary from 0.0014 M£/GWh for pelletisation up to 0.0046 M£/GWh for RCRP. Table 6.1 summarises conversion efficiencies for different pretreatment technologies, capex, and opex for facilities processing woody biomass with an input capacity of 100 MW.

Table 6.1. Capex, Opex and technical specifications of processing facilities.

	Torrefaction	Pelletisation	RCRP	FBRP
Feedstock	Woody biomass	Woody biomass	Woody biomass	Woody biomass
Capacity [MW]	100	100	100	100
Capex [£M]	25.8	17.7	16.6	30.7
Fixed cost [M£/y]	1.0	0.9	2.0	1.3
Variable cost [M£/GWh]	$1.7x10^{-3}$	$1.4x10^{-3}$	$4.6x10^{-3}$	$2.1x10^{-3}$
Efficiency [%] (based on LHV)	93.8	95.0	73.6	92.4
Heat recovery efficiency [%]	0	0	0	0
References	[113,310]	[321,322]	[113,323–325]	[32,113]

6.4 Results and discussion

The production of BioSNG and cogeneration of power generation along with their corresponding incentives, feed-in tariff for BioSNG and ROCs for power generation, are included for all the cases discussed in this section. First, the relevance of pretreatment technologies in the design of BioSNG supply chains is addressed and their benefits are identified by comparing with a scenario in which only integrated technologies are considered. Second, the role of the government in developing these technologies is investigated using feed-in tariffs. For this purpose, a parametric analysis was carried out in which different levels of subsidisation are explored and their impact on feedstock procurement, installation of facilities and production of BioSNG is discussed. Finally, the repercussion of uncertainty associated with 6 parameters: capital costs, feedstock cost, technology efficiency, feed-in tariff, gas and power prices, is studied through global sensitivity analysis (GSA). GSA allows to simultaneously address uncertainty in the input data described by means of a probability distribution function (PDF) and prioritised those parameters with major impact on the global performance of the supply chain.

The optimisation problems were solved using GAMS 24.7.1 with CPLEX 12.6.3. All runs were performed on a Dell OptiPlex 9010 with Intel® Core™ i7-3770 CPU @3.40 GHz and 16 GB RAM running Windows 7® Enterprise (64-bit operating system). The optimality gap was set to less or equal to 1% for all cases. The corresponding statistics for the extended mathematical model are compared to the original formulation and presented in Table 6.2.

Table 6.2. Model statistics

	Without pretreatment technologies	With pretreatment technologies
Total number of variables	16,553	71,865
Continuous variables	13,613	53,105
Binary variables	2,940	18,760
Total number of constraints	12,245	68,533
Non zero constraint matrix elements	56,589	265,231
CPU time [s]	183	15,247
Optimal NPV [£M]	21,446	25,524

6.4.1 The role of pretreatment technologies in the development of BioSNG supply chains

The results for a case study in which two different paths are considered for production of BioSNG and power cogeneration are discussed in this section. The first path, which has been addressed in Chapter 4, can be regarded as a centralised route since it consists merely of integrated facilities in which raw feedstocks are directly processed into BioSNG. The second path, which can be seen as a distributed route, considers installation and operation of pretreatment plants for processing raw feedstocks into intermediate products of higher energy density. The intermediate products are then transported to upgrading plants where gasification and methanation processes take place to produce BioSNG along with power cogeneration. Regarding government subsidisation, a feed-in tariff was set to £70/MWh for injection of BioSNG into the national gas pipeline transmission system. For power generation, ROCs were set to 1.8 per MWh at a price of £45/ROC [326,327].

The economic performance of the case study is summarised in Figure 6.2. In general, the total costs associated with the development of the BioSNG supply chain are mostly dominated by operational costs (51.2%), with the rest equally distributed between capital investments (24.2%) and taxes (24.6%) (see Figure 6.2a). The results show that tax payments are an important component of the total cost. Consequently, this could be used as an additional mechanism for the government to stimulate the development of BioSNG as a sustainable primary energy source.

The capital expenditures are largely defined by the development of infrastructure for BioSNG production rather than for transportation. 46.3% of the investments are destined to develop the first path, whereas the development of the second path, in which pretreatment and gasification-methanation processes are decoupled, accounted for 34.5% of the total investments.

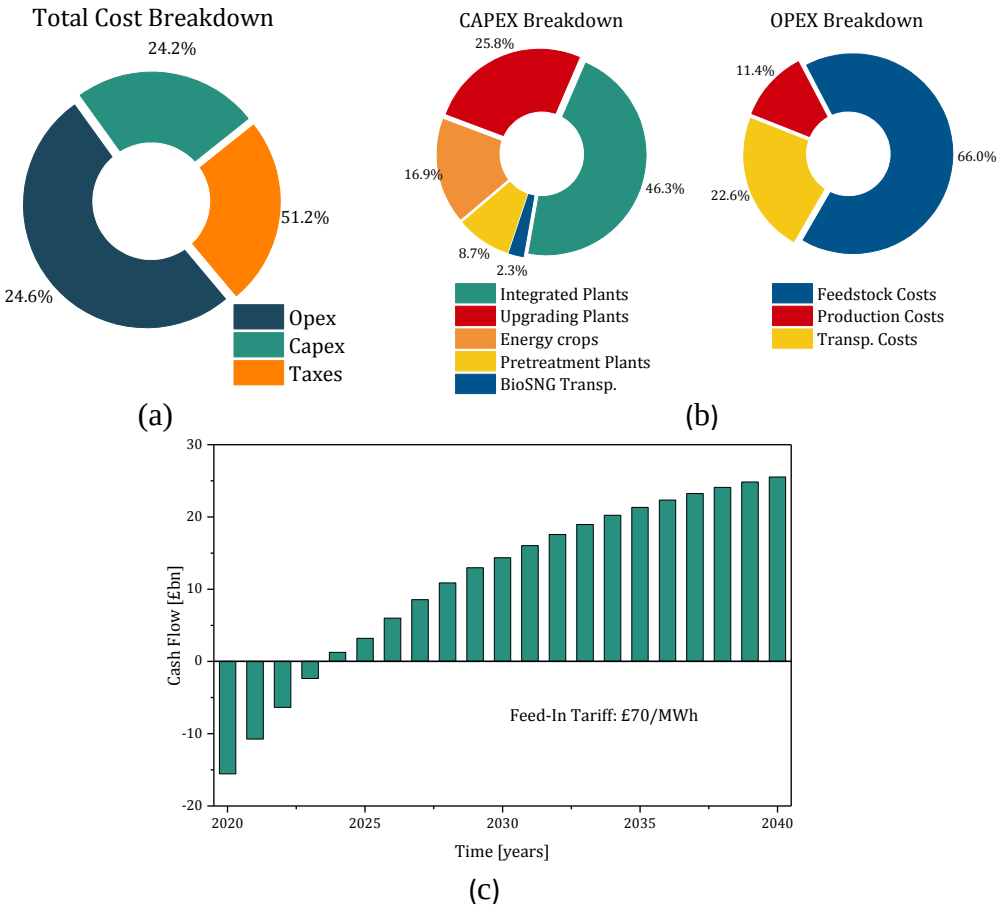

Figure 6.2. Summary of the economic performance: (a) total cost breakdown. (b). Capex and Opex Breakdown. (c) Cumulative net cash flow

Energy crops, in this case miscanthus, required 16.9% of the total capital cost whereas investment in infrastructure for local and regional transportation of BioSNG by road is only 2.3%. Concerning operational expenditures, 66% corresponds to feedstock purchases and 22.6% was required for transportation of feedstocks and intermediate products. This means that 33.8% of the total cost is due to feedstock purchases, whereas 19.5% are associated with facilities investment. Moreover, the transportation component is almost double of what is spent on the actual operation of the production facilities. These figures highlight the considerable impact of feedstock acquisition and transportation on the economy of these types of supply chains. Finally, the cumulative discounted cash flow (Figure 6.2c) shows that the production of BioSNG is profitable with a net present value of £25.5bn after 20 years and a breakeven time of 5 years.

On average, 21.2% of the total gas demand was supplied by the production of BioSNG and 4.3% of the power demand was supplied by cogeneration. Miscanthus plays a crucial role in these figures since 65.1% of the total BioSNG production comes from this energy crop. Residual waste comes in second place with enough resources to provide 17.5% of the BioSNG production. Woody biomass and straw only contributes with 9.4% and 7.9%, respectively. The design of the BioSNG supply chain for each feedstock is shown in Figure 6.3 and Figure 6.4.

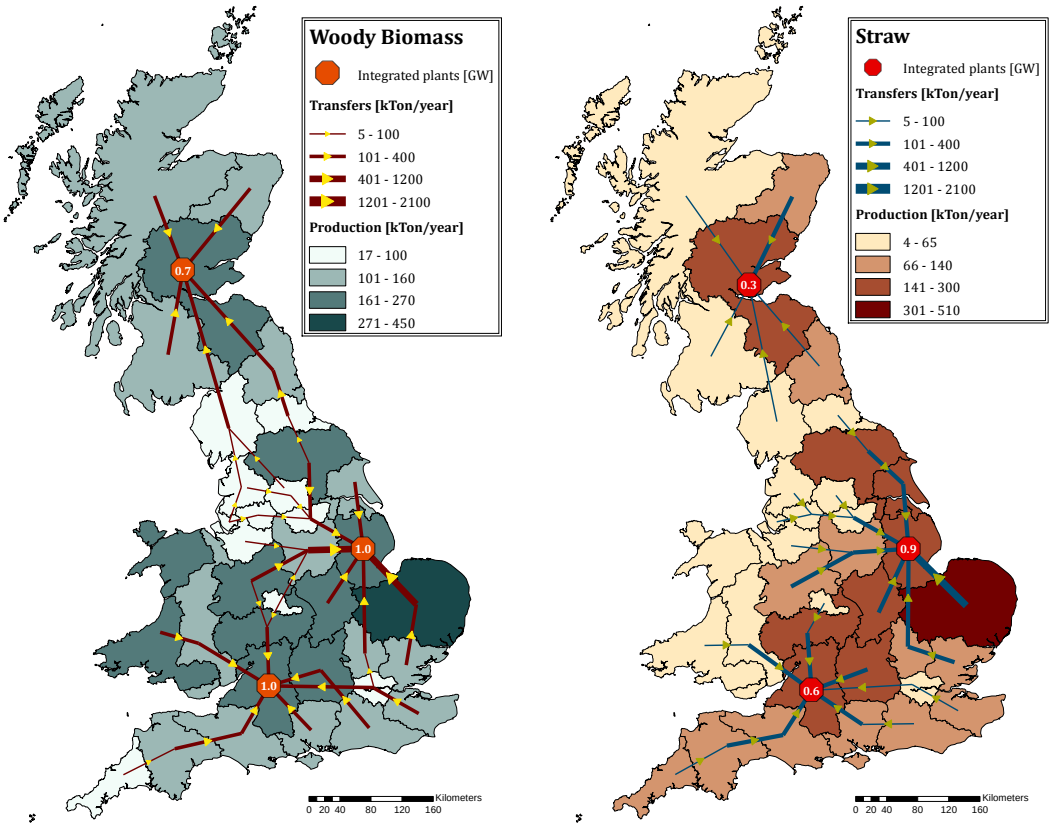

(a) (b)

Figure 6.3. Design of the BioSNG supply chain for different feedstocks: (a) Woody biomass. (b) Straw.

The supply chains for producing BioSNG from woody biomass and straw were designed following a centralised scheme in which only integrated technologies intervene. The total installed capacity was 2.7 GW for woody biomass and 1.8 GW for straw. The location of facilities in the south, central area and north of the UK aims to minimise the transportation costs of the raw materials, considering that they are fairly distributed across the regions. England produced 80% and 85% of woody

biomass and straw, respectively. The processing of woody biomass and straw takes place mostly in England where 79% of woody biomass and 85% of straw is converted into BioSNG. The remaining 11% of woody biomass and 15% of straw is processed in Scotland. Both resources are being utilised at their maximum availability. The fact that no pretreatment technologies were chosen can be explained by the low contribution of these resources in the production of BioSNG due to low availability. Consequently, the volume of these resources is not enough to compensate for investment in pretreatment facilities in order to reduce costs on transportation. Regarding the transportation modes, 90% of the woody biomass is transported via rail and only 10% by truck. In the case of straw, truck is the preferred mode with 65% of the straw delivered by this mode, whereas the remaining 35% was delivered by rail. By contrast, the production of BioSNG from miscanthus and waste involves torrefaction and pelletisation, respectively (Figure 6.4).

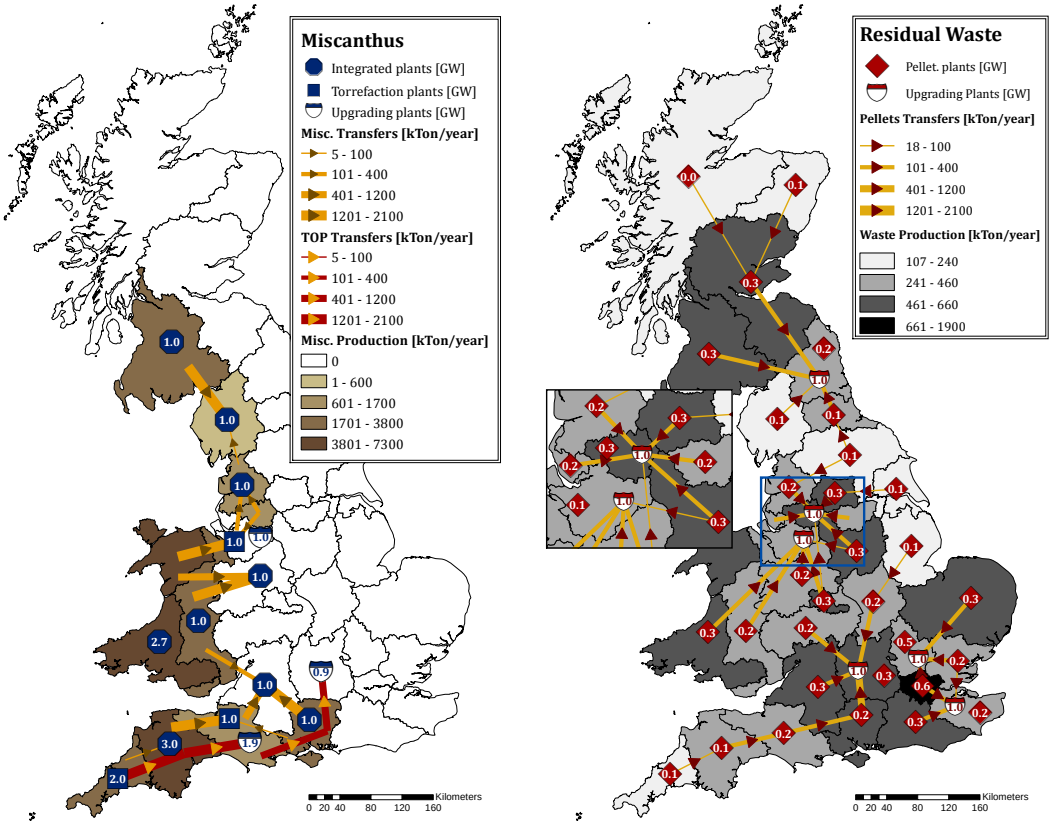

(a) (b)

Figure 6.4. Design of the BioSNG supply chain for different feedstocks: (a) Miscanthus. (b) Residual waste.

In the case of miscanthus, the cultivation of this energy crop is primarily developed along the west part of the UK. These regions have in common favourable conditions for energy crops cultivation that lead to high productivity in terms of tonnes per hectare. England contributes with 54% of the total production of miscanthus, followed by Wales (34%) and finally Scotland (12%). The total installed capacity for processing miscanthus in integrated plants is 12.7 GW. An alternative path was selected to produce BioSNG from miscanthus in which torrefaction-pelletisation was chosen as pretreatment technology with a final capacity of 4 GW, followed by further processing in upgrading plants, whose final capacity is 3.8 GW. This path is mostly developed in the south region of the UK, where the production of miscanthus is comparatively higher than in the other regions. Moreover, 67% of miscanthus was processed through integrated facilities, whereas the other 33% was processed through pretreatment and upgrading facilities. Regarding the transportation modes, 60% of raw miscanthus was delivered by rail, and the rest was delivered by truck. Torrefied miscanthus, on the other hand, was transported exclusively by rail. Regarding residual waste, its procurement is primarily focused in England which supplies 83% of the total residual waste resources. Scotland and Wales contribute with 10% and 7%, respectively. The supply chain design features a distributed scheme in which pretreatment facilities were installed in each of the 35 regions to process 100% of the resources into pellets (or RDF). Only 2% of the residual waste was transported to a different region without previous pretreatment (not shown in the map for the sake of simplicity). The residual waste pellets are processed in upgrading facilities distributed in five regions across England. This arrangement allows to reduce considerably not only transportation-related costs but also the size of facilities required for final conversion into BioSNG, which is reflected on the capital investments. The total installed capacity was 7.5 GW for pelletisation plants and 6 GW for upgrading plants. Despite the high generation of residual waste in London, none of the upgrading plants are located in this city. Instead, the facilities were installed in surrounding regions, acting as “hubs” for the residual waste pellets produced in the east part, including London. The preferred mode for transportation of residual waste pellets is rail, which delivered 95% of the total production. The marked preference for pelletisation of residual waste as a first

step stems mainly from a considerable potential for volume reduction, and therefore increase in energy density, which has positive effects on the transportation infrastructure and processing facilities.

In summary, in terms of energy units, England leads the production of feedstocks with 65% of the total production in 20 years, being miscanthus the main feedstock. Wales contributes with 23% driven mostly by the production of miscanthus, and Scotland comes in third place with 12% of the total feedstock production, also with miscanthus as main feedstock. Rail is a crucial transportation mode since it delivered 79% of the combined production of raw feedstocks and intermediate products. The remaining 21% was transported via trucks. Regarding processing infrastructure, 53% of the total installed capacity, including integrated, pretreatment, and upgrading facilities, was built for processing miscanthus. Similarly, the infrastructure for processing residual waste equals 35% of the total capacity, whereas woody biomass and straw required only 7% and 5%, respectively. In terms of geographic distribution, the infrastructure for BioSNG production is largely located in England (82% of the total installed capacity), followed by Wales (11%), and Scotland (7%). Accordingly, England is the major BioSNG supplier with 79% of the total production. Moreover, the transportation of BioSNG takes place only locally between the facilities and the injection points located in the same region.

The benefits of including pretreatment technologies are identified by comparing with a scenario in which only integrated technologies are considered. A summary for both cases is presented in Table 6.3.

Table 6.3. Results comparison

Feed-in tariff: 70 £/MWh	With pretreatment technologies	Without pretreatment technologies	Variation [%]
Net Present Value [£M]	25,524	21,446	-16.0
Capex [£M]	17,461	20,404	16.9
Integrated plants	8,079	17,044	111.0
Pretreatment plants	1,516	-	-
Upgrading plants	4,506	-	-
BioSNG transportation	408	408	-0.1
Energy crops	2,952	2,952	0.0
Opex [£M]	36,866	41,126	11.6
FeedCosts	24,328	24,214	-0.5
ProdCosts	4,190	7,590	81.1
Transportation [£M]	8,349	9,322	11.7
• *Feedstocks and intermediate products*	6,976	7,953	14.0
• *BioSNG*	1,372	1,369	-0.2
Income [£M]	27,332	27,790	1.7
BioSNG sales	19,296	19,505	1.1
Power sales	8,036	8,284	3.1
Incentives [£M]	70,222	71,172	1.4
Feed-in tariff	61,550	62,229	1.1
ROC	8,672	8,944	3.1
Taxes [£M]	17,702	15,986	-9.7
Cash Flow [£M]	42,985	41,849	-2.6
Production			
BioSNG [GWh/y]	104,052	105,070	1.0
Power [GWh/y]	12,862	13,234	2.9
Woody biomass [kTon/y]	4,975	4,975	0.0
Miscanthus [kTon/y]	31,696	31,563	-0.4
Straw [kTon/y]	3,750	3,750	0.0
Waste [kTon/y]	15,191	15,216	0.2
BioSNG penetration [%]	21.22	21.43	1.0
Integrated plants [MW]			
Woody biomass [kTon/y]	2,645	2,645	0.0
Miscanthus	12,692	16,637	31.1
Straw	1,784	1,784	0.0
Waste	-	7,535	-
Pretreatment plants [MW]			
Pelletisation - Waste	7,500	-	-
Torrefaction - Miscanthus	3,973	-	-
Upgrading plants [MW]	9,791	-	-

If only integrated technologies are considered, the NPV drops to £21.4bn, which corresponds to a reduction of 16% in profitability. This is mainly caused by an increment in infrastructure investment (16.9%) and operational costs (11.6%). Specifically, investment in integrated plants is 21% higher than the total investment in facilities for the scenario in which pretreatment technologies are also an alternate option. This is mainly a result of pelletisation of residual waste, which allows installation of less expensive facilities for producing BioSNG. Namely, when pretreatment technologies are included, the optimisation framework selects a total capacity of 7500 MW for pelletisation, and 6000 MW for upgrading pretreated waste. The combined investment does not surpass the investment for installing 7500 MW to process directly residual waste. The key is the extremely low energy density of residual waste in comparison to waste pellets. Therefore, a higher capacity in terms of Ton/y is required in order to reach the same output in MW. Correspondingly, the operational costs increased 11.6% due to a drastic increase in production costs of 81%, which is a result of installing larger facilities. In addition, the transportation costs increased 14% when no pretreatment technologies are included. Notably, the income component from BioSNG and Power sales increased 1.7%. Similarly, incentives from feed-in tariff and ROCs increased 1.4%. This is related to the fact that a supply chain based merely on integrated technologies is more efficient in terms of utilisation of feedstocks which reflects on a higher production of BioSNG in 1%. By contrast, when pretreatment technologies are added to the supply chain, the global energy losses are higher and therefore the net production of BioSNG decreases. In addition, the power sales increase by 2.9% due to intensification of cogeneration which is related to installation of more integrated technologies. This is also reflected in income through the subsidisation schemes. Woody biomass and straw are used at their maximum availability; nonetheless their contribution to the production of BioSNG is overshadowed by miscanthus which continues to be the dominant feedstock. The results show that the integration of pretreatment technologies in the design of BioSNG supply chains benefits the global economic performance.

6.4.2 Implications of subsidisation tariffs

This section discusses the impact of different subsidisation schemes on the general performance of the BioSNG supply chain. In this case, a parametric analysis was implemented in which the feed-in tariff was systematically increased from £0/MWh up to £100/MWh. In reality, based on the current policies established by the UK government, it is unlikely that the subsidisation for gasification through feed-in tariffs will reach £100/MWh. Nonetheless, these levels of subsidisation are included in the analysis for the sake of completeness. The corresponding results are summarised in Figure 6.5.

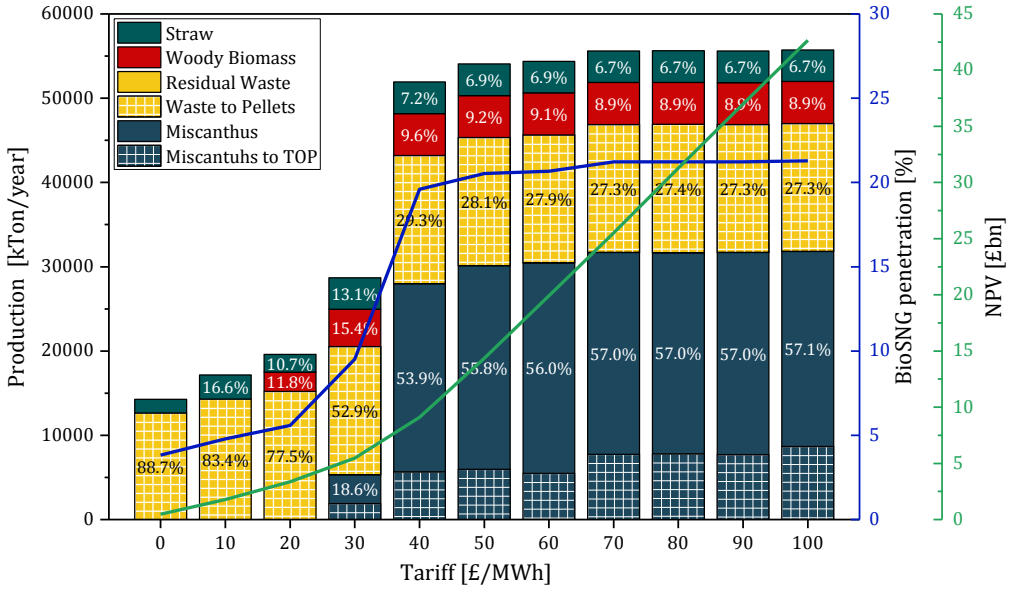

Figure 6.5. Impact of government policies on the development of BioSNG supply chains.

The production of BioSNG is economically feasible even when the feed-in tariff is set to £0/MWh. However, the NPV is only £0.5bn and the BioSNG penetration is 3.8%. The production of BioSNG is based largely on residual waste and a small fraction of straw. The utilisation of both feedstocks is 83% and 43% for residual waste and straw, respectively. The white grid represents how much of the feedstock was sent to pretreatment facilities. In this case, 100% of the residual waste was sent to pelletisation. It is worth to mention that in absence of subsidisation, a BioSNG supply chain based exclusively on integrated plants is not economically feasible. When the tariff is set to £10/MWh, the procurement of residual waste and straw increases reaching a utilisation of 94% and 76%, respectively. The NPV increased almost four times to £1.8bn and the supply reached 4.8%. At £20/MWh, residual

waste is used at its maximum availability, and woody biomass is included as an additional feedstock for production of BioSNG. At this level, only pelletisation is being used. The NPV is £3.4bn and the BioSNG penetration is 5.6%. Comparatively, when only integrated technologies are considered, the minimum tariff required for a feasible development is £20/MWh, in which the NPV is £0.2bn and only a supply of 2.6% is reached. The cultivation of miscanthus starts only after the tariff is set to £30/MWh, part of the production of miscanthus is pretreated with torrefaction (white grid). Residual waste and straw are being used at their maximum availability, and woody biomass utilisation is 88%. The NPV increased 62% from the previous case reaching £5.5bn. The BioSNG supply is 9.5% of the total demand. A tariff of £40/MWh increases drastically the BioSNG supply up to 19.6%. This is particularly driven by a boost in miscanthus cultivation. At this point miscanthus becomes a dominant feedstock. The economy performance largely benefits from this, reaching an NPV of £9.1bn. Further increments in the level of subsidisation are reflected on the NPV but do not have major impact on the cultivation of miscanthus and therefore the percentage of demand met by BioSNG. Finally, at £100/MWh, it was possible to reach 21.3% of penetration of BioSNG with a corresponding NPV of £42.6bn. The production of BioSNG across the UK with variation of feed-in tariffs is summarised in Figure 6.6.

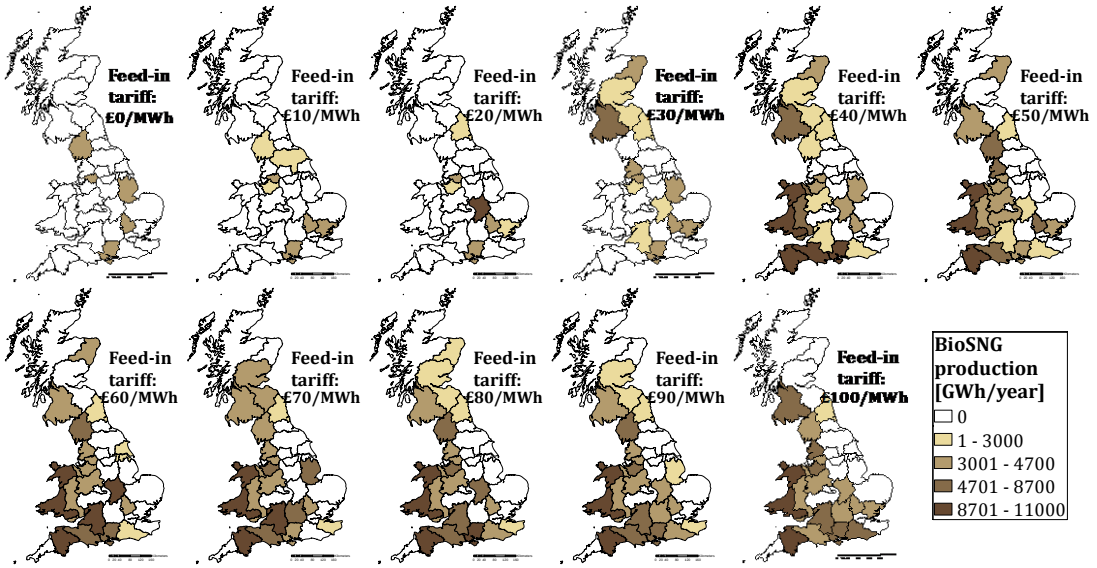

Figure 6.6. Geographic distribution of production of BioSNG with different levels of subsidisation.

Initially the production of BioSNG is scattered across England, as the tariff increases up to £20/MWh the production intensifies but continues to be centred in England. At a tariff of £30/MWh, the production of BioSNG initiates in three regions of Scotland. At this point all the resources of residual waste and straw, and most of the woody biomass are being transported to these regions. Once the tariff reaches the critical point of £40/MWh, Wales starts producing BioSNG. This production depends almost exclusively from cultivation of miscanthus. Similarly, more facilities are installed in the south of England whose production of BioSNG is based mainly on miscanthus. Therefore, the drastic increase in BioSNG supply discussed previously can be traced to Wales and three regions in the south of England. As the subsidisation increases the production in Scotland alternates between 2 and 3 regions. Similarly, the production of BioSNG in the east and central part of England presents variability in the location of facilities. By contrast, the regions whose BioSNG production relies mostly on local resources of miscanthus are consistently selected as the feed-in tariff increases.

6.4.3 Key parameters in BioSNG supply chains – A global sensitivity analysis (GSA) approach

The results presented in previous sections showed favourable economic metrics for the introduction of BioSNG in the energy mix of the UK. Nonetheless, the information that serves as the basis for this type of analysis is usually subject to substantial uncertainty that undoubtedly affects the economic performance of a supply chain. Therefore, it is essential to quantify the consequences of uncertainty and identify those parameters that can potentially have a major impact on the economics of a BioSNG supply chain. Accordingly, the effects of uncertainty in six parameters on the design of the BioSNG supply chain are addressed via GSA [328–330]. The parameters selected for the analysis are: technology efficiency, feedstock cost, capital cost of facilities, feed-in tariff, and gas and power spot prices. The data regarding the uncertainty for gas and power prices was based on three scenarios (low, medium, high) published by National Grid UK [331]. Additionally, a ±10% of variation was considered for technology efficiency, whereas capital costs and feedstock costs were assumed to vary ±30% from the base case. In the case of feed-in tariff, based on the analysis discussed in section 6.4.2, the subsidisation level was

allowed to range between £0/MWh and £50/MWh. Initially, the implementation of the GSA requires setting probability distribution functions for each uncertain parameter. In this work, beta distribution function is assumed for gas and power prices. For technology efficiency a normal distribution was chosen so that approximately 95% of the data falls within ±10% of variability. Finally, a uniform distribution was chosen for capex, feedstock costs, and feed-in tariff. A Quasi Monte Carlo method based on Sobol sequences [332] was implemented along with a Random Sampling-High dimensional model representation (RS-HDMR) method [332–334] was used which allows to approximate the input-output behaviour of high dimensional systems with minimum sampling effort. Therefore, despite the complexity of the optimisation model, this methodology allows to estimate sensitivity indices based on few samples. In this work, 128 scenarios were generated from sampling the uncertain parameters in order to calculate first order effects and total effects. First order effects determine the impact of changes in one parameter on the variance of the output variables without considering interactions with other parameters. Total effects account for the variance of the output variables due to the combined contribution of changes in the uncertain parameter as well as its interaction with the other parameters. The GSA was implemented with the software SobolGSA [335]. The corresponding results are summarised in Figure 6.7.

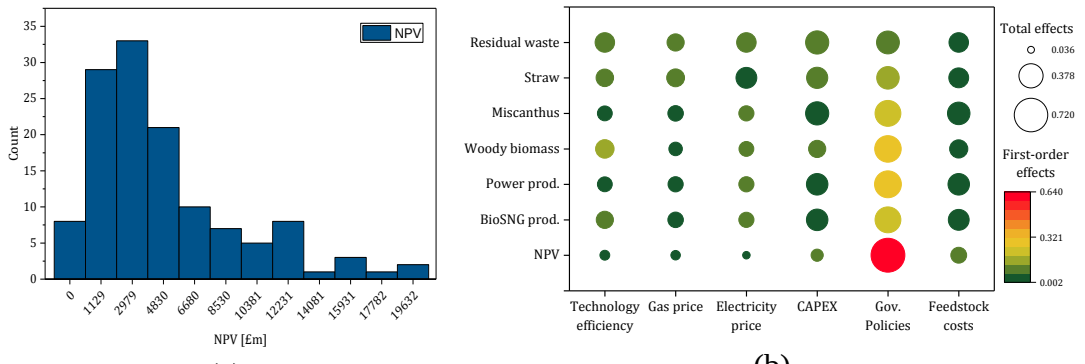

(a) (b)

Figure 6.7. Global sensitivity analysis for the BioSNG supply chain: (a) Distribution of NPV. (b) First order and total effects

The distribution of the NPV for 128 scenarios is presented in Figure 6.7a. The NPV presents high variability, with some scenarios not economically feasible, and a few scenarios with an NPV of around £19.6bn. The median is £3.7bn which is

considerably lower than the values reported in previous sections. Likewise, the BioSNG supply ranges from 0% up to 25%, with median of 9%. It is important to clarify that the distribution presented in Figure 6.7a is derived from the optimisation of each scenario individually, and it is not a result of the implementation of a method for stochastic optimisation.

Figure 6.7b presents a summary of the first order effects, represented by a colour scale, and the total effects, represented by the size of the bubbles. The results indicate that government policies i.e. subsidisation level, is the component with the largest impact on the economic performance of the BioSNG supply chain. 63.7% of the variance of the NPV is related to individual effect of subsidisation policies. Feedstock costs come in second place whose associated uncertainty accounted for 9.7% of the variance in NPV. Similarly, the interaction of government policies and feedstock costs with other parameters accounted for 71.8% and 15.9% of the variance of NPV, respectively. Moreover, the subsidisation policies have a dominant impact on the utilisation of woody biomass and miscanthus. The latter relates to the predominant influence of subsidisation on the production of BioSNG and power whose corresponding first order effects are 24.1% and 27.8%, respectively. The independent effects of capital costs of facilities, feedstock costs, electricity price, gas price and technology efficiency are in general low for the rest of the output variables (6% on average), with exception of technology efficiency on woody biomass utilisation with a corresponding first order effects of 14.7%. Moreover, when the interactions of capital costs and feedstock costs with all the parameters are considered, they have a comparable effect to subsidisation policies on the miscanthus utilisation, which also reflects on the BioSNG production and power cogeneration. Notably, the first order effects and total effects of subsidisation policies on residual waste and straw utilisation are comparable to the rest of the uncertain parameters. This indicates that, in comparison to the other feedstocks, the development of BioSNG supply chains based on residual waste and straw is not strongly dependant on subsidisation tariffs. This had been previously hinted by the results presented in Figure 6.5. In fact, both feedstocks are consistently selected for production of BioSNG in most of the 128 scenarios as shown in Figure 6.8.

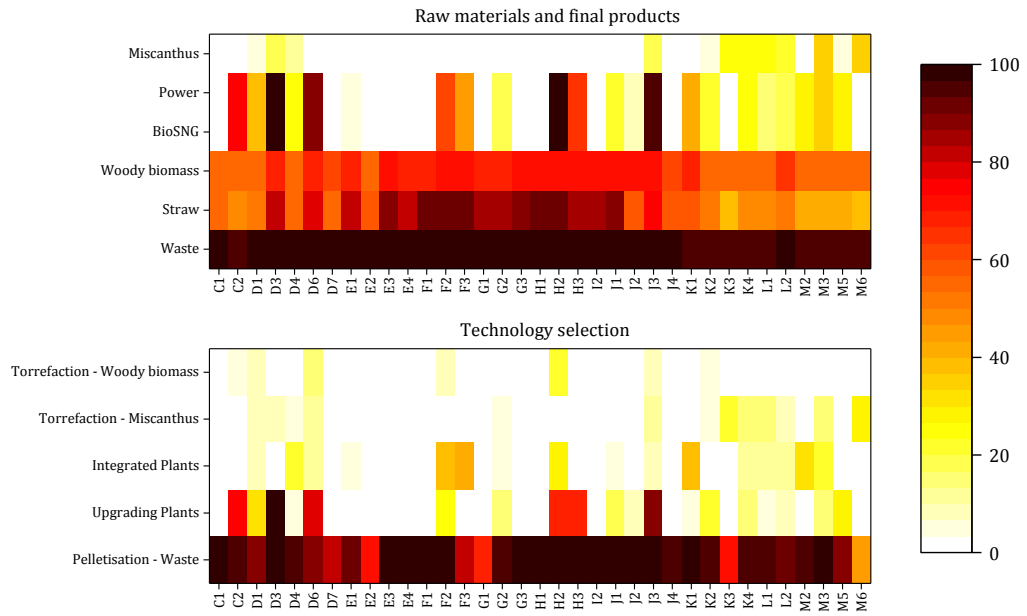

Figure 6.8. Heat maps for feedstocks and technology selection based on GSA

Figure 6.8 summarises the percentage of number of times (with respect to 128 scenarios) that raw materials, final products, and processing technologies are active in each one of the regions of the UK. Regarding raw materials and final products, it is clear that despite the variability of the uncertain parameters, the utilisation of residual waste across the UK is considerably high (above 94%), which makes it the preferred feedstock for production of BioSNG. The utilisation rate of straw is relatively high in England with certain preference towards East Midlands (F1-F3), West Midlands (G1-G3), and East of England (H1-H3) where straw was used in 90% of the scenarios. In Scotland (M2-M3, M5-M6), straw was produced in around 40% of the scenarios. The utilisation rate of Woody biomass is more homogenous across the UK, ranging between 54%, in Scotland and north of England (C1, C2, and D1), and 70% in England (E3-J3). The results for miscanthus show that the cultivation of this energy crop is mostly concentrated on Wales (L1-L2), five regions in England (D3, D4, J3, K3, and K4), and two regions in Scotland (M3 and M6). However, the selection rate of miscanthus is 17% which is very low in comparison to the other three feedstocks. Despite being crucial to achieve high BioSNG supply, the production of miscanthus is vulnerable to unfavourable government policies, which can hinder its development across the UK. Four regions in England (D3, D6, H2, and

J3) are selected in 94% of the scenarios to install facilities for BioSNG production and power cogeneration. From the figure it seems that upgrading plants are the preferred choice in these regions, which reaffirms the importance of a distributed route for BioSNG production. The selection of integrated facilities is low in comparison to the upgrading facilities. This can be explained by the fact that most of the installation of integrated facilities is linked to the cultivation of miscanthus; since this feedstock is severely affected by the variability in the subsidisation tariffs, this is reflected on the infrastructure development. Among the pretreatment technologies, the selection of pelletisation for residual waste is prevalent across the UK regardless of the variability in the uncertain parameters. Torrefaction of miscanthus is also selected as pretreatment technology; however, this occurs only in 10% of the scenarios. Similarly, torrefaction of woody biomass is active in 7% of the scenarios.

6.5 Conclusions

The mathematical formulation which is the basis of Chapter 5 has been extended to account for a second path for producing BioSNG. This path consists of pretreatment technologies, for generation of intermediate products, and upgrading facilities for final processing. The results show that when pretreatment technologies are considered, the profitability increases by 16%. Regarding the cost structure, feedstock purchases continue to be the major component cost, with investments in facilities in second place. Moreover, the operating costs related to transportation are almost double the operating costs of the facilities. In terms of transportation modes, rail is preferred over trucks, delivering around 71% of the feedstocks and intermediate products. Regarding feedstocks, in accordance to Chapter 5, miscanthus cultivation is main source of biomass since it contributes with 65.1% of the total BioSNG production. For the base scenario only torrefaction for miscanthus and pelletisation for residual waste were selected as pretreatment technologies.

A parametric analysis revealed that without subsidisation, the production of BioSNG is economically feasible if pretreatment technologies are included. In this case, the production of BioSNG is mostly based on pelletisation of residual waste. By contrast, when only integrated technologies are considered, the production of

BioSNG takes off only after the subsidisation tariff is £20/MWh. This result indicates that the early stages of a development of a BioSNG supply chain can be based on residual waste since this feedstock can be used at maximum availability with relatively low levels of subsidisation. A critical tariff of £40/MWh has been identified which triggers the cultivation of miscanthus making possible to achieve a supply of ~20%.

Finally, a global sensitivity analysis was carried out in order to simultaneously address the impact of uncertainty in 6 parameters: technology efficiency, gas price, power price, capital investments, subsidisation levels, and feedstock costs. It was demonstrated that miscanthus cultivation and woody biomass utilisation are strongly dependant on the subsidisation levels which also reflects on the general economic performance. Residual waste and straw, on the other hand, showed a balanced dependency with other factors such as capital investments and feedstock costs. Despite the variability in the input data, residual waste was consistently selected for production of BioSNG. Straw and woody biomass come in second and third place, respectively. Miscanthus showed a low rate of usage in comparison to the other three feedstocks, and therefore the installation of integrated facilities is affected. Among pretreatment technologies, pyrolysis (FBRP and RCRP) is not competitive with technologies such as pelletisation which is selected in most of the scenarios to process residual waste. Torrefaction is installed in some scenarios to process miscanthus and in some cases woody biomass.

Chapter 7. Concluding remarks and future work

This thesis presents comprehensive mathematical frameworks and their implementation for the strategic design and optimisation of two energy systems: Shale gas supply chains and BioSNG supply chains. Several aspects of both energy systems were addressed. In the case of shale gas supply chains, the research focused on developing an integrated approach that includes not only decisions regarding the production and processing of shale gas but also water management strategies associated with the exploitation of these resources. In the case of BioSNG supply chains, the research was focused on developing a framework that includes different routes for BioSNG production, evaluate the economic feasibility of this energy source, and identify key aspects for large-scale development. The main insights of each chapter are summarised next and possible venues for future work are discussed.

Chapter 2 provides insights of the current state of shale gas development and BioSNG supply chains. A detailed discussion regarding these energy systems serves as the motivation for the research presented in this thesis.

In Chapter 3, a methodology for the preliminary assessment of well-pad designs is proposed. This is an alternative approach that allows to include well-pad designs as decision variable in an optimisation framework without impacting considerably the complexity of the model. A thorough discussion of relevant aspects such as petrophysical properties of a shale reservoir and key elements for the design of well-pads is provided. Reservoir simulation tools were implemented in order to estimate the productivity of several well-pad designs. Economic and environmental metrics were proposed in order to evaluate the performance of these well-pads in different aspects. The findings from this chapter are the basis for the set of case studies discussed in Chapter 4.

In Chapter 4, the optimisation of integrated shale gas supply chains is addressed. The results reveal that the assessment of both supply chains (gas and water) cannot be decoupled from each other. The full understanding of the intrinsic synergies between these components requires that these types of planning problems be analysed in an integrated fashion. The analysis of water-energy nexus was based on parametric analysis of fresh water availability and TDS concentration in wastewater, which are two key parameters that could affect the optimal drilling and fracturing scheme as well as the water management strategy and thus the economics of the shale gas development. Under water scarcity scenarios, which are becoming progressively more frequent nowadays given global climate events such as El Niño/La Niña, it seems that the selection of less water intensive well-pad designs is more cost-effective than intensifying water treatment processes for water re-use and/or recycle in the development of shale gas resources. In addition, the role of economies of scale was investigated by varying the number of potential well-pads. It was found that shale gas development benefits from economies of scale, since not only the economic performance is improved but also the shale gas supply chain becomes more resilient to changes in water resources availability and water quality in terms of TDS. Moreover, water resources are used more efficiently as the number of installed well-pads increases.

In Chapter 5, an optimisation framework was developed in order to address the strategic optimisation of BioSNG supply chains in a regional and national context. Several insights are drawn from the implementation of a case study based on the UK. Initially, the results show that operating costs, specifically feedstock purchases, are the main cost component in the development of a BioSNG supply chain, followed by investments in integrated facilities. With the current domestic resources, it is possible to supply ~21% of the lower pressure gas demand. Among four feedstocks, the cultivation of miscanthus stands out as a critical source of biomass in order to achieve significant production of BioSNG in the UK. Moreover, the results indicate that the economics of BioSNG supply chains greatly benefits from cogeneration of power as a by-product of the gasification process. Therefore, a policy framework that allows power sales to the grid would encourage the development of this renewable

resource. It has been shown, however, that with the current capital and operating costs, a successful development of BioSNG nationwide depends greatly on subsidisation schemes developed by the government.

Chapter 6 extends the mathematical framework presented in Chapter 5 in order to account for a distributed route for production of BioSNG. It was found that pyrolysis is not economically viable, whereas torrefaction and especially pelletisation of residual waste are the preferred pretreatment technologies. Nonetheless, integrated technologies continue to be a crucial component in the design of BioSNG supply chains. A critical subsidisation point was found in which the supply of BioSNG increases sharply. This occurs due to cultivation of miscanthus, which is fundamental for the development of BioSNG supply chains but it is also highly susceptible to favourable subsidisation schemes. Finally, inclusion of pretreatment technologies improve considerably the economic performance, however, their impact is not enough to detach the development from government subsidisation which influences tremendously the possibility of a large scale deployment as was demonstrated by means of a global sensitivity analysis.

There are several aspects of the energy systems discussed in this work that require further investigation from the scientific community. The possible directions for extension of the research presented for shale gas supply chains are summarised next:

- One of the main challenges is related to taking into account spatial and temporal variations in shale gas composition and concentration of TDS in wastewater. However, this results in MINLP models which are highly complex and computationally expensive to solve.
- A real-world development of a shale gas reservoir entails drilling and fracturing of hundreds of well-pads. An implementation of the proposed optimisation framework for such scenarios will result in an intractable problem due to the size of the resulting model. Therefore, efficient solution strategies should be developed in order to expand the capabilities of the proposed framework.

- The features of the optimisation framework can also be extended. For instance, once a well-pad has reached low production, it is possible to reactivate the production via secondary recovery. The decision-support tool does not consider secondary recovery and well-pad shut-in operations, which can be relevant from an operational viewpoint.
- A fully integration of reservoir properties, well-pad designs, and supply chain optimisation is a possible extension. This can be done by coupling the optimisation framework with black-box models that allow to estimate the production of gas and wastewater having as inputs the main properties of the reservoirs and as decision variables the design parameters of the well-pads.
- Usually, several companies are involved in the development of a shale gas play. Therefore, the proposed optimisation framework can be extended to multiobjective optimisation to design shale gas supply chains that improve the economic performance of each of the companies involved.
- Finally, there are several sources of uncertainty in the development of shale gas resources. Therefore, multi-stage stochastic optimisation can be considered for the design of robust shale gas supply chains in face of uncertainty.

The work presented for the design of BioSNG supply chains can be extended in several aspects. Some possible routes for further investigation are summarised as follows:

- As commercial applications of gasification of biomass and waste are scarce, it is expected that the installation costs would decrease as research continues and more experience is gained (learning-by-doing). Hence, as future work, the optimisation framework can be extended in order to take into account learning curves.
- The current optimisation framework only considers transportation of BioSNG by road. Transportation of BioSNG via regional and local pipelines can be implemented so as to increase the capabilities of the proposed mathematical model.

- Seasonal variability of biomass resources can have important implications in the design of BioSNG supply chains. This can be addressed by extending the optimisation framework to multiscale capabilities which requires increasing the resolution of the planning horizon up to days. This would increase considerably the combinatorial complexity of the problem. Therefore, the use of typical days, weeks, and seasons is recommended so that the resulting problem can be solved in reasonable time.
- Finally, aspects such as the geographical distribution of the resources, associated production and investment costs, and market conditions are subject to high uncertainty. Therefore, the design of BioSNG supply chains can be extended by taking into account uncertainty in input data through rigorous stochastic optimisation frameworks.

Appendix A. Supporting information for shale gas case studies

Set of time periods T	Set of fresh water sources F	Set of well-pads W	Set of well-pads design D	Set of compressors C
t1*t40	RiverI RiverII RiverIII	w1*w10	MaxNPV MinWI	Comp1 Comp2

Set of compressors sizes M	Set of water treatment plants H	Set of gas treatment plants P	Set of demand centres J	Set of disposal sites S
m1	Waterplant1	Gasplant1	Power1	Disp1
m2	Waterplant2	Gasplant2	Petro1	Disp2
				Inject1

Set of gas plants sizes G	Set of water treatment plants sizes K	Set of pipeline sizes Q	Set of products I	Set of gas demand centres JG
g1	k1	l1*l3	Methane	Power1
g2	k2	u1*u2	Ethane	
g3	k3		C3plus	

Connections between water sources and well-pads LFW	Connections between water plants and disposal sites LHS	Connections between well-pads and compressors LWC	Set of connections between well-pads and disposal sites LWS	Set of connections between well-pads and gas plants LWP
RiverI.w6	waterplant1.disp1	w10.comp1	w1.injec1	w10.gasplant2
RiverI.w7	waterplant2.disp2	w4.comp1	w2.injec1	
RiverI.w5		w1.comp1	w3.injec1	
RiverII.w3		w6.comp1	w4.injec1	
RiverII.w8		w2.comp2	w5.injec1	
RiverII.w9		w3.comp2	w6.injec1	
RiverIII.w1		w6.comp2	w7.injec1	
RiverIII.w2		w7.comp2	w8.injec1	

RiverIII.w4	w8.comp2	w9.injec1	
RiverIII.w10	w9.comp2	w10.injec1	

Set of liquid demand centres ***JL***	**Set of liquid products pipeline sizes** ***U***	**Set of gas products pipeline sizes** ***L***	**Set of connections between compressors** ***LCC***	**Set of connections between compressors and plants** ***LCP***
Petro1	u1*u2	l1*l3	Comp2.Comp1	comp1.gasplant1 comp1.gasplant2 comp2.gasplant2

Set of connections between water plants and well-pads ***LHW***		**Set of connections between products and demand centres** ***LIJ***
waterplant1.w1	waterplant1.w9	methane.power1
waterplant1.w2	waterplant1.w11	ethane.petro1
waterplant1.w3	waterplant2.w2	
waterplant1.w4	waterplant2.w3	
waterplant1.w5	waterplant2.w5	
waterplant1.w6	waterplant2.w7	
waterplant1.w7	waterplant2.w8	
waterplant1.w8	waterplant2.w9	

Scalars		
$MaxExp$	3	Maximum number of expansions for gas processing plants
$MaxInv$	$10x10^9$	Maximum budget available for investment [USD]
$MaxTDS$	15,000	Max TDS concentration on water blend for hydraulic fracturing [mg/L]
$MaxWell$	14	Maximum number of wells that can be drilled per period
roy	8	Royalty rate [%]
tc	4	Lead time for installing a new compressor
td	4	Lead time for building a pipeline either for liquids or gas transportation
tg	4	Lead time for installing a new gas treatment plant
th	4	Lead time for installing a new water treatment plant
tx	35	Taxes rate [35%]
γ	3	Discount rate [%/period]

$CapDisp(s,t)$ [gallon/day]	t1*t40
disp1	40000
disp2	200000
injec1	336000

$CapexComp(m,c)$ [USD]	Comp1	Comp2
m1	1614300	1614300
m2	2659800	2659800

$CapexGas(g,p)$ [USD]	GasPlant1	GasPlant2
g1	442331224	442331224
g2	596055438.05	596055438.05
g3	758351674.68	758351674.68

$CapexPcc(c,c',q)$ [USD]	l1	l2	l3
Comp1.Comp2	12205772	17321774	22437777

$CapexPcp(c,p,q)$ [USD]	l1	l2	l3
comp1.gasplant1	3483130	5022320	6869347
comp1.gasplant2	8586083	14163809	18347103
comp2.gasplant2	5036087	8151702	11712405

$CapexPpj(p,j,q)$ [USD]	l1	l2	l3	u1	u2
gasplant1.power1	30088903	43385145	59340635	0	0
gasplant1.petro1	0	0	0	26175460	33332294
gasplant2.power1	26803205	38647502	52860658	0	0
gasplant2.petro1	0	0	0	21609760	27518251

$CapexPwc(w,c,q)$ [USD]	l1	l2	l3
w9.comp1	2582546	4084781	5587016
w4.comp1	3328304	4799077	6564004
w1.comp1	5793485	8616176	12379763
w5.comp1	4720785	7641337	10979109
w2.comp2	3358539	4842672	6623633
w3.comp2	4088120	6617267	8062494
w5.comp2	5971947	8881587	12761107
w6.comp2	1549691	2150648	3052084
w7.comp2	2097710	3317922	4131397
w8.comp2	5030893	8143296	11700327

$CapexPwp(w,p,q)$ [USD]	l1	l2	l3
w11.gasplant2	2392767	3784610	5176454

$CapexWate(k,h)$ [USD]	WaterPlant1	WaterPlant2
k1	300735.00	420000.00
k2	500000.00	698289.26
k3	757858.00	1058408.60

$Comp(i,d,w,t)$ [-]	t1*t40
methane.MaxNPV.w1*w10	0.75
ethane.MaxNPV.w1*w10	0.08
C3plus.MaxNPV.w1*w10	0.17
methane.MinWI.w1*w10	0.75
ethane.MinWI.w1*w10	0.08
C3plus.MinWI.w1*w10	0.17

$CapexWell(d,w)$ [USD]	w1*w10
MaxNPV	195300000
MinWI	52500000

$CostFres(f,w)$ [USD/gallon x10^{-3}]	w1	w2	w3	w4	w5	w6	w7	w8	w9	w10
RiverI					3.16	2.58	9.03			
RiverII			3.19					1.37	2.71	
RiverIII	6.03	7.23		8.83						1.23

$CostRech(h,w)$ [USD/gallon x10^{-3}]	w1	w2	w3	w4	w5	w6	w7	w8	w9	w10
WaterPlant1	7.13	5.70	11.43	9.93	2.11	1.31	4.73	6.86	10.04	13.41
WaterPlant2		4.58	5.18		3.57		2.13	1.40	4.58	

$CostRecs(h,s)$ [USD/gallon x10^{-3}]	disp1	disp2
WaterPlant1	1.17	
WaterPlant2		0.6

$CostWateh(w,h)$ [USD/gallon x10^{-3}]	WaterPlant1	WaterPlant2
w1	7.1	
w2	5.7	4.6
w3	11.4	5.2
w4	9.9	0.0
w5	2.1	3.6
w6	1.3	0.0
w7	4.7	2.1
w8	6.9	1.4
w9	10.0	4.6
w10	13.4	

$Dem(i,j,t)$ [MMSCFD]										
	t1	**t2**	**t3**	**t4**	**t5**	**t6**	**t7**	**t8**	**t9**	**t10**
methane.power1	187.3	215.6	218.9	240.8	63.0	76.1	93.9	110	215.7	238.3
ethane.power1	60.0	60.0	60.0	60.0	60.0	60.0	60.0	60.0	60.0	60.0
	t11	**t12**	**t13**	**t14**	**t15**	**t16**	**t17**	**t18**	**t19**	**t20**
methane.power1	253.9	266.9	299.2	306.4	317.7	334.7	456.0	393.2	398.4	412.6
ethane.power1	60.0	60.0	60.0	60.0	60.0	60.0	60.0	60.0	60.0	60.0
	t21	**t22**	**t23**	**t24**	**t25**	**t26**	**t27**	**t28**	**t29**	**t30**
methane.power1	450.4	451.6	464.8	475.5	503.4	591.2	525.0	537.1	573.7	577.4
ethane.power1	60.0	60.0	60.0	60.0	60.0	60.0	60.0	60.0	60.0	60.0
	t31	**t32**	**t33**	**t34**	**t35**	**t36**	**t37**	**t38**	**T39**	**t40**
methane.power1	582.4	599.7	628.1	636.2	643.1	654.7	679.4	682.8	695.1	707.0
ethane.power1	60.0	60.0	60.0	60.0	60.0	60.0	60.0	60.0	60.0	60.0

$Dep(t,t')$ [-]										
	t1	**t2**	**t3**	**t4**	**t5**	**t6**	**t7**	**t8**	**t9**	**t10**
t1	0.05	0.05	0.05	0.05	0.05	0.05	0.05	0.05	0.05	0.05
t2		0.05	0.05	0.05	0.05	0.05	0.05	0.05	0.05	0.05
t3			0.05	0.05	0.05	0.05	0.05	0.05	0.05	0.05
t4				0.05	0.05	0.05	0.05	0.05	0.05	0.05
t5					0.05	0.05	0.05	0.05	0.05	0.05
t6						0.05	0.05	0.05	0.05	0.05
t7							0.05	0.05	0.05	0.05
t8								0.05	0.05	0.05
t9									0.05	0.05
t10										0.05
	t11	**t12**	**t13**	**t14**	**t15**	**t16**	**t17**	**t18**	**t19**	**t20**
t11	0.05	0.05	0.05	0.05	0.05	0.05	0.05	0.05	0.05	0.05
t12		0.05	0.05	0.05	0.05	0.05	0.05	0.05	0.05	0.05
t13			0.05	0.05	0.05	0.05	0.05	0.05	0.05	0.05
t14				0.05	0.05	0.05	0.05	0.05	0.05	0.05
t15					0.05	0.05	0.05	0.05	0.05	0.05
t16						0.05	0.05	0.05	0.05	0.05
t17							0.05	0.05	0.05	0.05
t18								0.05	0.05	0.05
t19									0.05	0.05
t20										0.05

	t21	t22	t23	t24	t25	t26	t27	t28	t29	t30
t21	0.05	0.05	0.05	0.05	0.05	0.05	0.05	0.05	0.05	0.05
t22		0.05	0.05	0.05	0.05	0.05	0.05	0.05	0.05	0.05
t23			0.05	0.05	0.05	0.05	0.05	0.05	0.05	0.05
t24				0.05	0.05	0.05	0.05	0.05	0.05	0.05
t25					0.05	0.05	0.05	0.05	0.05	0.05
t26						0.05	0.05	0.05	0.05	0.05
t27							0.05	0.05	0.05	0.05
t28								0.05	0.05	0.05
t29									0.05	0.05
t30										0.05

	t31	t32	t33	t34	t35	t36	t37	t38	T39	t40
t31	0.05	0.05	0.05	0.05	0.05	0.05	0.05	0.05	0.05	0.05
t32		0.05	0.05	0.05	0.05	0.05	0.05	0.05	0.05	0.05
t33			0.05	0.05	0.05	0.05	0.05	0.05	0.05	0.05
t34				0.05	0.05	0.05	0.05	0.05	0.05	0.05
t35					0.05	0.05	0.05	0.05	0.05	0.05
t36						0.05	0.05	0.05	0.05	0.05
t37							0.05	0.05	0.05	0.05
t38								0.05	0.05	0.05
t39									0.05	0.05
t40										0.05

$CostWates(w,s)$ [USD/gallon x10^{-3}]	
	l1
w1	78.3
w2	80.3
w3	61.6
w4	81.1
w5	69.7
w6	81.3
w7	68.1
w8	65.4
w9	67.5
w10	84.5

$MaxTDSt(w,p,q)$ [mg/L]	
	l1
waterplant1	50000
waterplant2	120000

$NumWell(w)$ [-]	
MaxNPV	14
MinWI	6

$OpexWell(w)$ [USD/MMSCF]	
w1*w10	160

$OpexComp(c)$ [USD/MMSCF]	
Comp1	36.88
Comp2	36.88

$OpexDisp(s)$ [USD/gallon]	
Injec1	0.7518

$OpexGas(p)$ [USD/MMSCF]	
gasplant1	142.749
gasplant2	142.749

$OpexWate(h)$ [USD/gallon]	
Wateplant1	0.02
Wateplant2	0.03

$Price(i,j,t)$ [USD/MMSCFD]										
	t1	**t2**	**t3**	**t4**	**t5**	**t6**	**t7**	**t8**	**t9**	**t10**
methane.power1	4143.3	3986.7	4126.7	4253.3	5196.7	5276.7	5353.3	5433.3	5580.0	5586.7
ethane.power1	8398.7	8398.7	8398.7	8398.7	8398.7	8398.7	8398.7	8398.7	8398.7	8398.7

	t11	**t12**	**t13**	**t14**	**t15**	**t16**	**t17**	**t18**	**t19**	**t20**
methane.power1	5753.3	5703.3	6296.7	6283.3	6463.3	6456.7	7113.3	7076.7	7203.3	7126.7
ethane.power1	8398.7	8398.7	8398.7	8398.7	8398.7	8398.7	8398.7	8398.7	8398.7	8398.7

	t21	**t22**	**t23**	**t24**	**t25**	**t26**	**t27**	**t28**	**t29**	**t30**
methane.power1	6420.0	6523.3	6700.0	6620.0	6883.3	7016.7	7230.0	7146.7	7363.3	7416.7
ethane.power1	8398.7	8398.7	8398.7	8398.7	8398.7	8398.7	8398.7	8398.7	8398.7	8398.7

	t31	**t32**	**t33**	**t34**	**t35**	**t36**	**t37**	**t38**	**T39**	**t40**
methane.power1	7540.0	7383.3	7460.0	7540.0	7720.0	7643.3	7983.3	8136.7	8383.3	8293.3
ethane.power1	8398.7	8398.7	8398.7	8398.7	8398.7	8398.7	8398.7	8398.7	8398.7	8398.7

$PriceC3(p,t)$ [USD/MMSCF]	
	t1*t40
Gasplant1	32370.6
Gasplant2	32370.6

$RawTankCap(k)$ [gallon]	
k1	283500
k2	661500
k3	1323000

$Sizec(m)$ [MMSCFD]	
m1	150
m2	300

$Sizeg(g)$ [MMSCFD]	
g1	100
g2	200
g3	350

$Sizeh(k)$ [gallon/day]	
k1	k1
k2	220500
k3	441000

$Sizep(q)$ [MMSCFD]	
l1	40
l2	150
l3	360

$Sizepl(q)$ [MMSCFD]	
u1	16
u2	40

$TankCap(k)$ [gallon]	
k1	283500
k2	661500
k3	1323000

$TDSf(f)$ [mg/L]	
RiverI	130
RiverII	150
RiverIII	140

$TDSh(h)$ [mg/L]	
waterplant1	50000
waterplant2	100

$WatDem(d,w)$ [gallon/day]	
	w1*w10
MaxNPV	4701910
MinWI	1127017

$TDSw(w)$ [mg/L]	
w1	53081.9
w2	34334.9
w3	36671.1
w4	106774.5
w5	79765.26
w6	61051.3
w7	73370.7
w8	51689.8
w9	88677.0
w10	39892.5

$WateAvai(f,t)$ [gallon/day]										
	t1	**t2**	**t3**	**t4**	**t5**	**t6**	**t7**	**t8**	**t9**	**t10**
RiverI	2,350,955	3,526,433	4,701,910	3,526,433	2,350,955	3,526,433	4,701,910	3,526,433	2,350,955	3,526,433
RiverII	2,350,955	3,526,433	4,701,910	3,526,433	2,350,955	3,526,433	4,701,910	3,526,433	2,350,955	3,526,433
RiverIII	2,350,955	3,526,433	4,701,910	3,526,433	2,350,955	3,526,433	4,701,910	3,526,433	2,350,955	3,526,433
	t11	**t12**	**t13**	**t14**	**t15**	**t16**	**t17**	**t18**	**t19**	**t20**
RiverI	4,701,910	3,526,433	2,350,955	3,526,433	4,701,910	3,526,433	2,350,955	3,526,433	4,701,910	3,526,433
RiverII	4,701,910	3,526,433	2,350,955	3,526,433	4,701,910	3,526,433	2,350,955	3,526,433	4,701,910	3,526,433
RiverIII	4,701,910	3,526,433	2,350,955	3,526,433	4,701,910	3,526,433	2,350,955	3,526,433	4,701,910	3,526,433
	t21	**t22**	**t23**	**t24**	**t25**	**t26**	**t27**	**t28**	**t29**	**t30**
RiverI	2,350,955	3,526,433	4,701,910	3,526,433	2,350,955	3,526,433	4,701,910	3,526,433	2,350,955	3,526,433
RiverII	2,350,955	3,526,433	4,701,910	3,526,433	2,350,955	3,526,433	4,701,910	3,526,433	2,350,955	3,526,433
RiverIII	2,350,955	3,526,433	4,701,910	3,526,433	2,350,955	3,526,433	4,701,910	3,526,433	2,350,955	3,526,433
	t31	**t32**	**t33**	**t34**	**t35**	**t36**	**t37**	**t38**	**T39**	**t40**
RiverI	4,701,910	3,526,433	2,350,955	3,526,433	4,701,910	3,526,433	2,350,955	3,526,433	4,701,910	3,526,433
RiverII	4,701,910	3,526,433	2,350,955	3,526,433	4,701,910	3,526,433	2,350,955	3,526,433	4,701,910	3,526,433
RiverIII	4,701,910	3,526,433	2,350,955	3,526,433	4,701,910	3,526,433	2,350,955	3,526,433	4,701,910	3,526,433

$WellGas(d,w,t)$ [MMSCFD]										
	t1	**t2**	**t3**	**t4**	**t5**	**t6**	**t7**	**t8**	**t9**	**t10**
MaxNPV.w1*w10	99.8	85.6	74.1	64.9	57.4	51.1	45.7	41.1	37.2	33.7
MinWI.w1*w10	32.4	27.1	22.9	19.6	16.9	14.8	12.9	11.4	10.1	9.0
	t11	**t12**	**t13**	**t14**	**t15**	**t16**	**t17**	**t18**	**t19**	**t20**
MaxNPV.w1*w10	30.7	28.0	25.7	23.6	21.7	19.9	18.4	17.0	15.8	14.6
MinWI.w1*w10	8.0	7.2	6.5	5.8	5.3	4.8	4.3	4.0	3.6	3.3
	t21	**t22**	**t23**	**t24**	**t25**	**t26**	**t27**	**t28**	**t29**	**t30**
MaxNPV.w1*w10	13.6	12.6	11.8	10.9	10.2	9.5	8.9	8.3	7.8	7.3
MinWI.w1*w10	3.0	2.8	2.5	2.3	2.1	2.0	1.8	1.7	1.6	1.4
	t31	**t32**	**t33**	**t34**	**t35**	**t36**	**t37**	**t38**	**T39**	**t40**
MaxNPV.w1*w10	6.9	6.4	6.0	5.7	5.3	5.0	4.7	4.4	4.2	3.9
MinWI.w1*w10	1.3	1.2	1.2	1.1	1.0	0.9	0.9	0.8	0.8	0.7

$WellGas(d,w,t)$ [MMSCFD]										
	t1	**t2**	**t3**	**t4**	**t5**	**t6**	**t7**	**t8**	**t9**	**t10**
MaxNPV.w1*w10	99.8	85.6	74.1	64.9	57.4	51.1	45.7	41.1	37.2	33.7
MinWI.w1*w10	32.4	27.1	22.9	19.6	16.9	14.8	12.9	11.4	10.1	9.0
	t11	**t12**	**t13**	**t14**	**t15**	**t16**	**t17**	**t18**	**t19**	**t20**
MaxNPV.w1*w10	30.7	28.0	25.7	23.6	21.7	19.9	18.4	17.0	15.8	14.6
MinWI.w1*w10	8.0	7.2	6.5	5.8	5.3	4.8	4.3	4.0	3.6	3.3
	t21	**t22**	**t23**	**t24**	**t25**	**t26**	**t27**	**t28**	**t29**	**t30**
MaxNPV.w1*w10	13.6	12.6	11.8	10.9	10.2	9.5	8.9	8.3	7.8	7.3
MinWI.w1*w10	3.0	2.8	2.5	2.3	2.1	2.0	1.8	1.7	1.6	1.4
	t31	**t32**	**t33**	**t34**	**t35**	**t36**	**t37**	**t38**	**T39**	**t40**
MaxNPV.w1*w10	6.9	6.4	6.0	5.7	5.3	5.0	4.7	4.4	4.2	3.9
MinWI.w1*w10	1.3	1.2	1.2	1.1	1.0	0.9	0.9	0.8	0.8	0.7

$WellWate(d,w,t)$ [gallon/day]										
	t1	**t2**	**t3**	**t4**	**t5**	**t6**	**t7**	**t8**	**t9**	**t10**
MaxNPV.w1*w10	1455622.7	39069.2	34177.6	30156.5	26814.4	23997.3	21565.3	19475.6	17676.7	16097.8
MinWI.w1*w10	352762.7	12423.1	10623.1	9167.2	7977.1	6990.7	6153.5	5446.3	4847.7	4331.0
	t11	**t12**	**t13**	**t14**	**t15**	**t16**	**t17**	**t18**	**t19**	**t20**
MaxNPV.w1*w10	14685.3	13438.1	12338.3	11353.0	10455.0	9648.5	8926.8	8271.5	7666.8	7117.8
MinWI.w1*w10	3876.5	3481.8	3139.5	2837.9	2567.6	2328.9	2118.9	1931.3	1761.1	1609.2
	t21	**t22**	**t23**	**t24**	**t25**	**t26**	**t27**	**t28**	**t29**	**t30**
MaxNPV.w1*w10	6617.9	6161.8	5738.7	5351.5	4998.9	4673.5	4368.6	4088.0	3830.9	3592.6
MinWI.w1*w10	1473.1	1351.1	1239.8	1139.7	1050.0	968.6	893.6	825.8	764.7	708.9
	t31	**t32**	**t33**	**t34**	**t35**	**t36**	**t37**	**t38**	**T39**	**t40**
MaxNPV.w1*w10	3368.2	3160.7	2969.8	2792.2	2624.2	2468.5	2323.7	2189.0	2061.9	1943.6
MinWI.w1*w10	657.3	610.4	567.9	529.0	492.8	459.8	429.6	401.9	376.2	352.6

$\psi(h)$ [-]	
waterplant1	0.97
waterplant2	0.85

$\phi(i,p)$ [-]		
	gasplant1	**gasplant2**
methane	0.95	0.95
ethane	0.90	0.90
c3plus	0.90	0.90

Appendix B. Supporting maps

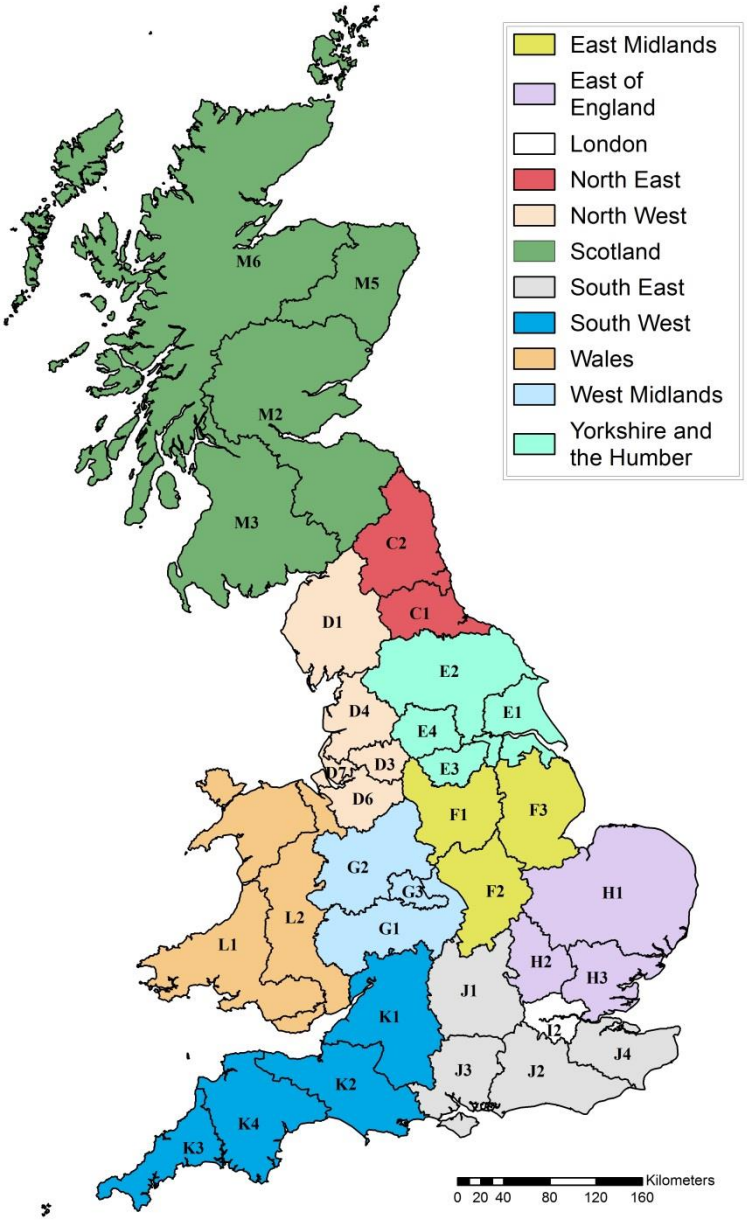

Figure A.1. UK statistical regions classified by NUTS 1 (colour) and NUTS 2 (labels)

Table A.1. UK NUTS1 and NUTS2 classification

UK NUTS 1	UK NUTS 2	REGIONS
East Midlands	F1	Derbyshire and Nottinghamshire
	F2	Leicestershire, Rutland and Northamptonshire
	F3	Lincolnshire
East of England	H1	East Anglia
	H2	Bedfordshire and Hertfordshire
	H3	Essex
Greater London	I2	Inner and outer London
North East England	C1	Tees Valley and Durham
	C2	Northumberland and Tyne and Wear
North West England	D1	Cumbria
	D3	Manchester
	D4	Lancashire
	D6	Cheshire
	D7	Merseyside
South East England	J1	Berkshire, Buckinghamshire and Oxfordshire
	J2	Surrey, East and West Sussex
	J3	Hampshire and Isle of Wight
	J4	Kent
South West England	K1	Gloucestershire, Wiltshire and Bristol/Bath area
	K2	Dorset and Somerset
	K3	Cornwall and Isles of Scilly
	K4	Devon
West Midlands	G1	Herefordshire, Worcestershire and Warwickshire
	G2	Shropshire and Staffordshire
	G3	West Midlands
Yorkshire and the Humber	E1	East Yorkshire and Northern Lincolnshire
	E2	North Yorkshire
	E3	South Yorkshire
	E4	West Yorkshire
Wales	L1	West Wales and The Valleys
	L2	East Wales
Scotland	M2	Eastern Scotland
	M3	South Western Scotland
	M5	North Eastern Scotland
	M6	Highlands and Islands

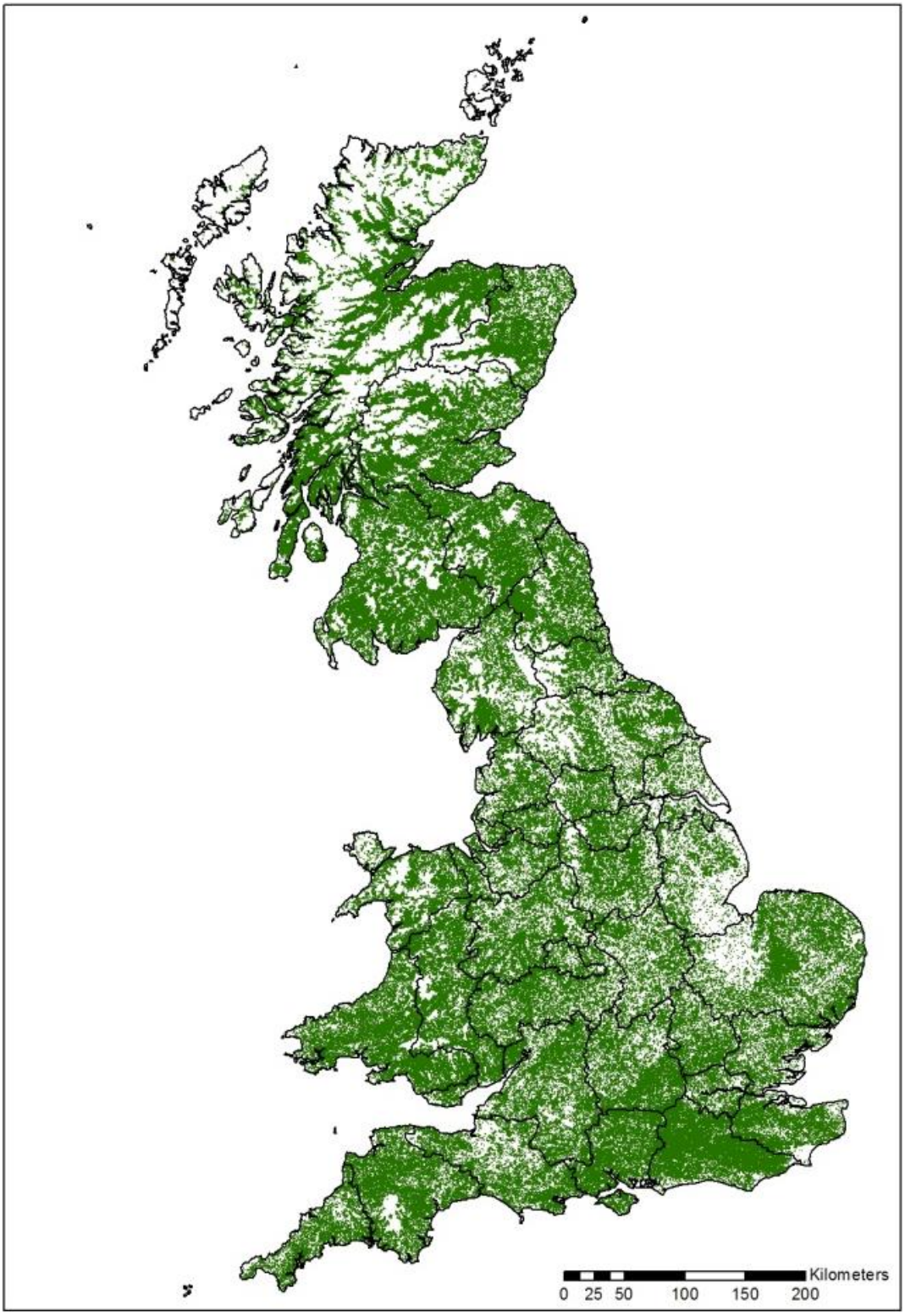

Figure A.2. Forestry land distribution across the UK [287]

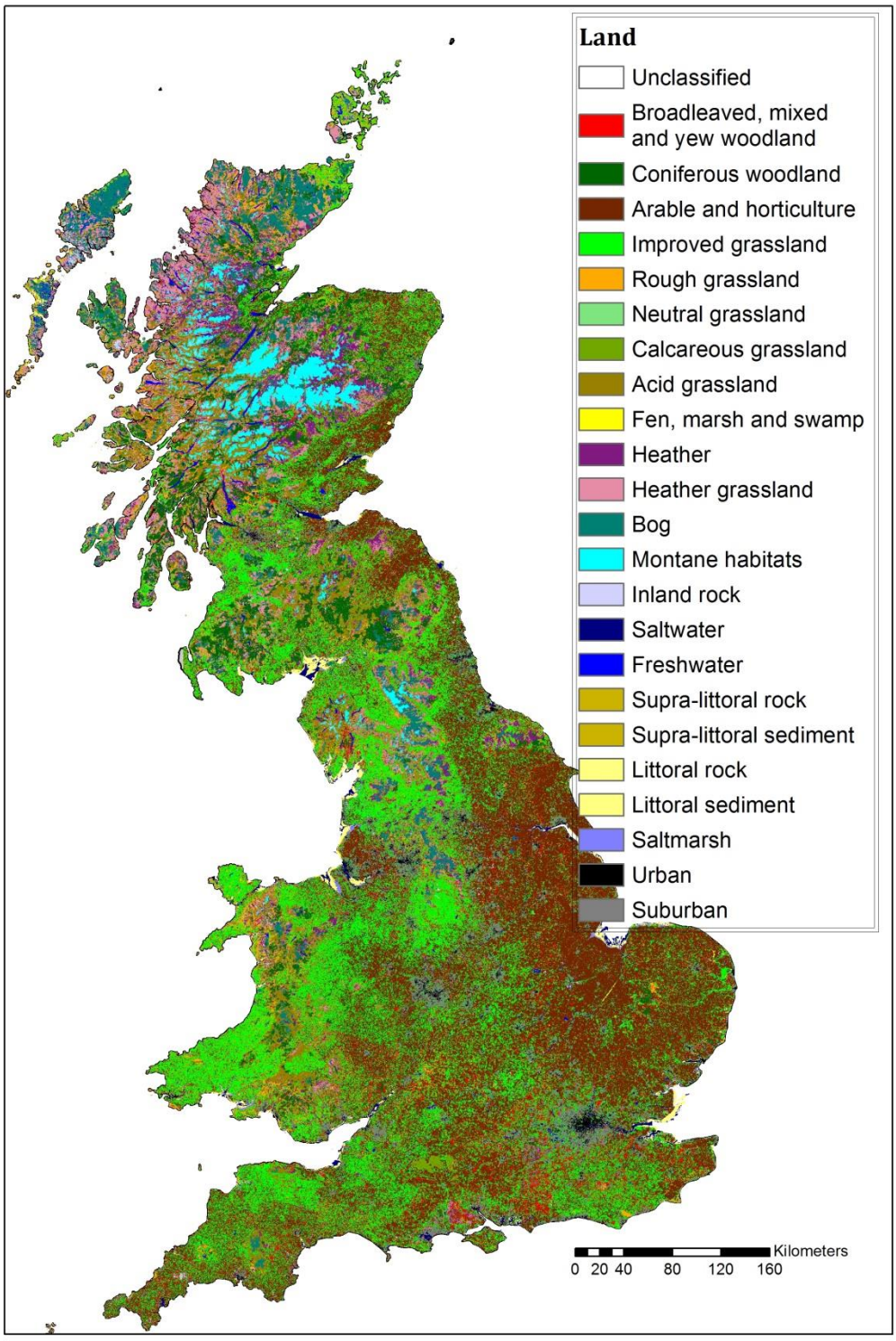

Figure A.3. UK Land Cover Area [289]

Figure A.4. UK map of active sawmills [130]

Publications

Peer-reviewed Publications

I. Calderón AJ, Guerra OJ, Papageorgiou LG, Siirola JJ, Reklaitis G V. Preliminary Evaluation of Shale Gas Reservoirs: Appraisal of Different Well-Pad Designs via Performance Metrics. Ind Eng Chem Res. 2015;54:10334–49. doi:10.1021/acs.iecr.5b01590.

II. Guerra OJ, Calderón AJ, Papageorgiou LG, Siirola JJ, Reklaitis G V. An optimization framework for the integration of water management and shale gas supply chain design. Comput Chem Eng. 2016;92:230–55. doi:10.1016/j.compchemeng.2016.03.025.

III. Guerra OJ, Calderón AJ, Papageorgiou LG, and Reklaitis GV. Strategic design and tactical planning for energy supply chain systems. In Advances in Energy Systems Engineering; Kopanos GM, Liu P, Georgiadis MC. Cham, Switzerland: Springer International Publishing Springer International Publishing, 2016.

IV. Calderón AJ, Agnolucci P, Papageorgiou LG. An optimisation framework for the strategic design of synthetic natural gas (BioSNG) supply chains. Appl Energy. 2017;187:929–55. doi:10.1016/j.apenergy.2016.10.074.

V. Calderón AJ, Guerra OJ, Papageorgiou LG, and Reklaitis GV. Water-Energy-Economics Nexus in Shale Gas Development (submitted for review, 2017).

VI. Guerra OJ, Calderón AJ, Papageorgiou LG, and Reklaitis GV. Integrated Shale Gas Supply Chain Design and Water Management under Uncertainty. (to be submitted for review, 2017).

VII. Calderón AJ, and Papageorgiou LG. The role of pretreatment technologies in the strategic development of synthetic natural gas (BioSNG) supply chains. (submitted for review, 2017).

Peer-reviewed Conference Proceedings

A. Calderón, AJ, Guerra OJ, Papageorgiou LG, Siirola JJ, and Reklaitis GV. Financial Considerations in Shale Gas Supply Chain Development. In: Krist V. Gernaey, Jakob K. Huusom and Rafiqul Gani, Editor(s), Computer Aided Chemical Engineering, Elsevier, 2015, Volume 37, Pages 2333-2338.

B. Guerra OJ, Calderón AJ, Papageorgiou LG, and Reklaitis GV. Wastewater Quality Impact on Water Management in Shale Gas Supply Chain. In: Zdravko Kravanja and Miloš Bogataj, Editor(s), Computer Aided Chemical Engineering, Elsevier, 2016, Volume 38, Pages 371-1376.

References

[1] Smil V. Energy in the twentieth century: Resources, Conversions, Costs, Uses, and Consequences. Annu Rev Energy Environ. 2000;25:21–51. doi:10.1146/annurev.energy.25.1.21.

[2] Smil V. The Long Slow Rise of Solar and Wind. Sci Am. 2013;310:52–7. doi:10.1038/scientificamerican0114-52.

[3] Nakata T, Silva D, Rodionov M. Application of energy system models for designing a low-carbon society. Prog Energy Combust Sci. 2011;37:462–502. doi:10.1016/j.pecs.2010.08.001.

[4] British Petroleum (BP). BP Statistical Review of World Energy. 2014. Available from: http://www.bp.com/en/global/corporate/energy-economics/statistical-review-of-world-energy.html.

[5] British Petroleum (BP). BP Energy Outlook 2035. 2014. Available from: http://www.bp.com/content/dam/bp/pdf/energy-economics/energy-outlook-2016/bp-energy-outlook-2014.pdf.

[6] Agerton M, Hartley P, Medlock III K, Temzelides T. Employment Impacts of Upstream Oil and Gas Investment in the United States. IMF Work Pap. 2015;62:171–80. doi:10.1016/j.eneco.2016.12.012.

[7] Clark CE, Horner RM, Harto CB. Life Cycle Water Consumption for Shale Gas and Conventional Natural Gas. Environ Sci Technol. 2013;47:11829–36. doi:10.1021/es4013855.

[8] Eaton TT. Science-based decision-making on complex issues: Marcellus shale gas hydrofracking and New York City water supply. Sci Total Environ. 2013;461–462:158–69. doi:10.1016/j.scitotenv.2013.04.093.

[9] Vidic RD, Brantley SL, Vandenbossche JM, Yoxtheimer D, Abad JD. Impact of Shale Gas Development on Regional Water Quality. Science. 2013;340:1235009–1235009. doi:10.1126/science.1235009.

[10] Warner NR, Christie CA, Jackson RB, Vengosh A. Impacts of shale gas wastewater disposal on water quality in western Pennsylvania. Environ Sci Technol. 2013;47:11849–57. doi:10.1021/es402165b.

[11] International Energy Agency (IEA). Golden rules for a golden age of gas. London: 2012. Available from: http://www.worldenergyoutlook.org/media/weowebsite/recentpresentations/PresentationtoPressWEOGoldenRulesforaGoldenAgeofGasspecialreport.pdf.

[12] International Energy Agency (IEA). CO2 Emissions From Fuel Combustion: Highlights 2014. Paris: 2013. Available from: http://www.iea.org/publications/freepublications/publication/co2-emissions-from-fuel-combustion-highlights-2015.html.

[13] European Commission (EC). Communication from the commission Europe 2020: A strategy for smart, sustainable and inclusive growth. Brussels: 2010. Available from: http://eur-lex.europa.eu/LexUriServ/LexUriServ.do?uri=COM:2010:2020:FIN:EN:PDF.

[14] European Commission (EC). Communication from the commission to the European parliament, the council, the European economic and social committee and the committee of the regions: A policy framework for climate and energy in the period from 2020 to 2030. Brussels: 2014. Available from: http://eur-lex.europa.eu/legal-content/EN/TXT/PDF/?uri=CELEX:52014DC0015&from=EN.

[15] Kim J, Sen SM, Maravelias CT. An optimization-based assessment framework for biomass-to-fuel conversion strategies. Energy Environ Sci. 2013;6:1093–104. doi:10.1039/c3ee24243a.

[16] Swanson RM, Platon A, Satrio J a., Brown RC. Techno-economic analysis of biomass-to-liquids production based on gasification. Fuel. 2010;89:S11–9. doi:10.1016/j.fuel.2010.07.027.

[17] Gebreslassie BH, Slivinsky M, Wang B, You F. Life cycle optimization for sustainable design and operations of hydrocarbon biorefinery via fast pyrolysis, hydrotreating and hydrocracking. Comput Chem Eng. 2013;50:71–91. doi:10.1016/j.compchemeng.2012.10.013.

[18] Wang B, Gebreslassie BH, You F. Sustainable design and synthesis of hydrocarbon biorefinery via gasification pathway: Integrated life cycle assessment and technoeconomic analysis with multiobjective superstructure optimization. Comput Chem Eng. 2013;52:55–76. doi:10.1016/j.compchemeng.2012.12.008.

[19] Pham V, El-Halwagi M. Process synthesis and optimization of biorefinery configurations. AIChE J. 2012;58:1212–21. doi:10.1002/aic.12640.

[20] Kelloway A, Daoutidis P. Process synthesis of biorefineries: Optimization of biomass conversion to fuels and chemicals. Ind Eng Chem Res. 2014;53:5261–73. doi:10.1021/ie4018572.

[21] Rooijers F, Wielders L, Schepers B, Croezen H, de Bruyn S. Natural gas as a transitional fuel for a sustainable energy future. Groningen, Netherlands: GasTerra/Castel International Publishers; 2009. Available from: http://www.gasterra.nl/uploads/fckconnector/ad10e972-6213-42e7-8063-52b1ffa39f71.

[22] Mozaffarian M, Zwart RW., Boerrigter H, Deurwaarder EP. Biomass and waste-related SNG production technologies: Technical, economic and

ecological feasibility. 2nd World Conf. Technol. Exhib. Biomass Energy, Ind. Clim. Prot., Rome, Italy: 2004.

[23] Heyne S, Thunman H, Harvey S. Extending existing combined heat and power plants for synthetic natural gas production. Int J Energy Res. 2012;36:670–81. doi:10.1002/er.1828.

[24] Tremel A, Gaderer M, Spliethoff H. Small-scale production of synthetic natural gas by allothermal biomass gasification. Int J Energy Res. 2013;37:1318–30. doi:10.1002/er.2933.

[25] van der Meijden CM, Veringa HJ, Rabou LPLM. The production of synthetic natural gas (SNG): A comparison of three wood gasification systems for energy balance and overall efficiency. Biomass and Bioenergy. 2010;34:302–11. doi:10.1016/j.biombioe.2009.11.001.

[26] Gassner M, Vogel F, Heyen G, Maréchal F. Optimal process design for the polygeneration of SNG, power and heat by hydrothermal gasification of waste biomass: Thermo-economic process modelling and integration. Energy Environ Sci. 2011;4:1726–41. doi:10.1039/c0ee00629g.

[27] Gassner M, Vogel F, Heyen G, Maréchal F. Optimal process design for the polygeneration of SNG, power and heat by hydrothermal gasification of waste biomass: Process optimisation for selected substrates. Energy Environ Sci. 2011;4:1742–58. doi:10.1039/c0ee00634c.

[28] Gassner M, Maréchal F. Thermo-economic optimisation of the polygeneration of synthetic natural gas (SNG), power and heat from lignocellulosic biomass by gasification and methanation. Energy Environ Sci. 2012;5:5768–89. doi:10.1039/c1ee02867g.

[29] Progressive Energy & CNG Services. Bio-SNG feasibility study. Establishment of a regional project. 2010. Available from: http://www.cngservices.co.uk/assets/Bio-SNG-Feasibility-Study.pdf.

[30] Akgul O, Zamboni A, Bezzo F, Shah N, Papageorgiou LG. Optimization-based approaches for bioethanol supply chains. Ind Eng Chem Res. 2011;50:4927–38. doi:10.1021/ie101392y.

[31] Elia JA, Baliban RC, Floudas CA. Nationwide, regional, and statewide energy supply chain optimization for natural gas to liquid transportation fuel (GTL) systems. Ind Eng Chem Res. 2013:130923121032000. doi:10.1021/ie401378r.

[32] You F, Wang B. Life cycle optimization of biomass-to-liquid supply chains with distributed - centralized processing networks. Ind Eng Chem Res. 2011;50:10102–27.

[33] Dal-Mas M, Giarola S, Zamboni A, Bezzo F. Strategic design and investment capacity planning of the ethanol supply chain under price uncertainty. Biomass and Bioenergy. 2011;35:2059–71. doi:10.1016/j.biombioe.2011.01.060.

[34] Almansoori A, Shah N. Design and operation of a future hydrogen supply chain: Multi-period model. Int J Hydrogen Energy. 2009;34:7883–97. doi:10.1016/j.ijhydene.2009.07.109.

[35] Cafaro D, Grossmann I. Strategic Planning, Design and Development of the Shale Gas Supply Chain Network. AIChE J. 2014;60:2122–42. doi:10.1002/aic.

[36] Zhang D, Yang T. Environmental impacts of hydraulic fracturing in shale gas development in the United States. Pet Explor Dev. 2015;42:876–83. doi:10.1016/S1876-3804(15)30085-9.

[37] Jarvie DM, Hill RJ, Ruble TE, Pollastro RM. Unconventional shale-gas systems: The Mississippian Barnett Shale of north-central Texas as one model for thermogenic shale-gas assessment. AAPG Bull. 2007;91:475–99. doi:10.1306/12190606068.

[38] Curtis JB. Fractured shale-gas systems. AAPG Bull. 2002;86:1921–38. doi:10.1306/61EEDDBE-173E-11D7-8645000102C1865D.

[39] Gale JFW, Laubach SE, Olson JE, Eichhuble P, Fall A. Natural Fractures in shale: A review and new observations. AAPG Bull. 2014;98:2165–216. doi:10.1306/08121413151.

[40] Cipolla C, Lolon E, Erdle J, Rubin B. Reservoir Modeling in Shale-Gas Reservoirs. SPE Reservoir Eval Eng. 2010;13:638–653. doi:10.2118/125530-PA.

[41] Mayerhofer MJ, Lolon E, Warpinski NR, Cipolla CL, Walser DW, Rightmire CM. What Is Stimulated Reservoir Volume?. SPE Prod Oper. 2013;25:89–98. doi:10.2118/119890-PA.

[42] Weijermars R. Economic appraisal of shale gas plays in Continental Europe. Appl Energy. 2013;106:100–15. doi:10.1016/j.apenergy.2013.01.025.

[43] Calderón AJ, Guerra OJ, Papageorgiou LG, Siirola JJ, Reklaitis G V. Preliminary Evaluation of Shale Gas Reservoirs: Appraisal of Different Well-Pad Designs via Performance Metrics. Ind Eng Chem Res. 2015;54:10334–49. doi:10.1021/acs.iecr.5b01590.

[44] Wilson KC, Durlofsky LJ. Optimization of shale gas field development using direct search techniques and reduced-physics models. J Pet Sci Eng. 2013;108:304–15. doi:10.1016/j.petrol.2013.04.019.

[45] Guerra OJ, Calderón AJ, Papageorgiou LG, Siirola JJ, Reklaitis G V. An optimization framework for the integration of water management and shale gas supply chain design. Comput Chem Eng. 2016;92:230–55. doi:10.1016/j.compchemeng.2016.03.025.

[46] Burnham A, Han J, Clark CE, Wang M, Dunn JB, Palou-Rivera I. Life-cycle greenhouse gas emissions of shale gas, natural gas, coal, and petroleum. Environ Sci Technol. 2012;46:619–27. doi:10.1021/es201942m.

[47] Howarth RW, Santoro R, Ingraffea A. Methane and the greenhouse-gas footprint of natural gas from shale formations. Clim Change. 2011;106:679–90. doi:10.1007/s10584-011-0061-5.

[48] Weber CL, Clavin C. Life cycle carbon footprint of shale gas: review of evidence and implications. Environ Sci Technol. 2012;46:5688–95. doi:10.1021/es300375n.

[49] International Energy Agency (IEA). World Energy Outlook 2015. Paris: 2015. Available from: http://www.worldenergyoutlook.org/weo2015/.

[50] Kavalov B, Petric H, Georgakaki A. Liquefied natural gas for Europe: some important issues for consideration. Brussels: 2009. Available from: http://orca.cf.ac.uk/27617/. doi:10.2790/1045.

[51] International Energy Agency (IEA). Natural Gas Information 2015. Paris: IEA; 2015. Available from: http://www.oecd-ilibrary.org/energy/natural-gas-information-2015_nat_gas-2015-en.

[52] West Virginia GIS Technical Center. Global Atlas of Unconventional Hydrocarbon Resources. 2014. Available online at: http://www.unconventionalenergyresources.com/ (accessed March 1, 2016).

[53] Reig P, Luo T, Proctor JN. Global shale gas development: Water availability and busines risks. Washington, D.C.: 2014. Available from: http://www.wri.org/publication/global-shale-gas-development-water-availability-business-risks.

[54] Gassert F, Landis M, Luck M, Reig P, Shiao T. Aqueduct Global Maps 2.1. Washington, DC: 2013. Available from: http://www.wri.org/our-work/project/aqueduct.

[55] Scanlon BR, Reedy RC, Philippe Nicot J. Will water scarcity in semiarid regions limit hydraulic fracturing of shale plays? Environ Res Lett. 2014;9:124011–25. doi:10.1088/1748-9326/9/12/124011.

[56] Breyer JA. Shale Reservoirs—Giant Resources for the 21st Century. American Association of Petroleum Geologists (AAPG); 2012.

[57] Lozano Maya JR. The united states experience as a reference of success for shale gas development: The case of mexico. Energy Policy. 2013;62:70–8. doi:10.1016/j.enpol.2013.07.088.

[58] Bilgili F, Koçak E, Bulut Ü, Sualp MN. How did the US economy react to shale gas production revolution? An advanced time series approach. Energy. 2016;116:963–77. doi:10.1016/j.energy.2016.10.056.

[59] Energy Information Administration (EIA). Natural Gas - U.S. Natural gas imports. 2016. Available online at: https://www.eia.gov/dnav/ng/hist/n9100us2a.htm (accessed June 5, 2016).

[60] Energy Information Administration (EIA). Total Energy - Electricity net generation: Electric power sector. n.d. Available online at:

http://www.eia.gov/beta/MER/?tbl=T07.02B#/?f=A (accessed June 5, 2016).

[61] American Chemistry Council (ACC). Shale Gas, Competitiveness, and New US Chemical Industry Investment: An analysis based on announced Projects. 2013. Available from: https://chemistrytoenergy.com/sites/chemistrytoenergy.com/files/shale-gas-full-study.pdf.

[62] American Chemistry Council (ACC). Shale gas and new u.s. chemical industry investment: $138 billion and counting. 2015. Available from: https://www.americanchemistry.com/Policy/Energy/Shale-Gas/Slides-Shale-Gas-and-New-US-Chemical-Industry-Investment138-Billion-and-Counting.pdf.

[63] Energy Information Administration (EIA). Shale in the United States. 2016. Available online at: http://www.eia.gov/energy_in_brief/article/shale_in_the_united_states.cfm (accessed July 1, 2016).

[64] Energy Information Administration (EIA). Short-Term Energy Outlook. 2016. Available online at: http://www.eia.gov/forecasts/steo/query/ (accessed March 1, 2016).

[65] Energy Information Administration (EIA). Spot Prices for Crude Oil and Petroleum Products. 2016. Available online at: http://www.eia.gov/dnav/pet/pet_pri_spt_s1_m.htm (accessed June 1, 2016).

[66] Energy Information Administration (EIA). Henry Hub Natural Gas Spot Price. 2016. Available online at: http://tonto.eia.gov/dnav/ng/hist/rngwhhdm.htm (accessed June 20, 2016).

[67] The World Bank. World Bank Commodity Price Data (The Pink Sheet). 2016. Available online at: http://www.worldbank.org/en/research/commodity-markets#1 (accessed May 1, 2016).

[68] Energy Information Administration (EIA). Annual Energy Outlook 2017. 2017. Available from: http://www.eia.gov/outlooks/aeo/pdf/0383(2017).pdf.

[69] Jiang M, Michael Griffin W, Hendrickson C, Jaramillo P, VanBriesen J, Venkatesh A. Life cycle greenhouse gas emissions of Marcellus shale gas. Environ Res Lett. 2011;6:034014–23. doi:10.1088/1748-9326/6/3/034014.

[70] Caulton DR, Shepson PB, Santoro RL, Sparks JP, Howarth RW, Ingraffea AR, et al. Toward a better understanding and quantification of methane emissions from shale gas development. Proc Natl Acad Sci. 2014;111:6237–42. doi:10.1073/pnas.1316546111.

[71] Heath GA, O'Donoughue P, Arent DJ, Bazilian M. Harmonization of initial estimates of shale gas life cycle greenhouse gas emissions for electric power generation. Proc Natl Acad Sci. 2014;111:E3167–76. doi:10.1073/pnas.1309334111.

[72] Tollefson J. Air sampling reveals high emissions from gas field. Nature. 2012;482:139–40. doi:10.1038/482139a.

[73] Karion A, Sweeney C, Pétron G, Frost G, Michael Hardesty R, Kofler J, et al. Methane emissions estimate from airborne measurements over a western United States natural gas field. Geophys Res Lett. 2013;40:4393–7. doi:10.1002/grl.50811.

[74] Pétron G, Frost G, Miller BR, Hirsch AI, Montzka SA, Karion A, et al. Hydrocarbon emissions characterization in the Colorado Front Range: A pilot study. J Geophys Res Atmos. 2012;117:1–19. doi:10.1029/2011JD016360.

[75] Newell RG, Raimi D. Implications of Shale Gas Development for Climate Change. Environ Sci Technol. 2014;48:8360–8. doi:10.1021/es4046154.

[76] Shearer C, Bistline J, Inman M, Davis SJ. The effect of natural gas supply on US renewable energy and CO2 emissions. Environ Res Lett. 2014;9:094008–16. doi:10.1088/1748-9326/9/9/094008.

[77] Jenner S, Lamadrid AJ. Shale gas vs. coal: Policy implications from environmental impact comparisons of shale gas, conventional gas, and coal on air, water, and land in the United States. Energy Policy. 2013;53:442–53. doi:10.1016/j.enpol.2012.11.010.

[78] McJeon H, Edmonds J, Bauer N, Clarke L, Fisher B, Flannery BP, et al. Limited impact on decadal-scale climate change from increased use of natural gas. Nature. 2014;514:482–5. doi:10.1038/nature13837.

[79] Zhang X, Myhrvold NP, Caldeira K. Key factors for assessing climate benefits of natural gas versus coal electricity generation. Environ Res Lett. 2014;9:114022. doi:10.1088/1748-9326/9/11/114022.

[80] Sovacool BK. How long will it take? Conceptualizing the temporal dynamics of energy transitions. Energy Res Soc Sci. 2016;13:202–15. doi:10.1016/j.erss.2015.12.020.

[81] Smil V. Examining energy transitions: A dozen insights based on performance. Energy Res Soc Sci. 2016;22:194–7. doi:10.1016/j.erss.2016.08.017.

[82] Nicot J-P, Scanlon BR. Water use for Shale-gas production in Texas, U.S. Environ Sci Technol. 2012;46:3580–6. doi:10.1021/es204602t.

[83] Jackson RB, Vengosh A, Carey JW, Davies RJ, Darrah TH, O'Sullivan F, et al. The Environmental Costs and Benefits of Fracking. Annu Rev Environ Resour. 2014;39:327–62. doi:10.1146/annurev-environ-031113-144051.

[84] Olmstead SM, Muehlenbachs LA, Shih J, Chu Z, Krupnick AJ. Shale gas development impacts on surface water quality in Pennsylvania. Proc Natl Acad Sci U S A. 2013;110:4962–7. doi:10.1073/pnas.1213871110.

[85] Vengosh A, Jackson RB, Warner N, Darrah TH, Kondash A. A Critical Review of the Risks to Water Resources from Unconventional Shale Gas

Development and Hydraulic Fracturing in the United States. Environ Sci Technol. 2014;48:8334–48. doi:10.1021/es405118y.

[86] Osborn SG, Vengosh A, Warner NR, Jackson RB. Methane contamination of drinking water accompanying gas-well drilling and hydraulic fracturing. Proc Natl Acad Sci U S A. 2011;108:8172–6. doi:10.1073/pnas.1100682108.

[87] Jackson RB, Vengosh A, Darrah TH, Warner NR, Down A, Poreda RJ, et al. Increased stray gas abundance in a subset of drinking water wells near Marcellus shale gas extraction. Proc Natl Acad Sci U S A. 2013;110:11250–5. doi:10.1073/pnas.1221635110.

[88] Ellsworth W. Injection-Induced Earthquakes. Science. 2013;341:142–9. doi:10.1126/science.1225942.

[89] Keranen K., Weingarten M, Abers G., Bekins B., Ge S. Sharp increase in central Oklahoma seismicity since 2008 induced by massive wastewater injection. Science. 2014;345:448–51. doi:10.1038/45144.

[90] Gregory KB, Vidic RD, Dzombak DA. Water management challenges associated with the production of shale gas by hydraulic fracturing. Elements. 2011;7:181–6. doi:10.2113/gselements.7.3.181.

[91] Lutz BD, Lewis AN, Doyle MW. Generation, transport, and disposal of wastewater associated with Marcellus Shale gas development. Water Resour Res. 2013;49:647–56. doi:10.1002/wrcr.20096.

[92] Rahm BG, Bates JT, Bertoia LR, Galford AE, Yoxtheimer DA, Riha SJ. Wastewater management and Marcellus Shale gas development: Trends, drivers, and planning implications. J Environ Manage. 2013;120:105–13. doi:10.1016/j.jenvman.2013.02.029.

[93] Horner P, Halldorson B, Slutz JA. Shale Gas Water Treatment Value Chain - A Review of Technologies, including Case Studies. SPE Annu. Tech. Conf. Exhib., Society of Petroleum Engineers; 2013. doi:10.2118/147264-MS.

[94] Boudet H, Clarke C, Bugden D, Maibach E, Roser-Renouf C, Leiserowitz A. “Fracking” controversy and communication: Using national survey data to understand public perceptions of hydraulic fracturing. Energy Policy. 2014;65:57–67. doi:10.1016/j.enpol.2013.10.017.

[95] Whitmarsh L, Nash N, Upham P, Lloyd A, Verdon JP, Kendall JM. UK public perceptions of shale gas hydraulic fracturing: The role of audience, message and contextual factors on risk perceptions and policy support. Appl Energy. 2015;160:419–30. doi:10.1016/j.apenergy.2015.09.004.

[96] Evensen D, Stedman R. Scale matters: Variation in perceptions of shale gas development across national, state, and local levels. Energy Res Soc Sci. 2016;20:14–21. doi:10.1016/j.erss.2016.06.010.

[97] Thomas M, Pidgeon N, Evensen D, Partridge T, Hasell A, Enders C, et al. Public perceptions of hydraulic fracturing for shale gas and oil in the United

States and Canada. Wiley Interdiscip Rev Clim Chang. 2017:1–19. doi:10.1002/wcc.450.

[98] Whitton J, Brasier K, Charnley-Parry I, Cotton M. Shale gas governance in the United Kingdom and the United States: Opportunities for public participation and the implications for social justice. Energy Res Soc Sci. 2017;26:11–22. doi:10.1016/j.erss.2017.01.015.

[99] Computer Modeling Group. GEM User's Guide: Advance Compositional Reservoir Simulatior, Version 2014. Houston: 2014. Available from: http://www.cmgl.ca/software/gem2015.

[100] Guarnone M, Rossi F, Negri E, Grassi C, Genazzi D, Zennaro R. An unconventional mindset for shale gas surface facilities. J Nat Gas Sci Eng. 2012;6:14–23. doi:10.1016/j.jngse.2012.01.002.

[101] Yuan J, Luo D, Xia L, Feng L. Policy recommendations to promote shale gas development in China based on a technical and economic evaluation. Energy Policy. 2015;85:194–206. doi:10.1016/j.enpol.2015.06.006.

[102] Lozano-Maya JR. Looking through the prism of shale gas development: Towards a holistic framework for analysis. Energy Res Soc Sci. 2016;20:63–72. doi:10.1016/j.erss.2016.05.014.

[103] Great Britain. Climate Change Act 2008: Elizabeth II. Chapter 27. London: 2008. Available from: http://www.legislation.gov.uk/ukpga/2008/27/pdfs/ukpga_20080027_en.pdf.

[104] Department of Energy & Climate Change (DECC). UK Renewable Energy Roadmap Update 2013. London: 2013. Available from: https://www.gov.uk/government/uploads/system/uploads/attachment_data/file/255182/UK_Renewable_Energy_Roadmap_-_5_November_-_FINAL_DOCUMENT_FOR_PUBLICATIO___.pdf.

[105] European Climate Foundation (ECF). Energy savings 2020: How to triple the impact of energy savings policies in Europe. 2010. Available from: http://www.roadmap2050.eu/attachments/files/EnergySavings2020-FullReport.pdf.

[106] Office of Gas and Electricity Markets (Ofgem). Feed-in tariff annual report. London: 2014. Available from: https://www.ofgem.gov.uk/publications-and-updates/feed-tariff-fit-annual-report-2013-14.

[107] Office of Gas and Electricity Markets (Ofgem). Renewables obligation annual report. London: 2014. Available from: https://www.ofgem.gov.uk/publications-and-updates/renewables-obligation-ro-annual-report-2012-2013.

[108] Office of Gas and Electricity Markets (Ofgem). Non-domestic renewable heat incentive (RHI) guidance volume one: Eligibility and how to apply. vol. 1. London: 2014. Available from: https://www.ofgem.gov.uk/ofgem-publications/89305/final3guidancevolumeone-august2014publication.pdf.

[109] VGB PowerTech. Investment and operation cost figures – Generation portfolio. Essen: 2011. Available from: http://www.eurelectric.org/Download/Download.aspx?DocumentFileID=72142.

[110] Sagar AD, Kartha S. Bioenergy and sustainable development? Annu Rev Environ Resour. 2007;32:131–67. doi:10.1146/annurev.energy.32.062706.132042.

[111] Committe on World Food Secutrity (CFS). Biofuels and food security: A report by the high level panel of experts of food security and nutrition. 2013. Available from: http://www.fao.org/fileadmin/user_upload/hlpe/hlpe_documents/HLPE_Reports/HLPE-Report-5_Biofuels_and_food_security.pdf.

[112] Eurolectric. Biomass 2020 : Opportunities , challenges and solutions. 2011. Available from: http://www.eurelectric.org/media/26720/resap_biomass_2020_8-11-11_prefinal-2011-113-0004-01-e.pdf.

[113] Magalhães AIP, Petrovic D, Rodriguez AL, Putra ZA, Thielemans G. Techno-economic assessment of biomass pre-conversion of biomass-to-liquids line-up. Biofuels, Bioprod Biorefining. 2009;3:584–600. doi:10.1002/bbb.

[114] Hamelinck CN, Suurs RAA, Faaij APC. International bioenergy transport costs and energy balance. Biomass and Bioenergy. 2005;29:114–34. doi:10.1016/j.biombioe.2005.04.002.

[115] Uslu A, Faaij APC, Bergman PCA. Pre-treatment technologies, and their effect on international bioenergy supply chain logistics. Techno-economic evaluation of torrefaction, fast pyrolysis and pelletisation. Energy. 2008;33:1206–23. doi:10.1016/j.energy.2008.03.007.

[116] Energy Information Administration (EIA). International Energy Statistics. 2012. Available online at: http://www.eia.gov/cfapps/ipdbproject/IEDIndex3.cfm (accessed June 1, 2014).

[117] Skea J, Chaudry M, Wang X. The role of gas infrastructure in promoting UK energy security. Energy Policy. 2012;43:202–13. doi:10.1016/j.enpol.2011.12.057.

[118] Department of Energy & Climate Change (DECC). Digest of United Kingdom Energy Statistics 2015 (DUKES). London: 2015. Available from: https://www.gov.uk/government/publications/digest-of-united-kingdom-energy-statistics-dukes-2013-printed-version-excluding-cover-pages.

[119] National Grid. The potential for Renewable Gas in the UK. London: 2009. Available from: http://www.nationalgrid.com/NR/rdonlyres/9122AEBA-5E50-43CA-81E5-8FD98C2CA4EC/32182/renewablegasWPfinal1.pdf.

[120] Kopyscinski J, Schildhauer TJ, Biollaz SMA. Production of synthetic natural

gas (SNG) from coal and dry biomass – A technology review from 1950 to 2009. Fuel. 2010;89:1763–83. doi:10.1016/j.fuel.2010.01.027.

[121] Li S, Ji X, Zhang X, Gao L, Jin H. Coal to SNG: Technical progress, modeling and system optimization through exergy analysis. Appl Energy. 2014;136:98–109. doi:10.1016/j.apenergy.2014.09.006.

[122] Zhou H, Yang S, Xiao H, Yang Q, Qian Y, Gao L. Modeling and techno-economic analysis of shale-to-liquid and coal-to-liquid fuels processes. Energy. 2016;109:201–10. doi:10.1016/j.energy.2016.04.108.

[123] National Energy Technology Laboratory (NETL). Coal Gasification Systems. 2015. Available online at: http://www.netl.doe.gov/research/coal/energy-systems/gasification (accessed March 1, 2016).

[124] van der Drift A, Zwart RW., Vreugdenhil B., Bleijendaal LP. Comparing the options to produce SNG from biomass. 18th Eur. Biomass Conf. Exhib., Lyon, France: 2010, p. 3–7.

[125] Juraščík M, Sues A, Ptasinski KJ. Exergy analysis of synthetic natural gas production method from biomass. Energy. 2010;35:880–8. doi:10.1016/j.energy.2009.07.031.

[126] Heyne S, Harvey S. Methane from biomass: process-integration aspects. Proc ICE - Energy. 2009;162:13–22. doi:10.1680/ener.2009.162.1.13.

[127] Zwart RW., Boerrigter H, Deurwaarder E., van der Meijden CM, van Paasen SV. Production of Synthetic Natural Gas (SNG) from Biomass: Development and operation of an integrated bio-SNG system. 2005. Available from: https://www.ecn.nl/docs/library/report/2006/e06018.pdf.

[128] Rehling B, Hofbauer H, Rauch R, Aichernig C. BioSNG—process simulation and comparison with first results from a 1-MW demonstration plant. Biomass Convers Biorefinery. 2011;1:111–9. doi:10.1007/s13399-011-0013-3.

[129] Zwart R. Synthetic Natural Gas (SNG) Large-scale introduction of green natural gas in existing gas grids. 2007. Available from: ftp://ftp.ecn.nl/pub/www/library/report/2007/l07069.pdf.

[130] E4tech. The potential for bioSNG production in the UK. London: 2010. Available from: http://www.nnfcc.co.uk/tools/potential-for-biosng-production-in-the-uk-nnfcc-10-008.

[131] Kinnaman TC. The economic impact of shale gas extraction: A review of existing studies. Ecol Econ. 2011;70:1243–9. doi:10.1016/j.ecolecon.2011.02.005.

[132] Siirola JJ. The impact of shale gas in the chemical industry. AIChE J. 2014;60:810–9. doi:10.1002/aic.14368.

[133] Logan J, Heath G, Macknick J, Paranhos E, Boyd W, Carlson K. Natural Gas and the Transformation of the U.S. Energy Sector: Electricity. 2012.

[134] Agencia Nacional de Hidrocarburos (ANH). Geophysics and Geological Information. 2014. Available online at: http://www.anh.gov.co/en-us/Informacion-Geologica-y-Geofisica (accessed November 15, 2014).

[135] Aguilera R. Flow Units: From Conventional to Tight Gas to Shale Gas to Tight Oil to Shale Oil Reservoirs. SPE West. Reg. AAPG Pacific Sect. Meet. 2013 Jt. Tech. Conf., Society of Petroleum Engineers; 2013. doi:10.2118/165360-MS.

[136] Peng D-Y, Robinson DB. A New Two-Constant Equation of State. Ind Eng Chem Fundam. 1976;15:59–64. doi:10.1021/i160057a011.

[137] Leahy-Dios A, Das M, Agarwal A, Kaminsky RD. Modeling of Transport Phenomena and Multicomponent Sorption for Shale Gas and Coalbed Methane in an Unstructured Grid Simulator. SPE Annu. Tech. Conf. Exhib., Society of Petroleum Engineers; 2013, p. 1–9. doi:10.2118/147352-MS.

[138] Hu H. Methane adsorption comparison of different thermal maturity kerogens in shale gas system. Chin J Geochem. 2014;33:425–30. doi:10.1007/s11631-014-0708-9.

[139] Heller R, Zoback M. Adsorption of methane and carbon dioxide on gas shale and pure mineral samples. J Unconv Oil Gas Resour. 2014;8:14–24. doi:10.1016/j.juogr.2014.06.001.

[140] Sigal R, Akkutlu I. The Laboratory Measurement of the Gas-Storage Capacity of Organic Shales. vol. c. 2013. Available from: http://shale.ou.edu/Content/Member Area/Papers/GasStorage.pdf.

[141] Freeman CM. Study of Multi-scale Transport Phenomena in Tight Gas and Shale Gas Reservoir Systems. Ph.D Thesis. Texas A&M University, 2013.

[142] Passey QR, Bohacs K, Esch WL, Klimentidis R, Sinha S. From Oil-Prone Source Rock to Gas-Producing Shale Reservoir - Geologic and Petrophysical Characterization of Unconventional Shale Gas Reservoirs. Int. Oil Gas Conf. Exhib. China, Society of Petroleum Engineers; 2013. doi:10.2118/131350-MS.

[143] Laubach S. Practical approaches to identifying sealed and open fractures. AAPG Bull. 2003;4:561–79.

[144] NETL. Modern Shale Gas Development in the United States: An Update. 2013. Available from: https://www.netl.doe.gov/File Library/Research/Oil-Gas/shale-gas-primer-update-2013.pdf.

[145] Ozkan E. Releasing Shale-Gas Potential with Fractured Horizontal Wells. SPE Disting. Lect., 2012.

[146] Walls JD, Diaz E, Cavanaugh T. Shale Reservoir Properties from Digital Rock Physics. SPE/EAGE Eur Unconv Resour Conf Exhib. 2013:1–9. doi:10.2118/152752-MS.

[147] Tovar E, Marfisi N, Diaz E, Walls JD. Looking into La Luna. Oilf Technol.

2013.

[148] Idowu N, Nardi C, Long H, Øren P-E, Bondino I. Improving digital rock physics predictive potential for relative permeabilities from equivalent pore networks. Int. Symp. Soc. Core, Napa Valley, California: 2013, p. 1–12.

[149] Novlesky A, Kumar A, Merkle S. Shale Gas Modeling Workflow: From Microseismic to Simulation -- A Horn River Case Study. Can. Unconv. Resour. Conf., Society of Petroleum Engineers; 2013. doi:10.2118/148710-MS.

[150] Rogers S, Elmo D, Dunphy R, Bearinger D. Understanding Hydraulic Fracture Geometry and Interactions in the Horn River Basin Through DFN and Numerical Modeling. Can. Unconv. Resour. Int. Pet. Conf., Society of Petroleum Engineers; 2013, p. 1–12. doi:10.2118/137488-MS.

[151] Gale JFW, Reed RM, Holder J. Natural fractures in the Barnett Shale and their importance for hydraulic fracture treatments. AAPG Bull. 2007;91:603–22. doi:10.1306/11010606061.

[152] Narr W, Suppe J. Joint spacing in sedimentary rocks. J Struct Geol. 1991;13:1037–48. doi:10.1016/0191-8141(91)90055-N.

[153] Olson JE, Laubach SE, Lander RH. Natural fracture characterization in tight gas sandstones: Integrating mechanics and diagenesis. AAPG Bull. 2009;93:1535–49. doi:10.1306/08110909100.

[154] Gross MR. The origin and spacing of cross joints: examples from the Monterey Formation, Santa Barbara Coastline, California. J Struct Geol. 1993;15:737–51. doi:10.1016/0191-8141(93)90059-J.

[155] Engelder T, Lash GG, Uzcátegui RS. Joint sets that enhance production from Middle and Upper Devonian gas shales of the Appalachian Basin. AAPG Bull. 2009;93:857–89. doi:10.1306/03230908032.

[156] Bonnet E, Bour O, Odling N. Scaling of fracture systems in geological media. Rev Geophys. 2001;39:347–83. doi:8755-1209.

[157] Odling NE. Natural fracture profiles, fractal dimension and joint roughness coefficients. Rock Mech Rock Eng. 1994;27:135–53. doi:10.1007/BF01020307.

[158] Syihab Z. Simulation of discrete fracture network using flexible voronoi gridding. PhD Thesis. Texas A&M University, 2009.

[159] Patwardhan SD, Famoori F, Gunaji RG, Govindarajan SK. Simulation and Mathematical Modeling of Stimulated Shale Gas Reservoirs. Ind Eng Chem Res. 2014;53:19788–805. doi:10.1021/ie501116j.

[160] Dake L. Fundamentals of reservoir engineering. Elsevier Science; 1983. Available from: http://www.ing.unp.edu.ar/asignaturas/reservorios/Fundamentals of Reservoir Engineering (L.P. Dake).pdf.

[161] Patzek TW, Male F, Marder M. Gas production in the Barnett Shale obeys a simple scaling theory. Proc Natl Acad Sci U S A. 2013;110:19731–6. doi:10.1073/pnas.1313380110.

[162] Lee DS, Herman JD, Elsworth D, Kim HT, Lee HS. A critical evaluation of unconventional gas recovery from the marcellus shale, northeastern United States. KSCE J Civ Eng. 2011;15:679–87. doi:10.1007/s12205-011-0008-4.

[163] Jiang M, Hendrickson CT, VanBriesen JM. Life Cycle Water Consumption and Wastewater Generation Impacts of a Marcellus Shale Gas Well. Environ Sci Technol. 2014;48:1911–20. doi:10.1021/es4047654.

[164] Goodwin S, Carlson K, Knox K, Douglas C, Rein L. Water intensity assessment of shale gas resources in the Wattenberg field in northeastern Colorado. Environ Sci Technol. 2014;48:5991–5. doi:10.1021/es404675h.

[165] Baca RG, Arnett RC, Langford DW. Modelling fluid flow in fractured-porous rock masses by finite-element techniques. Int J Numer Methods Fluids. 1984;4:337–48. doi:10.1002/fld.1650040404.

[166] Warren JE, Root PJ. The Behavior of Naturally Fractured Reservoirs. Soc Pet Eng J. 1963;3:245–55. doi:10.2118/426-PA.

[167] Moinfar A, Varavei A, Sepehrnoori K, Johns RT. Development of a Novel and Computationally-Efficient Discrete-Fracture Model to Study IOR Processes in Naturally Fractured Reservoirs. SPE Improv. Oil Recover. Symp., 2013, p. 1–17. doi:10.2118/154246-MS.

[168] Kazemi H. Pressure Transient Analysis of Naturally Fractured Reservoirs with Uniform Fracture Distribution. Soc Pet Eng J. 1969;9:451–62. doi:10.2118/2156-A.

[169] de Swaan O. A. Analytic Solutions for Determining Naturally Fractured Reservoir Properties by Well Testing. Soc Pet Eng J. 2013;16:117–22. doi:10.2118/5346-PA.

[170] Kazemi H, Merrill Jr. LS, Porterfield KL, Zeman PR. Numerical Simulation of Water-Oil Flow in Naturally Fractured Reservoirs. Soc Pet Eng J. 1976;16:317–26. doi:10.2118/5719-PA.

[171] Rossen RH. Simulation of Naturally Fractured Reservoirs With Semi-Implicit Source Terms. Soc Pet Eng J. 1977;17:201–10. doi:10.2118/5737-PA.

[172] Pruess K, Narasimhan TN. A practical method for modeling fluid and heat flow in fractured porous media. Sixth SPE Symp. Reserv. Simul., 1985, p. 41.

[173] Thomas LK, Dixon TN, Pierson RG. Fractured Reservoir Simulation. Soc Pet Eng J. 2013;23:42–54. doi:10.2118/9305-PA.

[174] Odling NE. Scaling and connectivity of joint systems in sandstones from western Norway. J Struct Geol. 1997;19:1257–71. doi:10.1016/S0191-8141(97)00041-2.

[175] Odling NE, Gillespie P, Bourgine B, Castaing C, Chiles JP, Christensen NP, et al. Variations in fracture system geometry and their implications for fluid flow in fractures hydrocarbon reservoirs. Pet Geosci. 1999;5:373–84. doi:10.1144/petgeo.5.4.373.

[176] Kim J-G, Deo MD. Finite element, discrete-fracture model for multiphase flow in porous media. AIChE J. 2000;46:1120–30. doi:10.1002/aic.690460604.

[177] Karimi-Fard M, Firoozabadi A. Numerical Simulation of Water Injection in Fractured Media Using the Discrete-Fracture Model and the Galerkin Method. SPE Reservoir Eval Eng. 2013;6:117–26. doi:10.2118/83633-PA.

[178] Karimi-Fard M, Durlofsky LJ, Aziz K. An Efficient Discrete-Fracture Model Applicable for General-Purpose Reservoir Simulators. Soc Pet Eng J. 2013;9:227–36. doi:10.2118/88812-PA.

[179] Huang T, Guo X, Chen F. Modeling transient flow behavior of a multiscale triple porosity model for shale gas reservoirs. J Nat Gas Sci Eng. 2015;23:33–46. doi:10.1016/j.jngse.2015.01.022.

[180] Ding YD, Wu Y, Farah N, Wang C, Bourbiaux B. Numerical Simulation of Low Permeability Unconventional Gas Reservoirs. SPE/EAGE Eur. Unconv. Resour. Conf. Exhib., Society of Petroleum Engineers; 2014, p. 1–30. doi:10.2118/167711-MS.

[181] Darishchev A, Rouvroy P, Lemouzy P. On Simulation of Flow in Tight and Shale Gas Reservoirs. SPE Unconv. Gas Conf. Exhib., Society of Petroleum Engineers; 2013. doi:10.2118/163990-MS.

[182] Wu Y, Li J, Ding D, Wang C, Di Y. A Generalized Framework Model for the Simulation of Gas Production in Unconventional Gas Reservoirs. Soc Pet Eng J. 2014;19:845–57. doi:10.2118/163609-PA.

[183] Blasingame TA. The Characteristic Flow Behavior of Low-Permeability Reservoir Systems. SPE Unconv. Reserv. Conf., Society of Petroleum Engineers; 2013, p. 10–2. doi:10.2118/114168-MS.

[184] Li J, Du C, Zhang X. Critical Evaluations of Shale Gas Reservoir Simulation Approaches: Single Porosity and Dual Porosity Modeling. SPE Middle East East Unconv. Gas Conf. Exhib. 31 January-2 February, Muscat, Oman, Society of Petroleum Engineers; 2011. doi:10.2118/141756-MS.

[185] Ding DY, Wu YS, Jeannin L. Efficient simulation of hydraulic fractured wells in unconventional reservoirs. J Pet Sci Eng. 2014;122:631–42. doi:10.1016/j.petrol.2014.09.005.

[186] Du CM, Zhang X, Zhan L, Gu H, Hay B, Tushingham K, et al. Modeling Hydraulic Fracturing Induced Fracture Networks in Shale Gas Reservoirs as a Dual Porosity System. Int. Oil Gas Conf. Exhib. China, Society of Petroleum Engineers; 2013. doi:10.2118/132180-MS.

[187] Rubin B. Accurate Simulation of Non Darcy Flow in Stimulated Fractured Shale Reservoirs. SPE West. Reg. Meet., Society of Petroleum Engineers; 2013. doi:10.2118/132093-MS.

[188] Sun H, Chawathe A, Hoteit H, Shi X, Li L. Understanding Shale Gas Flow Behavior Using Numerical Simulation. Soc Pet Eng J. 2015;20:142–54. doi:10.2118/167753-PA.

[189] Noorishad J, Mehran M. An upstream finite element method for solution of transient transport equation in fractured porous media. Water Resour Res. 1982;18:588–96. doi:10.1029/WR018i003p00588.

[190] Gong B, Qin G, Douglas C, Yuan S. Detailed Modeling of the Complex Fracture Network and Near-well Effects of Shale Gas Reservoirs. 2011. doi:10.2118/142705-MS.

[191] Moridis GJ, Freeman CM. The RealGas and RealGasH2O options of the TOUGH+ code for the simulation of coupled fluid and heat flow in tight/shale gas systems. Comput Geosci. 2014;65:56–71. doi:10.1016/j.cageo.2013.09.010.

[192] Bazan LW, Larkin SD, Lattibeaudiere MG, Palisch TT. Improving Production in the Eagle Ford Shale With Fracture Modeling, Increased Fracture Conductivity, and Optimized Stage and Cluster Spacing Along the Horizontal Wellbore. Tight Gas Complet. Conf., Society of Petroleum Engineers; 2013, p. 23. doi:10.2118/138425-MS.

[193] Chaudhri MM. Numerical Modeling of Multifracture Horizontal Well for Uncertainty Analysis and History Matching: Case Studies From Oklahoma and Texas Shale Gas Wells. SPE West. Reg. Meet. 21-23 March, Bak. California, USA, Society of Petroleum Engineers; 2012. doi:10.2118/153888-MS.

[194] Meyer BR, Bazan LW, Jacot RH, Lattibeaudiere MG. Optimization of Multiple Transverse Hydraulic Fractures in Horizontal Wellbores. Proc. SPE Unconv. Gas Conf., 2010, p. 1–37. doi:10.2118/131732-MS.

[195] Samandarli O. A new method for history matching and forecasting shale gas reservoir production performance with a dual porosity model. MSc Thesis. Texas A&M University, 2011.

[196] Diaz De Souza OC, Sharp A, Martinez RC, Foster RA, Piekenbrock E, Reeves Simpson M, et al. Integrated Unconventional Shale Gas Reservoir Modeling: A Worked Example From the Haynesville Shale, De Soto Parish, North Louisiana. SPE Am. Unconv. Resour. Conf. 5-7 June, Pittsburgh, Pennsylvania USA, Society of Petroleum Engineers; 2012. doi:10.2118/154692-MS.

[197] Altman RM, Viswanathan A, Xu J, Ussoltsev D, Indriati S, Grant D, et al. Understanding the Impact of Channel Fracturing in the Eagle Ford Shale Through Reservoir Simulation. SPE Lat. Am. Caribb. Pet. Eng. Conf. 16-18

April. Mex. City, Mex., Society of Petroleum Engineers; 2012. doi:10.2118/153728-MS.

[198] Kam P, Nadeem M, Omatsone EN, Novlesky A, Kumar A. Integrated Geoscience and Reservoir Simulation Approach to Understanding Fluid Flow in Multi-Well Pad Shale Gas Reservoirs. SPE/CSUR Unconv. Resour. Conf. – Canada, vol. Paper SPE, Calgary, Alberta, Canada: Society of Petroleum Engineers; 2014. doi:10.2118/171611-MS.

[199] Esmaili S, Mohaghegh SD. Full field reservoir modeling of shale assets using advanced data-driven analytics. Geosci Front. 2015:1–11. doi:10.1016/j.gsf.2014.12.006.

[200] Sadrpanah H, Charles T, Fulton J. Explicit Simulation of Multiple Hydraulic Fractures in Horizontal Wells. SPE Eur Annu Conf Exhib. 2006:12–5. doi:10.2118/99575-MS.

[201] Zhang X, Du C, Deimbacher F, Crick M, Harikesavanallur A. Sensitivity Studies of Horizontal Wells with Hydraulic Fractures in Shale Gas Reservoirs. Int. Pet. Technol. Conf. 7-9 December, Doha, Qatar, International Petroleum Technology Conference; 2009. doi:10.2523/13338-MS.

[202] Olorode O. Numerical Modeling of Fractured Shale-Gas and Tight-Gas Reservoirs Using Unstructured Grids. MS Thesis. Texas A&M University, 2011.

[203] Guo T, Zhang S, Qu Z, Zhou T, Xiao Y, Gao J. Experimental study of hydraulic fracturing for shale by stimulated reservoir volume. Fuel. 2014;128:373–80. doi:10.1016/j.fuel.2014.03.029.

[204] Balogun AS, Kazemi H, Ozkan E, Al-kobaisi M, Ramirez B. Verification and Proper Use of Water-Oil Transfer Function for Dual-Porosity and Dual-Permeability Reservoirs. SPE Middle East Oil Gas Show Conf. 11-14 March, Manama, Bahrain, Society of Petroleum Engineers; 2007, p. 189–99. doi:10.2118/104580-PA.

[205] Ramirez B, Kazemi H, Al-kobaisi M, Ozkan E, Atan S. A Critical Review for Proper Use of Water/Oil/Gas Transfer Functions in Dual-Porosity Naturally Fractured Reservoirs: Part I. SPE Reservoir Eval Eng. 2013;12:200–10. doi:10.2118/109821-PA.

[206] Al-kobaisi M, Kazemi H, Ramirez B, Ozkan E, Atan S. A Critical Review for Proper Use of Water/Oil/Gas Transfer Functions in Dual-Porosity Naturally Fractured Reservoirs: Part II. SPE Reservoir Eval Eng. 2013;12:211–7. doi:10.2118/124213-PA.

[207] Freeman CM, Moridis GJ, Blasingame TA. A Numerical Study of Microscale Flow Behavior in Tight Gas and Shale Gas Reservoir Systems. Transp Porous Media. 2011;90:253–68. doi:10.1007/s11242-011-9761-6.

[208] Boulis AS. A new series of rate decline relations based on the diagnosis of rate-time data a new series of rate decline relations based on the diagnosis of

rate-time data. 2010.

[209] Cheng Y, Wang Y, McVay D, Lee WJ. Practical Application of a Probabilistic Approach to Estimate Reserves Using Production Decline Data. SPE Econ Manag. 2010;2:19–31. doi:10.2118/95974-PA.

[210] Mattar L. SPE 119897 Production Analysis and Forecasting of Shale Gas Reservoirs: Case History-Based Approach. SPE Shale Gas Prod Conf. 2008:1–39.

[211] Johnson NL, Currie SM, Ilk D, Blasingame TA. A Simple Methodology for Direct Estimation of Gas-in-place and Reserves Using Rate-Time Data. SPE Rocky Mt. Pet. Technol. Conf., Society of Petroleum Engineers; 2013. doi:10.2118/123298-MS.

[212] Bello R, Wattenbarger R. Multi-stage Hydraulically Fractured Horizontal Shale Gas Well Rate Transient Analysis. Proc. North Africa Tech. Conf. Exhib., Society of Petroleum Engineers; 2010, p. 14–7. doi:10.2118/126754-MS.

[213] Al Ahmadi H, Almarzooq A, Wattenbarger R. Application of Linear Flow Analysis to Shale Gas Wells - Field Cases. Proc. SPE Unconv. Gas Conf., 2010, p. 23–5. doi:10.2118/130370-MS.

[214] Anderson D, Nobakht M, Moghadam S, Mattar L. Analysis of Production Data From Fractured Shale Gas Wells. Proc. SPE Unconv. Gas Conf., 2010, p. 1–15. doi:10.2118/131787-MS.

[215] Nobakht M, Clarkson CR. Analysis of production data in shale gas reservoirs: Rigorous corrections for fluid and flow properties. J Nat Gas Sci Eng. 2012;8:85–98. doi:10.1016/j.jngse.2012.02.002.

[216] Ilk D, Rushing JA, Blasingame TA. Integration of Production Analysis and Rate-Time Analysis via Parametric Correlations -- Theoretical Considerations and Practical Applications. SPE Hydraul. Fract. Technol. Conf., Society of Petroleum Engineers; 2013. doi:10.2118/140556-MS.

[217] Anderson DM, Turco F, Virues CJJ, Chin A. Application of Rate Transient Analysis Workflow in Unconventional Reservoirs: Horn River Shale Gas Case Study. SPE Unconv. Resour. Conf. Exhib. Pacific, 11-13 November, Brisbane, Aust., Society of Petroleum Engineers; 2013. doi:10.2118/167042-MS.

[218] Yin J, Xie J, Datta-Gupta A, Hill AD. Improved characterization and performance prediction of shale gas wells by integrating stimulated reservoir volume and dynamic production data. J Pet Sci Eng. 2015;127:124–36. doi:10.1016/j.petrol.2015.01.030.

[219] Lian Z, Yu H, Lin T, Guo J. A study on casing deformation failure during multi-stage hydraulic fracturing for the stimulated reservoir volume of horizontal shale wells. J Nat Gas Sci Eng. 2015;23:538–46. doi:10.1016/j.jngse.2015.02.028.

[220] Ikewun PO, Ahmadi M. Production Optimization and Forecasting of Shale Gas Wells Using Simulation Models and Decline Curve Analysis. SPE West. Reg. Meet., Society of Petroleum Engineers; 2013, p. 1–27. doi:10.2118/153914-MS.

[221] Can B, Kabir S. Probabilistic Production Forecasting for Unconventional Reservoirs With Stretched Exponential Production Decline Model. SPE Reservoir Eval Eng. 2012;15:41–50. doi:10.2118/143666-PA.

[222] Can B, Kabir CS. Simple tools for forecasting waterflood performance. J Pet Sci Eng. 2014;120:111–8. doi:10.1016/j.petrol.2014.05.028.

[223] Ning Y, Jiang Y, Qin G. Numerical Simulation of Natural Gas Transport in Shale Formation Using Generalized Lattice Boltzmann Method. Int. Pet. Technol. Conf., International Petroleum Technology Conference; 2014. doi:10.2523/18117-MS.

[224] Mohaghegh SD. Reservoir simulation and modeling based on artificial intelligence and data mining (AI&DM). J Nat Gas Sci Eng. 2011;3:697–705. doi:10.1016/j.jngse.2011.08.003.

[225] Mohaghegh SD. Reservoir modeling of shale formations. J Nat Gas Sci Eng. 2013;12:22–33. doi:10.1016/j.jngse.2013.01.003.

[226] Lai B, Miskimins JL, Wu Y-S. Non-Darcy Porous-Media Flow According to the Barree and Conway Model: Laboratory and Numerical-Modeling Studies. Soc Pet Eng J. 2013;17:70–9. doi:10.2118/122611-PA.

[227] Wang FP, Reed RM. Pore Networks and Fluid Flow in Gas Shales. SPE Annu. Tech. Conf. Exhib., Society of Petroleum Engineers; 2013. doi:10.2118/124253-MS.

[228] Klinkenberg LJ. The permeability of porous media to liquids and gases. API Drill Prod Pract. 1941:200–13. doi:10.5510/OGP20120200114.

[229] Yu W, Sepehrnoori K. Simulation of gas desorption and geomechanics effects for unconventional gas reservoirs. Fuel. 2014;116:455–64. doi:10.1016/j.fuel.2013.08.032.

[230] Cipolla CL, Lolon EP, Erdle JC, Rubin B. Reservoir Modeling in Shale-Gas Reservoirs. SPE Reservoir Eval Eng. 2013;13:638–53. doi:10.2118/125530-PA.

[231] Wilson KC. Optimization of shale resource development using reduced-physics surrogate models. MS Thesis. Standford University, 2012.

[232] Gao J, You F. Shale Gas Supply Chain Design and Operations toward Better Economic and Life Cycle Environmental Performance: MINLP Model and Global Optimization Algorithm. ACS Sustain Chem Eng. 2015;3:1282–91. doi:10.1021/acssuschemeng.5b00122.

[233] Yang L, Grossmann IE, Manno J. Optimization models for shale gas water management. AIChE J. 2014;60:3490–501. doi:10.1002/aic.14526.

[234] Gao J, You F. Optimal design and operations of supply chain networks for water management in shale gas production: MILFP model and algorithms for the water-energy nexus. AIChE J. 2015;61:1184–208. doi:10.1002/aic.14705.

[235] Lira-Barragán LF, Ponce-Ortega JM, Serna-González M, El-Halwagi MM. Optimal reuse of flowback wastewater in hydraulic fracturing including seasonal and environmental constraints. AIChE J. 2016;7. doi:10.1002/aic.15167.

[236] Gao J, You F. Deciphering and handling uncertainty in shale gas supply chain design and optimization: Novel modeling framework and computationally efficient solution algorithm. AIChE J. 2015;61:3739–55. doi:10.1002/aic.15032.

[237] Lira-Barragán LF, Ponce-Ortega JM, Guillén-Gosálbez G, El-Halwagi MM. Optimal Water Management under Uncertainty for Shale Gas Production. Ind Eng Chem Res. 2016;55:1322–35. doi:10.1021/acs.iecr.5b02748.

[238] Fedotov V, Gallo D, Hagemeijer P, Kuijvenhoven C. Water Management Approach for Shale Operations in North America. SPE Unconv. Resour. Conf. Exhib. Pacific, Society of Petroleum Engineers; 2013. doi:10.2118/167057-MS.

[239] Slutz J, Anderson J, Broderick R, Horner P. Key Shale Gas Water Management Strategies: An Economic Assessment Tool. SPE Annu. Tech. Conf. Exhib., Society of Petroleum Engineers; 2012.

[240] ESRI. ArcGIS Desktop: Release 10.2.2. Redlands, CA: Environmental Systems Research Institute. 2014. Available from: http://www.esri.com/software/arcgis/arcgis-for-desktop.

[241] Wicaksono DS, Karimi I a. Piecewise MILP under- and overestimators for global optimization of bilinear programs. AIChE J. 2008;54:991–1008. doi:10.1002/aic.11425.

[242] Castro PM. Tightening piecewise McCormick relaxations for bilinear problems. Comput Chem Eng. 2015;72:300–11. doi:10.1016/j.compchemeng.2014.03.025.

[243] McCormick G. Computability of global solutions to factorable nonconvex programs: Part I—Convex underestimating problems. Math Program. 1976;10:147–75.

[244] Sherali HD, Adams WP. A hierarchy of relaxations and convex hull characterizations for mixed-integer zero—one programming problems. Discret Appl Math. 1994;52:83–106. doi:10.1016/0166-218X(92)00190-W.

[245] Duran MA, Grossmann IE. An outer-approximation algorithm for a class of mixed-integer nonlinear programs. Math Program. 1986;36:307–39. doi:10.1007/BF02592064.

[246] Bussieck MR, Drud AS. SBB: A new solver for mixed integer nonlinear

programming. Duisburg: GAMS; 2001. Available from: http://www.gams.com/presentations/or01/sbb.pdf.

[247] Misener R, Floudas CA. ANTIGONE: Algorithms for coNTinuous / Integer Global Optimization of Nonlinear Equations. J Glob Optim. 2014;59:503–26. doi:10.1007/s10898-014-0166-2.

[248] Misener R, Floudas CA. GloMIQO: Global mixed-integer quadratic optimizer. J Glob Optim. 2012;57:3–50. doi:10.1007/s10898-012-9874-7.

[249] Tawarmalani M, Sahinidis N V. A polyhedral branch-and-cut approach to global optimization. Math Program. 2005;103:225–49. doi:10.1007/s10107-005-0581-8.

[250] Sahinidis N V. BARON 14.3.1: Global Optimization of Mixed-Integer Nonlinear Programs, User's Manual 2014. 2014. Available from: http://www.minlp.com/downloads/docs/baron manual.pdf.

[251] Lin Y, Schrage L. The global solver in the LINDO API. Optim Methods Softw. 2009;24:657–68. doi:10.1080/10556780902753221.

[252] Martín M, Grossmann IE. On the systematic synthesis of sustainable biorefineries. Ind Eng Chem Res. 2013;52:3044–64. doi:10.1021/ie2030213.

[253] Floudas CA, Elia JA, Baliban RC. Hybrid and single feedstock energy processes for liquid transportation fuels: A critical review. Comput Chem Eng. 2012;41:24–51. doi:10.1016/j.compchemeng.2012.02.008.

[254] Bai Y, Hwang T, Kang S, Ouyang Y. Biofuel refinery location and supply chain planning under traffic congestion. Transp Res Part B Methodol. 2011;45:162–75. doi:10.1016/j.trb.2010.04.006.

[255] Zamboni A, Shah N, Bezzo F. Spatially explicit static model for the strategic design of future bioethanol production systems. 1. Cost minimization. Energy & Fuels. 2009;23:5121–33. doi:10.1021/ef900456w.

[256] Corsano G, Vecchietti AR, Montagna JM. Optimal design for sustainable bioethanol supply chain considering detailed plant performance model. Comput Chem Eng. 2011;35:1384–98. doi:10.1016/j.compchemeng.2011.01.008.

[257] Ekşioğlu SD, Acharya A, Leightley LE, Arora S. Analyzing the design and management of biomass-to-biorefinery supply chain. Comput Ind Eng. 2009;57:1342–52. doi:10.1016/j.cie.2009.07.003.

[258] Dunnett AJ, Adjiman CS, Shah N. A spatially explicit whole-system model of the lignocellulosic bioethanol supply chain: an assessment of decentralised processing potential. Biotechnol Biofuels. 2008;1:13. doi:10.1186/1754-6834-1-13.

[259] Samsatli S, Samsatli NJ, Shah N. BVCM: A comprehensive and flexible toolkit for whole system biomass value chain analysis and optimisation - Mathematical formulation. Appl Energy. 2015;147:131–60.

doi:10.1016/j.apenergy.2015.01.078.

[260] Samsatli S, Samsatli NJ. A general spatio-temporal model of energy systems with a detailed account of transport and storage. Comput Chem Eng. 2015;80:155–76. doi:10.1016/j.compchemeng.2015.05.019.

[261] Bowling IM, Ponce JM, El-Halwagi MM. Facility Location and Supply Chain Optimization for a Biorefinery. Ind Eng Chem Res. 2011;50:6276–86. doi:10.1021/ie101921y.

[262] Marvin WA, Schmidt LD, Daoutidis P. Biorefinery location and technology selection through supply chain optimization. Ind Eng Chem Res. 2013;52:3192–208. doi:10.1021/ie3010463.

[263] Leduc S, Starfelt F, Dotzauer E, Kindermann G, McCallum I, Obersteiner M, et al. Optimal location of lignocellulosic ethanol refineries with polygeneration in Sweden. Energy. 2010;35:2709–16. doi:10.1016/j.energy.2009.07.018.

[264] Leduc S, Schwab D, Dotzauer E, Schmid E, Obersteiner M. Optimal location of wood gasification plants for methanol production with heat recovery. Int J Energy Res. 2008;32:1080–91. doi:10.1002/er.1446.

[265] Wu J, Yan J, Jia H, Hatziargyriou N, Djilali N, Sun H. Integrated Energy Systems. Appl Energy. 2016;167:155–7. doi:10.1016/j.apenergy.2016.02.075.

[266] Tittmann PW, Parker NC, Hart QJ, Jenkins BM. A spatially explicit techno-economic model of bioenergy and biofuels production in California. J Transp Geogr. 2010;18:715–28. doi:10.1016/j.jtrangeo.2010.06.005.

[267] Chinese D, Patrizio P, Nardin G. Effects of changes in Italian bioenergy promotion schemes for agricultural biogas projects: Insights from a regional optimization model. Energy Policy. 2014;75:189–205. doi:10.1016/j.enpol.2014.09.014.

[268] Giarola S, Zamboni A, Bezzo F. Spatially explicit multi-objective optimisation for design and planning of hybrid first and second generation biorefineries. Comput Chem Eng. 2011;35:1782–97. doi:10.1016/j.compchemeng.2011.01.020.

[269] You F, Tao L, Graziano DJ, Snyder SW. Optimal design of sustainable cellulosic biofuel supply chains: Multiobjective optimization coupled with life cycle assessment and input – output analysis. AIChE J. 2012;58:1157–80. doi:10.1002/aic.

[270] Zamboni A, Bezzo F, Shah N. Spatially explicit static model for the strategic design of future bioethanol production systems. 2. Multi-objective environmental optimization. Energy & Fuels. 2009;23:5134–43. doi:10.1021/ef9004779.

[271] Akgul O, Shah N, Papageorgiou LG. An optimisation framework for a hybrid first/second generation bioethanol supply chain. Comput Chem Eng.

2012;42:101–14. doi:10.1016/j.compchemeng.2012.01.012.

[272] Mele FD, Kostin AM, Guillén-Gosálbez G, Jiménez L. Multiobjective model for more sustainable fuel supply chains. A case study of the sugar cane industry in argentina. Ind Eng Chem Res. 2011;50:4939–58. doi:10.1021/ie101400g.

[273] Kim J, Realff MJ, Lee JH. Optimal design and global sensitivity analysis of biomass supply chain networks for biofuels under uncertainty. Comput Chem Eng. 2011;35:1738–51. doi:10.1016/j.compchemeng.2011.02.008.

[274] Marvin WA, Schmidt LD, Benjaafar S, Tiffany DG, Daoutidis P. Economic optimization of a lignocellulosic biomass-to-ethanol supply chain. Chem Eng Sci. 2012;67:68–79. doi:10.1016/j.ces.2011.05.055.

[275] Steubing B, Ballmer I, Gassner M, Gerber L, Pampuri L, Bischof S, et al. Identifying environmentally and economically optimal bioenergy plant sizes and locations: A spatial model of wood-based SNG value chains. Renew Energy. 2014;61:57–68. doi:10.1016/j.renene.2012.08.018.

[276] Calderón AJ, Agnolucci P, Papageorgiou LG. An optimisation framework for the strategic design of synthetic natural gas (BioSNG) supply chains. Appl Energy. 2017;187:929–55. doi:10.1016/j.apenergy.2016.10.074.

[277] Koltsaklis NE, Dagoumas AS, Kopanos GM, Pistikopoulos EN, Georgiadis MC. A spatial multi-period long-term energy planning model: A case study of the Greek power system. Appl Energy. 2014;115:456–82. doi:10.1016/j.apenergy.2013.10.042.

[278] Guerra OJ, Tejada DA, Reklaitis G V. An optimization framework for the integrated planning of generation and transmission expansion in interconnected power systems. Appl Energy. 2016;170:1–21. doi:10.1016/j.apenergy.2016.02.014.

[279] Mazairac W, Salenbien R. Mixed-integer linear program for an optimal hybrid energy network topology. 4th Int. Conf. Renew. Res. Appl., vol. 5, Palermo: 2015, p. 861–6.

[280] Dorfner J, Hamacher T. Large-scale district heating network optimization. IEEE Trans Smart Grid. 2014;5:1884–91. doi:10.1109/TSG.2013.2295856.

[281] Bauen AW, Dunnett AJ, Richter GM, Dailey AG, Aylott M, Casella E, et al. Modelling supply and demand of bioenergy from short rotation coppice and Miscanthus in the UK. Bioresour Technol. 2010;101:8132–43. doi:10.1016/j.biortech.2010.05.002.

[282] European Environment Agency (EEA). Estimating the environmentally compatible bioenergy potential from agriculture. Copenhagen: 2007. Available from: http://www.eea.europa.eu/publications/technical_report_2007_12.

[283] Agnolucci P, Akgul O, McDowall W, Papageorgiou LG. The importance of

economies of scale, transport costs and demand patterns in optimising hydrogen fuelling infrastructure: An exploration with SHIPMod (Spatial hydrogen infrastructure planning model). Int J Hydrogen Energy. 2013;38:11189–201. doi:10.1016/j.ijhydene.2013.06.071.

[284] Eurostat. NUTS - Nomenclature of territorial units for statistics. 2013. Available online at: http://ec.europa.eu/eurostat/web/nuts/overview.

[285] Forestry Research. Woodfuel Resource: Study into the potentially available woodfuel resource of Great Britain. 2002. Available online at: https://www.eforestry.gov.uk/woodfuel/pages/home.jsp (accessed May 15, 2014).

[286] European Environmental Agency (EEA). How much bioenergy can Europe produce without harming the environment?. vol. No. 7. Copenhagen: 2006. Available from: http://www.eea.europa.eu/publications/eea_report_2006_7.

[287] Forestry Commission. National forest inventory Great Britain. 2013. Available online at: http://www.forestry.gov.uk/.

[288] McKay H, Hudson JB, Hudson RJ. Woodfuel resource in Britain: main report. 2003. Available from: http://www.biomassenergycentre.org.uk/pls/portal/docs/PAGE/RESOURCES/REF_LIB_RES/PUBLICATIONS/RESOURCE AVAILABILITY/WOODFUEL RESOURCE IN BRITAIN FILE15006.PDF.

[289] EDINA Environment Digimap Service. Great Britain 25m [TIFF geospatial data], Scale 1:250000, Tiles: GB. 2008. Available online at: http://digimap.edina.ac.uk.

[290] E4tech. Biomass prices in the heat and electricity sectors in the UK. 2010. Available from: http://www.rhincentive.co.uk/library/regulation/100201Biomass_prices.pdf.

[291] Department for Environment Food & Rural Affairs (DEFRA). Experimental Statistics: Area of crops grown for bioenergy in England and the UK: 2008 - 2012. 2014. Available from: https://www.gov.uk/government/uploads/system/uploads/attachment_data/file/289168/nonfood-statsnotice2012-12mar14.pdf.

[292] Department for Environment Food & Rural Affairs (DEFRA). UK Biomass Strategy. London: 2007. Available from: http://www.biomassenergycentre.org.uk/pls/portal/docs/PAGE/RESOURCES/REF_LIB_RES/PUBLICATIONS/UKBIOMASSSTRATEGY.PDF.

[293] Department for Environment Food & Rural Affairs (DEFRA). Hay & Straw, Eng & Wales average prices. London: 2014. Available from: https://www.gov.uk/government/statistical-data-sets/commodity-prices.

[294] NNFCC. Domestic energy crops; potential and constraints review. York: 2012. Available from: https://www.gov.uk/government/uploads/system/uploads/attachment_data/file

/48342/5138-domestic-energy-crops-potential-and-constraints-r.PDF.

[295] Hastings A, Tallis MJ, Casella E, Matthews RW, Henshall PA, Milner S, et al. The technical potential of Great Britain to produce ligno-cellulosic biomass for bioenergy in current and future climates. GCB Bioenergy. 2014;6:108–22. doi:10.1111/gcbb.12103.

[296] Lovett A, Sünnenberg G, Dockerty T. The availability of land for perennial energy crops in Great Britain. GCB Bioenergy. 2014;6:99–107. doi:10.1111/gcbb.12147.

[297] Department for Environment Food & Rural Affairs (DEFRA). Waste strategy for England 2007. London: 2007. Available from: https://www.gov.uk/government/publications/waste-strategy-for-england-2007.

[298] WRAP. The composition of municipal solid waste in Wales. 2010. Available from: http://www.wrapcymru.org.uk/sites/files/wrap/Wales_compositional_analysis_report__2_.9076.pdf.

[299] Welsh Assembly Government. The overarching waste strategy document for wales: Towards zero waste. Cardiff: 2010. Available from: http://wales.gov.uk/docs/desh/publications/100621wastetowardszeroen.pdf.

[300] Welsh Assembly Government. Survey of Industrial & Commercial waste generated in Wales 2012. Cardiff: 2012. Available from: https://www.naturalresources.wales/media/1995/survey-of-industrial-and-commercial-waste-generated-in-wales-2012pdf.pdf.

[301] Welsh Assembly Government. Consultation document towards zero waste one wales: One planet. Cardiff: 2013. Available from: www.cymru.gov.uk.

[302] The Scottish Government. Scotland's Zero Waste Plan. Edinburgh: 2010. Available from: http://www.gov.scot/Resource/0045/00458945.pdf.

[303] Department for Environment Food & Rural Affairs (DEFRA). Household waste forecasts for England. London: 2013. Available from: https://www.gov.uk/government/uploads/system/uploads/attachment_data/file/286332/Household_Waste_Forecasts_for_England_Feb13_and_Oct13.pdf.

[304] Department for Environment Food & Rural Affairs (DEFRA). Survey of commercial and industrial waste arisings. London: 2011. Available from: https://www.gov.uk/government/uploads/system/uploads/attachment_data/file/400595/ci-statistics-release.pdf.

[305] Department for Environment Food & Rural Affairs (DEFRA). Forecasting 2020 waste arisings and treatment capacity. London: 2013. Available from: https://www.gov.uk/government/uploads/system/uploads/attachment_data/file/364243/forecasting-2020-hertfordshire-analysis-20141016.pdf.

[306] Department for Environment Food & Rural Affairs (DEFRA). Government

review of waste policy in England 2011. London: 2011. Available from: https://www.gov.uk/government/uploads/system/uploads/attachment_data/file/69401/pb13540-waste-policy-review110614.pdf. doi:10.1016/j.jclepro.2012.11.037.

[307] EDENext. Eurostat: Population projections by NUTS2 admin areas for 2008, 2010, 2030. 2012. Available online at: http://www.edenextdata.com/?q=data.

[308] WRAP. Comparing the cost of alternative waste treatment options. 2013. Available from: http://www.wrap.org.uk/sites/files/wrap/Gate_Fees_Report_2013_h%282%29.pdf.

[309] National Grid. Gas network innovation competition: Project NGGDGN01. 2014. Available from: http://www.smarternetworks.org/Files/BioSNG_Demonstration_Plant_131203151750.pdf.

[310] Batidzirai B. Design of sustainable biomass value chains: Optimising the supply logistics and use of biomass over time. PhD Thesis. Utrecht University, 2013.

[311] van der Meijden CM, Rabou LPLM, van der Drift A, Vreugdenhil BJ, Smit R. Large scale production of bio methane from wood. Int. Gas Union Res. Conf. IGRC, Seoul, South Korea: 2011.

[312] Searcy E, Flynn P, Ghafoori E, Kumar A. The relative cost of biomass energy transport. Appl Biochem Biotechnol. 2007;137–140:639–52. doi:10.1007/s12010-007-9085-8.

[313] Almansoori A, Shah N. Design and operation of a stochastic hydrogen supply chain network under demand uncertainty. Int J Hydrogen Energy. 2012;37:3965–77. doi:10.1016/j.ijhydene.2011.11.091.

[314] Ordnance Survey (OS). MERIDIAN2 [geospatial data], Scale 1:50000, Tiles: GB. 2014. Available online at: http://www.ordnancesurvey.co.uk/business-and-government/products/meridian2.html (accessed March 30, 2015).

[315] National Grid. Gas Ten Year Statement. London: 2013. Available from: http://www2.nationalgrid.com/UK/Industry-information/Future-of-Energy/Gas-ten-year-statement/Archive/.

[316] National Grid. UK Future Energy Secenarios. London: 2013. Available from: http://www2.nationalgrid.com/uk/industry-information/future-of-energy/fes/Documents/.

[317] National Grid UK. Electricity and gas transmission assets: Gas pipe [geospatial data], tiles: GB. 2014. Available online at: http://www2.nationalgrid.com/uk/services/land-and-development/planning-authority/shape-files/ (accessed December 1, 2014).

[318] Energy Solutions. Networks/LDZ Map. 2014. Available online at:

http://www.energybrokers.co.uk/gas/gas-network.htm (accessed December 1, 2015).

[319] MacRonald C. Modelling the UK gas transmission network. 2015. Available online at: http://www.see.ed.ac.uk/~mzaiser/4thyear/websites05/MacRonald/Website/home.html.

[320] Giarola S, Zamboni A, Bezzo F. Environmentally conscious capacity planning and technology selection for bioethanol supply chains. Renew Energy. 2012;43:61–72. doi:10.1016/j.renene.2011.12.011.

[321] Pirraglia A, Gonzalez R, Saloni D. Techno-economical analysis of wood pellets production for US manufacturers. BioResources. 2010;5:2374–90.

[322] Qian Y, Mcdow W. The wood pellet value chain. An economic analysis of the wood pellet supply chain from the Southeast United States to European Consumers. Greenville: 2013. Available from: http://www.usendowment.org/images/The_Wood_Pellet_Value_Chain_Revised_Final.pdf.

[323] Jahirul MI, Rasul MG, Chowdhury AA, Ashwath N. Biofuels production through biomass pyrolysis- A technological review. Energies. 2012;5:4952–5001. doi:10.3390/en5124952.

[324] Rogers JG, Brammer JG. Estimation of the production cost of fast pyrolysis bio-oil. Biomass and Bioenergy. 2012;36:208–17. doi:10.1016/j.biombioe.2011.10.028.

[325] Heo HS, Park HJ, Yim JH, Sohn JM, Park J, Kim SS, et al. Influence of operation variables on fast pyrolysis of Miscanthus sinensis var. purpurascens. Bioresour Technol. 2010;101:3672–7. doi:10.1016/j.biortech.2009.12.078.

[326] Office of Gas and Electricity Markets (Ofgem). Renewables Obligation : Guidance for generators. 2014. Available from: https://www.ofgem.gov.uk/ofgem-publications/87997/renewablesobligation-guidanceforgenerators1june2014.pdf.

[327] Office of Gas and Electricity Markets (Ofgem). Renewables Obligation (RO) buy-out price and mutualisation ceilings for 2017-18. 2017. Available online at: https://www.ofgem.gov.uk/publications-and-updates/renewables-obligation-ro-buy-out-price-and-mutualisation-ceilings-2017-18 (accessed March 1, 2017).

[328] Sobol IM. Global sensitivity indices for nonlinear mathematical models and their Monte Carlo estimates. Math Comput Simul. 2001;55:271–80. doi:10.1016/S0378-4754(00)00270-6.

[329] Saltelli A, Ratto M, Andres T, Campolongo F, Cariboni J, Gatelli D, et al. Global Sensitivity Analysis. The Primer. Chichester, UK: John Wiley & Sons, Ltd; 2007. doi:10.1002/9780470725184.

[330] Kucherenko S, Rodriguez-Fernandez M, Pantelides C, Shah N. Monte Carlo evaluation of derivative-based global sensitivity measures. Reliab Eng Syst Saf. 2009;94:1135–48. doi:10.1016/j.ress.2008.05.006.

[331] National Grid. Future Energy Scenarios: GB gas and electricity transmission. London: 2016. Available from: http://www2.nationalgrid.com/uk/industry-information/future-of-energy/future-energy-scenarios/.

[332] Feil B, Kucherenko S, Shah N. Comparison of Monte Carlo and Quasi Monte Carlo Sampling Methods in High Dimensional Model Representation. 2009 First Int Conf Adv Syst Simul. 2009:12–7. doi:10.1109/SIMUL.2009.34.

[333] Li G, Wang SW, Rabitz H. Practical approaches to construct RS-HDMR component functions. J Phys Chem A. 2002;106:8721–33. doi:10.1021/jp014567t.

[334] Zuniga MM, Kucherenko S, Shah N. Metamodelling with independent and dependent inputs. Comput Phys Commun. 2013;184:1570–80. doi:10.1016/j.cpc.2013.02.005.

[335] Kucherenko S, Zaccheus O. SobolGSA Software. 2017. Available online at: http://www.imperial.ac.uk/process-systems-engineering/research/free-software/sobolgsa-software/ (accessed November 1, 2016).